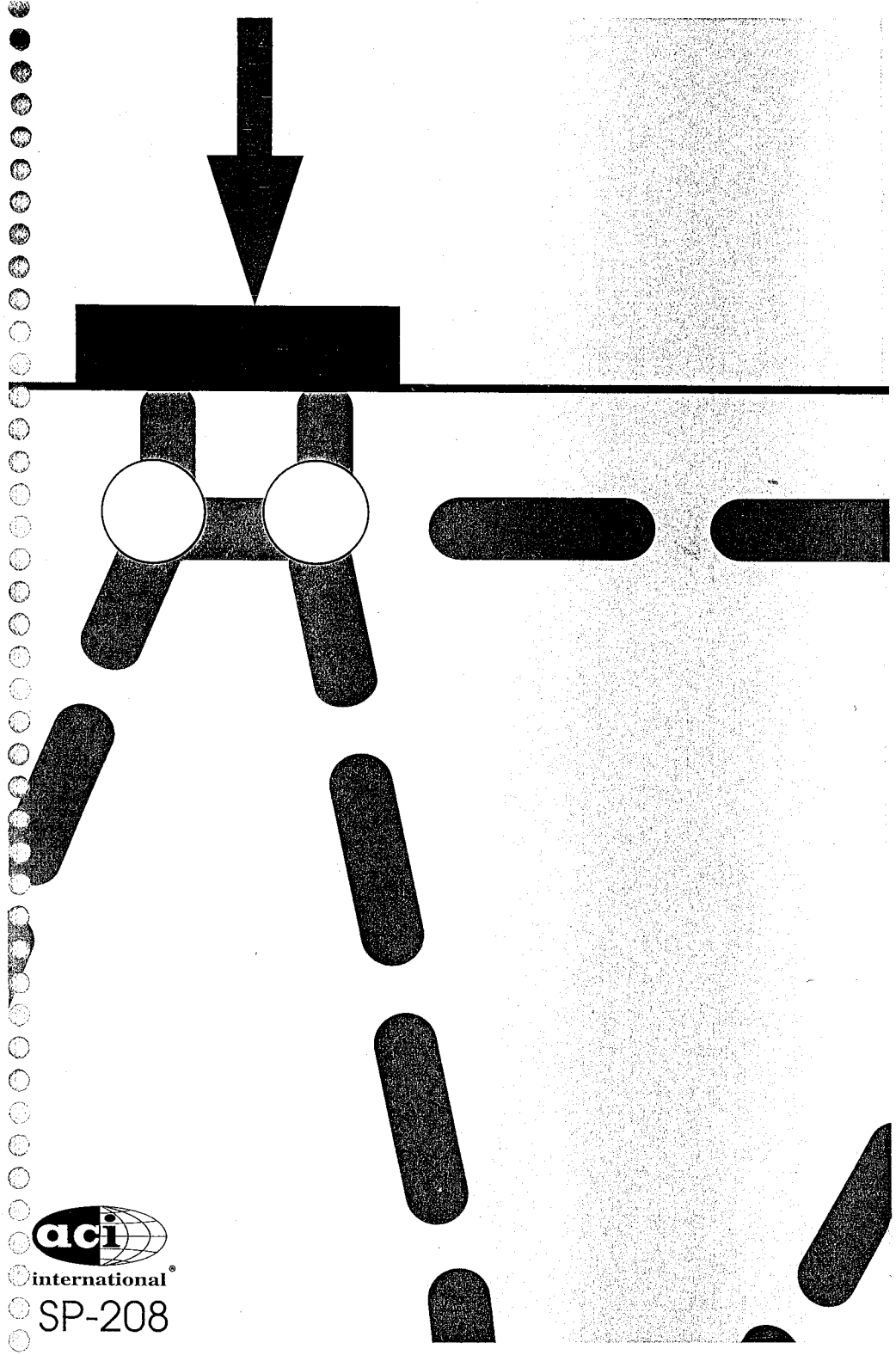

aci international
SP-208

Examples for the Design of Structural Concrete with Strut-and-Tie Models

aci international
SP-208

Examples for
the Design of
Structural Concrete with

Strut-and-Tie Mod

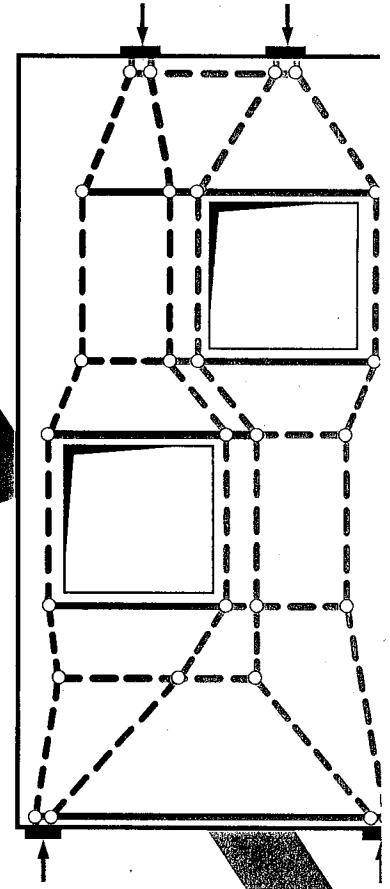

aci international
SP-208

Editor:
Karl-Heinz Reineck

Examples for the Design of Structural Concrete with Strut-and-Tie Models

Prepared by members of ACI Subcommittee 445-1, Strut and Tie Models, for sessions at the Fall Convention in Phoenix, October 27 to November 1, 2002, and sponsored by Joint ACI-ASCE Committee 445, Shear and Torsion, and ACI Committee 318-E, Shear and Torsion

Editor
Karl-Heinz Reineck

international®
SP-208

DISCUSSION of individual papers in this symposium may be submitted in accordance with general requirements of the ACI Publication Policy to ACI headquarters at the address given below. Closing date for submission of discussion is June 2003. All discussion approved by the Technical Activities Committee along with closing remarks by the authors will be published in the September/October 2003 issue of either ACI Structural Journal or ACI Materials Journal depending on the subject emphasis of the individual paper.

The Institute is not responsible for the statements or opinions expressed in its publications. Institute publications are not able to, nor intended to, supplant individual training, responsibility, or judgment of the user, or the supplier, of the information presented.

The papers in this volume have been reviewed under Institute publication procedures by individuals expert in the subject areas of the papers.

AMERICAN CONCRETE INSTITUTE
P.O. Box 9094
Farmington Hills, Michigan 48333-9094

Printed in the United States of America

Editorial production: Bonnie L. Schmick

Library of Congress catalog card number: 2002112515
ISBN: 0-87031-086-0

Preface

The new Appendix A of ACI 318-2002 on strut-and-tie models provides an excellent tool for the design of structural concrete where sectional design procedures for flexure and shear do not apply. This is the case in discontinuity regions (D-regions), which if not properly detailed, may exhibit structural damage or even brittle failure. This special publication presents examples for the use of strut-and-tie models following Appendix A of ACI 318-2002 for designing D-regions such as corbels, deep beams with and without openings, dapped beam ends, beams with indirect supports, anchorage zones of prestressed members, shear walls with openings, bridge pier tables, and pile caps.

The contributions and the examples were prepared by members of *ACI Subcommittee 445-A Shear and Torsion: Strut-and-Tie Models* and were presented at two sessions at the ACI Fall Convention in Phoenix, October 27 – November 1, 2002, co-sponsored by the technical committee *ACI-ASCE Committee 445: Shear and Torsion* and *ACI Subcommittee 318E: Shear and Torsion*. The papers of this special publication were reviewed in accordance with American Concrete Institute policies. The cooperation of the authors in the preparation of the manuscripts and their revision considering comments by reviewers is greatly appreciated.

In addition, the efforts of the reviewers and of the ACI Headquarters staff, especially Mr. Todd Watson, Manager of Technical Documents, are appreciated.

The editor also acknowledges the efforts of several individuals at ILEK, University of Stuttgart, including Elfriede Schnee, Ali Daghigni, Hussein Coskun, and Angela Siller for their assistance in producing the document.

The editor finally wishes to thank Cathy French, Chair of ACI-ASCE Committee 445, and Jim Wight, former Chair of ACI Subcommittee 318E, for their continuous support of the work of ACI Subcommittee 445-A and of this special publication.

Karl-Heinz Reineck
Editor and Chair of ACI Subcommittee 445-A Shear and Torsion: Strut and Tie Models
ILEK, University of Stuttgart, Germany

ACI Subcommittee 445-A Shear and Torsion: Strut and Tie Models

Members: Sergio M. Alcocer, Robert B. Anderson, Robert W. Barnes, Jay Holombo, Gary J. Klein, Daniel Kuchma, Denis Mitchell, Karl H. Reineck (chair), Julio A. Ramirez, Mario Rodriguez , David Sanders, Sri S. Sritharan, Claudia M. Uribe, Fernando Yanez

Examples for the design of structural concrete with strut-and-tie models

List of contents

Part 1

Introduction

Karl - Heinz Reineck

Karl-Heinz Reineck received his Dipl.-Ing. and Dr.-Ing. degrees from the University of Stuttgart. He is involved in both research and teaching at the Institute for Lightweight Structures Conceptual and Structural Design (ILEK), University of Stuttgart, and he is head of two research groups and managing director of the institute. His research covers the shear design of structural concrete, the design with strut-and-tie models and detailing of structural concrete and the design of high-performance concrete hot-water tanks. He is member of ASCE-ACI Committee 445 "Shear and Torsion" and chairs two subcommittees and also is a member of *fib* Task Group 1.1 "Practical Design".

Part 1: Introduction

1 Historical remarks

The last fifteen years has brought a major breakthrough in design methods for concrete structures which reflected in the terminology used. The term "structural concrete" was proposed as a unifying term for all kinds of applications of concrete and steel in order to overcome the traditional divisions between reinforced concrete, prestressed concrete and partially prestressed concrete and even externally prestressed concrete or unreinforced concrete. These differentiations were identified as artificial, leading to confusion in codes and in teaching as well as to unnecessary restrictions in practice, as pointed out at the IABSE Colloquium "Structural Concrete" April 1991 in Stuttgart [IABSE (1991 a, b)]. Shortly thereafter the American Concrete Institute renamed the ACI 318 code accordingly.

The limitations of purely empirical design procedures has been increasingly realized, driving the demand for the development of clear design models. The theory of plasticity was applied to the design of members under shear and torsion, especially by Thürlimann (1975, 1983) and Nielsen (1978, 1984) and their co-workers. This also formed the basis for strut-and-tie models after the works of Schlaich et al. (1987, 2001). Strut-and-tie models are a valuable design tool used since the beginning of reinforced concrete design, as demonstrated by the use of truss models for the shear design e.g. by Ritter (1899), Mörsch (1909, 1912,1922), Rausch (1938, 1953) and others. This is especially true for discontinuity regions (D-regions), which have been poorly addressed in codes, even though improper design and detailing of D-regions led to structural damages including some failures [Breen (1991), Podolny (1985)]. The development of strut-and-tie models has brought the unique chance toward gaining consistency in the design concept covering D-regions and B-regions with similar models. Furthermore, the application of strut-and-tie models emphasizes the essential role of detailing in design. All this was pointed out in the State-of-the-Art Report on shear by the ASCE-ACI Committee 445 (1998).

The Appendix A of ACI 318-2002 consequently reflects this international development in research and thus is in line with some codes like the CEB-FIP Model Codes 1990, EC 2, Canadian Code and AASHTO, as well as the recent FIP Recommendations (1999) and the new German code DIN 1045-1 (2001-07).

2 Dimensioning procedures according to the present codes

The principles for the design are clearly defined in most codes, and they address the whole structure and not only sections when defining the requirements and principles for the design. Contrary to the principles, however, the dimensioning procedures and the checking procedures focus on sections, and separate checks are carried out for the different actions, such as moments and shear forces. In addition, the detailing rules given finally in codes are meant to ensure the overall safety of the structure.

The danger of a sectional design approach is that the overall flow of forces may be overlooked and that critical regions are not covered. Especially the regions with discontinuities due to the loading or/and the geometry, the D-regions, are not dimensioned but left to be covered by detailing rules, apart from some special cases (e.g. frame corners or corbels). All these considerations triggered discussions at the IABSE Colloquium "Structural Concrete" in 1991 and to the conclusions published thereafter [IABSE (1991 a, b)]. The demand for developing clear models, like strut-and-tie models, was expressed by Schlaich (1991) and Breen (1991). Most of these ideas were taken up by the FIP Commission 3 "Practical Design", chaired by Julio Appleton, and one of its Working Groups developed the FIP Recommendations "Practical design of structural concrete" published in 1999 by *fib*. These recommendations are fully based on strut-and-tie models and show the direction for future developments. However, most codes still keep to the traditional concepts and only added a new chapter or appendix without integrating the new concept throughout the code. One exception is the case of the shear design where a truss model has been used for steel contribution for many years.

3 Aim and contents of this Special Publication

The implementation of strut-and-tie models in ACI 318-2002 with Appendix A is an important step in direction towards a more consistent design concept. Even more, it is a major achievement for the engineers in practice and should trigger efforts to apply strut-and-tie models in daily practice. Therefore, the main objective of this Special Publication is to show with design examples the application of strut-and-tie models according to the Appendix A of ACI 318-2002.

This Special Publication contains five parts. After the introduction (Part 1), Part 2 gives an insight into the development of Appendix A of ACI 318-2002 and of the discussions in ACI Committee 318 E "Shear and Torsion". The scope and aim of the Appendix A is described and extensive explanations are given in addition to those already presented in the Commentary of Appendix A.

Part 3 presents a summary of important tests, which justify the use of strut-and-tie models for the design of structural concrete. Among the tests are the classical examples for D-regions like deep beams, corbels and dapped beam ends.

Part 4 forms the major part of this Special Publication presenting nine different examples designed with strut-and-tie models using Appendix A of ACI 318-2002. Most of these examples were taken from practice:

- The Example 1 (deep beam), Example 2 (dapped beam end) and Example 3 (double corbel and corbel at column) are classical D-regions, which have been designed with strut-and-tie models since long, and for which even tests were carried out, as described in Part 3.
- The Example 5 (beam with indirect supports) and Example 6 (prestessed beam) deal with well known D-regions of beams, which so far have mostly been dealt with in codes by rules for the shear design.
- The Examples 7 (pier table) and Example 9 (pile cap) deal with D-regions of 3D-structures, for the design which most codes give only rare information.

Some examples were selected to demonstrate the potential of strut-and-tie models to solve uncommon design problems, such as like Example 4 (deep beam with opening) and Example 8 (high wall with two openings).

All examples show the approach of finding a model, which is the first and an important step in a design with strut-and-tie models. The examples also point out where problems in dimensioning or in detailing and anchoring the reinforcement occur and how the design could be improved.

Part 5 gives a summary and discusses some issues which are either common for all examples or turned up in several examples. After a brief review of the procedures for finding a model, the uniqueness of a model is discussed and why different models may be selected by several engineers. The other issue addresses the transition between D- and B-regions of beams and is of general importance for many examples, because many D-regions are part of a larger structure and have to be "cut out" of it, i.e. the correct actions and forces have to be applied at the border of the D-region. Finally in Part 5 the importance of detailing is pointed out as it was demonstrated in several examples.

References

AASHTO (1994): AASHTO LRFD Bridge design specifications, section 5 Concrete Structures. American Association of State Highway and Transportation Officials, Washington, D.C. 2001, 1994

ACI 318 (2002): Building Code Requirements for Structural Concrete and Commentary. American Concrete Institute, Farmington Hills

ASCE-ACI 445 (1998): Recent approaches to shear design of structural concrete. State-of-the-Art-Report by ASCE-ACI Committee 445 on Shear and Torsion. ASCE-Journ. of Struct. Eng. 124 (1998), No.12, 1375-1417

Breen, J.E. (1991): Why Structural Concrete? p. 15-26 in: IABSE Colloquium Structural Concrete, Stuttgart April 1991. IABSE Rep. V.62, 1991

CEB-FIP MC 90 (1993): Design of concrete structures. CEB-FIP-Model-Code 1990. Thomas Telford, 1993

CSA (1994): Design of Concrete Structures - Structures (Design). Canadian Standards Association (CAN3-A23.3-M84), 178 Rexdale Boulevard, Rexdale (Toronto), Ontario, December 1994

DIN 1045-1 (2001): Deutsche Norm: Tragwerke aus Beton, Stahlbeton und Spannbeton - Teil 1: Bemessung und Konstruktion. S. 1 - 148. (Concrete, reinforced and prestressed concrete strutures - Part 1: Design). Normenausschuss Bauwesen (NABau) im DIN Deutsches Institut für Normung e.V. Beuth Verl. Berlin, Juli (2001)

EC 2 (1992): Eurocode 2: design of concrete structures - Part 1: General rules and rules for buildings. DD ENV 1992-1-1. BSI 1992

FIP Recommendations (1999): "Practical Design of Structural Concrete". FIP-Commission 3 "Practical Design", Sept. 1996. Publ.: SETO, London, Sept. 1999. (Distributed by: *fib*, Lausanne)

IABSE (1991 a): IABSE-Colloquium Stuttgart 1991: Structural Concrete. IABSE-Report V.62 (1991 a), 1-872, Zürich 1991

IABSE (1991 b): IABSE-Colloquium Stuttgart 1991: Structural Concrete - Summarizing statement.
publ. in: - Structural Engineering International V.1 (1991), No.3, 52-54
- Concrete International 13 (1991), No.10, Oct., 74-77
- PCI-Journal 36 (1991), Nov.-Dec., 60-63
and: IVBH-Kolloquium "Konstruktionsbeton" - Schlußbericht.
publ. in: - BuStb 86 (1991), H.9, 228-230
- Bautechnik 68 (1991), H.9, 318-320
- Schweizer Ingenieur und Architekt Nr.36, 5. Sept. 1991
- Zement und Beton 1991, H.4, 25-28

Mörsch, E. (1909): Concrete Steel Construction. McGraw-Hill, New York, (1909), pp. 368 (English translation of "Der Eisenbetonbau", 1902)

Mörsch, E. (1912): Der Eisenbetonbau. 4. Aufl., K. Wittwer, Stuttgart, 1912

Mörsch, E. (1922): Der Eisenbetonbau - Seine Theorie und Anwendung (Reinforced concrete Construction - Theory and Application). 5th Edition, Vol.1, Part 2, K. Wittwer, Stuttgart, 1922

Nielsen, M.P.; Braestrup, M.W.; Jensen, B.C.; Bach, F. (1978): Concrete Plasticity: Beam Shear-Shear in Joints-Punching Shear. Special Publ. Danish Society for Structural Science and Engineering, Dec. 1978, 1-129

Nielsen, M.P. (1984): Limit State Analysis and Concrete Plasticity. Prentice-Hall, Englewood Cliffs, New Jersey, 1984, pp. 420

Podolny, W. (1985): The cause of cracking in past-tensioned concrete box girder bridges and retrofit procedures. PCI Journal V.30 (1985), No.2, March-April, 82-139

Rausch, E. (1938): Berechnung des Eisenbetons gegen Verdrehung (Torsion) und Abscheren. 2. Aufl.. Springer Verlag, Berlin, 1938. pp. 92

Rausch, E. (1953): Drillung (Torsion), Schub und Scheren im Stahlbetonbau. 3. Aufl. Deutscher Ingenieur-Verlag, Düsseldorf, 1953 pp. 168

Ritter, W. (1899): Die Bauweise Hennebique. Schweizerische Bauzeitung, Bd. XXXIII, Nr. 7., Jan., 1899

Schlaich, J.; Schäfer, K; Jennewein, M. (1987): Toward a consistent design for structural concrete. PCI-Journ. V.32 (1987), No.3, 75-150

Schlaich, J.; Schäfer, K. (2001): Konstruieren im Stahlbetonbau (Detailing of reinforced concrete). Betonkalender 90 (2001), Teil II, 311 - 492. Ernst & Sohn Verlag, Berlin 2001

Schlaich, J. (1991): The need for consistent and translucent models. p. 169-184 in: IABSE Colloquium Structural Concrete, Stuttgart April 1991. IABSE Rep. V.62, 1991

Thürlimann, B.; Grob, J.; Lüchinger, P. (1975): Torsion, Biegung und Schub in Stahlbetonträgern. Fortbildungskurs für Bauingenieure, Institut für Baustatik und Konstruktion, ETH Zürich. April 1975.

Thürlimann, B.; Marti, P.; Pralong, J.; Ritz, P.; Zimmerli, B. (1983): Anwendung der Plastizitätstheorie auf Stahlbeton. Fortbildungskurs für Bauingenieure, Institut für Baustatik und Konstruktion, ETH Zürich. April 1983

Part 2

Derivation of strut-and-tie models for the 2002 ACI Code

James G. MacGregor

Synopsis

This paper documents the decisions made by ACI Committee 318 to introduce strut-and-tie models into the 2002 ACI Code. Sections 3 and 4 of this paper review code statements concerning the layout of strut-and-tie models for design. The format and values of the effective compression strength of struts are presented in Sec. 5. The first step was to derive an effective compression strength which gave the same cross-sectional area and strength using Appendix A as required by another code for the same concrete strength and same unfactored loads. The final selection of design values of the effective compression strength considered test results, design values from the literature, values from other codes, and ACI Code design strengths for similar stress situations. A similar derivation of the effective compression strengths of nodal zones is summarized in Sec. 6 of the paper. The description of the geometry of nodal zones in code language proved difficult. The design of ties is described in Sec. 7 of this paper and requirements for nominal reinforcement are in Sec. 8. Nominal reinforcement is provided to add ductility, to improve the possibility of redistribution of internal forces, and to control cracks at service loads.

James G. MacGregor received a B.Sc. in Civil Engineering from the University of Alberta, Canada in 1956, and a Ph.D. from the University of Illinois in 1960. He joined the Department of Civil Engineering at the University of Alberta in 1960, employed there until 1993. Dr. MacGregor serves on ACI technical committees on shear and torsion, columns, and the ACI Code committee. He chaired Canadian code committees on reinforced concrete design, and structural design. In 1992-93 he was president of ACI. Dr. MacGregor is an Honorary Member of ACI, a Fellow of the Royal Society of Canada, and a Fellow of the Canadian Academy of Engineering. In 1998 he received an honorary Doctor of Engineering degree from Lakehead University, and in 1999, an honorary Doctor of Science degree from the University of Alberta.

1 Introduction

The 2002 ACI Code (2002) includes a new Appendix A, "*Strut-and-Tie Models*" and changes to a number of code sections to allow the use of strut-and-tie models (STM) in design. In developing Appendix A, concepts were drawn from the AASHTO LRFD Specification (1998), the CEB/FIP Model Code (1993) as interpreted in the FIP Recommendations (1999), and the Canadian concrete design code, CSA A23.3-94 (1994). Research reports [ACI Committee 445 (1997)] also provided some of the basis for the appendix This paper, in combination with the ACI 318 Commentary for Appendix A [ACI (2002)] explains the decisions and assumptions made in the development of Appendix A.

2 Research significance

This paper documents major decisions made in the development of Appendix A, "*Strut-and-Tie Models*" in the 2002 ACI Code.

3 What are strut-and-tie models?

3.1 B-Regions and D-Regions

Concrete structures can be divided into beam-like regions where the assumption of the straight line strain distribution of flexure theory applies, and disturbed regions, adjacent to abrupt changes in loading at concentrated loads and reactions; or adjacent to abrupt changes in geometry such as holes or changes in cross section. In the latter regions the strain distributions are not linear. These different portions are referred to *B-regions* and *D-regions*, respectively.

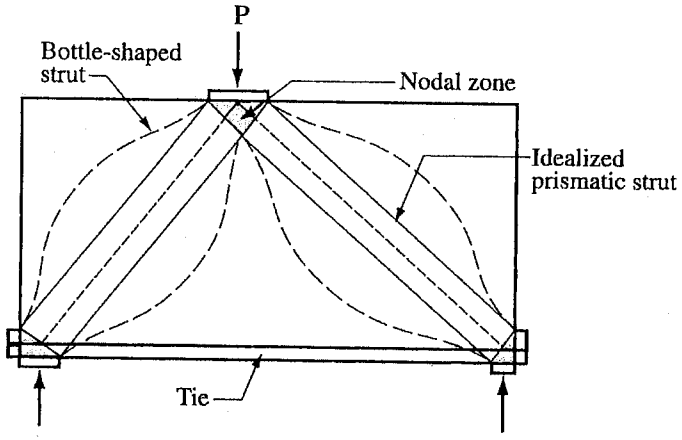

Fig. 1: A strut-and-tie model for a deep beam.

The traditional theory of flexure for reinforced concrete, and the traditional ($V_c + V_s$) design approach for shear apply in B-regions. In D-regions, on the other hand, a major portion of the load is transferred directly to the supports by in-plane compressive forces in the concrete and tensile forces in reinforcement and a different design approach is needed. D-regions may be modeled using hypothetical trusses consisting of concrete *struts* stressed in compression, steel *ties* stressed in tension, joined together at joints referred to as *nodes*. These trusses are referred to as *strut-and-tie models* (STM's).The strut and tie model of a single span deep beam shown in Fig. 1 is composed of two inclined struts, and a horizontal tie joined together at three nodes [ACI 318 (2002)]. The nodes are enclosed within *nodal zones* which transfer forces from the struts to the ties and reactions. Strut-and-tie models are assumed to fail due to yielding of the ties, crushing of the struts, failure of the nodal zones connecting the struts and ties, or anchorage failure of the ties. The struts and the nodal zones are assumed to reach their capacities when the compressive stresses acting on the ends of the struts or on the faces of the nodal zones, reach the appropriate *effective compressive strength*, f_{cu}.

De St. Venant's principle and elastic stress analyses suggest that the localized effect of a concentrated load or a geometric discontinuity will die out *about* one member depth away from the load or discontinuity. For this reason, D-regions are assumed to extend *approximately* one member depth from the load or discontinuity. The words "about" and "approximately" are emphasized here because the extent of D-regions can vary from case to case (see ACI Sec. A.1.).

If two D-regions each of length d or less, come together and touch or overlap, they are considered in Appendix A to act as a combined D-region. For a shear span in a deep beam the combined D-region has a depth of d and a length up to 2d one way or two ways from the disturbance. This establishes the smallest angle between a strut and a tie attached to one end of the strut as arctan (d / 2d) = 26.5°, rounded off to 25° (see ACI Sec. A.2.5.)

Figure 2, reproduced from *"Prestressed Concrete Structures"* [Collins and Mitchell (1991)], compares the experimental shear strengths of simply supported beams with various shear-span-to-depth ratios, a/d, from 1 to 7. B-region behavior controlled the strengths of beams with a/d greater than 2.5 as shown by the approximately horizontal line to the right of a/d = 2.5. D-region behavior controlled the strengths of beams with a/d ratios less than about 2.5 as shown by the steeply sloping line to the left of a/d = 2.5 in Fig. 2.

ACI Committee 318 limited the maximum lengths of isolated D-regions to d, and to 2d for overlapping D-regions. Strut-and-tie models can also be used in the design of B-regions [Marti (1985)]. However, the V_c term in the traditional ACI shear strength equation is not included.

Two-dimensional strut-and-tie models are used to represent planar structures such as deep beams, corbels and joints. Three-dimensional strut-and-tie models are used for structures such as pile caps for two or more rows of piles.

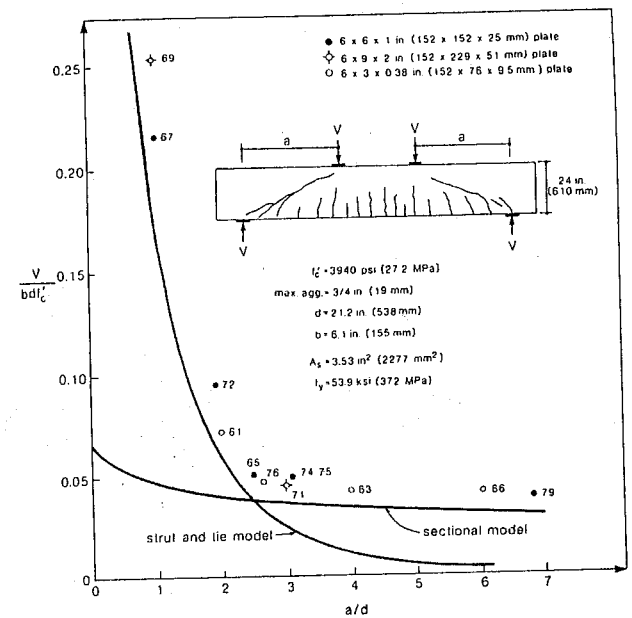

Fig. 2: Strengths of concrete beams failing in shear for various a/d ratios.

3.2 Decisions necessary to develop design rules for strut-and-tie models

To codify strut-and-tie models for design, the major items to be defined and specified are:

(a) the geometric layout of strut-and-tie models,

(b) what effective concrete strengths and ϕ factors should be used,

(c) the shape and strength of the struts,

(d) the arrangement and strength of the nodal zones,

(e) the layout, strength, and anchorage of the ties, and

(f) the detailing requirements.

The definitions of these items differ considerably in various codes and other design documents. The effective concrete strength and the strength reduction factors in Appendix A were originally derived using the load and resistance factors in Chapter 9 of the 1999 ACI Code. The changes necessitated by the new load and resistance factors in the 2002 ACI Code are presented briefly.

3.3 Geometric layout of strut-and-tie models

A strut-and-tie model is a hypothetical truss that transmits forces from loading points to supports. The selection of STM's, the calculation of the forces in the struts and ties, and the design of reinforcement in the ties are discussed, with examples, in "*Toward a Consistent Design of Structural Concrete*" [Schlaich, Schäfer and Jennewein (1987)] "*Prestressed Concrete Structures*" [Collins and Mitchell (1991)], ., and "*Basic Tools of Reinforced Concrete Beam Design*" [Marti (1985), and [*Reinforced Concrete: Mechanics and Design*, MacGregor (1997)].

Appendix A is formulated on the assumption that strut-and-tie models will be used in design. It is not intended that design be reduced to equations for the shear resisted by struts and web reinforcement. The selection of the model and the production of a drawing of the model are integral parts of

Commentary RA.2.1 in Appendix A [ACI(2002)] gives a step-by-step procedure for laying out a strut-and-tie model. Various authors have suggested methods of doing this [ACI (1999)], Collins and Mitchell (1991), Schlaich, Schäfer and Jennewein (1987) and MacGregor (1997). The starting point is usually the computation of the reactions for the structure and loads. Generally speaking, a strut-and-tie model which minimizes the amount of reinforcement approaches the ideal model. For two-dimensional structures some researchers [Schlaich, Schäfer and Jennewein (1987)] recommend using a finite element analysis to determine the stress trajectories for a given load case. The struts are then aligned within ± 15° of the resultant compression forces from such an analysis, and the ties within ± 15° of the resultant tensile forces.

On the other hand, the Canadian code [CSA(1994)] requires that finite element analyses be checked by independent analyses satisfying equilibrium, and suggests using strut-and-tie models for this check.

In developing a strut-and-tie model for a given application it is frequently useful to select initial trial locations for the nodes and use these in the initial cycle of calculations of the member forces. If pictures of the cracking pattern in similar structures are available, the location of the struts and ties can be arranged within the structure such that struts fall between cracks. Struts should not cross cracked regions.

Section A.2 of the 2002 ACI presents several major requirements that must be satisfied by a strut-and-tie model:

1. *First and foremost, the strut-and-tie model must be in equilibrium with the factored applied loads and factored dead loads (ACI Sec. A2.2). The calculation of the reactions and strut and tie forces satisfies statics. It therefore produces a* statically adnissible force field.
2. *The strengths of the struts, ties, and nodal zones must equal or exceed the forces in these members. (ACI Sec. A.2.6). If the strength at every cross section equals or exceeds the strength required by the analysis in item 1, the structure is said to have a* safe *distribution of strengths.*
3. *In the early stages in the design of a D-region it may be sufficient to consider only the axes of the struts and ties when laying out a strut-and-tie model. It is generally necessary, however, to consider the widths of the struts, ties, and nodal zones and support regions when laying out a strut-and-tie model (Sec. A.2.3).*
4. *Struts must not cross or overlap each other (Sec. A.2.4). The widths of struts are chosen to carry the forces in the struts using the effective strength of the concrete in the struts. If struts overlapped, the overlapping parts of the struts would be overstressed.*
5. *Ties are permitted to cross struts or other ties. (Sec. A.2.4)*
6. *The smallest angle between a strut and a tie that are joined at a node is set at 25°. (Sec. A2.5).*

A structural design that is both statically admissible and safe, satisfies the requirements of a lower bound solution *in the theory of plasticity. This implies that the failure load computed by a strut-and-tie model underestimates the actual failure load. For this to be true, the structure must have enough ductility to accommodate any needed redistribution of forces.*

4 Forces in struts and ties, and strength reduction factors, ϕ

After the initial strut-and-tie model has been selected, the reactions to the applied loads and self weight loads are computed. Once the reactions have been computed, the forces, F_u, in all the struts, ties, and nodal zones loads are computed using truss analysis. The struts, ties and nodal zones are then proportioned based on:

$$\phi F_n \geq F_u \qquad (1)$$

where F_u is the force in the member (strut, tie, or nodal zone) due to the factored loads, F_n is the nominal strength of the member, and ϕ is a strength reduction factor. The nominal strengths of struts, ties, and nodal zones are F_{ns}, F_{nt}, and F_{nn}, respectively.

Equation 1 includes the factored resistance ϕF_n. In the CEB/FIP Model Code (1993) the Canadian Code [CSA(1994)], and the FIP Recommendations (1999), material strength reduction factors, ϕ_c and ϕ_s, or γ_c and γ_s, are applied to the concrete and steel strengths, f_c' and f_y. The 1999 ACI Code used different strength reduction factors for each type of structural resistance, $\phi_f = 0.9$ for flexure and $\phi_V = 0.85$ for shear in beams, corbels, and deep beams. (Subscripts have been added to the ϕ factors in this paper to indicate the structural action corresponding to the various ϕ factors.)

In the 2002 ACI Code, the load combinations and ϕ factors in Appendix C of ACI 318-99, were interchanged with those in Chapter 9 of ACI 318-99. In the 2002 Code, ϕ_V and ϕ_{STM} were changed to 0.75 for the design of strut-and-tie models using the load factors and strength reduction factors in Chapter 9 of the 2002 ACI Code. A re-evaluation of the ϕ factor for flexure indicated ϕ_f could remain equal to 0.90.

ACI 318–99 included a new Sec. 18.13 on the design of post-tensioned tendon anchorage zones, based in part on strut-and-tie models. That code specified $\phi_{PA} = 0.85$ in the design of post-tensioned anchorage zones to be used with a load factor of 1.2 (Sec. 9.2.8) on the prestressing force. Strut-and-tie models of prestress anchorage zones retain this ϕ factor and load factor because the tendon forces and the load factor on the tendon forces are unchanged.

5 Struts

5.1 Types of struts

Struts vary in shape. In strut-and-tie models, they are generally idealized as prismatic or uniformly tapered members as shown by the straight sides of the idealized prismatic struts in the shear spans of the deep beam shown in Fig. 1. In that strut-and-tie model, the concrete in the beam webs adjacent to a strut is stressed by the lateral spread of the strut stresses into the adjacent concrete in the shear spans. If there is room for this spread to occur, the struts are said to be *bottle-shaped.* Most struts in two-dimensional strut-and-tie models will be bottle-shaped.

5.2 Design of struts

Struts are designed to satisfy Eqs. 1 to 4. The factored strength of a strut is computed as:

$$F_{ns} = f_{cu} A_c \qquad (2)$$

where f_{cu} is the *effective compressive* strength of the concrete in a strut, taken equal to:

$$f_{cu} = \nu f_c' \qquad (3)$$

or:

$$\phi f_{cu} = \phi \nu f_c' = \phi_{STM} \alpha_1 \beta_s f_c' \qquad (4)$$

where ν (nu) is called the effectiveness factor, A_c is the end area of the strut acted on by f_{cu}, ϕ_{STM} is the value of ϕ for struts, ties, and nodal zones in strut-and-tie models, α_1 is the 0.85 factor in ACI Sec. 10.2.7.1 and β_s is the effectiveness factor for a strut. If f_{cu} is different at the two ends of a strut, the strut is idealized as being uniformly tapered. The term ν is introduced as an intermediate step in the derivation of Eq. 4 because different codes and researchers include different factors in their definitions of the effective compressive strength.

5.3 Effective compressive strength of struts, f_{cu}

5.3.1 Factors affecting the effective concrete strength of struts

The stress acting in a strut is assumed to be constant over the cross-sectional area at the end of the strut. Three major factors that affect the effectiveness factor are given in the following paragraphs. Depending on the emphasis placed on each factor when deriving values of the effectiveness factor, the values of f_{cu} differ from code to code.

(a) Load Duration Effects. The effective strength of the struts is given by Eqs. 1 and 4 where $\nu = \alpha_1 \beta_s$, and α_1 is the 0.85 factor defined in ACI Sec. 10.2.7.1, explained in various references as accounting for load duration effects, or accounting for different stress regimes in the cylinders and the flexural stress blocks, or accounting for the vertical migration of bleed water. In Eq. 4, α_1 was taken equal to 0.85 from ACI Sec. 10.2.7.1. This factor probably should be a function of f_c', decreasing as f_c' increases [Ibrahim and MacGregor (1997)]. Recently, several relationships have been suggested as replacements for the $\alpha_1 = 0.85$ in ACI Sec. 10.2.7.1. In the event that one of these proposed revisions is accepted, the α_1 in Eq. 4 would be modified to agree. The subscript "s" in β_s refers to strut.

(b) Cracking of the struts. Typically, the struts develop axial, diagonal, or transverse cracks. The resulting reduction in the compressive strength of the struts is explained in the following paragraphs.

(i) Bottle-shaped struts. Struts frequently are wider at midlength than at their ends because the width of concrete that the strut stresses can spread into is greater at midlength than at the ends of the strut. The curved, dashed outlines of the struts in Fig. 1 represent the effective boundaries of a typical strut. Such a strut is said to be *bottle-shaped*. In design, bottle-shaped struts are idealized as the prismatic struts shown by the straight, solid-line boundaries of the struts in Fig. 1.

The divergence of the forces along the length of the strut tends to cause longitudinal splitting near the ends of the strut as shown in Fig. 3. In the absence of reinforcement to confine this splitting, these cracks may weaken the strut. Schlaich et al. (1987) have analyzed this type of cracking and predict that it will occur when the compressive stress on the end of the strut exceeds approximately $0.55f_c'$. Schlaich et al. and Breen et al. (1994) suggest that a the diverging struts in Fig. 3 have a slope of 1:2 as shown.

(ii) Cracked struts. The strut may be crossed by cracks which will tend to weaken the strut [Schlaich, Schäfer and Jennewein (1987)]. The effective compressive strengths given in Appendix A and Sec. 5.3.5 of this paper reflect this concept.

(iii) Transverse tensile strains. Tensile strains perpendicular to the axis of a cracked strut connected to a tie may reduce the compressive strength of the strut [Vecchio and Collins (1982)]. In the Canadian Code [CSA(1994)] and the AASHTO Specifications (1998) it is assumed that the strength of a strut is a function of the transverse tensile

strain in the strut due to the tie attached to one or other end of the strut, computed as a function of the angle between the axis of the strut and the axis of the tie. Tests of uniformly-stressed, square concrete panels by Vecchio and Collins (1982) have given rise to the values of f_{cu} given by Eqs. 11 and 12 in Sec. 5.3.3.

(c) Confinement from surrounding concrete. In three-dimensional concrete structures like pile caps, the compressive strength of a strut may be increased by the confinement resulting from the large volume of concrete around the strut. Adebar and Zhou (1993) have proposed equations for the effective compressive strength for use in designing pile caps.

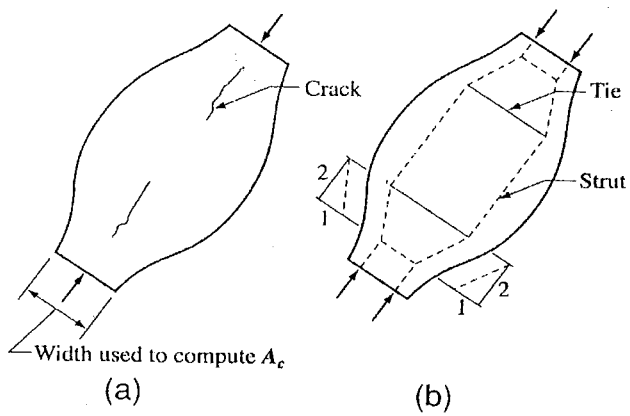

Fig. 3: Splitting of a bottle-shaped strut.

5.3.2 Effective compressive strength of struts—from tests and literature

Various researchers have proposed values of the effectiveness factor ν. A few comparisons are made here. Many more references are listed in a Bibliography on Strut-and-Tie Models, collected by the ACI-ASCE committee on Shear and Torsion [ACI 445(1997)].

- Based on tests of 24, one- and two-span deep beams, Rogowsky and MacGregor (1986) proposed $f_{cu} = \nu f_c' = 0.85 f_c'$. They observed that the selection of an appropriate truss was more important than the choice of ν.
- Ricketts (1985) reported ratios of test to calculated strengths of six two-span continuous deep beams. The failure loads predicted using strut-and-tie models, had a mean ratio of test / calculated strengths of 0.96 for ν = 1.0. When ν was taken as 0.6, the mean test to calculated strength ratio increased to 1.13. This indicates that ν was closer to 1.0 than to 0.6.
- Rogowsky (1983) stated that ν = 1.0 conservatively predicted the strengths of the corbels tested by Kriz and Raths (1965). Virtually all of the corbel tests had effectiveness factors, ν, between 1.0 and 1.3.
- Ramirez and Breen (1991) proposed a relationship between ν and $\sqrt{f_c'}$ with ν ranging from 0.55 to 0.39 for f_c' ranging from 3000 to 6000 psi.
- Bergmeister et al. (1991) related ν and f_c' with ν ranging from 0.77 to 0.69 for concrete strengths ranging from 3000 psi to 6000 psi.
- Schlaich et al. (1987) recommended values of ν similar to those given in Section 5.3.5 of this paper.
- Marti (1985) suggested a constant value of ν = 0.6.

5.3.3 Effective concrete strength of struts—from other codes

The values of β_s from other codes cannot be used directly in Appendix A because other codes have different load factors, different resistance factors, and different ways of specifying the concrete strength. A further complication is introduced by the fact that the load and resistance factors in Chapter 9 of the 2002 ACI Code differ from those in Chapter 9 of the 1999 ACI Code.

Initial values of $\phi_{STM}\alpha_1\beta_s$ corresponding to the 1999 ACI Code load factors and the ACI definition of f_c' were derived by calibration to the FIP Recommendations (1999).The cross-sectional areas of struts required by the FIP Recommendations, for example, were computed for the axial forces in a hypothetical strut due to assumed combinations of dead and live load, based on the load factors in the FIP Recommendations and for the corresponding concrete strengths, f_c'.

The values of $\phi_{STM}\ \alpha_1\ \beta_s$ needed in the ACI Code so that the strut area from the two codes givethe same load capacities were then computed using ..

$\phi_{STM} = 0.85$ and $\alpha_1 = 0.85$.

FIP Recommendations. The FIP Recommendations (1999) give the cross-sectional area of a strut required for a given set of loads as:

$$A_{c,FIP} = \frac{F_{uFIP}}{f_{cdeff}} \tag{5}$$

where $A_{c,FIP}$ is the cross-sectional area of the strut computed using the FIP Recommendations, $F_{u,FIP}$ is the strut force due to the sum of the factored loads acting on the strut., and $f_{cd,eff}$ is the effective concrete strength from FIP. For unfactored strut loads of 100 kips dead load and 50 or 200 kips live load, values of $A_{c,FIP}$ were computed using Eq. 5 for specified concrete strengths, f_c' of 3000 psi and 6000 psi. These were set equal to the corresponding areas, $A_{c,ACI}$, from Appendix A:

$$A_{c,ACI} = \frac{F_{uACI}}{\phi_{STM}\alpha_1\beta_s f_c'} \tag{6}$$

where $A_{c,ACI}$ is the area of the strut or the compression stress block for a member designed using the ACI Code, and $F_{u,ACI}$ is the force in the strut due to ACI factored loads on the strut-and-tie model.

Setting $A_{c,FIP}$ equal to $A_{c,ACI}$, assuming that the unfactored loads are defined in the same way in both the ACI and FIP, and rearranging, gives:

$$\phi_{STM}\ \beta_s = \frac{F_{uACI} f_{cdeff}}{\alpha_1 f_c' F_{uFIP}} \tag{7}$$

where α_1 is the factor from ACI Sec. 10.2.7.1.

Load Factors and Loadings. The basic load case considered is dead load plus live load (D + L), where D = 100 kips, with L either 50 kips (0.5D) or 200 kips (2.0D). It is reasonable to assume that D and L are defined in a similar fashion in both American and European codes.

In FIP, the basic load case is U = 1.35D + 1.5 L, where U stands for ultimate load. For L = 0.5D, U = 2.10D (210 kips) and for L = 2D, U = 4.35D (435 kips).

In Sec. 9.2.1 of the 1999 ACI Code, U = 1.4D +1.7L. For L = 0.5D, U = 2.25D (225 kips) and for L = 2D, U = 4.8D (480 kips).

In Sec. 9.2.1 of the 2002 ACI Code, the basic load combination changes to U = 1.2D + 1.6L, giving U = 200 kips and 440 kips for the two loading cases.

Concrete Strengths. Two concrete strengths were considered, 3000 and 6000 psi.

3000 psi Concrete. Consider 3000 psi (20.7 MPa) concrete with a standard deviation of 450 psi (3.1 MPa), and a coefficient of variation = 0.15. From ACI Sec. 5.3.2.1, the required mean strength, $f_{cr}' = 3000 + 1.34 \times 450 = 3600$ psi. FIP defines concrete strength using the characteristic or 5th %ile strength, f_{ck}, which is a lower fractile than used in ACI to define f_c'. For concrete with an ACI specified strength of 3000 psi,

$$f_{ck} = 3600\,(1 - 1.645 \times 0.15) = 2710 \text{ psi (18.7 MPa)}.$$

The design strength for uniaxial compression from FIP is:

$$f_{1cd} = \alpha \times \frac{f_{ck}}{\gamma_c} \tag{8}$$

where $\alpha = 0.85$ is similar to the $\alpha_1 = 0.85$ in ACI 10.2.7.1 and Eq. 4, and γ_C is a resistance factor for concrete, equal to 1.5. For $f_c' = 3000$ psi:

$$f_{1cd} = \frac{0.85 \times 2710}{1.5} = 1540 \text{ psi}$$

6000 psi Concrete. Consider 6000 psi (41.4 MPa) concrete with a standard deviation of 600 psi (4.14 MPa), and a coefficient of variation = 0.10. From ACI Sec. 5.3.2.1, the required mean strength, $f_{cr}' = (6000 + 2.33 \times 600) - 500 = 6900$ psi. The FIP uses the 5th % fractile strength, $f_{ck} = f_{cr}'(1 - 1.645 \times 0.10) = 5760$ psi (39.8 MPa). From Eq. 8 the design strength for uniaxial compression from FIP is $f_{1cd} = 3260$ psi.

In the FIP Recommendations, the strength of the concrete in a strut is taken as the smaller of

$$f_{cd,eff} = \nu_1 f_{1cd} \tag{9}$$

or

$$f_{cd,eff} = \nu_2 f_{1cd} \tag{10}$$

where Eq. 9 is applicable only in the compression zones for beams or axially loaded columns that are assumed to be uniformly stressed with $f_{cd,eff} = \nu_1 f_{1cd}$ acting over the distance c from the neutral axis to the extreme compression fiber. Because this locates the resultant compression force at c/2 from the extreme compression fiber, rather than at a/2 as assumed in the ACI Code rectangular stress block, values of $f_{cd,eff}$ based on ν_1 will not be considered.

FIP defines ν_2 in Eq. 10 using the following descriptions:

5.3.2(3) a) *Uncracked struts with uniform strain distribution.* $\nu_2 = 1.00$.
For 3000 psi concrete, $f_{cd,eff}$ is 1.00 x 1540 psi = 1540 psi and, for $\phi_{STM} = 0.85$, β_s ranged from 0.76 to 0.83 for the 1999 load factors and $\phi_{STM} = 0.85$. For the 2002 load and resistance factors β_s ranged from 0.77 to 0.86 .

5.3.2(3) b) *Struts with cracks parallel to the strut and bonded transverse reinforcement*; The reduction in strut strength is due to the transverse tension and to the disturbances by the reinforcement and the irregular crack surfaces. FIP gives $\nu_2 = 0.80$. For the 1999 ACI load factors α_1 v β_s $\phi = 0.75$, and the values of β_s ranged from 0.61 to 0.63. For the 2002 load and ϕ factors, the range was 0.64 to 0.66.

5.3.2(3) c) *Struts transferring compression across cracks with normal crack widths, e.g. in webs of beams.* FIP gives $\nu_2 = 0.60$. For 1999 Code load and ϕ factors, β_s ranged from 0.46 to 0.50. For the 2002 load and resistance factors, the range was 0.46 to 0.52.

5.3.2(3) d) *Struts transferring compression across large cracks, as e.g. in members with axial tension or in tension flanges.* FIP gives $\nu_2 = 0.45$. For 3000 psi concrete, the corresponding values of β_s ranged from 0.34 to 0.37 for the 1999 Code. For the 2002 Code the range is 0.35 to 0.39.

These values are listed in Table 1 for comparison with values of β_s derived from other codes, and those proposed for Appendix A. Because the verbal descriptions used in ACI Appendix A differ from those given in the FIP Recommendations, some FIP cases and ACI cases overlap and are listed two or more times.

Canadian Concrete Design Code and AASHTO LRFD Specification. These two codes define f_{cu} based on transverse tensile strains in the struts. One definition of f_{cu} is assumed to apply for all types of struts.

In the Canadian code [CSA(1994)] design is carried out using a factored concrete strength $\phi_c f_c'$ and a factored steel strength $\phi_s f_y$ where $\phi_c = 0.60$ and $\phi_s = 0.85$. The strength of concrete is defined in the same way as in ACI 318. The load factors in the Canadian Code are U = 1.25D + 1.5L. The effective compressive strength of the concrete in struts is:

$$f_{cu} = \frac{f_c'}{0.80 + 170\varepsilon_1} \le 0.85 f_c' \tag{11}$$

where

$$\varepsilon_1 = \varepsilon_s + (\varepsilon_s + 0.002)\cot^2\theta_s \tag{12}$$

ε_s = tensile strain in the tie.

θ_s = the smallest angle between the axis of the compressive strut and the axis of the tie attached to one end of the strut.

In the strut-and-tie model in Fig. 1, the strut is anchored by the longitudinal tie and is crossed by stirrups or minimum reinforcement. Here, θ_s is taken as the angle between the axis of the strut and the tie which is limited in ACI Sec. A.2.5 to 25° and by implication to to an upper limit of 90 – 25 = 65° relative to the tie. The stirrups and minimum surface reinforcement are ignored when computing θ_s and ε_1.

TABLE 1—Values of β_s for Struts in Strut-and-Tie Models. $\phi f_{cu} = \phi_{STM} \alpha_1 \beta_s f_c'$

Case	Code	β_s for $\phi = 0.85$, $\alpha_1 = 0.85$, 1999 load factors		β_n for $\phi = 0.75$, $\alpha_1 = 0.85$, 2002 loads factors	
		Values	Chosen	Values	Chosen
A.3.2.1—Struts in which the area of the mid-strut cross section is the same as that at the nodal zones, such as the compression zone of a beam.	**ACI App. A**		**1.0**		**1.0**
• Uncracked strut with a uniform strain distribution, $\nu_2 = 1.00$	FIP 5.3.2(3)a)	0.76-0.83		0.77–0.86	
• Compression zone in a beam	ACI 10.2.7	1.06		1.20	
• Compression zone in a tied column	ACI Chapter 10	0.82		0.87	
A.3.2.2—Struts located such that the width of the mid-section of the strut is larger than the width at the nodal zones (Bottle-shaped struts)	**ACI App. A**		**0.75**		**0.75**
(a) with reinforcement satisfying A.3.3					
• Struts with cracks and bonded transverse reinforcement, $\nu_2 = 0.80$	FIP 5.3.2(3)b)	0.61-0.66		0.61-0.69	
• Struts transferring compression across cracks of normal width, $\nu_2 = 0.6$	FIP 5.3.2(3)c)	0.46-0.50		0.46-0.52	
• Struts in STM's of post-tensioned anchorage zones	ACI 18.13	0.82 λ			
• Struts crossed by reinforcement at an angle θ with the axis of the strut	CSA $\theta = 60°$ $\theta = 45°$ $\theta = 30°$	0.683 0.513 0.293			
• Back calculated from tests of one and two span deep beams	Ref. 21	0.95			

TABLE 1—(Continued)

Case	Code	β_s for $\phi = 0.85$, $\alpha_1 = 0.85$, 1999 load factors		β_n for $\phi = 0.75$, $\alpha_1 = 0.85$, 2002 loads factors	
		Values	Chosen	Values	Chosen
(b) without reinforcement satisfying A.3.3	**ACI App. A**		**0.60 λ**		**0.60 λ**
• Struts transferring compression across cracks of normal width, $\nu_2 = 0.60$	FIP 5.3.2(3)c)	0.46-0.50		0.46-0.52	
A.3.2.3—Struts in tension members, or the tension flanges of members	**ACI App. A**		**0.40**		**0.40**
• Struts transferring compression across large cracks	FIP 5.3.2(3)d)	0.34-0-0.37		0.35-0.39	
A.3.2.4—For all other cases	**ACI App. A**		**0.60**		**0.60**

For $\theta_s = 60°$ and $\varepsilon_s = \varepsilon_y = 0.002$, Eq. 11 from the Canadian Code [CSA(1994)] gives $f_{cu} = 0.73 f_c'$.

For $\theta_s = 45°$ and $\varepsilon_s = 0.002$, Eq. 11 gives $f_{cu} = 0.55 f_c'$.

For $\theta_s = 30°$., and $\varepsilon_s = 0.002$, $f_{cu} = 0.31 f_c'$.

Assuming $\phi f_{cu} = \phi_{STM} \alpha_1 \beta_s f_c'$, the values of β_s for these angles θ are 0.68, 0.51, and 0.29 respectively, based on $\alpha_1 = 0.85$ and $\phi_{STM} = 0.85$.

For strut-and-tie models, the AASHTO LRFD Specification [AASHTO(2002)] gives the following values of ϕ:

- for compression in strut-and-tie models . . . 0.70
- for compression in anchorage zones:
  - normal weight concrete 0.80
  - lightweight concrete 0.65

For strut-and-tie models of prestress anchorage zones AASHTO gives

$$f_{cu} = 0.7 \phi f_c'$$

except that, in areas where the concrete may be extensively cracked at ultimate due to other force effects, or if large inelastic rotations are expected, the factored effective compressive strength is limited to $0.6 \phi f_c'$.

Setting ϕf_{cu} equal to $\phi \alpha_1 \beta_s f_c'$ and neglecting differences in the load factors gives $\beta_s = 0.82$ and 0.71 for $\phi f_{cu} = 0.7 \phi f_c'$ and $0.6 \phi f_c'$, respectively, with $\alpha_1 = 0.85$.

5.3.4 Effective Concrete Strength of Struts - From Other Sections of ACI 318–99

The effective concrete strength of a strut is given as the product $\phi f_{cu} = \phi_{STM} \alpha_1 \beta_s f_c'$. It would be desirable that $\phi \nu f_c'$ agree with $\phi_{STM} \alpha_1 \beta_s f_c'$ for the following three cases to minimize the differences at the interface between B-regions designed using the traditional flexure and shear design theory, and D-regions designed using strut-and-tie models.

The Flexural Stress Block in Beams. For flexure by the 1999 ACI Code, $\phi_f = 0.90$, and $\alpha_1 = 0.85$, the flexural compressive force, C_u, acting on the height, $a = \beta_1 c$, of the rectangular stress block is:

$$C_{u,flex} = \phi_f \alpha_1 f_c' a b \qquad (13)$$

If we assume the compressive force in a strut-and-tie model of the same beam is also equal to C_u:

$$C_{u,STM} = \phi_{STM} \alpha_1 \beta_s f_c' a b \qquad (14)$$

Setting these equal and substituting $\phi_{STM} = 0.85$ we get $\beta_s = \phi_f / \phi_{STM} = 1.06$.

For the same case using $\phi_{STM} = 0.75$ and $\phi_f = 0.90$ from the 2002 ACI Code,

$\beta_s = 0.90/0.75 = 1.20$.

The Flexural Stress Block in Columns Failing in Compression. The ϕ factor for tied columns is $\phi_{tc} = 0.70$ and for spiral columns $\phi_{sc} = 0.75$. For the 1999 ACI Code, $\phi_{tc} \nu f_c' = \phi_{STM} \alpha_1 \beta_s f_c'$. The corresponding value of β_s is 0.70/0.85 = 0.82 for tied columns and 0.88 for spiral columns. This value for the compression zone in a tied column is lower than the value of β_s for the compression zone in a beam because the ACI ϕ factors for columns were arbitrarily set below the ϕ for flexure to account for the more serious and more brittle nature of column failures.

Prestressed Tendon Anchorage Zones--ACI 318-99 Section 18.13.4.2 In 1999, ACI 318 included a new Section 18.13 on tendon anchorage zones based in large part on strut-and-tie models. This revision used $f_{cu} = 0.7 \lambda f_c'$ and $\phi = 0.85$. Rewriting the expression for f_{cu} as $\phi f_{cu} = \phi_{STM} \alpha_1 \beta_s f_c'$ gives $\beta_s = 0.7 \lambda / \alpha_1 = 0.824 \lambda$.

5.3.5 Selection of f_{cu} for Struts for Appendix A

The values of f_{cu} presented in ACI Code Appendix A were chosen to satisfy four criteria:

(a) Simplicity in application.

(b) Compatibility with tests of D-regions, such as deep beams, dapped ends or corbels.

(c) Compatibility with other sections of ACI 318.

(d) Compatibility with other codes or design recommendations.

Because these four criteria lead to different values of f_{cu} for a given application, judgement was required in selecting the values of f_{cu}.

Values of β_s are summarized in Table 1. The bold headings numbered A.3.2.1 through A.3.2.4 are the descriptions of the types of struts used in Appendix A of ACI 318-02. Values of β_s for related cases from other documents are also listed in each section. Two different methods of specifying f_{cu} are given in the various codes cited: (a) FIP uses descriptions of the cracking of the struts to select the applicable values of ν. (b) CSA and AASHTO base f_{cu} on Eqs. 11 and 12 which require ε_s to be computed. The first option depends on finding unambiguous descriptions of the state of cracking in the member. The second, depends on being able to compute a poorly defined strain in the web of the member. In Appendix A, the first option, verbal descriptions was adopted. The italicized words in the following paragraphs are directly from ACI 318-02.

A.3.2.1 For a strut of uniform cross-sectional area over its length, ... $\beta_s = 1.0$.

Table 1 lists values of β_s ranging from 0.76 to 1.20 for related cases. β_s was taken equal to 1.0, or $\beta_s = 0.85$ has been proposed to correspond to the rectangular stress block for flexure. In making this choice, evidence of β_s approaching 1.0 in tests was also strongly weighted.

A.3.2.2 For struts located such that the width of the mid-section of the strut is larger than the width at the nodes (bottle-shaped struts):

(a) with reinforcement satisfying A.3.3 . . . . . $\beta_s = 0.75$.

Other codes give β_s ranging from 0.46 to 0.824. The CSA code values are based on a different concept and will be disregarded. Experiments gave β_s as high as 0.94.

(b) without reinforcement satisfying A.3.3. . . . . . $\beta_s = 0.60\,\lambda$

The term λ for cracking of lightweight concrete was included in the β_s value for A.3.2.2(b) because the stabilizing effect of reinforcement transverse to the struts is not present and failure is assumed to occur shortly after cracking.

A.3.2.3 For struts in tension members or tension flanges of members. $\beta_s = 0.40$.

The similar case from FIP corresponds to $\beta_s = 0.34$ to 0.37.

A.3.2.4 For all other cases. . . . . . $\beta_s = 0.60$

The selected values of β_s are generally higher than those from other codes because more weight was given to values of f_{cu} corresponding to related design cases in the ACI Code and values of f_{cu} from tests, than was given to f_{cu} from other codes.

6 Nodes and nodal zones

6.1 Classification of nodes and nodal zones

It is desirable to distinguish between nodes and nodal zones. *Nodes* are the points where the axial forces in the struts and ties intersect, and *nodal zones* are the regions around the joint areas in which the members are connected. For vertical and horizontal equilibrium at a node, there must be a minimum of three forces acting on the node in a planar structure like a deep beam.

Nodes are classified by the types of forces that meet at the node. Thus a C-C-C node anchors three struts, a C-C-T node anchors two struts and one tie, a C-T-T node anchors one strut and two ties. Appendix A assumes the faces of the nodal zone that are loaded in compression have the same width as the ends of the struts. The width of the faces anchoring ties will be discussed more fully in Sec. 7.1.

6.2 Types of nodal zones and their use in strut-and-tie models

The literature on nodes in strut-and-tie models is based on two quite different concepts.

Hydrostatic Nodal Zones. Originally, nodal zones were assumed to have equal stress on all in-plane sides. Because the Mohr's circle for the in-plane stresses acting on such nodal zones plots as a point, this class of nodes was referred to as *hydrostatic nodal zones*. If the stresses were equal on all sides of the nodal zone, the ratio of the lengths of the sides of a hydrostatic nodal zone, w_{n1}: w_{n2}: w_{n3} are in the same proportions as the forces, C_1: C_2: C_3 acting on the sides.

Hydrostatic nodal zones were extended to C-C-T or C-T-T nodes by assuming the ties extended through the nodal zones to be anchored on the far side by hooks or bond on the tie reinforcement beyond the nodal zone. This concept is represented using a *hypothetical* anchor plate behind the joint. The area of the hypothetical anchor plate is chosen so that the bearing pressure on the plate was equal to the stresses acting on the other sides of the nodal zone. The effective area of the tie is the tie force divided by the permissible bearing stress for the struts meeting at a node. The requirement for equal stresses on all faces of a hydrostatic nodal zone tends to complicate the use of such nodal zones.

Extended Nodal Zones. These are nodal zones bounded by the outlines of the compressed zones at the intersection of:

(a) the struts,

(b) the reactions, and

(c) the assumed widths of ties including a prism of concrete concentric with the ties.

This is illustrated in Fig. 4(a) where the darker shaded area is the hydrostatic nodal zone and the total shaded zone is the extended nodal zone. The extended nodal zone falls within the area stressed in compression due to the reactions and struts. The compression stresses assist in the transfer of forces from strut to strut, or strut to tie. In general, Appendix A uses extended nodal zones in place of hydrostatic nodal zones.

Relationships between the dimensions of a nodal zone. Equations can be derived relating the widths of the struts, ties, and bearing areas if it is assumed that the stresses are equal in all three members meeting at a C-C-T nodal zone.

$$w_s = w_t \cos\theta + \ell_b \sin\theta \qquad (15)$$

where w_s is the width of the strut, w_t is the effective width of the tie, ℓ_b is the length of the bearing plate, and θ is the angle between the axis of the strut and the horizontal axis of the member. This relationship is useful for adjusting the size of nodal zones in a strut-and-tie model. The strut width can be adjusted by changing w_t or ℓ_b, one at a time. Once this has been done, it is necessary to check the stresses on all the faces of the nodal zone. The accuracy of Eq. 15 decreases as the stresses on the sides become more and more unequal. Equation 15 was included in Fig. 4 (ACI Fig. RA.1.6), but not in the code itself. Future code committees should consider adding such equations to the Commentary.

Resolution of forces acting on nodal zones. If more than three forces act on a nodal zone in a two-dimensional structure, it is frequently necessary to resolve some of the forces to end up with three intersecting forces. Alternatively, the nodes in the strut-and-tie model acted on by more than three forces could be analyzed assuming that all the strut and tie forces act through the node, with the forces on one side of the nodal zone being resolved into a single resultant strut during the design of the nodal zone. This concept is illustrated in ACI Commentary Fig. RA.2.3.

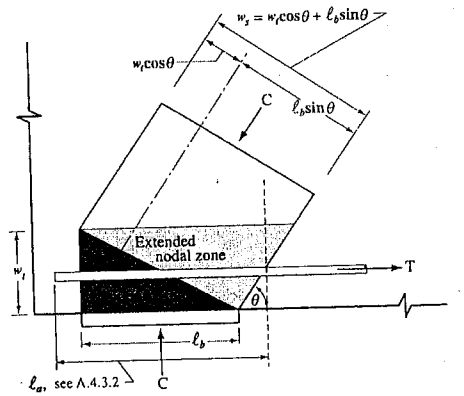

(a) One layer of steel

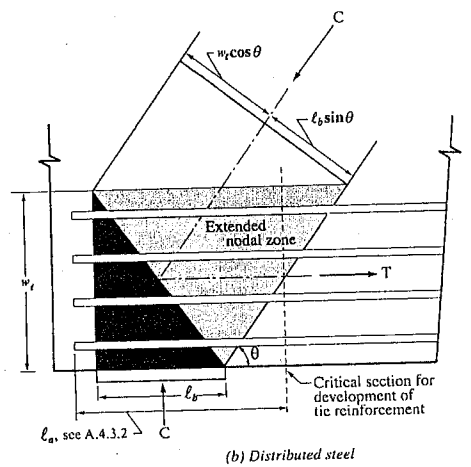

(b) Distributed steel

Fig. 4: An extended nodal zone.

6.3 Effective compressive strength of nodal zones

6.3.1 Effective compressive strength of nodal zones from tests

Very few tests of the strength of nodal zones are available. Tests of ten isolated C-C-T and nine C-T-T nodal zones reported by Jirsa et al. (1991) indicate that $f_{cu} = 0.80f_c'$ can be developed in such nodal zones if properly detailed For C-C-T nodal zones the average test / calculated strengths were 1.17 with a standard deviation of 0.14. For C-T-T nodal zones the mean test / calculated strength was 1.02. Assuming $\phi = 1.0$ for comparison with the strength of test specimens and $\alpha_1 = 0.85$, this corresponds to $\beta_n = 0.94$.

6.3.2 Effective compressive strength of nodal zones from other codes

6.3.2.1 FIP Recommendations "Practical design of structural concrete"

The FIP Recommendations limit f_{cu} on nodal zones to the following values:

- for node regions anchoring one or more ties: *0.85 f_{1cd} where f_{1cd} is given by Eq. 8. For $\alpha_1 = 0.85$ and $\phi_{STM} = 0.85$ this corresponds to $\beta_n = 0.65$ to 0.71.*
- for biaxially- or triaxially-loaded C-C-C nodal zones anchoring only struts:
  - biaxial stress state: up to 1.20 f_{1cd} *($\beta_n = 0.91$)*
  - triaxial stress state: up to 3.88 f_{1cd} *($\beta_n = 2.9$)*

6.3.2.2 Canadian Code and AASHTO LRFD Specification

The Canadian Code (1994) defines the effective compressive strength of nodal zones, ϕf_{cu}, as:

- for nodal zones loaded by compressive struts and bearing areas: $0.85 \phi_c f_c'$
- for nodal zones anchoring only one tie: $0.75 \phi_c f_c'$
- for nodal zones anchoring more than one tie: $0.65 \phi_c f_c'$,

where $\phi_c = 0.60$ in the Canadian code.

The β_n values are intended to reflect the weakening effect of the discontinuity of strains introduced when ties stressed in tension are anchored in a node stressed in compression. The values from the Canadian code are equivalent to β_n equal to 0.80, 0.70 and 0.61 in ACI.

The AASHTO LRFD Specification uses similar values of ϕf_{cu}.

6.3.3 Selection of the Effective Compression Strength of Nodal Zones, f_{cu}.

The values of f_{cu} for nodal zones from other codes are summarized in Table 2.

For the 1999 Code, the strength reduction factor for nodal zones was taken as $\phi_{STM} = 0.85$. The effective compressive strength, f_{cu}, will be based on the AASHTO and CSA values, modified to agree with the ACI load factors, the α_1 factor, and $\phi_{STM} = 0.85$ using Eq. 4.

The following values were selected for inclusion in the 2002 ACI Code:

- for C-C-C nodal zones bounded by compressive struts and bearing areas $\beta_n = 1.0$
- for C-C-T nodal zones anchoring only one tie $\beta_n = 0.80$
- for C-T-T or T-T-T nodal zones anchoring ties in more than one direction $\beta_n = 0.60$.

Table 2 shows these are a reasonable fit to the β_n values for each type of nodal zone.

7 Ties

7.1 Ties in strut-and-tie models

In strut-and-tie models based on hydrostatic nodal zones, the tie reinforcement is spread over the height of the tie computed as

$$w_t = \frac{F_u / \phi}{f_{cu} b_w} \qquad (16)$$

The tie is assumed to consist of the reinforcement and a hypothetical prism of concrete concentric with the axis of the tensile force. Thus, ACI Sec. A.4.2 requires the tie reinforcement to be distributed approximately uniformly over the width of the tie, w_t. This may entail putting the reinforcement in several layers as shown in Fig. 4(b), rather than concentrating it near the tension face of the beam as shown in Fig. 4(a).

If extended nodal zones are being used, the lower extreme value of the height of the tie corresponds to the steel being placed in one layer with w_t taken equal to the diameter of the bars plus twice the cover to the bars as in Fig. 4(a). (See also Section RA.4.2 of the Commentary to Appendix A.)

7.2 Strength of ties

A non-prestressed tie is assumed to reach its capacity when the force in the tie reaches

$$T_n = A_s f_y \qquad (17)$$

A second term is added for prestressed ties, ACI Eq.A–6 assumes Δf_p equals 60 ksi. This is a reasonable approximation to the change in stress in the prestressed reinforcement as a member is loaded to failure. Generally the major problem in the design of ties is the anchorage of a tie in a nodal zone. The hypothetical concrete prism concentric with the tie does not resist any of the tie force. In serviceability checks the reduced strain in the tie due to this concrete may reduce the elongation of the tie, leading to less deflection of the member.

Table 2: Recommended values of β_n for nodal zones in strut-and-tie models, $\phi = 0.85$ and 1999 load factors and $\phi = 0.75$ and 2002 load factors $\phi f_{cu} = \phi\, \alpha_1\, \beta_n\, f_c'$

Case	Code	Range of β_n	β_n[1] and 1999 Load Factors	Range of β_n	β_n[2] and 2002 Load Factors
C-C-C Nodal zones • Nodal zones anchoring only compression struts.	CSA A23.3 FIP	0.79 - 0.80 0.91 - 1.00	**1.0**	0.76-0.83 0.92-1.03	**1.0**
C-C-T Nodal zones • Nodal zones anchoring one or more ties.	CSA A23.3 FIP	0.70-0.71 0.65 - 0.71	**0.80**	0.67-0.73 0.65-0.73	**0.80**
C-T-T Nodal zones • Nodal zones anchoring one or more ties.	CSA A23.3 FIP	0.61 0.65 - 0.71	**0.60**	0.58-0.63 0.65-0.73	**0.60**
Tests of Nodal zones $\phi = 1.0$ for tests.	Ref. 15	0.94			

Notes: [1] The first set of recommended values of β_n are for use with the 1999 load factors assume $\alpha_1 = 0.85$ and $\phi_{STM} = 0.85$.

[2] The second set of recommended values of β_n are for use with the 2002 load factors assume $\alpha_1 = 0.85$ and $\phi_{STM} = 0.75$.

7.3 Anchorage of ties

ACI Secs. A.4.3.1, A.4.3.2 and A.4.3.3 require that the anchorage of the tie forces be achieved completely by the time the geometric centroid of the bars in a tie leaves the extended nodal zone. This point is shown in Fig. 4. Hooks or mechanical anchorages may be required. ACI Section A.4.3 itemizes other requirements for anchoring ties. At nodal zones in beam-like structures where diagonal struts are anchored by stirrups, the change in the tie forces at the truss node must occur within the width of the nodal zone.

8 Reinforcing Requirements

8.1 Effect of minimum confinement reinforcement from tests

Grids of reinforcement are desirable in the side faces of D-regions to restrain the splitting cracks near the ends of bottle-shaped struts, and to give some ductility to the struts.

Three, two-span continuous deep beams tested by Rogowsky (1983) and Ricketts (1985), with clear shear span to depth ratios of 0.8 with vertical stirrups giving a stirrup reinforcement ratio, ρ_v, of 0.0015 and no horizontal web reinforcement, failed after the positive moment (bottom) reinforcement yielded but before the top steel did, and as a result, these two beams did not develop their full plastic load capacity. This ρ_v did not allow adequate moment redistribution.

Three similar beams with vertical stirrup ratios in the order of 0.0035, again without horizontal web reinforcement, had varying distributions of flexural reinforcement. In these beams the relative amounts of top and bottom steel from an elastic analysis of a slender beam were 4 top bars and 3 bottom bars. The three beams varied the amounts of top and bottom bars from 2 top bars and 5 bottom bars, 4 top and 3 bottom bars in the second beam, and 5 top and 2 bottom bars in the third. All three beams failed after both top and bottom steel yielded. This required some moment redistribution. The trends from these tests and others with varying web reinforcement ratios suggested that in beams with vertical stirrups only, the full plastic capacity would be reached with a stirrup reinforcement ratio of 0.0025.

8.2 Minimum reinforcement required in bottle-shaped struts.

ACI Secs. A.3.2.2(a) and (b) allow the use of $\beta_s = 0.75$ when computing the effective compression strength of bottle-shaped struts with reinforcement satisfying ACI Sec. A.3.3. The value of β_s drops to $0.60\,\lambda$ if this reinforcement is not provided. ACI Sec. A.3.3 requires reinforcement transverse to the axis of the strut proportioned to resist the tensile force lost when the strut cracks due to the lateral spread of the strut forces. ACI Sec. A.3.3 allows the designer to compute the necessary steel either from an assumed localized strut-and-tie model of the strut as shown in Fig. 3(b), or, for beams with a concrete strength of 6000 psi or less,

ACI Sec. A.3.3.1 allows the results of the strut-and-tie model to be approximated using the empirical equation, Eq. A–4. This equation was derived assuming the normal stress, σ_1, acting on the crack resulting from a layer of confinement steel is

$$\sigma_1 = \frac{A_{s1} f_{s1}}{b s_1} \sin \gamma_1 \qquad (18)$$

where A_{s1} is the area of the bars in one direction and the angle γ_1 is the angle between the crack and the component of the force in the bar in question. The direction of the bar is chosen so that a tensile bar force in the bar causes a compressive force in the concrete perpendicular to the crack. It has been written without the term f_{si} to simplify the presentation.

A.3.3.1 allows this requirement to be satisfied using layers of steel crossing the strut which satisfy

$$\Sigma \frac{A_{si}}{b s_i} \sin \gamma_i \geq 0.003 \qquad (19)$$

where A_{si} is the total area of reinforcement at a spacing s_i in a layer of bars at an angle γ_i to the axis of the strut. ACI Sec. A.3.3.1 states that this steel generally is placed in grids in two orthogonal directions in each face, but allows it to be placed in one layer in cases such as corbels.

8.3 Minimum shear reinforcement in deep beams

There is a major discontinuity in the amount of shear reinforcement required at the limit between the deep beams and shallow beams in the 1999 and earlier codes. The FIP Recommendations (1998) provide a transition from a D-region to a B-region for a/d ratios close to the limit of 2. For shear spans with a/z between 0.5 and 2, where z = jd is the internal lever arm between the resultant tensile and compressive forces in flexure, FIP requires that a portion, V_2, of the total shear, V, on the shear span be transferred to the supports by an inclined strut, and the rest, V_1, = V – V_2, be transferred by vertical web reinforcement.

For a/z between 0.5 and 2.0, the amount V_1 is given by:

$$V_1 = V \frac{\left(\frac{2a}{z} - 1\right)}{3} \qquad (20)$$

At the limits, a/z = 0.5 and 2.0, this equation gives $V_1 = 0$, and $V_1 = V$. Thus, for a/z = 0.5, FIP recommends that all of the shear V be transferred by the inclined strut, and for a/z = 2, FIP recommends that all the shear should be resisted by stirrups. This, or a similar provision, should be considered by ACI Committee 318 Sub E as a possible addition to Appendix A. Such a provision prevents strut-and-tie models with struts which are at too small an angle with the longitudinal axis of the member. ACI Sec. A.2.5 limits the angle to 25° for the same reason.

8.4 Minimum web reinforcement from codes

• The 1994 CSA Code requires an orthogonal grid of reinforcing bars near each face with a ratio of total steel area to gross concrete area in each direction of at least 0.002. This is referred to as crack control reinforcement. The portion of this reinforcement parallel to a tie and located within the assumed cross-sectional area of the tie can be considered as part of the tie reinforcement.

• AASHTO (2002) has similar requirements to CSA but the minimum total reinforcement ratio is set at 0.003 in each direction. The Commentary to the AASHTO LRFD Specification states that, in thinner members, there should be a grid of bars at each face, while for thicker members it may be necessary to have multiple grids throughout the thickness.

• The FIP Recommendations (1999) suggest that deep beams should have a minimum reinforcement ratio of 0.001 in each direction, in each face, for a total of not less than 0.002 each way.

• Sections 11.8.4 and 11.8.5 of ACI 318-99 require minimum ratios of vertical and horizontal web reinforcement of $0.0015b_ws$ and $0.0025b_ws_2$, respectively in deep beams.

These minimum amounts provide a considerable shear capacity. Each $0.0010b_ws$ of vertical web reinforcement corresponds to a shear stress resistance, V_s corresponding to v = 60 psi, calculated using ACI Eq. 11–15. Horizontal web reinforcement is much less efficient in transferring shear. The additional capacity provided by the vertical web reinforcement is not implicitly included in the strength calculation using ACI Eqs. A–1 and A–2. It is accounted for by the increase in β_s.

For some D-regions, such as those in a deep beam, it is feasible to provide orthogonal grids of steel near the side faces of the deep beam. In other cases, such as corbels or dapped ends, it is easier to place the web steel in one direction, horizontal in the case of a corbel. ACI Sec. A.3.3.2 allows uni-directional confining steel in corbels or similar cases. If in one layer, the steel is placed in one direction at an angle of at least 40° with the axis of the strut.

In some structures, such as pile caps for more than two piles, it is frequently not feasible to place web steel in the three-dimensional strut-and-tie model. A reduced strut strength is imposed by ACI Sec. A.3.2.2(b) in such cases.

8.5 Selection of minimum web reinforcement.

The two structural functions of minimum web steel in a D-region are to resist the transverse tension in the bottle-shaped areas near the ends of the strut after splitting cracks occur, and to provide ductility to the struts and nodal zones by confinement. The minimum steel was given in Eq. A– 4 in terms of equivalent amounts perpendicular to the axis of the strut.

In the Rogowsky (1983) and Ricketts (1985) tests quoted earlier, the full plastic capacity was obtained with a ratio of vertical steel equal to 0.0035.

These beams did not have horizontal web steel. The strut-and-tie model of the failure region indicated that the critical strut had a slope of about 55°. with the vertical steel.

The critical web steel ratio taken perpendicular to the strut is $\rho_v \sin\gamma$, where γ is the angle between the reinforcement and the axis of the strut. In the Rogowsky and Ricketts tests quoted above, γ was 55°, and the steel area provided was equivalent to

$$\Sigma \frac{A_{si}}{bs_i} \sin\gamma_i = 0.0029$$

In design this crack restraint is achieved by providing minimum web steel satisfying:

$$\Sigma (\rho_{vi} \sin\gamma_i) \geq 0.003 \qquad (21)$$

where ρ_{vi} is the reinforcement ratio for web reinforcement at an angle γ_i to the axis of the strut.

8.6 Comparison of strut-and-tie models to tests of deep beams.

A range of test results were considered in developing the ACI Code provisions for strut-and-tie models as reported in Section 5.3.2 of this paper. In addition, the final code statements were compared to tests of each end of six simple-span, deep beams tested by Rogowsky and MacGregor (1986). These beams were relatively large, having overall depths of 500 to 1000 mm, and spans of 2000 mm, and a / d ratios of 1.03, 1.86 and 2.21.

Each beam was assumed to have five failure limit states, ranging from yield of the ties, to crushing of each end of each strut, and crushing of the nodal zones at each end of each strut. The strength of each shear span was taken to be the lowest of the five shear strengths for that shear span. The ratios of the lowest test/calculated shear strength ranged from 0.96 to 2.14, with an overall mean of 1.54, with a coefficient of variation of 0.247. The mean test/calculated ratios decreased from 2.0 for beams with a/d = 1.06, to 1.32 for beams with a/d = 2.0 This is reasonable agreement for shear test data. Further checks against test data are presented by D. Mitchell in another paper in this symposium.

9 Other details

9.1 Changes to 1999 ACI Code sections. 10–7.1 and 11–8

When strut-and-tie models were introduced, it was necessary to change the definitions of deep beams in 1999 ACI Code Secs. 10.7.1 and 11.8.1. The new definitions are based on the definition of deep beams in ACI 2002 Sec. A.1.

The 1999 and earlier ACI Code design equations for deep beams were based on the ($V_c + V_s$)approach to shear design. The 1999 Code Eqs. 11–29 and 11–30 for V_c and V_s were deleted, without replacements in Chap. 11, because these equations did not reflect the true behavior of deep beams. This is especially true for continuous deep beams where the moment approaches zero at the critical section defined in ACI Sec. 11.8.5. As a result, the second term on the right-hand side of ACI Eq. 11–29 for V_c approaches zero. In addition, there was a major discontinuity in the magnitude of V_s from 1999 ACI Eq. 11 – 30. At $\ell_n / d = 5.0$, the V_s provided by horizontal stirrups dropped step-wise from 0.5 $A_v f_y$ at $\ell_n / d = 4.99$ to zero at $\ell_n / d = 5.01$. In the same region, the V_s provided by vertical stirrups increased step-wise from 0.5 to 1.0 $A_v f_y$.

ACI Sec. 11.8, "Deep Beams" was shortened by omitting the these sections and design was permitted either by non-linear analysis or by strut-and-tie models.

9.2 Pile caps

Revisions were made to ACI Sec. 15.5.3 to allow the use of strut-and-tie models in the design of pile caps. In a pile cap the strut-and-tie model is three-dimensional. The nodal zones are also three-dimensional with the struts from the various piles converging on the nodal zone at the base of the column. Section A.5.3 is intended to simplify the design of three-dimensional strut-and-tie models by requiring that the individual faces of the nodal zone have the areas computed from Eq. A.—7, but not requiring an exact match between the shape of the end of the strut and the corresponding shape of the face of the nodal zone acted on by the strut, provided that enough bearing area is provided.

9.3 Serviceability

The last paragraph of RA.2.1 mentions serviceability. Deflections can be estimated using an elastic frame analysis of the strut-and-tie model. The axial stiffness of the ties can be modeled as cracked regions with axial stiffnesses of $A_s E_s / \ell_{cr}$ and uncracked regions with axial stiffnesses of $A_c E_c / \ell_{uncr}$, where ℓ_{cr} and ℓ_{uncr} are the portions of the length of tie which can be assumed to have a cracked section stiffness, and the fraction having an uncracked stiffness respectively. This allows the elongation of the tie to be modelled in a simple manner. Further study is needed in this area.

10 Summary

The development of Appendix A of the 2002 ACI Code and the selection of the ϕ factors and effective concrete strengths is explained. The layout of strut-and-tie models is reviewed.

11 Acknowledgements

ACI Code Appendix A was developed by ACI Committee 318, Subcommittee E, *Shear and Torsion*, chaired by J.O. Jirsa, who was succeeded as chair by J.K. Wight during the period in which the Appendix was letter balloted. Extensive assistance and a number of widely differing design checks were provided by ACI Committee 445–A, *Strut-and-Tie Models*, chaired by K-H Reineck. Design checks and comparisons to tests were carried out by members of ACI 445.A.. Appendix A was reviewed by ACI Committee 318 and approved over the course of four letter ballots.

12 Notation

The following notation is used in this paper:

w_{n1}, w_{n2}, w_{n3} = lengths of the sides of a nodal zone.

A_c = smaller end area of a strut.

A_v = area of vertical web reinforcement within a spacing s.

b_w = width of the web of a beam.

f_c' = specified concrete compressive strength.

$F_{cd\ eff}$ = strength of the concrete in a strut—FIP.

f_{cu} = effective compression strength of struts or nodal zones—ACI.

f_{1cd} = design concrete strength for uni-axial compression—FIP.

F_n, F_{nn}, F_{ns}, F_{nt} = nominal strength, the nominal strength of a nodal zone, the nominal strength of a strut, and the nominal strength of a tie.

F_u = force in a strut, tie, or node due to the factored loads.

jd = internal lever arm between the resultant compressive and tensile forces in a beam. from ACI Sec. 10.2.7.

s = spacing of vertical web reinforcement.

V_c = shear strength provided by concrete.

V_s = shear strength provided by stirrups.

w_t = height of a tie and its surrounding concrete.

z = internal lever arm between the resultant compressive and tensile forces in a beam.

α_1 = ratio of the average stress in the rectangular stress block to the concrete strength.

β_s, β_n = ratio of the design strength of the concrete in a strut or node to the specified strength.

ε_1 = principal tension strain in the concrete.

ε_2 = strain in a tie.

ϕ, ϕ_F, ϕ_V, ϕ_{STM} = strength reduction factor, strength reduction factors for flexure, for shear, for strut-and-tie models.

γ = angle from axis of strut and axis of a layer of confining reinforcement.

λ = correction factor for the strength of lightweight concrete.

ν = effectiveness factor.

ρ_v = reinforcement ratio for vertical web reinforcement $= \dfrac{A_v}{b_w s}$

13 References.

AASHTO (1998): *LRFD Bridge Specifications and Commentary*. 2nd Edition, American Association of Highway and Transportation Officials, Washington, 1998, 1216 pp.

ACI Committee 318 (2002): *Building Code Requirements for Structural Concrete* (ACI 318-02) *and Commentary* (ACI 318R-02). American Concrete Institute, Farmington Hills, MI, 2002, 443pp.

ACI Committee 445 (1997): *Strut-and-Tie Bibliography,* ACI Bibliography No. 16, 1997, 50 pp.

ACI ASCE Committee 445 (1998): *Recent approaches to shear design of structural concrete*. State-of-the-Art-Report by ASCE-ACI Committee 445 on Shear and Torsion. ASCE-Journ. of Struct. Eng. 124 (1998), No.12, 1375-1417 (see also ACI 445R-99, American Concrete Institute, Farmington Hills, MI (1999), 55 pp.)

Adebar, P. and Zhou, Z. (1993): *Bearing Strength of Compressive Struts Confined by Plain Concrete*. ACI Structural Journal, Vol. 90 (1993), No. 5, September-October 1993, pp 534-541.

Bergmeister, K., Breen, J.E. and Jirsa, J.O. (1991): Dimensioning of Nodal zones and Anchorage of Reinforcement, *Structural Concrete*. IABSE Colloquium Structural Concrete, Stuttgart, 1991, pp 551-564.

Breen, J.E.; Burdet, O; Roberts, C; Sanders, D; Wollmann, G: and Falconer, B. (1994): NCHRP *Report* 356, Transportation Research Board, National Academy Press, Washington, D.C.

Canadian Standards Association (CSA) (1994): A23.3-94, *Design of Concrete Structures*, Canadian Standards Association, Rexdale, Dec. 1994, 199 pp

CEB-FIP Model Code 1990 (1993): *Design of concrete structures*. Comité Euro-International du Beton, Thomas Telford Services Ltd., London, 1993, 437 pp

Collins, M P and Mitchell, Denis (1991): *Prestressed Concrete Structures*, Prentice Hall Inc., Englewood Cliffs, 1991, 766 pp

FIP Recommendations (1999): *Practical Design of Structural Concrete*. FIP-Commission 3 "*Practical Design*", Sept. 1996. Publ.: SETO, London, Sept. 1999. (Distributed by: *fib*, Lausanne)

Ibrahim, Hisham H.H. and MacGregor, James G. (1997): *Modification of the ACI Rectangular Stress Block for High-Strength Concrete*. ACI Structural Journal Vol. 94 (1997), No. 1, Jan. - Febr. 1997, pp 40-48

Jirsa, J.O., Bergmeister, K., Anderson, R., Breen, J.E., Barton, D., and Bouadi, H. (1991): *Experimental Studies of Nodes in Strut-and-Tie Models*. Structural Concrete, IABSE Colloquium Structural Concrete, Stuttgart, 1991, pp 525-532

Kriz, L.B. and Raths, C.H. (1965): *Connections in Precast Concrete Structures: Strength of Corbels*. PCI Journal, Vol. 10 (1965), No. 1, 1965, pp 16-47

MacGregor, J.G. (1997): *Reinforced Concrete: Mechanics and Design*, 3rd Edition. Prentice Hall, 1997, 939 pp

Marti, P. (1985): *Basic Tools of Reinforced Concrete Beam Design*. ACI Journal, Vol. 82 (1985), No. 1, Jan.-Feb. 1985, pp 46-56

Ramirez, J.A. and Breen, J.E. (1991): *Evaluation of a Modified Truss-Model Approach for Beams in Shear*. ACI Structural Journal, Vol. 88 (1991), No. 5, September-October 1991, pp 562-571

Ricketts, D. (1985): *Continuous Reinforced Concrete Deep Beams*. M.Sc. Thesis, University of Alberta, Edmonton, 1985

Rogowsky, D.M. and MacGregor, J.G. (1986): *Design of Deep Reinforced Concrete Continuous Beams*. Concrete International: Design and Construction, Vol. 8 (1986), No. 8, August, pp 49-58

Rogowsky, D.M. (1983): *Shear Strength of Deep Reinforced Concrete Continuous Beams*. Ph.D. Thesis, University of Alberta, November 1983, 178 pp

Schlaich, J.; Schäfer, K.; Jennewein, M. (1987): *Toward a Consistent Design of Structural Concrete*. PCI Journal, Vol. 32 (1987), No. 3, May-June, p. 74-150

Vecchio, F.J.; Collins, M.P. (1982): *The Response of Reinforced Concrete to In-plane Shear and Normal Stresses*. Publication 82-03, Department of Civil Engineering, University of Toronto, Toronto, March 1982, 332 pp

Part 3: Experimental verification of strut-and-tie models

Denis Mitchell, William D. Cook, Claudia M. Uribe and Sergio M. Alcocer

Synopsis
Results of experiments on a corbel, deep beams and a beam with dapped ends are presented to illustrate how strut-and-tie models are applied to these cases and to provide some experimental verification of the accuracy of the predictions. Both simple strut-and-tie models, as well as refined strut-and-tie models are presented.

Denis Mitchell, FACI, is a professor in the Department of Civil Engineering at McGill University. He is a member of ACI Committees 408, Bond and Development of Reinforcement; 318B, Standard Building Code, Reinforcement and Development; and Joint ACI-ASCE Committee 445, Shear and Torsion. He chairs the Canadian Standard CSA A23.3 on the Design of Concrete Structures and the Canadian Highway Bridge Design Subcommittee on Seismic Design.

ACI member, **William D. Cook** is a Research Engineer in the Department of Civil Engineering at McGill University. He received his Ph.D. degree from McGill University in 1987, specializing in the behavior and design of regions near discontinuities in reinforced concrete members. His research interests include nonlinear analysis of reinforced concrete structures and the structural use of high-strength concrete.

Claudia M. Uribe is a former graduate research assistant in the Structural Engineering and Geotechnical Area at the National Center for Disaster Prevention (CENAPRED). She holds a B.Sc. degree from EAFIT, Medellin, Colombia and a M.Sc. degree from the National Autonomous University of Mexico (UNAM).

Sergio M. Alcocer, FACI, is a research professor at the Institute of Engineering of the UNAM and Director of Research at CENAPRED. He is a member of ACI Committees 318, Building Code Requirements, and 374, Performance Based Seismic Design of Concrete Buildings, as well as a member of Joint ACI-ASCE Committee 352, Joints and Connections in Monolithic Concrete Structures.

1 Introduction

Although truss models have been used since the turn of the century [Ritter (1899) and Mörsch (1909)], they have gained increased popularity in recent years. The reason for this increased popularity is that they provide the designer with a simple, yet powerful tool, for the design of complex regions in reinforced concrete. This increased popularity is due to the fact that the designer can model the flow of the forces with struts and ties, even for complex design situations. Thus, rather than using empirically based design approaches, the designer can apply a strut-and-tie model, which not only illustrates the flow of the forces, but also provides a clear understanding of the various resisting elements. Design approaches using strut-and-tie models have been codified in Appendix A of the 2002 ACI Code (2002), as well as in the 1984 and 1994 CSA Standards (1984, 1994) and the FIP Recommendations (1999). Design using strut-and-tie models provides an alternative to the empirically based code approaches for disturbed regions, such as brackets, corbels and deep beams. Empirically based approaches are not only limited in their applicability, but do not provide the designer with insight into the actual behavior. An additional advantage of using strut-and-tie models is that sketching the flow of the forces within a member highlights the need for careful details of the reinforcement in key regions. This paper illustrates some simple strut-and-tie models and compares these predictions with experiments. In selecting the experiments only well-instrumented, full-size tests were chosen. Walraven and Lehwalter (1994) have summarized the importance of size effects not only for slender beams, but for deep beams as well. The testing of geometrically similar deep beams demonstrated that, compared to larger beams, smaller beams exhibit less severe crack propagation and as a result exhibit higher stresses for the crushing of the concrete near the bearing plates. Therefore, the response of small-scale specimens may not be representative of the response of actual structural elements.

2 Corbel

Figure 1 illustrates the strut-and-tie model for a double-sided corbel tested by Cook and Mitchell (1988). Figure 1(a) shows the details of the reinforcement and the dimensions of the test specimen. During testing, the corbel was subjected to a vertically applied load, V, and an outwards horizontal load that was kept equal to 0.2V. This horizontal force of 0.2V represented the minimum horizontal design force required in the ACI Code (Clause 11.9.3.4), unless special provisions are made to avoid tensile forces. The 50 mm·300 mm (2 in.·11.8 in.) bearing plate was 25 mm (1 in.) thick and was welded to four No. 15 (16 mm dia. (0.63 in.)) weldable grade bars. The concrete strength at the time of testing was 40.4 MPa (5860 psi). Figure 1(c) shows the strut-and-tie model for this corbel. This simplified model used the conservative assumption that only the main tie reinforcement contributed to the strength of the corbel. The forces shown in Fig. 1(c) are those resulting from yielding of the four No. 15 bars. The total yield force is $A_s f_y = 4 \cdot 200 \text{ mm}^2 \cdot 444 \text{ MPa} = 355 \text{ kN}$ (79.8 kips). In order to predict the capacity, it was necessary to find the geometry of the strut-and-tie model. While the ACI Code and CSA Standard do not recommend strut-and-tie models for different cases, the FIP Recommendations (1999) provide guidance on suitable strut-and-tie models for different types of regions. For a corbel, the inclined struts are equilibrated by vertical struts with dimensions of a_1 by b in the column and a horizontal strut with dimensions of a_2 by b near the bottom of the corbel (see Fig. 1(c)), where b is the width of the column and corbel. In solving for the geometry, a uniform stress of 0.85 f_c' was assumed in the stress blocks. From equilibrium, a_1 was calculated to be 39.2 mm (1.54 in.) and a_2 was 21.7 mm (0.85 in.). The corresponding predicted capacity, V, was 471 kN (106 kips) which is 94% of the measured failure load, V, of 502 kN (113 kips).

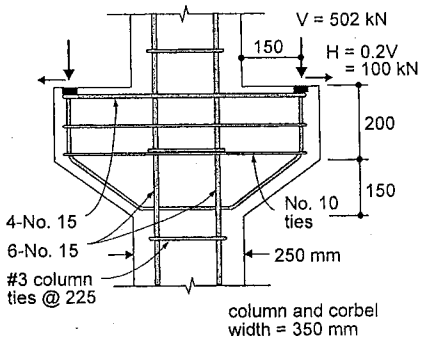

(a) Details

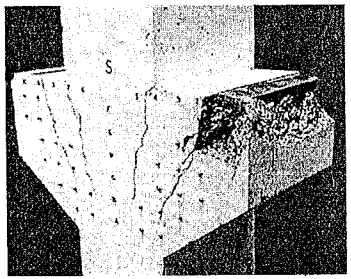

(b) Specimen after failure

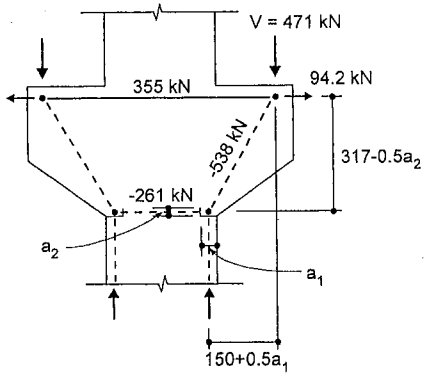

(c) Strut-and-tie model

Fig. 1: Double-sided corbel, tested by Cook and Mitchell (1988).

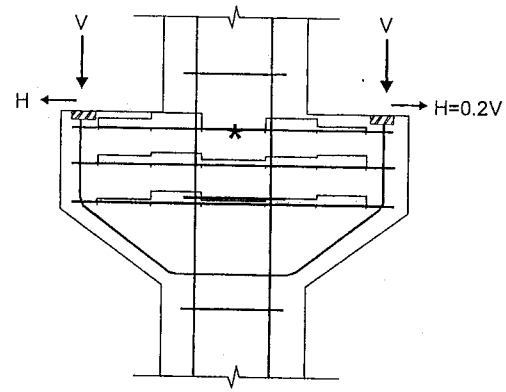

(a) Load, V = 336 kN

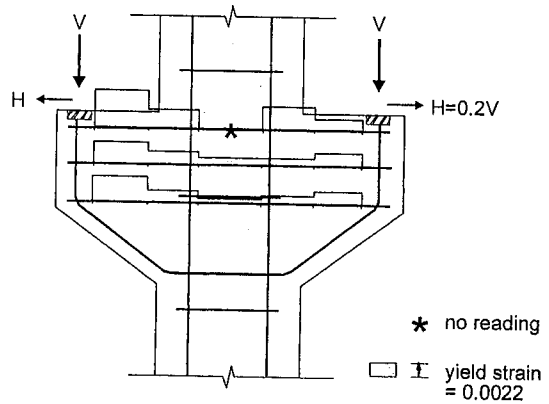

(b) Load, V = 502 kN

Fig. 2: Measured strains in reinforcing bars of double-sided corbel [Cook and Mitchell (1988)].

A small bearing plate was intentionally chosen for this test specimen to determine the crushing strength of the concrete under the bearing plate. In design, a larger bearing plate would typically be used. As shown in Fig. 1(b) there was considerable spalling of the concrete in the region around the bearing plate. At the predicted failure load of 471 kN (106 kips) the compressive stress at the node under the bearing plate was (471·1000)/(50·300) = 31.4 MPa (4550 psi), or $0.78f_c'$. The 2002 ACI Code limits this stress to $0.85\beta_n f_c' = 0.68f_c'$. The 1994 CSA Standard and the FIP Recommendations (1999) limit the nodal zone stress to $0.75f_c'$ and $0.80f_c'$, respectively, for this compression-tension node. It is clear that these limits are somewhat conservative for this particular case because a bearing stress of $0.83f_c'$ was reached at the failure load of 502 kN (113 kips).

In design, the main tie is often selected using such a simplified strut-and-tie model, and then additional reinforcement is added to control cracking. Clause 11.9.4 of the ACI Code requires that this additional reinforcement, with an area equal to $0.5\ (A_s\text{-}A_n)$ be provided by closed stirrups, uniformly distributed within two-thirds of the effective depth adjacent to A_s. The area, A_s, is the total area of the tie and A_n is the area of tension reinforcement resisting the horizontal tension applied to the corbel.

Figure 2 shows the measured strains obtained from a mechanical extensometer, measuring change of length on strain targets glued to the reinforcing bars. The measurements were taken on these targets through small access holes in the concrete cover. First yielding occurred in the main tie at the face of the column at a load, V, of 336 kN (75.5 kips) as shown in Fig. 2(a). Failure occurred by yielding of the main tie, as well as yielding in the stirrups, followed by crushing of the concrete under the bearing plate. Figure 2(b) shows the measured strains in the horizontal reinforcement just before failure. It is interesting to note that at failure the maximum strain in the main tie occurred close to the bearing plate. These experimental results emphasize the need to properly anchor the main tie at its ends. In this case, the loading plates were welded to the four No. 15 bars making up the main tie, providing the necessary anchorage (see Fig. 1(a)).

3 Deep beam subjected to concentrated load

Figure 3 illustrates the details and the strut-and-tie model for a deep beam tested by Rogowsky, MacGregor and Ong (1986). This 200 mm (7.9 in.) thick beam was supported on columns which were, in turn, supported on rollers. The shear span-to-depth ratio, a/d, was 1.4. The concrete strength at the time of testing was 42.4 MPa (6150 psi). The main tie reinforcement consisted of six No. 15 bars (16 mm dia. (0.63 in.)) having a total yield force, $A_s f_y = 6{\cdot}200\ \text{mm}^2{\cdot}455\ \text{MPa} = 546$ kN (123 kips). On the left side of the beam, the member contained additional reinforcement consisting of five sets of 6 mm (0.24 in.) diameter closed stirrups (see Fig. 3(a)). The reinforcement in the columns is not shown in Fig. 3(a). The failure of the beam was governed by yielding of the main tie reinforcement. The basic strut-and-tie model shown in Fig. 3(c) neglected the presence of the additional stirrups on the left side of the beam. The two lower nodes of the truss were located at the intersections of the centerlines of the support reactions and the line of action of the main tie. The equivalent rectangular stress block depth, a, required to equilibrate the yield force of the tie was 76 mm (3.0 in.). The top two nodes were located a distance of a/2 below the top surface of the beam and in line with the resultant forces in the column (assumed to act at the quarter points of the column). The predicted capacity of 586 kN (132 kips) is 97% of the actual capacity of 606 kN (136 kips). As expected, failure took place on the side without the stirrups. Figure 3(b) shows the crushing that took place in the concrete after yielding occurred in the main tie. Figure 3(d) shows the strains measured in the main tie reinforcement at two load levels. At a load of 550 kN (124 kips) the tie had experienced yielding along most of its length. The hooks at the ends of the tie reinforcement provided adequate anchorage of this steel. The strut-and-tie model and the measured strains illustrate the need to adequately anchor the tie yield force at the support reaction areas.

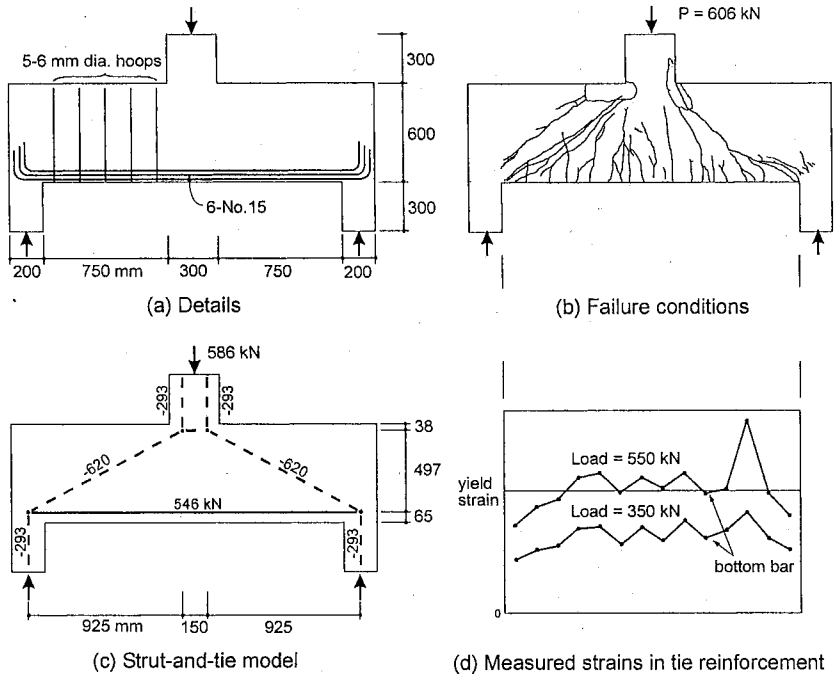

Fig. 3: Deep beam subjected to concentrated load, tested by Rogowsky, MacGregor and Ong (1986).

4 Deep beam subjected to uniform loading

Figure 4 shows a deep beam, loaded uniformly on the top, tested by Leonhardt and Walther (1966). This 100 mm (3.9 in.) thick beam was supported on 160 mm (6.3 in.) long bearing plates. The concrete strength (equivalent prism strength) at the time of testing was 30.2 MPa (4380 psi). The main tie reinforcement consisted of four 8 mm (0.32 in.) diameter reinforcing bars having a total yield force, $A_s f_y = 4 \cdot 50.26\ mm^2 \cdot 428\ MPa = 86.1\ kN$ (19.4 kips). The center-to-center span was 1440 mm (56.7 in.) and the uniform loading applied to the top of the beam was located over the clear span distance of 1280 mm (50.4 in.). Figure 4(c) shows a simplified strut- and-tie model suitable for design. In the strut-and-tie model, the uniform loading was replaced by two point loads at the quarter points of the clear span.

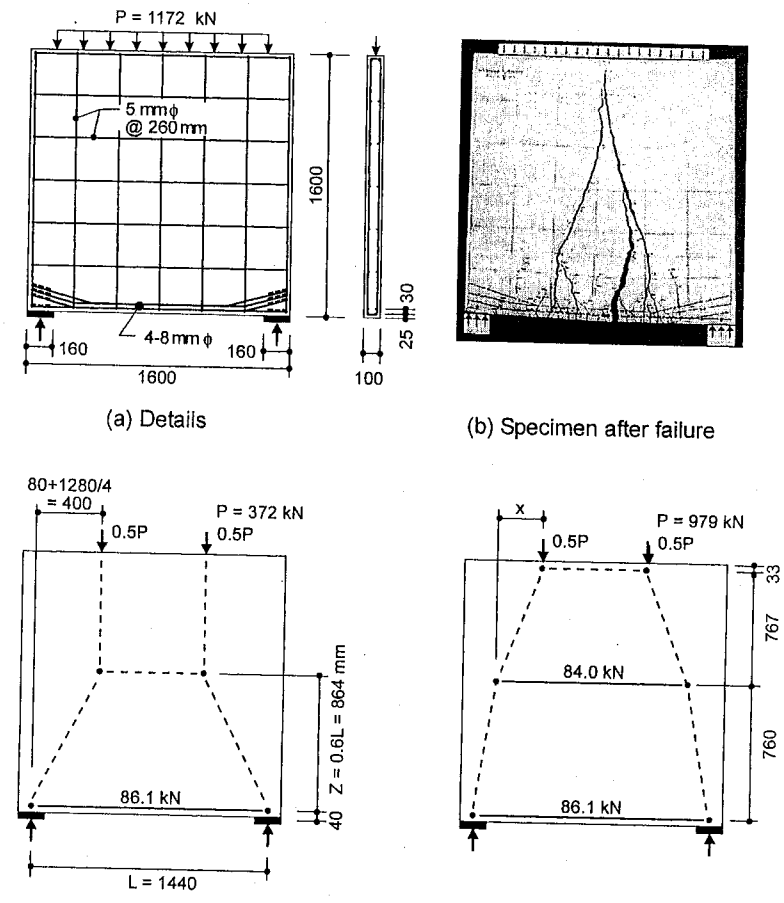

Fig. 4: Deep beam subjected to uniform loading, tested by Leonhardt and Walther (1966)

While the ACI Code and CSA Standard do not provide specific guidance on suitable strut-and-tie models for different cases, the FIP Recommendations provide suggested geometries for some standard disturbed regions. Following the FIP Recommendations (1999), the distance from the centroid of the main tie to the centroid of compression was taken as $Z = 0.6L = 864$ mm (34.0 in.). With the geometry of the strut-and-tie model established, the capacity of the deep beam, in terms of the resultant of the uniformly distributed load, was predicted to be 372 kN (83.6 kips). This predicted value is considerably below the measured capacity of 1172 kN (263 kips).

In order to provide a better estimate of the failure load the strut-and-tie model shown in Fig. 4(d) was developed. This more refined model utilized the additional horizontal reinforcement that was spread uniformly over the beam depth and assumed that considerable redistribution of the tension and compressive resultants occurred. The two top nodes were located a distance of a/2 down from the top face of the beam. The horizontal tie, representing five 5 mm (0.20 in.) diameter horizontal closed stirrups, was located at mid-depth of the beam and was assumed to yield with $A_s f_y$ = 84.0 kN (18.9 kips). From equilibrium of the strut-and-tie model shown in Fig. 4(d), the distance, x, was found to be 266 mm (10.5 in.) and the resulting predicted capacity was 979 kN (220 kips), that is 84% of the actual failure load. Although this provides a good prediction of the capacity it must be emphasized that considerable redistribution was assumed and extremely large strains would occur in the bottom horizontal tie. If the beam were designed using this more refined model then unacceptably wide cracks might occur at service load levels. The model illustrated in Fig. 4(c) would give a conservative design with acceptable service load performance. The ACI Code, the CSA Standard, the FIP Recommendations all require additional, uniformly distributed reinforcement in the beam for crack control at service load levels.

It is noted that at the experimentally determined failure load of 1172 kN (263 kips), the bearing stress was $(1172 \cdot 1000)/(2 \cdot 100 \cdot 160) = 36.6$ MPa (5310 psi) = 1.21 f_c'. This very high bearing stress was achieved by providing special confinement reinforcement directly above the bearing plates. This test demonstrates that high bearing stresses can be attained with the use of confinement in the bearing areas.

5 Deep beam subjected to bottom loading

Figure 5 shows a deep beam tested by Leonhardt and Walther (1966) that was bottom-loaded. The center-to-center span was 1440 mm (56.7 in.) and the simulated uniform loading was applied to the top of the bottom ledge over the clear span of 1280 mm (50.4 in.). This bottom loading was achieved by hanging loads applied to a 400 mm (15.7 in.) wide bottom ledge as shown in Fig. 5(a). The beam was supported on 160 mm (6.3 in.) long bearing plates and the thickness of the deep beam above the ledge was 100 mm (3.9 in.). The concrete strength at the time of testing was 30.2 MPa (4380 psi). The main tie reinforcement consisted of eight 8 mm (0.32 in.) diameter reinforcing bars having a total yield force, $A_s f_y = 8 \cdot 50.26\ mm^2 \cdot 428$ MPa = 172 kN (38.7 kips).

Figure 5(c) shows the simplified strut-and-tie model suitable for design. For this beam it was assumed that the bottom load was transferred to the beam by bond stresses between the vertical stirrups, that hang-up the load, and the concrete. A uniform stress transfer was assumed over the height of the beam and hence the deviation in the struts was assumed to occur at mid-height of the beam as shown in Fig. 5(c). The distance from the centroid of the main tie to the centroid of compression was taken as 800 – 67.5 = 732.5 mm (28.8 in.). With the geometry of the strut-and-tie model established, the capacity of the deep beam, in terms of the total applied load, was calculated to be 630 kN (142 kips). This prediction is considerably below the measured capacity of 1102 kN (248 kips).

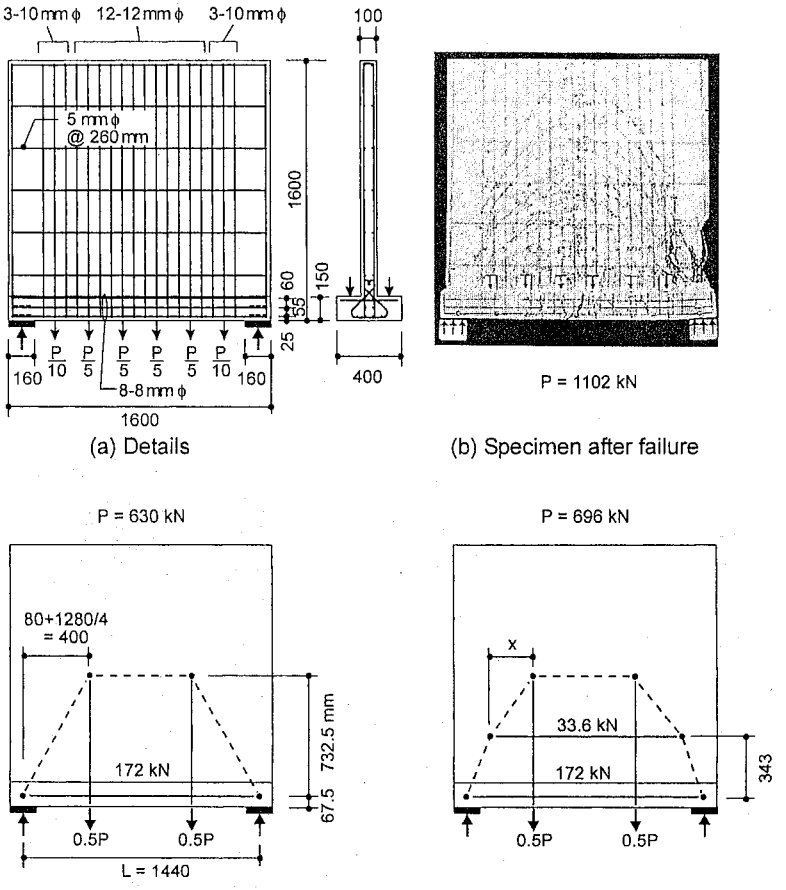

Fig. 5: Deep beam subjected to bottom loading, tested by Leonhardt and Walther (1966)

The refined strut-and tie model for this deep beam is shown in Fig. 5(d). This model accounted for two of the horizontal, 5 mm (0.20 in.) diameter, closed stirrups that were considered to yield in the tension zone. The additional horizontal tie, representing these two stirrups, was located at their centroid. From equilibrium of the truss, the distance, x, was found to be 231 mm (9.1 in.) and the resulting predicted capacity was 696 kN (156 kips), which is also a conservative prediction.

At the failure load of the beam of 1102 kN (248 kips), the concrete crushed in the 100 mm (3.9 in.) thick portion just above the bottom flange. At this load level, the refined strut–and-tie model predicted a force of 614 kN (138 kips) in the strut just above the reaction. From geometry, the angle of this strut was found to be 63.8° from the horizontal, giving a strut width,
$w_s = 150 \cos 63.8° + 160 \sin 63.8° = 210$ mm (8.3 in.). Hence at failure, the stress in the strut was $614 \cdot 1000/(210 \cdot 100) = 29.2$ MPa (4240 psi) or $0.97f_c'$. For the case with parallel diagonal cracks in a web the 2002 ACI Code limits the stress in the strut to $0.85\beta_s f_c' = 0.85 \cdot 0.60f_c' = 0.51f_c'$. The 1994 CSA Standard limits the strut stress based on the amount of strain in the tie crossing the strut and on the angle between the strut and the tie. For this case a strut stress of $0.76f_c'$ would be permitted. The FIP Recommendations (1999) limit the stress in the strut to $0.60f_c'$ for the webs of beams. It is evident that these code requirements are conservative in predicting the crushing of the struts, for this case.

6 Deep beam with transverse reinforcement

Figure 6(a) shows a deep beam, containing transverse reinforcement tested under monotonic loading by Uribe and Alcocer (2001). The 350 mm thick by 1200 mm (13.8 by 47.2 in.) deep beam was supported on 400 mm (15.7 in.) long bearing plates. The top loading was applied through two 400 mm (15.7 in.) long plates centered 800 mm (31.5 in.) apart. The center-to-center span was 3600 mm (141.7 in.) and the shear-span-to-effective depth ratio was 1.17. The concrete cylinder compressive strength at the time of testing was 35 MPa (5075 psi). The transverse reinforcement consisted of #4 closed stirrups (12.7 mm dia.) spaced at 140 mm (5.5 in.) in the clear shear span and the longitudinal reinforcement, consisted of #8 bars (25.4 mm dia.). The actual yield stresses of the #4 stirrups and #8 longitudinal bars were 429 and 445 MPa (62.2 and 64.5 ksi), respectively. At the bottom of the beam, five bars were continuous over the span, having a total measured yield force of $5 \cdot 507$ mm$^2 \cdot 445$ MPa = 1128 kN (254 kips). Three additional shorter #8 bars were placed at the bottom to resist the forces required by the strut-and-tie model assumed. The total measured yield force of the 8-#8 bars was 1806 kN (406 kips). A total of 12-#8 bars were placed at midspan (Fig. 6(a)). The longitudinal reinforcement was anchored with 90° standard hooks following ACI 318-02. To assess the effect of confinement along the bar anchorage, no stirrups were placed along the bearing region at one end of the beam (see Fig. 6(a)).

Figure 7 shows the strut-and-tie model developed in accordance with the FIP Recommendations (1999). It was assumed that, at each beam end, part of the load is transferred from the loading plate directly to the support through an inclined strut (i.e., direct strut mechanism). The remainder was assumed to be carried by stirrups (tie) in a truss with two inclined struts at each beam end, which were, in turn, superimposed onto the direct strut mechanism. In accordance with the FIP Recommendations (1999), the part of the load resisted by the stirrups depends on the shear span-to-internal lever arm ratio, a/z, as given by $1/3\ (2\ a/z - 1)$. For this beam, with a = 1400 mm (55.1 in.) and z = 942 mm (37.1 in.), the stirrups were predicted to carry 0.657 of the total load.

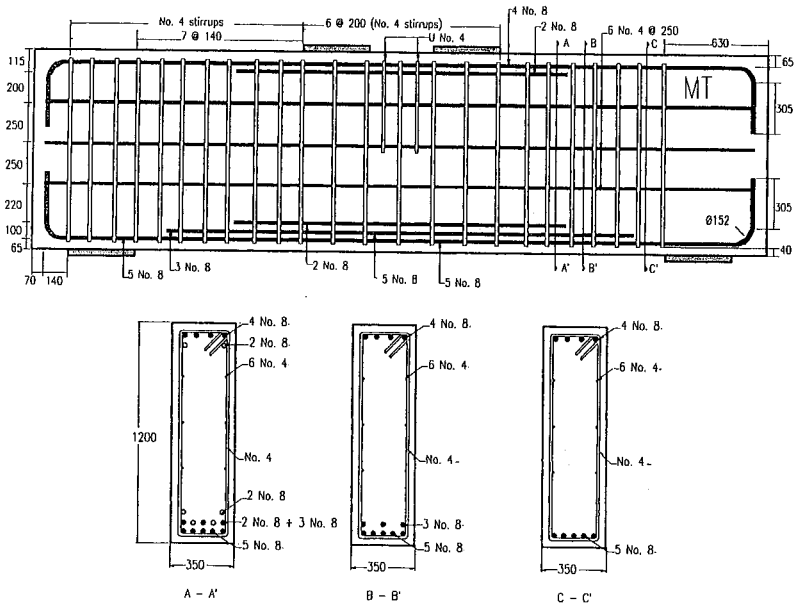

(a) Details

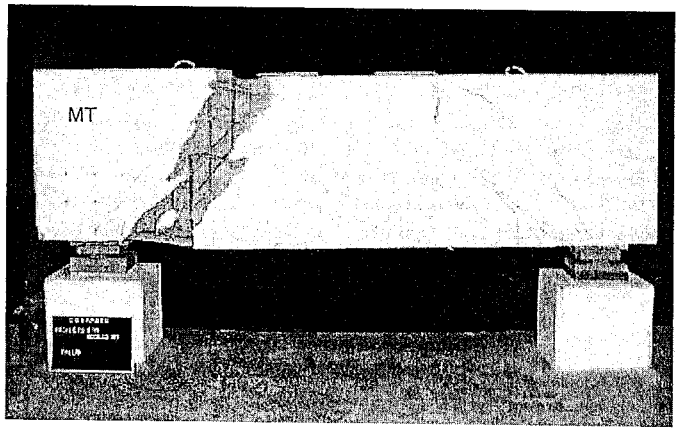

(b) Beam after failure

Fig. 6: Deep beam with transverse reinforcement, tested by Uribe and Alcocer (2001)

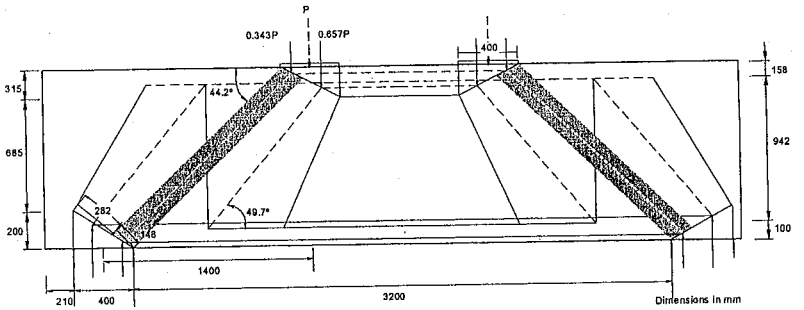

(a) Strut and tie model

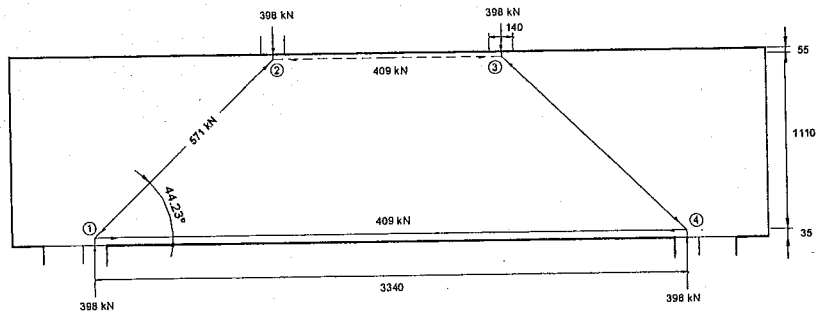

(b) Direct strut mechanism

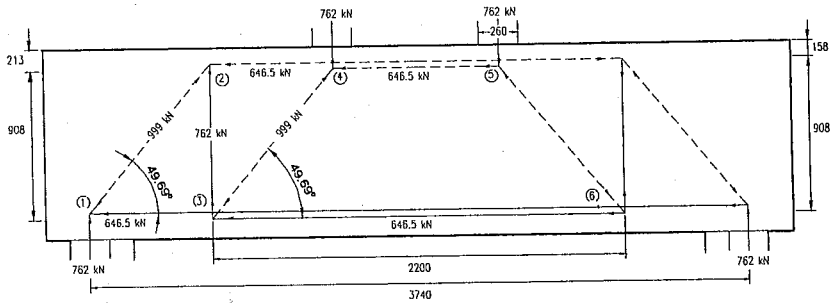

(c) Truss mechanism

Fig. 7: Strut and tie models for deep beam with transverse reinforcement, tested by Uribe and Alcocer (2001)

In predicting the strength of this beam, it was assumed that stirrup yielding controlled the failure mode. The FIP Recommendations (1999) require that the part of the total load carried by the stirrups be provided along the length $a_w = 0.85a - z/4$. For this beam, $a_w = 0.85 \cdot 1400 - 942/4 = 955$ mm (37.6 in.) and hence with a stirrup spacing of 140 mm (5.5 in.) seven stirrups were considered effective. Figure 7(c) shows the predicted truss mechanism assuming that the seven stirrups yielded.

This yield force is $7 \cdot 2 \cdot 127$ mm$^2 \cdot 429$ MPa = 762 kN (171 kips).

Hence the predicted capacity of the truss mechanism is 762 kN. Therefore the beam capacity is predicted to be 762 kN/0.657 = 1160 kN (261 kips).

The load carried by the direct strut mechanism (see Fig. 7(b)) is thus 1160 kN – 762 kN = 398 kN (89.5 kips). In order to check the capacity of the longitudinal reinforcement it is necessary to combine the direct strut mechanism with the truss mechanism to give the complete strut and tie model (see Fig. 7(a)). The force required in the 5-#8 bars is 409 kN + 646.5 kN = 1056 kN (237 kips) and in the 8-#8 bars is 409 kN + (2 · 646.5 kN) = 1702 kN (383 kips). Because both of these forces are less than the yield forces of the bars provided, it was concluded that the correct yielding mechanism was chosen. The additional 4-#8 bars in the midspan region were not included in the strut-and-tie model because they were not long enough to participate in the strut-and-tie model assumed.

The strength of the deep beam was predicted to be 1160 kN (261 kips), which is less than the measured strength of 1578 kN (355 kips). The failure of the beam was governed by yielding of the stirrup reinforcement, followed by wide cracking, extending from the outer edge of the loading plate to a region near the inner edge of the bearing plate, by concrete crushing, as well as by local bending of the longitudinal reinforcement. Figure 6(b) shows the specimen after failure.

Figure 8(a) shows the strains measured in the stirrup reinforcement of the beam when the maximum load was attained. Yielding was recorded in nearly all of the stirrups. The largest strains were recorded in the second, third and fourth stirrups from the inner edge of the bearing plates.

Figure 8(b) shows the predicted and measured stirrup forces as the applied load increased. The actual contribution was calculated from strains recorded in the test, which were converted to stresses using the measured stress-strain relation of the steel reinforcement. The prediction was calculated assuming that all seven stirrups participated and that the part of the load resisted by the stirrups (i.e., 0.657 times the applied load) was constant throughout the tests. Although the stirrup contribution followed the trend of the prediction, it had smaller values. This implies that the assumed contribution of the direct strut (0.343 times the applied load) was a little larger.

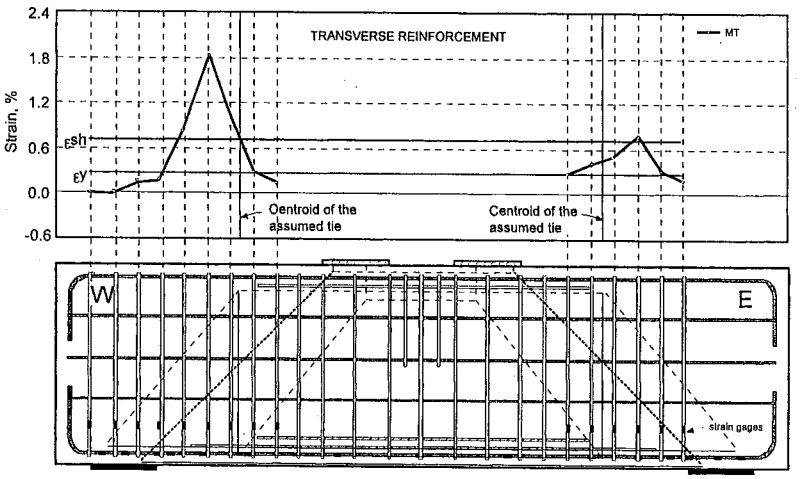

(a) Measured strains in stirrup reinforcement

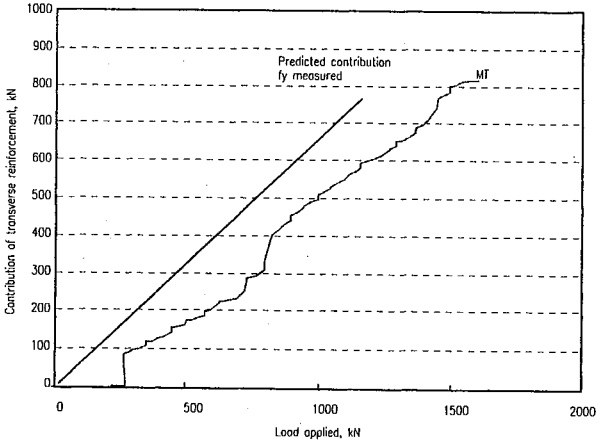

(b) Contribution of stirrup reinforcement to shear strength

Fig. 8: Stirrup contribution for deep beam tested by Uribe and Alcocer (2001)

7 Beam with dapped ends

Figure 9 shows a beam with dapped ends tested by Cook and Mitchell (1988). The 600 mm deep by 300 mm wide (23.6 by 11.8 in.) beam spanned 3200 mm (126 in.) between roller supports and was subjected to a concentrated load at midspan. The dapped ends resulted in a 250 mm (9.8 in.) deep projection at each end. The concrete strength at the time of testing was 29.8 MPa (4320 psi). The beam was designed using the strut-and-tie model shown in Fig. 9(c). It was assumed that the shear at the end of the beam collected at the bottom of the full-depth beam (node C) and then was lifted by the main vertical tie B-C to the top of the beam (node B). It was assumed that the shear in the end projection flowed into the support reaction by means of the inclined concrete strut A-B. Horizontal tie A-D was required to provide equilibrium at the node just above the support reaction to equilibrate the outward thrust of strut A-B. The main vertical tie B-C consisted of four No. 10 (11.3 mm (0.44 in.) dia.) closed stirrups. At node A the horizontal tie, consisting of four No. 15 (16 mm (0.63 in.) dia) weldable grade bars, was welded to a 75×75·6 mm (3·3·0.25 in.) steel angle to provide the necessary end anchorage. These bars were extended well into the full-depth portion of the beam to provide sufficient development length. Node D represented the fanning compressive stresses resulting from bond stresses and was assumed to be at a distance equal to one-half of the development length beyond the main vertical tie. The struts represented the centerlines of the fanning compressive stresses, assuming that uniform bond stresses were developed. The addition of three No. 10 U-bars at the end of the horizontal tension tie at the bottom of the full depth beam provided the additional force necessary to anchor the five No. 30 (29.9 mm (1.18 in.) dia.) bottom bars (see Fig. 9(a)). In the full-depth portion of the beam, No. 10 U-stirrups spaced at 225 mm (8.9 in.) were provided.

The centroid of the top chord was assumed to be located at a distance of a/2 down from the top surface and the bottom tie was located at the centroid of the tension reinforcement. The failure of the test specimen was predicted to occur by yielding of the main vertical tie B-C. The yield force of the main vertical tie was $A_s f_y = 4{\cdot}2{\cdot}100\ mm^2{\cdot}445\ MPa = 356\ kN$ (80.0 kips). The predicted reaction at failure was 260 kN (58.5 kips). The actual failure load was 307 kN (69.0 kips). At the predicted failure load none of the other ties reached yield and no nodal zones or struts reached their limiting stresses.

Figure 10(a) and (b) show the strains in the reinforcement at first yielding and at the maximum load level of 307 kN (69.0 kips), respectively. As can be seen from Fig. 10(b) considerable yielding occurred in both the horizontal and vertical main ties. The significant tensile strains in the horizontal tie at the bottom of the end projection illustrate the need to anchor this tie at the bearing area.

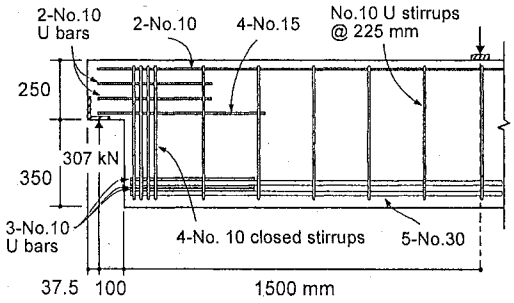

(a) Details

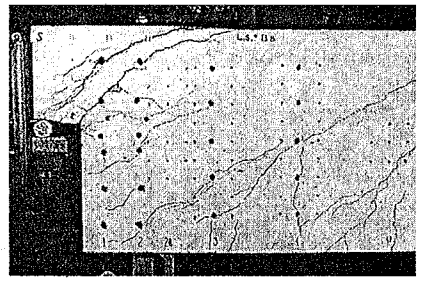

(b) Specimen after failure

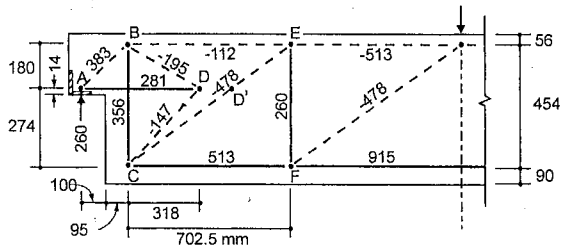

(c) Strut-and-tie model (forces in kN)

Figure 9: Beam with dapped ends, tested by Cook and Mitchell (1988).

It is noted that in checking the stresses at node B, the spalling of the 40 mm concrete cover on the vertical tie reinforcement must be taken into account and hence the nodal zone stress is predicted to be $356 \cdot 1000/(110 \cdot 220) = 14.7$ MPa (2130 psi) $= 0.49 f_c'$. In order to provide adequate bearing at this nodal zone, closed stirrups with 135°-bend anchorages were used for the main vertical tie. A companion specimen, with four No. 10 open U-stirrups instead of closed stirrups was constructed and tested. Because of this detail, the nodal zone area at node B was effectively reduced and the specimen with open stirrups failed at a lower load by crushing of the compressive strut at this node. This emphasizes the need to provide closed stirrups for the main ties.

In using the strut-and-tie model shown in Fig. 9(c) for design, the number of nodes may be reduced by shifting node D to location D', provided that the horizontal tie extends beyond D' by a distance of at least one-half the development length of the bar. Other strut-and-tie models for the design of beams with dapped ends are given by Jirsa et al. (1991) and in the FIP Recommendations (1999).

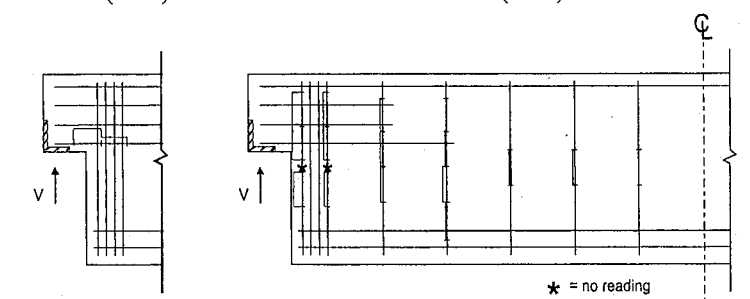

(a) Support reaction, V = 173 kN

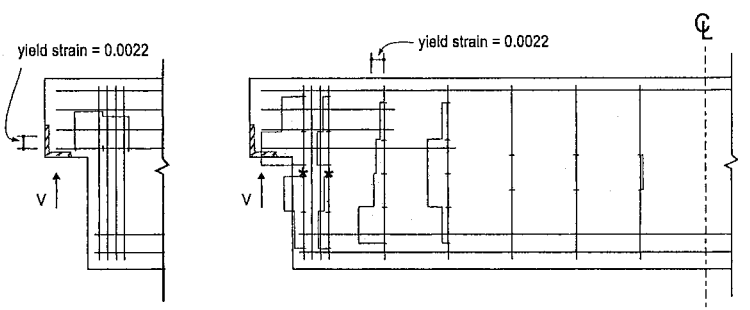

(b) Support reaction, V = 307 kN

Fig. 10: Measured strains in reinforcing bars of beam with dapped ends [Cook and Mitchell (1988)].

8 Conclusions

This paper presents the results of a number of experiments that have been carried out on disturbed regions. The strut-and-tie design approach of the ACI Code (2002), the CSA Standard (1984 and 1994) and the FIP Recommendations (1999) were used to predict the capacities of these test specimens. The predicted capacities were compared with the measured failure loads and it is concluded that the strut-and-tie design approach for disturbed regions gives conservative predictions. The FIP Recommendations (1999) provide useful guidance to the designer for the strut-and-tie geometries of a number of different standard cases such as deep beams and corbels. The paper also discusses some important detailing considerations for disturbed regions. The strut-and-tie model provides a conservative, simple tool enabling the designer to visualize the flow of forces and to appreciate the need for careful detailing.

9 References

ACI Committee 318 (2002): "Building Code Requirements for Structural Concrete (ACI 318-02) and Commentary ACI 318-R-02", American Concrete Institute, Farmington Hills, MI, 443 pp.

Jirsa, J.O., Breen J.E., Bergmeister, K., Barton, D., Anderson, R. and Bouadi, H., (1991): "Experimental Studies of Nodes in Strut-and Tie Models", IABSE Colloquium Stuttgart 1991- Structural Concrete", International Association of Bridge and Structural Engineering, Zurich, pp. 525-532.

CSA Committee A23.3 (1984): "Design of Concrete Structures for Buildings", CAN3-A23.3-M84, Canadian Standards Association, Rexdale, Canada, 281 pp.

CSA Committee A23.3 (1994): "Design of Concrete Structures", CSA A23.3-94, Canadian Standards Association, Rexdale, Canada, 199 pp.

Cook, W.D. and Mitchell, D. (1988): "Studies of Disturbed Regions near Discontinuities in Reinforced Concrete Members", ACI Structural Journal, V. 85, No. 2, pp. 206-216.

FIP Recommendations (1999): *Practical Design of Structural Concrete*. FIP-Commission 3 "*Practical Design*", Sept. 1996.
Publ.: SETO, London, Sept. 1999. (Distributed by: *fib*, Lausanne)

Leonhardt F. and Walther R. (1966): "Wandartiger Träger", Deutscher Ausschuss für Stahlbeton, Bulletin No. 178, Wilhelm Ernst & Sohn, Berlin, 159 pp.

Mörsch, E. (1909): "Concrete-Steel Construction (Der Eisenbetonbau)", Translation of the third German Edition by E.P. Goodrich, McGraw-Hill Book Co., New York, 368 pp.

Ritter, W. (1899): "The Hennebique Design Method (Die Bauweise Hennebique)", Schweizerische Bauzeitung (Zürich), V. 33, No. 7, Feb., pp. 59-61.

Rogowsky, D.M., MacGregor, J.G. and Ong, S.Y. (1986): "Tests of Reinforced Concrete Deep Beams", ACI Journal, V. 83, No. 4, July-August, pp. 614-623.

Uribe C.M., and Alcocer S.M., (2001): "Comportamiento de vigas peraltadas diseñadas con el modelo de puntales y tensores", (In Spanish), Centro Nacional de Prevención de Desastres, ISBN 970-628-607-1, México.

Walraven, J. and Lehwalter, N., (1994): "Size Effects in Short Beams Loaded in Shear", ACI Structural Journal, V. 91, No. 5, September-October, pp. 585- 593.

Part 4

Examples

Example 1 a: Deep beam design in accordance with ACI 318-2002

Claudia M. Uribe

Sergio M. Alcocer

Synopsis

A deep beam, supporting two concentrated loads at the top, was designed in accordance with Appendix A of the ACI 318-2002. The analysis and design using the strut and tie model were performed in an efficient and straight forward manner. The strut and tie methodology provides a framework to understand and assess the flow of forces and the resisting mechanisms. Also, it is a valuable tool for achieving proper detailing of ductile concrete members.

Claudia M. Uribe is a former graduate research assistant in the Structural Engineering and Geotechnical Area at the National Center for Disaster Prevention (CENAPRED). She holds a B.Sc. degree from EAFIT, Medellin, Colombia and a M.Sc. degree from the National Autonomous University of Mexico (UNAM). Her research interests include the seismic behavior of reinforced concrete structures.

Sergio M. Alcocer, FACI, is a research professor at the Institute of Engineering of the UNAM and Director of Research at CENAPRED. He is a member of ACI Committees 318, Building Code Requirements, and 374, Performance Based Seismic Design of Concrete Buildings, as well as a member of Joint ACI-ASCE Committee 352, Joints and Connections in Monolithic Concrete Structures. He is Chairman of the Committee on Masonry Standards and a member of the committee on Reinforced Concrete Standards of the Mexico City Building Code. His research interests include earthquake-resistant design of reinforced concrete and masonry structures.

1 Problem statement

Design the simply supported beam that carries two concentrated factored loads of $134^k \times 1.6 = 214^k$ (952 kN) each on a clear span of 12 ft (3.66 m), as shown in Fig. (1-1).

The beam has a thickness of 14 in. (356 mm) and a 48 in. (1.22 m) overall depth. The length of the bearing plate at each concentrated load location is 16 in. (406 mm) and the width is the same as the beam thickness, i.e. 14 in. (356 mm).

Use $f_c' = 4\,000$ psi (27.6 MPa) and $f_y = 60\,000$ psi (414 MPa). Neglect the self-weight.

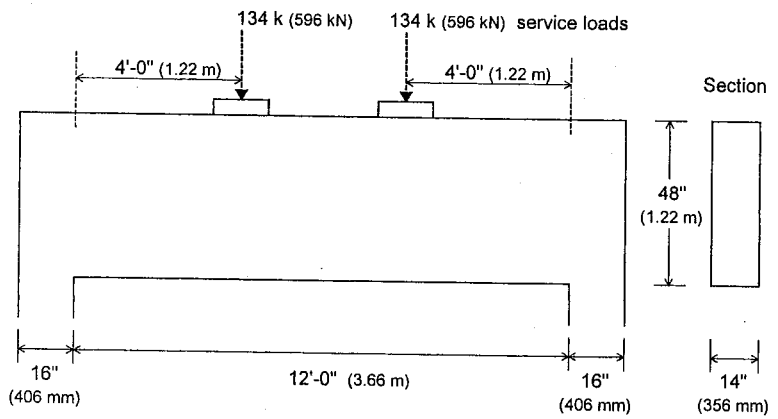

$P = 134\text{ k} \times 1.6 = 214\text{ k}$ (952 kN)

$b = 14$ in. (356 mm)

$h = 48$ in. (1.22 m)

$f_c' = 4\,000$ psi (27.6 MPa)

$f_y = 60\,000$ psi (414 MPa)

Fig. 1-1: Member and loads

2 Strut and tie model parameters

2.1 Compressive strength of the concrete (Sections A.3.2 and A.5.2 of ACI 318-2002)

$f_{cu}=0.85\beta_2 f_c'$ β_2 = factor to account for the effect of cracking and confining reinforcement on the effective compressive strength of a strut, β_s, or a nodal zone, β_n

f_c' = specified compressive strength of concrete

f_{cu} = $0.85 \times 4000 \times \beta_2 = 3400\beta_2$, psi ($23.4\beta_2$, MPa) (1-1)

the values of β_2 in this example are

Struts, β_s (Section A.3.2 of ACI 318-2002):

a. Struts in uncracked zones and located such that the mid-strut cross section is the same as that at the nodes, such as the compression zone of a beam (to be referred to as type *a* in this example), 1.00

c. Struts located such that the width of the mid-section of the strut, is or could be, larger than the width at the nodes, with reinforcement satisfying A.3.3 (to be referred to as type *c* in this example) 0.75

Nodal zones, β_n (Section A.5.2 of ACI 318-2002):

e. Nodal zones bounded by struts, or bearing areas or both (type CCC) 1.00

f. Nodal zones anchoring a tie in one direction only (type CCT) 0.80

g Nodal zones anchoring ties in more than one direction (type CTT) 0.60

Table 1-1: Strength of concrete in struts and nodal zones

	Struts			Nodal zones		
	Type	$\beta_2=\beta_s$	f_{cu}, psi* (MPa)	Type	$\beta_2=\beta_n$	f_{cu}, psi* (MPa)
a.	Uncracked chord (prismatic)	1.0	3400 (23.4)	*e.* CCC	1.0	3400 (23.4)
c.	Inclined strut (bottle-shaped)	0.75	2550 (17.6)	*f.* CCT	0.8	2720 (18.8)
				g. CTT	0.6	2040 (14.1)

*from eq. (1-1) in this example

2.2 Strength of struts, ties and nodal zones

The following shall be met:

$\phi F_n \geq F_u$ (eq. A-1)

F_u = force in the strut or tie, or force acting on a node due to the factored loads

F_n = nominal strength of the strut

ϕ = strength reduction factor (according to 9.3.2.6); for all truss elements, $\phi = 0.75$

Strength of struts (Section A.3)

$F_{ns} = f_{cu} A_c$ (eq. A-2)

F_{ns} = nominal compressive strength of the concrete in a strut

f_{cu} = effective compressive strength

A_c = smallest effective cross-sectional area of the strut

Strength of ties (Section A.4)

Because the tie is made of nonprestressed reinforcement:

$F_{nt} = A_{st} f_y$ (eq. A-6)

F_{nt} = nominal strength of a tie

A_{st} = area of nonprestressed reinforcement in a tie

f_y = specified yield strength of nonprestressed tie

Strength of nodal zones (Section A.5)

$F_{nn} = f_{cu} A_n$ (eq. A-7)

F_{nn} = nominal compressive strength of a nodal zone

f_{cu} = effective compressive strength of a nodal zone

A_n = area of the face of the nodal zone

3 Strut-and-tie model design procedure (Section A.2 of ACI 318-2002)

3.1 Flexure design

To develop the strut-and-tie model, it is convenient to know the size (depth) of the compression block of concrete.

Assuming that two layers of No.8 bars are provided for positive moment, the effective depth would be:

$$d = h - cover - d_{b\ \text{No. 5 stirrup}} - d_{b\ \text{No.8}} - \tfrac{1}{2} s_v \qquad (1\text{-}2)$$

$= 48$ in. $- 1.5$ in. $- 0.625$ in. $- 1.0$ in. $- \tfrac{1}{2}$ in. $= 44.4$ in. (1.13 m)

where s_v is the vertical spacing between the two layers of No. 8 bars.

According to Section R9.1 of ACI 318-2002

$M_u \leq \phi M_n$

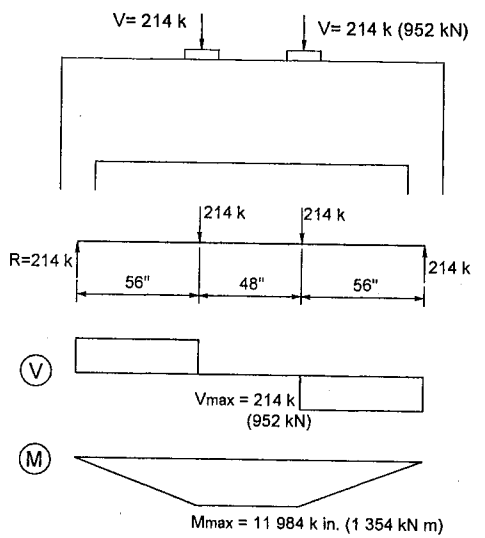

Fig. 1-2: Moment and shear diagrams

where:

ϕ = strength reduction factor. For flexure, $\phi = 0.9$ (Section 9.3.2.1)

M_u = 11 984 k·in. (1 354 kN m).

$$M_n = A_s f_y\left(d - \frac{a}{2}\right) = A_s f_y\left(d - \frac{A_s f_y}{2\times 0.85 f_c' b}\right) \qquad (1\text{-}3)$$

Therefore,

$$11984 \text{ k·in} \le 0.9 A_s \times 60000 \text{ psi}\left(44.4 - \frac{A_s \times 60\,000 \text{ psi}}{2\times 0.85\times 4000 \text{ psi}\times 14 \text{ in.}}\right)$$

solving for A_s, $A_s \ge 5.4$ in.^{2} (3 480 mm²), c = 8.5 in. (216 mm)

3.2 Strut-and-tie model

From 3.1: c (distance from extreme compression fiber to neutral axis) = 8.5 in. (216 mm). For the strut and tie model try a depth of horizontal strut (a) equal to 10 in. (254 mm) (in the constant-moment region).

The following is the strut-and-tie model proposed (Fig. 1-3).

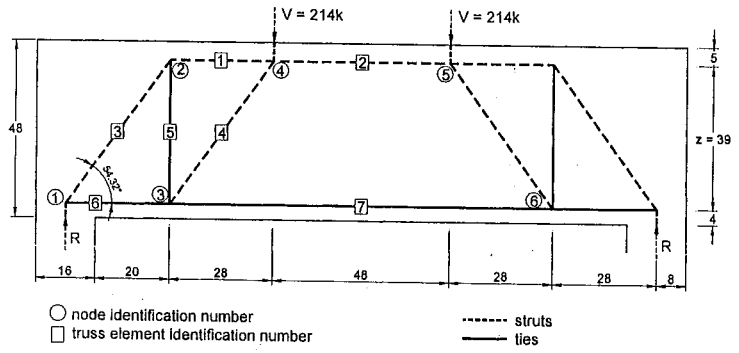

Dimensions in inches (1 in. = 25.4 mm)

V = 214 000 lb (952 kN)
R = 214 000 lb (952 kN)
f_c' = 4 000 psi (27.6 MPa)
f_y = 60 000 psi (414 MPa)

b = 14 in. (356 mm)
h = 48 in. (1.22 m)
l_b = 16 in. (406 mm)
a = 10 in. (254 mm)

Fig. 1-3: Proposed strut-and-tie model (z =39 in. [990 mm])

3.3 Truss solved

Forces in the truss, calculated according to geometry, are shown in Fig. (1-4).

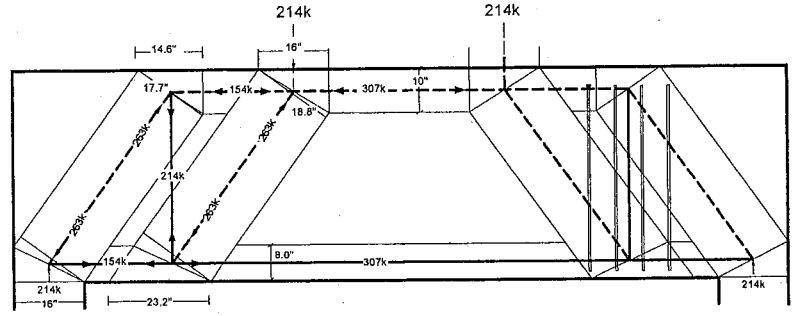

Fig. 1-4: Forces in the truss

3.4 Verification of the strut and nodal zone strength

The verification of the strut and nodal zone strengths should be done through comparing the available strut or nodal area with that required. In this example, because the thickness of the beam, and the width of the loading plates and supports are the same (i.e. 14 in. or 356 mm), the verification will be done by comparing the available strut or nodal width, w_{prov}, with that required, w_{req}. Therefore, for struts and nodes, w_{req} will be calculated using eq. (1-4), see Figs. (1-5a) to (1-5d).

$$w_{req} = \frac{F_u}{\phi f_{cu} b} = \frac{F_u}{\phi\, 0.85 \beta_2 f_c' b} \qquad (1\text{-}4)$$

Node 1

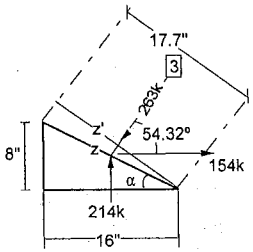

z = 17.89 in. [454.4 mm]

α= 26.6°; θ= 54.3°

z' = l_b sin θ + w_t cos θ =

16 sin 54.3° + 8 cos 54.3° = 17.7 in.

Therefore, for strut 3,

w_{prov} = 17.7 in. (450 mm)

Fig. 1-5a: Node 1

Node 2

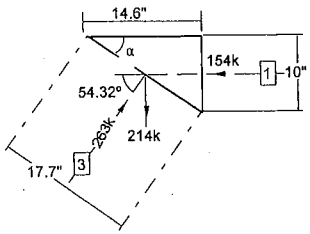

Fig. 1-5b: Node 2

For strut 1, w_{prov} = 10 in. (254 mm) (from flexure design)

z' = 17.69 in. (449 mm)

Therefore,
width of nodal zone = 14.6 in. (371 mm)

Node 3

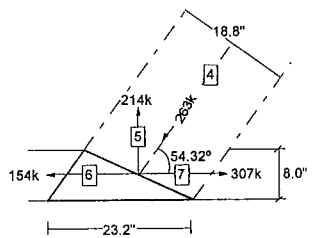

Fig. 1-5c: Node 3

The width 18.8 in. comes from solving Node 4 (Fig. 1-5d).

Node 4

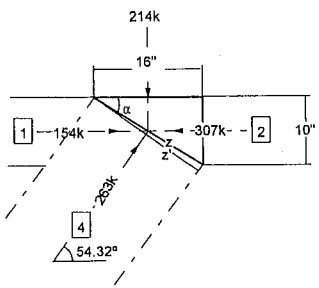

Fig. 1-5d: Node 4

z = 18.88 in. (480 mm)

α = 32°; θ= 54.3°

z' = $l_b \sin\theta + w_t \cos\theta$ =

16 sin 54.3° + 10 cos 54.3° = 18.8 in.

Therefore,
for strut 4, w_{prov} = 18.8 in. (478 mm)

Strut 1 (sample calculation)

$$w_{req} = \frac{F_u}{\phi f_{cu} b_w} = \frac{F_u}{\phi 0.85 \beta_2 f_c' b_w} = \frac{153661}{0.75 \times 0.85 \times 1.0 \times 4000 \times 14} = 4.3 \text{ in. (109 mm)}$$

where,

β_2 = 1.0; it is an uncracked chord, strut Type *a*, from Table (1-1)

b = thickness of member = 14 in.

According to the geometry of the nodal zone, shown in Fig. (1-5b), a width of 10.0 in. (254 mm) can be proposed (w_{prov} = 10 in.). Therefore, it is adequate.

Strength check for other struts is shown in Table (1-2) and for nodes, in Table (1-3) and Fig. (1-5).

Table 1-2: Verification of strength of struts

Element #	Node *i - j*	β_2 [1]	θ [2] (°)	F_{uc} [3] lb (kN)	w_{req} [4] in. (mm)	w_{prov} [5] in. (mm)	Adequacy ✓:OK	Proposed solution
1	*2-4*	1.00	0	153661 (684)	4.3 (109)	10.0 (254)	✓	
						10.0 (254)	✓	
2	*4-5*	1.00	0	307323 (1367)	8.6 (219)	10.0 (254)	✓	
						10.0 (254)	✓	
3	*1-2*	0.80	54.32	263454 (1172)	9.2 (234)	17.7 (450)	✓	
						17.7 (450)	✓	
4	*3-4*	0.80	54.32	263454 (1172)	9.2 (234)	18.8 (478)	✓	
						18.8 (478)	✓	

Notes: [1] From Table 1-1

[2] From STM proposed, Fig. (1-3); $\beta_2 = \beta_s$

[3] From truss solved (Section 3.3 and Fig. (1-4) in this example)

[4] Required width for struts (from eq. (1-4))

[5] Provided width for struts, considering geometry, and bearing and support conditions.

Table 1-3: Verification of strength of nodal zones

Node	β_2[1]	Type[2]	Force[3]	F_u[4] lb (kN)	$w_{p\,req}$[5] in. (mm)	$w_{p\,prov}$[6] in.	Adequacy ✓:OK	Proposed solution
1	0.8	CCT	R	214000 (952)	7.5 (190)	16.0 (406)	✓	
			S1-2	263454 (1172)	9.2 (234)	17.7 (450)	✓	
			T1-3	153661 (684)	5.4 (137)	8.0 (203)	✓	
2	0.8	CCT	S2-1	263454 (1172)	9.2 (234)	17.7 (450)	✓	
			S2-4	153661 (684)	5.4 (137)	10.0 (254)	✓	
			T2-3	214000 (952)	7.5 (190)	54.0 (1372)	✓	
3	0.6	CTTT	S3-4	263454 (1172)	12.3 (312)	18.8 (478)	✓	
			T3-2	214000 (952)	10 (254)	54.0 (1372)	✓	
			T3-1	153661 (684)	7.2 (182)	8.0 (203)	✓	
			T3-6	307323 (1367)	14.3 (364)	8.0 (203)	×	Distribution of steel
4	1.0	CCCC	V	214000 (952)	6.0 (152)	16.0 (406)	✓	
			S4-3	263454 (1172)	7.4 (187)	18.8 (478)	✓	
			S4-2	153661 (684)	4.3 (109)	10.0 (254)	✓	
			S4-5	307323 (1367)	8.6 (219)	10.0 (254)	✓	

Notes: [1] From Table (1-1); $\beta_2 = \beta_n$

[2] From STM proposed, Fig. (1-3)

[3] R = reaction, S = strut, T = tie, V = concentrated load

[4] From truss solved (Section 3.3 and Fig. (1-4) in this example)

[5] Required width for nodes (from eq. (1-4))

[6] Provided width for nodes, considering geometry, and bearing and support conditions.

Verification of the bearing strength at loading and reaction points

From Fig. (1-2), the ultimate load and the reactions are

$V = R = 214$ k (952 kN)

Since the loading plate is 16×14 in., its area is

$A_A = 16 \times 14$ in.² (406 x 356 mm²)

Therefore, the compressive stress is equal to

$$\sigma_A = \left(\frac{V}{\phi A_A} = 1274 \text{ psi} \right) \text{ (8.78 MPa)} \qquad (1\text{-}5)$$

According to Section 2.1 in this example, it must be satisfied that $\sigma_A \le f_u$, that is, $\sigma_A \le \phi\, 0.85\, \beta_2 f_c'$.

For node 4, type CCC,

1274 psi (8.78 MPa) ≤ $\phi 0.85 \beta_2 f'_c = \phi 3400$ psi = 2550 psi (17.6 MPa) (OK)

For node 1, type CCT,

1274 psi (8.78 MPa) ≤ $\phi 0.85 \beta_2 f'_c = \phi 2720$ psi = 2040 psi (14.1 MPa) (OK)

3.5 Steel required in ties

Once the strength of struts and nodes was verified, the amount of steel required in the ties is determined.

Table 1-4: Steel requirements

Element #	Node i-j	β_2	θ (°)	F_{ut} lb (kN)	$A_{s\,req}$[1] in.² (mm²)	$A_{s\,prov}$[2] in.² (mm²)	Adequacy	Proposed solution
5	*2-3*	---	90	214000 (952)	4.8 (3100)	4.96 (3200)	✓	8 No. 5 stirrups @ 4 in.
6	*1-3*	---	0	153661 (684)	3.4 (2190)	4.74 (3060)	✓	A_s = 6 No. 8
7	*3-6*	---	0	307323 (1367)	6.8 (4390)	7.2 (4650)	✓	A_s = 8 No. 8 and 2 No.6

Notes: [1] Required area of ties ($A_s = F_{ut}/\phi f_y$); $\phi = 0.75$

[2] Provided area of ties.

[3] For tie 7, No. 6 and No. 8 bars were used instead of No. 10 bars to be able to distribute them.

Tie 6 (from node 1 to 3)

From Table (1-4)

$A_{s\,req} = 3.4$ in.² (2190 mm²): Use 6 No. 8 bars ($A_{s\,prov} = 4.74$ in.² [3060 mm²]) in two layers.

It is necessary to anchor the bars either by hooks, headed bars, mechanical anchorages or straight bar development (Section A.4.3 of ACI 318-2002).

From Section 12.5.2 of ACI 318-2002, the anchorage length of a 90-deg hook bar is

$$l_{dh} = \frac{0.02\beta\lambda f_y}{\sqrt{f_c'}} d_b = 19 \text{ in. (483 mm) for No. 8 bars} \quad (1\text{-}6)$$

where $\beta = 1$; $\lambda = 1$; d_b = diameter of the bar (in this case, d_b=1 in. [25.4 mm])

l_{dh} is modified by factor (a) of Section 12.5.3

Section 12.5.3.a: factor = 0.7 because a concrete cover ≥ 2½ in. (64 mm) thick is provided in the perpendicular direction to the hook plane, and a concrete cover ≥ 2 in. (51 mm) thick is provided in the direction of the bar extension.

Thus, l_{dh} = 19 in. × 0.7 = 13.3 in. (338 mm) for No.8 bars.

Available anchorage is (Fig. 1-6):

$l_{dh\ available}$ = length of the extended nodal zone – cover – d_b horizontal shear reinforcement

$l_{dh\ available}$ = 16 + 4/tan 54.3° – 1.5 – 0.625 = 16.7 in. (425 mm)

$l_{dh\ available} > l_{dh}$ (OK)

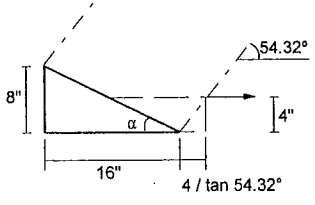

Fig. 1-6: Available anchorage length at the extended nodal zone in Node 1

Tie 7 (from node 3 to 6)

From Table (1-4)

$A_{s\ req}$ = 6.8 in.² (4390 mm²)

It is clear that extending the 6 No. 8 bars from tie 6 is not enough. Therefore, an extra area of steel is needed and is calculated as 6.8 in.² - 4.74 in.² = 2.06 in.² Use 8 No.8 and 2 No.6 ($A_{s\ prov}$ = 7.2 in.² [4650 mm²]).

It is convenient to spread the reinforcement uniformly over an area of concrete at least equal to the tension force in the tie, divided by the applicable limiting compressive stress for the node. In this example,

$$A = \frac{F_{u\ tie7}}{f_{cu}} = \frac{307323}{2040} = 151 \text{ in.}^2 \ (97420 \text{ mm}^2) \quad (1\text{-}7)$$

$$w = 151 / b = 11 \text{ in. (279 mm)} \quad (1\text{-}8)$$

Thus, spread the 8 No. 8 and 2 No. 6 vertically over a height of 11 in. (279 mm).

To anchor the No. 6 bars, use the table from Section 12.2.2 of ACI 318-2002

$$l_d = \frac{f_y\ \alpha\beta\lambda\ d_b}{25\sqrt{f_c'}} \quad (1\text{-}9)$$

$$l_d = \frac{60\,000 \times 1.0 \times 1.0 \times 1.0 \times 0.75}{25\sqrt{4\,000}} = 28.5 \text{ in. (724 mm)}$$

It was assumed that:

α = 1.0, since no more than 12 in. (305 mm) are cast below the bars,

β = 1.0, since it is uncoated reinforcement, and

λ = 1.0, since it is normal-weight concrete.

Available anchorage is:

$l_{dh\ available}$ = distance from critical section to edge of the beam – cover – d_b horizontal shear reinforcement, Fig. (1-3).

$l_{dh\ available}$ = 36 in. – 1.5 in. – 0.625 in. = 33.9 in. (861 mm)

$l_{dh\ available} > l_d$ (OK)

Therefore, place No. 8 bars spread (vertically) @ 3 in. (76 mm) and with l_d = 34 in. (864 mm) (to improve confinement in nodal zone). The straight No. 6 bars are extended over the full span of the beam.

Tie 5 (from node 2 to 3)

From Table (1-4)

$A_{s\ req}$ = 4.8 in.² (3100 mm²)

From Section 11.8.4 of ACI 318-2002

$$s \le \begin{cases} d/5 = 8.9 \text{ in. (226 mm)} & \text{(controls)} \\ 12 \text{ in. (305 mm)} \end{cases}$$

Use 8 No. 5 closed stirrups ($A_{s\ prov}$ = 4.96 in.² [3200 mm²]). Use 2 No.5 inside the top corners continuous along the beam. These stirrups shall have 135 deg bends alternatively around one or the other of these bars. Space stirrups @ 4 in. (102 mm).

3.6 Reinforcement for bottle-shaped struts 3 and 4

In Section A.3.3, it is specified that layers or grids of reinforcement parallel to the plane of the member must cross struts 3 and 4.

Also, because the web thickness is greater than 8 in. (203 mm), it is convenient that the layer or grid of reinforcement be near each face.

From eq. (A-4)

$$\sum \frac{A_{si}}{bs_i} \sin\gamma_i = \rho_{vi} \sin\gamma_i \geq 0.003 \qquad \text{(eq. A-4)}$$

where,

A_{si} = total area of reinforcement at spacing s_i in a layer of reinforcement with bars at an angle γ_i to the axis of the strut.

Suppose only horizontal reinforcement is provided, and $\gamma_i = 54.32°$

$$\frac{2A_{s,i}}{b\, s_i} = \frac{0.003}{\sin 54.3°} \qquad (1\text{-}10)$$

$a_{s,i} \geq 0.0259\, s_i$ But, from Section 11.8.5 of ACI 318-2002

$$s_2 \leq \begin{cases} d/5 = 8.9 \text{ in. (226 mm)} & \text{(controls)} \\ 12 \text{ in. (305 mm)} \end{cases}$$

Suppose s = 7 in. (178 mm), $a_{svh} \geq 0.18$ in.² (116 mm²). Use No.4 bars spaced 7 in. (178 mm) in each face.

4 Arrangement of reinforcement

The final layout of the reinforcement is shown in Fig. 1-7.

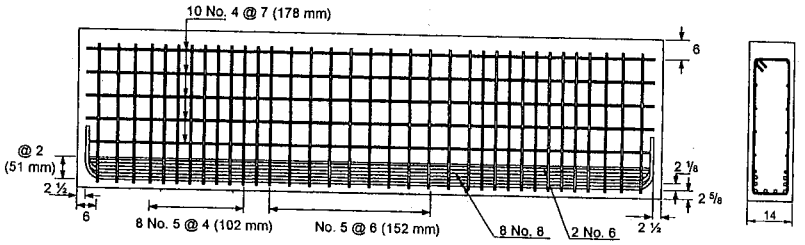

Dimensions in inches; 1 in. = 25.4 mm

Fig. 1-7: Arrangement of reinforcement

5 Optional models

The strut-and-tie model solved (see Fig. 1-3) is one of several models that could have been selected. In the model assumed, load transfer was considered to take place by the formation of a truss made of two inclined struts near each support. This model was selected because of its simplicity, and because it required stirrups along the shear span, which was considered a safe detail.

Optionally, two other strut-and-tie models could have been selected. In Fig. 1-8, the strut-and-tie model recommended in the 1999 FIP Recommendations is presented. In this model, part of the load is transferred from the loading plate directly to the support through an inclined strut. The remainder is resisted by the stirrups, through a simple truss, similar to that assumed in the solution of this example. The FIP Recommendations consider that both load-carrying mechanisms (i.e. direct strut and truss action) can be superimposed. The distribution of load between these two mechanisms depends on the shear span-to-internal lever arm ratio, and is determined from equations that have been verified with test results.

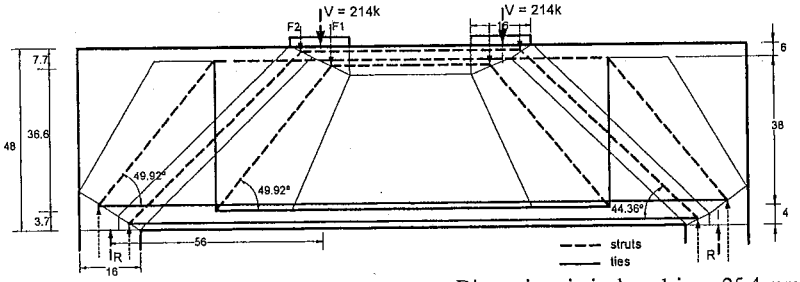

Dimensions in inches; 1 in. = 25.4 mm

Fig. 1-8: Model in accordance with FIP 1999

Another strut-and-tie model that could have been selected considers that at each beam end, the load is transferred to the support by a single inclined strut (Fig. 1-9). This model does not require vertical stirrups along the shear span (i.e. between the loading plate and the beam support) to maintain equilibrium. In the absence of stirrups, large cracking at loads well below ultimate may be expected, and therefore, is not recommended for design. Nevertheless, it can be argued about the suitability of a similar model, if minimum vertical stirrup reinforcement is provided.

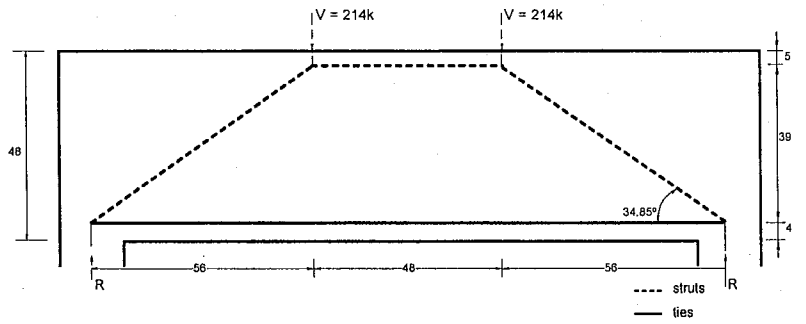

Dimensions in inches; 1 in. = 25.4 mm

Fig. 1-9: Load transferred directly to the support

6 Final comments

The strut-and-tie model selected was readily analyzed, and the design and strength verification of its components was easily performed. It was found that the strut and tie methodology provides a framework to understand and assess the flow of forces and the resisting mechanisms. Also, it was demonstrated that it is a valuable tool for achieving proper detailing of ductile concrete members.

References

ACI 318-2002: *Building Code Requirements for Reinforced Concrete and Commentary*. ACI Committee 318, American Concrete Institute, Farmington Hills, Michigan, 2002.

FIP Recommendations (1999): *Practical Design of Structural Concrete*. FIP-Commission 3 "*Practical Design*", Sept. 1996.
Publ.: SETO, London, Sept. 1999. (Distributed by: *fib*, Lausanne)

Acknowledgements

The authors gratefully acknowledge the participation and contribution of Mr. Leonardo Flores in the preparation of the final version of the paper.

Example 1b: Alternative design for the non-slender beam (deep beam)

Tjen N. Tjhin

Daniel A. Kuchma

Synopsis

A 20 ft (6.10 m) span deep beam was designed using the strut-and-tie method according to ACI 318-02 Appendix A. The beam is 20 in. (508 mm) wide and 80 in. (2032 mm) deep and carries two concentrated factored loads, V_u of 360 kips (1601 kN) each. Bearing plates of 18 in. × 20 in. (457 mm × 508 mm) are provided at all loading and support locations. The self-weight was not considered in the design. The compressive strength of concrete, f'_c and the yield strength of the steel reinforcement, f_y are taken as 4 ksi (27.6 MPa) and 60 ksi (414 MPa), respectively.

A simple strut-and-tie model shown in Fig. (1b-2) is used in the design. The provided reinforcement for the main tie is 2 layers of 5 #9 (#29 mm) bars. The anchorages of these bars are provided by means of standard 90° hooks. The reinforcement details are shown in Fig. (1b-6).

Tjen N. Tjhin is a doctoral candidate in the Department of Civil and Environmental Engineering at the University of Illinois at Urbana-Champaign. His research interests include nonlinear analysis and design of concrete structures.

Daniel (Dan) A. Kuchma is an Assistant Professor of Civil and Environmental Engineering at the University of Illinois at Urbana-Champaign. He is a member of ACI subcommittee 318E Shear and Torsion as well as joint ASCE/ACI Committee 445 Shear and Torsion and its subcommittee 445-A Strut and Tie.

1 Geometry and loads

The structure and loading under consideration are shown in Fig. (1b-1).

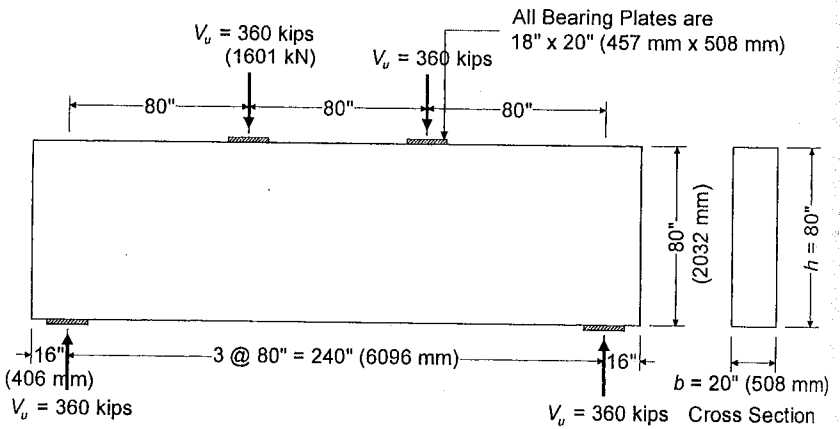

Fig. 1b-1: Structure and loading

Material strengths:

$f_c^{'}$ = 4 ksi (27.6 MPa) (normal-weight concrete)

f_y = 60 ksi (414 MPa)

2 Design procedure

The entire deep beam is a disturbed region because it is near statical discontinuities, i.e., the concentrated forces, within one section depth of the beam on either side of the discontinuity. However, it is only necessary to consider the left third of the structure to complete the design because the geometry and loading are symmetric about a vertical axis passing the midspan of the beam. The structure will be designed using the strut-and-tie method according to ACI 318-02 Appendix A. The step-by-step design procedure is as follows:

- Step 1: Check bearing capacity at loading and support locations.
- Step 2: Establish the strut-and-tie model and determine the required truss forces.
- Step 3: Select the tie reinforcement.
- Step 4: Design the nodal zones and check the anchorages.
- Step 5: Check the diagonal struts.
- Step 6: Calculate the minimum reinforcement required for crack control.
- Step 7: Arrange the reinforcement.

3 Design calculations

3.1 Step 1: Check bearing capacity at loading and support locations

The area of bearing plate is $A_c = 18(20) = 360$ in.^{2} (232258 mm^2).

The bearing stresses at points of loading and at supports are

$$\frac{V_u}{A_c} = \frac{360(1000)}{360} = 1000 \text{ psi (6.89 MPa).}$$

The nodal zone beneath the loading locations is an all-compression (CCC) node per ACI Sec. A.5.2 definition. The effective compressive strength of this node is limited to

$$f_{cu} = 0.85\beta_n f_c^{'} = 0.85(1.00)(4000) = 3400 \text{ psi.} \quad \text{[ACI Sec. A.5.2 eq. (A-8)]}$$

The nodal zone over the support locations is a compression-tension (CCT) node. The effective compressive strength of this node is

$$f_{cu} = 0.85\beta_n f_c^{'} = 0.85(0.80)(4000) = 2720 \text{ psi.} \quad \text{[ACI Sec. A.5.2 eq. (A-8)]}$$

Because the bearing stresses are less than their corresponding limits, i.e., $\phi f_{cu} = 0.75(3400) = 2550$ psi (17.58 MPa) at points of loading and $\phi f_{cu} = 0.75(2720) = 2040$ psi (14.07 MPa) at supports, the area of bearing plates provided is adequate.

3.2 Step 2: Establish the strut-and-tie model and determine the required truss forces

A simple strut-and-tie model shown in Fig. (1b-2) is selected. The truss consists of a direct strut *AB* (or strut *CD*) running from the applied load to the support. Strut *BC* and tie *AD* are required to equilibrate the truss. As shown in Fig. (1b-3), these strut and tie form a force couple,

$$F_{u,BC} = F_{u,AD}. \qquad \text{(1b-1)}$$

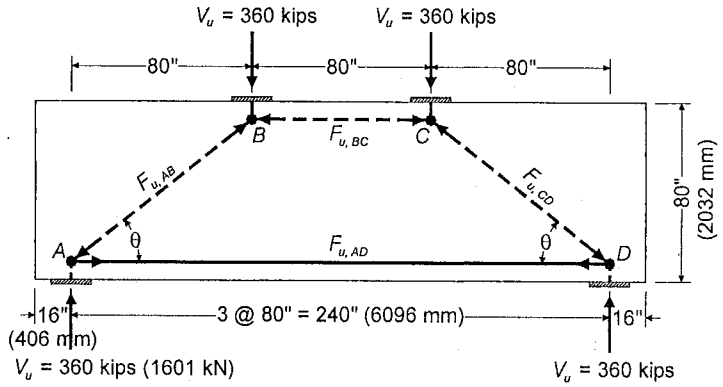

Fig. 1b-2: Selected strut-and-tie model

The horizontal position of nodes *A* and *B* is easy to define, but the vertical position of these nodes must be estimated or determined. To fully utilize the beam, the positions of these nodes have to be as close to the top and bottom of the beam. In other words, the lever arm, *jd*, of the force couple must be set maximum, and this means that the width of strut *BC*, w_s and the width to anchor tie *AD*, w_t must be minimum.

To minimize w_s strut force *BC*, $F_{u,BC}$, must reach its capacity defined in ACI Sec. A.3.2, or

$$F_{u,BC} = \phi F_{nc} = \phi f_{cu} A_c = \phi\left(0.85\beta_s f_c'\right) b w_s, \text{ where } \beta_s = 1.0 \text{ (prismatic).} \qquad \text{(1b-2)}$$

To minimize w_t tie force *AD*, $F_{u,AD}$, must reach the node capacity to anchor this tie, which is defined in ACI Sec. A.5.2, or

$$F_{u,AD} = \phi F_{nt} = \phi f_{cu} A_c = \phi\left(0.85\beta_n f_c'\right) b w_t, \text{ where } \beta_n = 0.8 \text{ (CCT node).} \qquad \text{(1b-3)}$$

Subtituting eqs. (1b-2) and (1b-3) into eq. (1b-1) gives $w_t = 1.25 w_s$ and

$$jd = 80 - w_s/2 - w_t/2 = 80 - 1.125 w_s. \qquad \text{(1b-4)}$$

Writing the moment equilibrium equation about point *A* as described in eq. (1b-5) and substituting eqs. (1b-2) and (1b-4) into the equation give $w_s = 7.95$ in., and therefore $w_t = 9.94$ in.

$$V_u(80) - F_{u,BC}\, jd = 0 \qquad \text{(1b-5)}$$

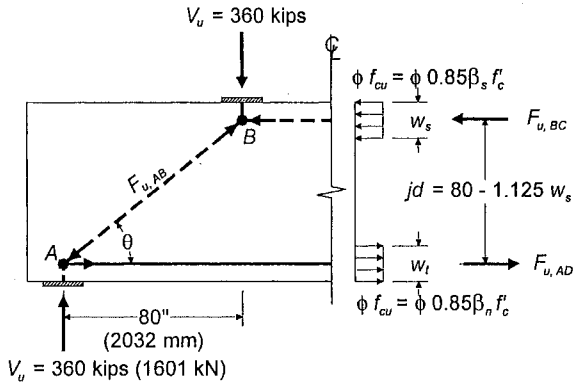

Fig. 1b-3: Free body diagram of the left third of the deep beam

If the values of w_s and w_t just obtained are used for the dimensions of the struts and ties, the stress in strut *BC*, $F_{u,BC}$ will be at its limit, and the force in tie *AD*, $F_{u,AD}$ will be anchored in just sufficient area. In this design, w_s will be selected to be 8 in. (203 mm), and w_t will be selected to be 10 in. (254 mm). Therefore, $d = 80 - 10/2 = 75$ in., $jd = 80 - 8/2 - 10/2 = 71$ in., and $F_{u,BC} = F_{u,AD} = 360(80)/71 = 406$ kips (1806 kN). Strut *BC* is located 8/2 = 4 in. (102 mm) from the top of the beam and tie AD is located 10/2 = 5 in. (127 mm) from bottom of the beam. This fixes the geometry of the truss and is illustrated in Fig. (1b-4).

The angle and the force of diagonal strut *AB* are $\theta = \arctan(71/80) = 41.6°$ and $F_{u,AB} = 360/\sin 41.6° = 542$ kips (2411 kN), respectively.

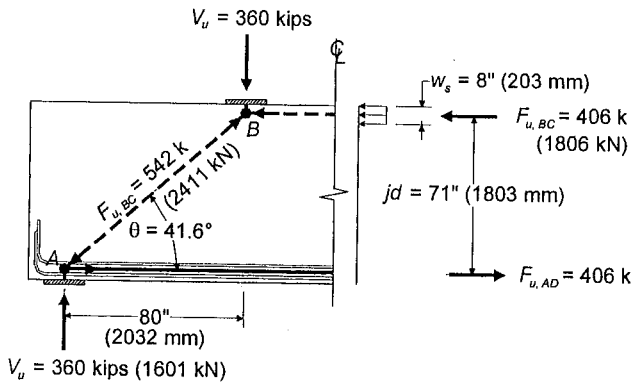

Fig. 1b-4: Strut-and-tie model dimensions and forces

3.3 Step 3: Select the tie reinforcement

Minimum tie reinforcement provided must satisfy

$$\phi F_{nt} = \phi A_{st} f_y \geq F_{u,AD} = 406 \text{ kips (1806 kN).} \quad \text{[ACI Secs. A.4.1 and A.2.6]}$$

Thus, the required area of reinforcement for tie *AD* is

$$\frac{F_{u,AD}}{\phi f_y} = \frac{406}{0.75(60)} = 9.02 \text{ in.}^2$$

Consider the following three steel arrangements:

- 1 layer of 6 #11 bars, $A_{st} = 6(1.56) = 9.36$ in.^{2}, @ 5 in. from bottom
- 2 layers of 5 #9 bars, $A_{st} = 2(5)(1.00) = 10$ in.^{2}, @ 2.5 and 7.5 in. from bottom
- 3 layers of 6 #7 bars, $A_{st} = 10.8$ in.^{2}, @ 2, 5, and 8 in. from bottom

For better steel distribution and for ease of anchorage length requirement, choose 2 layers of 5 #9 (#29 mm) bars, $A_{st} = 10$ in.^{2} (6452 mm^2).

3.4 Step 4: Design the nodal zones and check the anchorages

The 90° standard hook is used to anchor tie *AD*. The required anchorage length is

$$l_{dh} = \lambda \frac{0.02 f_y d_b}{\sqrt{f_c'}} = \frac{9.02}{10.0} \frac{0.02(60000)(1.128)}{\sqrt{4000}} = 19.3 \text{ in.,} \quad \text{[ACI Sec 12.5]}$$

where $\lambda = \dfrac{\text{required } A_{st}}{\text{provided } A_{st}}$ represents the correction factor for excess of reinforcement. ACI A.4.3.2 requires that this development length start at the point where the centroid of the reinforcement in a tie leaves the extended nodal zone and enters the span. As shown in Fig. (1b-5) left, the available development length is 27.0 in. (686 mm). Because this is greater than 19.3 in. (490 mm), the anchorage length is adequate.

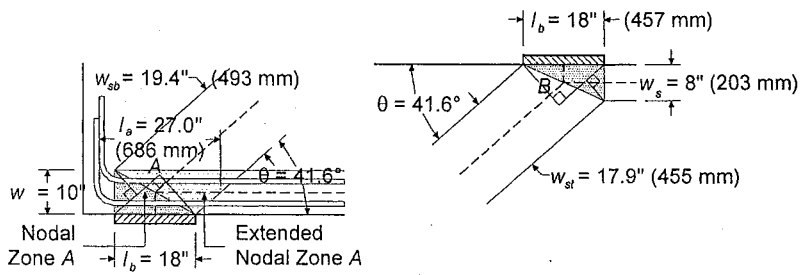

Fig. 1b-5: Nodal zones *A* and *B*

3.5 Step 5: Check the diagonal struts

From Sec. 3.2, the angle of strut *AB* (or *CD*) is $\theta = 41.6°$, and the force is $F_{u,AB} = 542$ kips (2411 kN).

As shown in Fig. (1b-5), the width at top of the strut is

$$w_{st} = l_b \sin\theta + w_s \cos\theta$$
$$= 18\sin 41.6° + 8\cos 41.6° = 17.9 \text{ in. } (455 \text{ mm}),$$

and the width at bottom of the strut is

$$w_{sb} = l_b \sin\theta + w_t \cos\theta$$
$$= 18\sin 41.6° + 10\cos 41.6° = 19.4 \text{ in. } (493 \text{ mm}).$$

Strut *AB* is expected to be a bottle-shaped strut. By assuming that sufficient crack control reinforcement is used to resist bursting force in the strut ($\beta_s = 0.75$) the capacity of strut *AB* is limited to

$$\phi F_{ns} = \phi(0.85\beta_s f_c')bw_{st}$$
$$= 0.75(0.85)(0.75)(4)(20)(17.9) \quad \text{[ACI Secs. A.2.6 and A.3.2]}$$
$$= 685 \text{ kips } (3047 \text{ kN}).$$

Because this is higher than the required force, strut *AB* (or *CD*) is adequate.

3.6 Step 6: Calculate the minimum reinforcement required for crack control

Vertical web reinforcement provided must be at least

$$A_v = 0.0025bs, \quad \text{[ACI Sec. 11.8.4]}$$

and horizontal web reinforcement provided must be at least

$$A_{vh} = 0.0015bs_2, \quad \text{[ACI Sec. 11.8.5]}$$

where s and s_2 cannot exceed $d/5$ or 12 in.

For vertical web reinforcement, use #5 (#16 mm) @ 12 in. (305 mm) on each face over entire length, $A_v / bs = 2(0.31)/20/12 = 0.0026 > 0.0025$.

For horizontal web reinforcement, use #4 (#13 mm) @ 12 in. (305 mm) on each face over entire length, $A_{vh} / bs_2 = 2(0.20)/20/12 = 0.0017 > 0.0015$.

Because β_s equal to 0.75 is used to calculate the strength of strut *AB*, minimum reinforcement provided must also satisfy

$$\sum \frac{A_{si}}{bs_i} \sin\gamma_i \geq 0.0030, \quad \text{[ACI Sec. A.3.3.1 eq. (A-4)]}$$

where γ_i is the angle between the axis of minimum reinforcement and the axis of strut. Based on the provided web reinforcement,

$$\sum \frac{A_{si}}{bs_i} \sin\gamma_i = 0.0017\sin 41.6° + 0.0026\sin 48.4° = 0.0031 \geq 0.003.$$

3.7 Step 7: Arrange the reinforcement

The reinforcement details are shown in Fig. (1b-6).

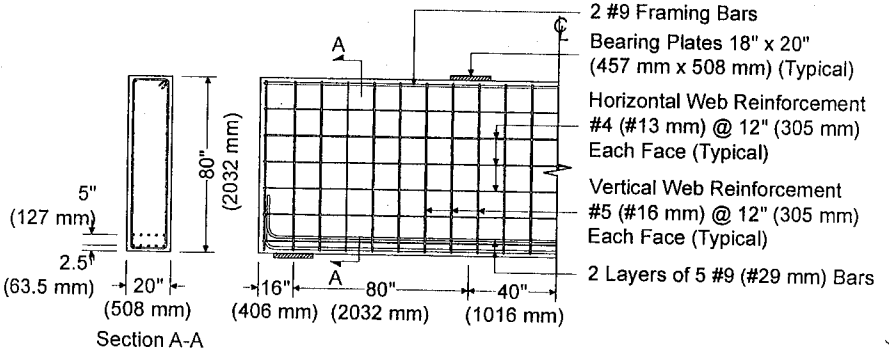

Fig. 1b-6: Reinforcement details

4 Summary

A design of a simply-supported deep beam under two point loads has been presented. This design was completed using the provisions in ACI 318-02 Appendix A "Strut-and-Tie Models."

The main steps in the design process of this deep beam involve defining the D-region and the boundary forces acting on the region, visualizing a truss carrying the boundary forces in the D-region (i.e., the strut-and-tie model), solving for the truss member forces, providing reinforcement to serve as the steel ties, dimensioning the struts and nodes, and providing distributed reinforcement for ductility.

The entire deep beam is the D-region because it is near statical discontinuities, i.e., the concentrated forces, within one section depth of the beam on either side of the discontinuity. A simple strut-and-tie model was employed in the design. This strut-and-tie model resulted in the use of 2 layers of 5 #9 (#29 mm) bars for the main tie. Particular attention was given to the anchorage of this main tie to ensure that it can carry the required force without having anchorage failure. The anchorage requirements were satisfied by the use of standard 90° hooks.

References

ACI 318.(2002): *Building Code Requirements for Structural Concrete and Commentary*. ACI Committee 318, American Concrete Institute, Detroit, Michigan, 2002, 443 pp.

Example 2: Dapped-end T-beam supported by an inverted T-beam

David H. Sanders

Synopsis

At the ends of dapped-end beams, the transfer of load from the support into the beam is a D-region. The STM is excellent for modeling such a region. In a number of applications, for example parking structures, dapped-end beams are used in conjunction with inverted T-Beams. At each point where the load of the dapped-end beam sets on the inverted T-beam, a D-region is formed. The following example used ACI 318-02 Appendix A to design both the end region of the dapped-end beam as well as the tie back and vertical reinforcement needed for each point load on the inverted T-beam. Conventional B-regions in the dapped-end beam are designed using conventional ACI beam design.

David H. Sanders received his Civil Engineering BS degree from Iowa State University and his MS and PhD degrees from the University of Texas at Austin. He is ACI Fellow. He is chair of ACI 341 Earthquake Resistant Concrete Bridges and a member of TAC. His research involves the behavior and design of concrete system with particular emphasis in bridges and seismic applications.

1 Geometry and loads

A reinforced concrete dapped-end T-beam is supported by an inverted T-beam. The web is 10 inches (254 mm) wide and the section has an overall depth of 19 inches (483 m) (see Fig. 2-1). The inverted T-beam is also 19 inches (483 mm) deep and has a seat width of 7 inches (178 mm)(see Fig. 2-2). The T-beams are spaced at 10 feet (3048 mm) along the length of the inverted T-beam and span 32 feet (9900 mm). There is a live load of 100 psf (4.79 kN/m²) and a superimposed dead load of 10 psf (0.48 kN/m²).

Each T-beam has a tributary width of 10 feet (3048 mm). Therefore, effective live load is 1.0 k/ft (14.6 kN/m) and the dead load including the superimposed dead load is 0.87 k/ft (12.7 kN/m). This produces a factored distributed load of 2.64 k/ft (38.6 kN/m) based on 1.2 Dead Load + 1.6 Live Load. The design positive moment (M_u) is 1/8 x 2.64 x 32.5^2 x 12 = 4183 in-kips (473 kN-m). The horizontal force at the support is taken as 10 kips (44.5 kN).

The concrete strength is 5500 psi (38 MPa). The reinforcement has a yield stress of 60,000 psi (414 MPa).

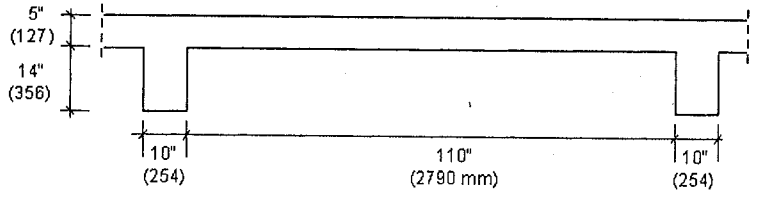

Fig. 2-1: Geometry for T-beam

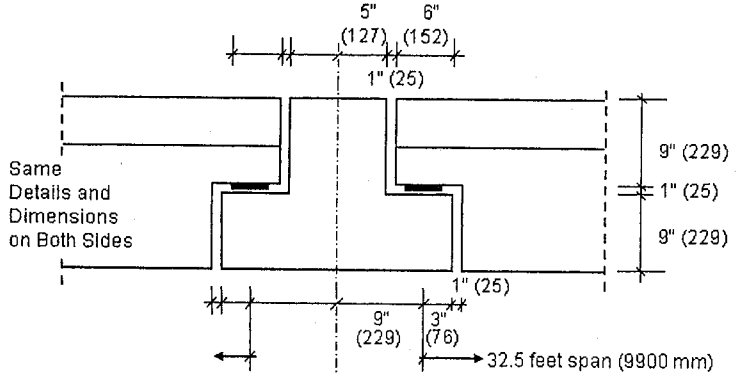

Fig. 2-2: Details of dapped end and inverted T-beam

2 Design procedure

The structure is a combination of D-Regions at the dapped end of the T-beam and near the load points of the inverted T-beam. The remaining portions of the beams are B-Regions. The simply supported dapped-end T-beam will be designed for standard beam moment and shear. The strut-and-tie model will be used to transition the forces from the beam section to the concentrated support load. The concentrated support load will then be distributed into the inverted T-beam. The following steps will be used.

- Step 1: B-region flexural design.
- Step 2: B-region shear design.
- Step 3: Strut-and-tie model for dapped end layout.
- Step 4: Design and check capacities of struts, ties and nodes.
- Step 5: Strut-and-tie model for inverted T-beam.
- Step 6: Design and check capacities of struts, ties and nodes

3 Design calculations

3.1 Step 1: B-region flexural design

The tension reinforcement was assumed to be 2 rows of #9 (29 mm) bars. Therefore effective depth, d = 19 – 1.5 – 3/8 – 9/8 – 1.25/2 = 15.375" (391 mm), see Fig. 2-3. The middle bars shown in Fig. 2-3 will be used as part of strut-and-tie model in the dapped-end region and are not part of the standard flexural design.

The effective width $b_e = b_w + 16(t) = 10 + 16(5) = 90$" (2286 mm)
Setting $M_u = 4183$ in-kips $= \Phi M_n = 0.9A_sf_y(d-a/2)$
$A_s = 5.21$ in^2 (3363 mm^2) and a = 0.74" (19 mm)
=> Use 6 #9 (29 mm) bars, $A_s = 6.0$ in^2 (3871 mm^2)
Amount of tension reinforcement satisfies both minimum and maximum A_s.

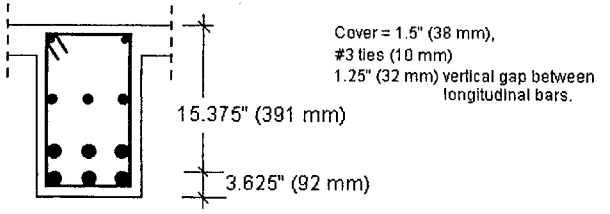

Fig. 2-3: T-beam cross-section

3.2 Step 2: Shear design

ACI 318 (1) permits the design shear to be taken at a distance d from the face of the support. Because of the dapped end, the design shear was determined at a distance d from the face of the short section (d = 7 inches (178 mm)).

$V_u = 2.64/12 \times (32.5/2 \times 12 - 4 - 7) = 40.5$ kips (180 kN)

$V_c = 2\ \text{sqrt}(f'_c)\ b_w\ d = 2\ \text{sqrt}(5500)\ 10 \times 15.375/1000 = 22.8$ kips (101 kN)

$V_u = 40.5 = \Phi V_n = \Phi\ (V_c + V_s) = 0.75\ (22.8 + V_s) \Rightarrow V_s = 31.2$ kips (139 kN)

$V_s = 31.2 = A_v f_y\ d/s = A_v/s\ 60 \times 15.375 \Rightarrow A_v/s = 0.0338$ in^2/in (0.86 mm^2/mm)

If use #3 (10 mm) hoops, $A_v = 0.22$ in^2 (142 mm^2) and s = 6 in (152 mm).

OK Since s < d/2 = 7.7 inches (196 mm)

3.3 Step 3: Develop strut-and-tie model for the dapped-end beam

The assumed strut-and-tie model is shown in Fig. 2-4. On the right side of the strut-and-tie model, the tie at the bottom of the section is assumed to be located in the center of the longitudinal tension reinforcement. The strut at the top of the section was assumed to be located at a depth equal to 10% of the overall depth. This could also be taken at the center of the compression zone as calculated in step 1. The distance between the centerlines of the top strut and the bottom tie is equal to (15.375 –0.1x19) 13.48 in (342 mm). The distributed load is divided to the closest node by using the tributary width on each side of the node.

In order to determine remaining geometry of the strut-and-tie model, the location of Tie AD, Tie BC and Tie EF must be assumed. The location of Tie AD permits sufficient room for an end plate and the cover requirements (1.5 in (38 mm)) over the reinforcement. Tie BC will consist of several stirrups and therefore the centroid must be placed away from the end of the beam. Tie EF was placed at two stirrup spacings away (12 in (305 mm)) from BC. See Fig. 2-4.

From geometry

$\tan\theta_1 = 5.1/8 \Rightarrow \theta_1 = 32.5°$ $\quad\quad$ $\tan\theta_2 = 5.1/7 \Rightarrow \theta_2 = 36.1°$

$\tan\theta_3 = 8.38/7 \Rightarrow \theta_3 = 50.1°$ $\quad\quad$ $\tan\theta_4 = 5.1/5 \Rightarrow \theta_4 = 45.6°$

From statics

Strut AB =	78.2 kips (348 kN)	Tie AD =	76.0 kips (338 kN)
Strut BD =	62.9 kips (280 kN)	Strut BE =	15.2 kips (67.6 kN)
Tie BC =	76.9 kips (342 kN)	Strut CD =	100 kips (445 kN)
Tie CF =	64.3 kips (286 kN)	Tie EF =	37.0 kips (164 kN)
Strut DE=	55.9 kips (249 kN)		

Vertical Reaction = 43.6 kips (194 kN)

Horizontal Reaction = 10 kips (44.5 kN)

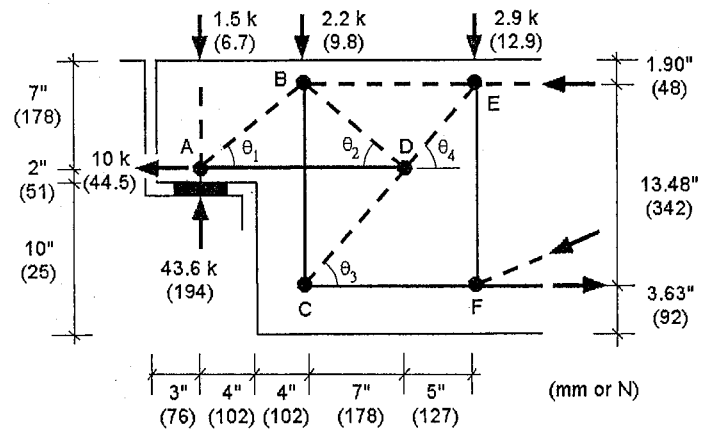

Fig. 2-4: Assumed strut-and-tie model

3.4 Step 4: Design and check capacities of struts, ties and nodes

3.4.1 Node A

Node A, the connection of Strut AB and Tie AD at the end support, must be checked (see Fig. 2-5). The bearing surface is 4 in x 7 in (102 mm x 178 mm). The potential development length for Tie AD extends to the point where Tie AD exits from Strut AB. Because of the very short development length, an end plate must be used on the end of the tie reinforcement to provide development. This plate was also taken as 4 in x 7 in (102 mm x 178 mm). A plate may not be necessary if a greater distance beyond the support or extra tie reinforcement was provided. Current ACI does not allow a reduction in development length due to a high compression load on the bar.

For the node, β_n is 0.80 because there is one tie being anchored. For Strut AB, β_S can either be 0.6 or 0.75 if sufficient stirrups are provided: $\Sigma A_{si}/bs_i \sin\gamma_i \geq 0.003$. AB=> 0.22/(10x2) x sin(90-32.5) = 0.009 > > 0.003. So, β_s = 0.75 could be used if the #3 (10 mm) ties at 2 in (51 mm) were extended into the dapped end. It will be shown that this is not necessary in order to provide capacity.

Support Capacity (A) = 0.75 (0.85 x 0.8 x 5.5) (4 x 7) = 79 kips (351 kN)

> 43.6 kips (194 kN) OK

Tie Bearing Plate Capacity (A) = 0.75 (0.85 x 0.8 x 5.5) (4 x 7) =

79 kips (351 kN) > 75.9 kips (338 kN) OK

Tie Reinf.(AD) => 75.9 kips = 0.75 ($A_{s,AD}$) 60 => $A_{S,AD}$ = 1.69 in^2 (1090 mm^2)

Use 3 #7 (22 mm) bars, $A_{S,AD}$ = 1.80 in^2 (1161 mm^2) (Could use more than one layer if wanted to shorten development length or increase node size.).

Strut AB width (perpendicular to line of action) = $l_b \sin\theta_1 + h_t \cos\theta_1$

$\doteq$ 4 sin(32.5) + 4cos(32.5) = 5.52 in (140 mm)

Assume that strut thickness equals beam width (10 inches (254 mm)).

Strut AB Capacity = 0.75 (0.85 x 0.6 x 5.5) (5.52 x10) = 116 kips (516 kN)

>78.2 kips (348 kN) OK No strut reinforcement is needed.

The dimension given in Fig. 2-5 from the bottom of the section to Tie CF is slightly different than the one in Fig. 2-4 and used to calculate the angles. This occurred because of the need to accommodate the reinforcement for Tie BC. Because the change was slight, the angles and the forces were not recalculated.

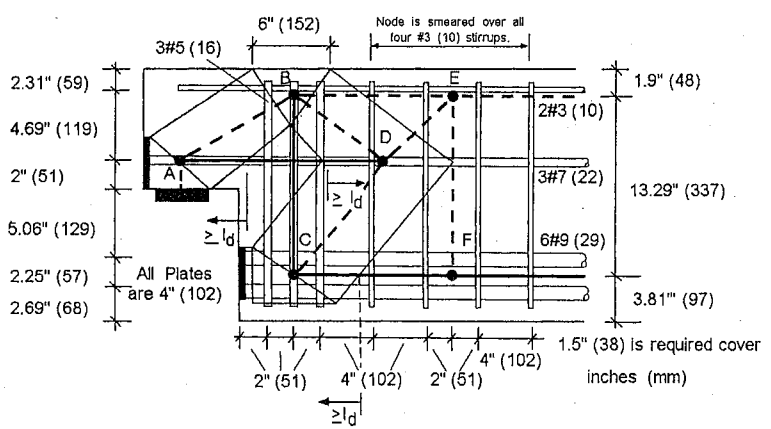

Fig. 2-5: Strut and tie details with proposed reinforcement

3.4.2 Node B

For Node B, β_n is 0.80 because there is one tie being anchored. For Strut BE, β_S is 1. The BE strut will not control because the node has a lower β than the strut. Struts AB and BD have β_s values of 0.60 and therefore will control the design for compression. The size of the struts is determined by the width of the Tie BC.

Tie BC = 76.8 kips = 0.75 ($A_{S,BC}$) 60 => $A_{S,BC}$ = 1.71 in^2 (1103 mm)

Use 3 #5 (16 mm) stirrups bars $A_{S,BC}$ = 1.86 in^2 (1200 mm)

Figure 2-5 shows the configuration of Node B. The #5 (16 mm) stirrups have been placed 2 in (51 mm) apart creating a node face of 2 x 2 + 2 = 6 inches (152 mm). The plus 2 inches (51 mm) comes from allowing some (spacing/2) spreading of the tie width beyond the reinforcement.

Strut AB width = $l_b \sin\theta + h_t \cos\theta \doteq$

6/2sin(32.5) + 3.8cos(32.5) = 4.82 in (122 mm)

Strut BD width = $l_b \sin\theta + h_t \cos\theta$ =

6/2sin(36.1) + 3.8cos(36.1) = 4.84 in (123 mm)

For Struts AB and BD, use the web thickness for strut thickness (10 inches (25 mm)). The β_S for the struts is 0.60 (bottled shaped) if reinforcement is neglected. Therefore β_S could be increased to 0.75 by providing reinforcement that satisfies A3.3.1 ($\Sigma A_{si}/bs_i \sin\gamma_i \geq 0.003$). In Fig. 2-5, the upper boundary of Strut BD is not show because the area is all compression. In addition, the strut is headed towards Node D, which is a smeared node.

Strut Capacity AB & BD = 0.75 (0.85 x 0.6 x 5.5) (4.8 x 10) = 101 kips (449 kN)

> 78.2 & 62.9 kips (348 kN & 280 kN) OK

Development for Tie BC at Node B is governed by the stirrup development checks of ACI 318 12.13 and 7.1.3. The tie must be anchored at both the top and the bottom.

3.4.3 Node C

For the node, β_n is 0.60 because there are two ties being anchored. The bottom width of the node was set by the vertical reinforcement of Tie BC, 6 inches (152 mm). In Fig. 2-5, a bearing plate is shown, this could be eliminated by moving the node/center of the reinforcement to the right or by increasing the distance between the vertical reinforcement. The development length is measured from the far right boundary of the node towards the bearing plate.

Tie CF Reinf. => 64.2 kips = 0.75 ($A_{s,CF}$) 60 => $A_{s,CF}$ = 1.43 in^2 (920 mm^2). If all 6 #9 (29 mm) bars are extended into Node C then $A_{s,CF}$ = 6.0 in^2 (3871 mm^2). The extra reinforcement will help with reducing the needed development length but it is still more than what is available. The distance available for developing Tie CF at the node is the distance from the concrete edge minus cover to where the tie leaves Strut CD: 6 – 1.5 + 2tan(50.1) = 6.9 inches (175 mm). In this case, a 5-inch x 7-inch (127 mm x178 mm) bearing plate was added to the #9 bars (29 mm).

Tie CF Bearing Plate Capacity = 0.75 (0.85 x 0.6 x 5.5) (5 x 7)

= 73.6 kips (327 kN) > 64.2 kips (286 kN) OK

Strut CD width = $l_b \sin\theta + h_t \cos\theta$ = 6sin(50.1)+4cos(50.1) = 7.2 in (182 mm)

Assume that strut thickness equals beam width (10 in (254 mm)) and that β_s = 0.6.

Strut CD Capacity = 0.75 (0.85 x 0.6 x 5.5) (7.2 x10) = 179 kips (796 kN)

100 kips (445 kN) OK

3.4.4 Node D

For Node D, the only issue is the development of Tie AD. The struts coming into Node D are distributed (smeared). The width of a strut at Node D will be equal to or greater than the strut width at the other end (Node B and Node C). Therefore, the capacity checks at Node D are satisfied by the checks in 3.4.3 and 3.4.4. The width of the strut was assumed to be constant between Nodes C and D. This defines the left boundary of the node and the point from which Tie AD can be developed.

Development length for AD => l_d/d_b = 60000 (1)(1)(1)/(25 x sqrt 5500) =>

l_d = 28.3 in (719 mm) measured from left side of Node D.

3.4.5 Nodes E and F

Both nodes are smeared over multiple stirrups. The number of stirrups is based on the force in Tie EF.

Tie EF = 37.0 kips = 0.75 ($A_{s,EF}$) 60 => $A_{s,EF}$ = 0.82 in^2 (529 mm^2). Use 4 #3 (10 mm) stirrups at 4 inches (102 mm) ($A_{s,EF}$ = 0.88 in^2 (567 mm^2). The 4 inches (102 mm) spacing provides a centroid at line EF and a distribution of stirrups between Node C and Node F.

3.4.6 Alternative models

There are other potential models that have been developed for dapped-end beams. One such model is given in the FIP Recommendations "Practical design of structural concrete" (2) (see Fig. 2-6). In experiments, a crack forms in the corner to the right of the support. In the first model (see Fig. 2-4), a strut (BD) crosses the crack, whereas in this model that compression area does not exist. This is more consistent with the crack formation since it would allow the tension area to spread further into the beam. In the alternative model, the value of Tie AD is the same as that shown in first model but the value of Tie BC and CF are much less in the FIP model. This is an acceptable strut-and-tie model solution.

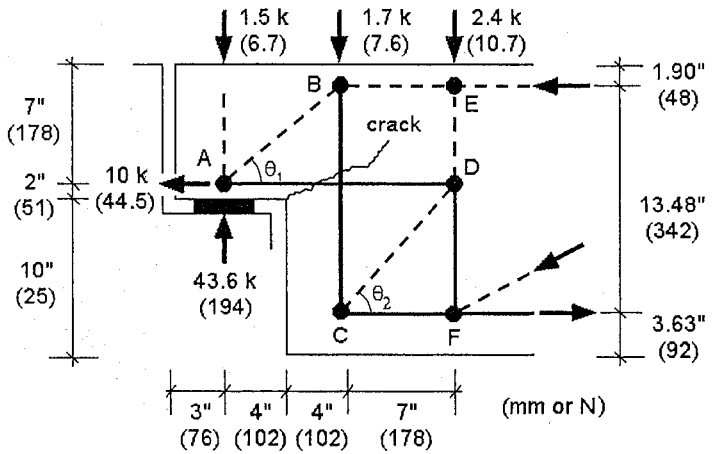

Fig. 2-6: Alternative model

From geometry

$\tan\theta_1 = 5.1/8 \Rightarrow \theta_1 = 32.5°$ $\tan\theta_2 = 8.38/7 \Rightarrow \theta_2 = 50.1°$

From statics

Strut AB =	78.2 kips (348 kN)	Tie AD =	76.0 kips (338 kN)
Strut BE =	76.0 kips (338 kN)	Tie BC =	40.4 kips (180 kN)
Strut CD =	52.7 kips (234 kN)	Tie DF =	38.0 kips (169 kN)
Tie CF =	33.8 kips (150 kN)		

Vertical Reaction = 43.6 kips (194 kN)

Horizontal Reaction = 10 kips (44.6 kN)

3.5 Step 5: Strut-and tie model layout for inverted T-beam

Fig. 2-7 shows the assumed strut-and-tie model. Along the longitudinal axis of the inverted T-beam, normal beam theory will be used.

From geometry: $\tan\theta = (5.1)/6.625) \Rightarrow \theta = 37.6$ degrees

From statics

Strut AC =	71.5 kips (318 kN)	Tie AB =	66.6 kips (296 kN)
Tie CE =	43.6 kips (194 kN)	Strut CD =	56.6 kips (252 kN)

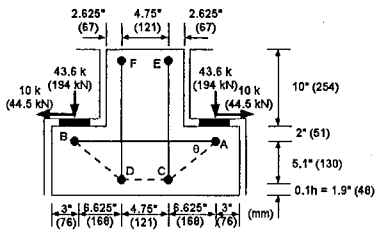

Fig. 2-7: STM for inverted T-beam for struts and ties

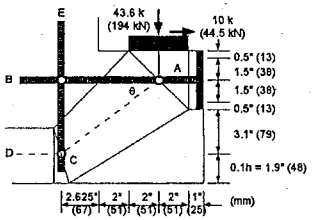

Fig. 2-8: STM details

3.6 Step 6: Design and check capacities of struts, ties and nodes for an inverted T-beam.

3.6.1 Node A

The resultant of Strut AC and Tie AB at the inverted T-beam support must be checked/designed (see Fig. 2-8). The bearing surface for the stem of the T-beam is 4 inches x 7 inches (127 mm x 178 mm). Because of the very short development length, an end plate must be used. This plate was taken as 4 inches x 7 inches (102 mm x 178 mm). It is a common practice to use this type of plate and to weld the bars to the plate.

For the node, β_n is 0.80 because there is one tie being anchored. For Strut AB, β_S can either be 0.6 or 0.75 if sufficient stirrups are provided. $\Sigma A_{si}/bs_i \sin\gamma_i \geq 0.003$.

Support Capacity = 0.75 (0.85 x 0.8 x 5.5) (4 x 7) = 78.5 kips (349 kN)
> 43.6 kips (194 kN) OK
Tie Bearing Plate Capacity = 0.75 (0.85 x 0.8 x 5.5) (4 x 7) = 78.5 kips (349 kN)
> 66.6 kips (796 kN) OK
Tie AB Reinf. => 66.6 kips = 0.75 ($A_{S,AB}$) 60 => $A_{S,AB} = 1.48$ in^2,
Use 3 #7 (22 mm) bars, $A_{S,AB} = 1.80$ in^2 (1161 mm^2)

Strut AC width (perpendicular to line of action) $= l_b \sin\theta + h_t \cos\theta$
$= 4 \sin(37.6) + 4\cos(37.6) = 5.61$ in (142 mm)
Assume that strut thickness equals the section width 10 inches (254 mm).
Strut AC Capacity @ A = 0.75 (0.85 x 0.6 x 5.5) (5.61 x 10) = 118 kips (525 kN)
> 71.5 kips (318 kN) OK

3.6.2 Node C

For Node C, there is transverse tension that comes from the longitudinal bending of the inverted T-beam. Therefore β_n is 0.60 because there would be two or more ties anchored in a three dimensional STM. For Strut AC and CD, β_S would be 0.4 because they are located in the tension zone of the member.

Tie CE Reinf. => 43.6 kips = 0.75 ($A_{S,CE}$) 60 => $A_{S,CE} = 0.97$ in^2. Use 4#5 (16 mm), $A_{S,CE} = 1.24$ in^2 (800 mm^2). Distribute as shown in Figure 2-9. Bars will be at 3 inches (76 mm) on center in the longitudinal axis of the inverted T-beam. The 3-inch (76 mm) spacing provides a distribution of stirrups over the T-beam seat width.

The location of Node C was taken at 0.1h above the bottom of the beam, therefore the height of the node is two times that or 3.8 inches (96 mm). The width of the node is governed by the vertical reinforcement (Tie CE). The width was taken as the bar size plus 1 inch (25 mm) on either side. Currently this type of guidance is not given in the Appendix. The strut width of Strut AC is equal to $l_b \sin\theta + h_t \cos\theta = (2.62) \sin(37.6) + (3.8)\cos(37.6) = 4.61$ in (117 mm). The strut thickness is equal to the width of Tie CE reinforcement in the longitudinal axis of the inverted T-beam (9") plus half the spacing (1.5" (38 mm)) on each side of the reinforcement (11.5 inches (292 mm)). Strut AC Capacity @ A = 0.75 (0.85 x 0.4 x 5.5) (4.61 x 11.5) = 74.4 kips (331 kN) > 71.5 kips (318 kN) OK

For Strut CD, the strut thickness is the same as Strut AC (11.5 inches (292 mm)) and the width is 1.9 x 2 = 3.8 inches (96 mm).
Strut CD Capacity @ C = 0.75 (0.85 x 0.4 x 5.5) (3.8 x 11.5) = 61.3 kips (273 kN)
> 56.6 kips (252 kN) OK

The node does not control the design because of the larger β value in comparison to the struts.

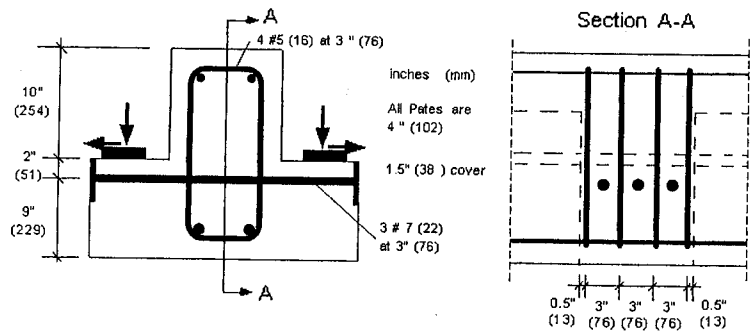

Fig. 2-9: Reinforcement details for inverted T-beam

4 Closure

The example shows the ability of the provisions of Appendix A to model the flow of forces through a structure. The models provide an engineer with a rational design tool for portions of a structure where standard beam theory does not apply.

5 Notation

a	=	depth of equivalent rectangular stress block, in (mm)
A_s	=	area of nonprestressed tension reinforcement, in^2 (mm^2)
A_{si}	=	area of surface reinforcement in the ith layer crossing a strut
$A_{s,IJ}$	=	area of reinforcement in Tie IJ, in^2 (mm^2)
A_v	=	area of shear reinforcement within a distance s, in^2 (mm^2)
b	=	width of a member, in (mm)
b_e	=	effective flange width of a T-beam based, in (mm)
d	=	distance from extreme compression fiber to centroid of tension rebar (effective depth) , in (mm)
f'_c	=	specified compressive strength of concrete, psi (MPa)
f_y	=	specified yield strength of nonprestressed reinforcement, psi (MPa)
h_t	=	effective height of a tie, in (mm)
l_b	=	length of the bearing surface, in (mm)
M_u	=	factored moment at a section, in-kips (kN-m)
s	=	spacing of stirrups along longitudinal axis of the member, in (mm)

s_i	=	spacing of reinforcement in the ith layer adjacent to the surface of the member, in (mm)
V_c	=	nominal shear strength provided by concrete, kips (kN)
V_n	=	nominal shear strength at a section, kips (kN)
V_s	=	nominal shear strength provided by shear reinforcement, kips (kN)
V_u	=	factored shear load, kips (kN)
β_n	=	factor to account for the effect of the anchorage strength of a nodal zone
β_S	=	factor to account for the effect of cracking and confining inforcement on the effective compressive strength of the concrete in a strut
γ_i	=	angle between the axis of a strut and the bars in the ith layer of reinforcement crossing that strut, degrees
Φ	=	strength reduction factor
θ	=	angle between two struts or ties at a node, degrees

6 References

American Concrete Institute (2002): *Building Code Requirements for Structural Concrete* (ACI 318-02) and Commentary (ACI 318R-02), Appendix A

FIP Recommendations (1999): *Practical Design of Structural Concrete*. FIP-Commission 3 "*Practical Design*", Sept. 1996. Publ.: SETO, London, Sept. 1999. (Distributed by: *fib*, Lausanne)

Example 3.1: Corbel at column

Tjen N. Tjhin

Daniel A. Kuchma

Synopsis

A single corbel projecting from a 14 in. (356 mm) square column is designed using the strut-and-tie method according to ACI 318-02 Appendix A. The corbel is to support a precast beam reaction force, V_u of 56.2 kips (250 kN) acting at 4 in. (102 mm) from the face of the column. A horizontal tensile force, N_{uc} of 11.2 kips (49.8 kN) is assumed to develop at the corbel top, accounting for creep and shrinkage deformations. The structure and the loads are described in Fig. (3.1-1). Normal-weight concrete with a specified compressive strength, f'_c of 5 ksi (34.5 MPa) is assumed. The yield strength of reinforcement, f_y is taken as 60 ksi (414 MPa).

The selected corbel dimensions including its bearing plate are shown in Fig. (3.1-2). The corresponding shear span to depth ratio, *a/d*, is 0.24. A simple strut-and-tie model shown in Fig. (3.1-3) is selected to satisfy the code requirements. The main tie reinforcement provided is 5 #4 (#13 mm) bars. These bars are welded to a structural steel angle of 3½ in. × 3½ in. × ½ in. (89 mm × 89 mm × 13 mm). The reinforcement details are shown in Fig. (3.1-5).

Tjen N. Tjhin is a doctoral candidate in the Department of Civil and Environmental Engineering at the University of Illinois at Urbana-Champaign. His research interests include nonlinear analysis and design of concrete structures.

Daniel (Dan) A. Kuchma is an Assistant Professor of Civil and Environmental Engineering at the University of Illinois at Urbana-Champaign. He is a member of ACI subcommittee 318E Shear and Torsion as well as joint ASCE/ACI Committee 445 Shear and Torsion and its subcommittee 445-A Strut and Tie.

1 Geometry and loads

The corbel to be designed and its loads are shown in Fig. (3.1-1).

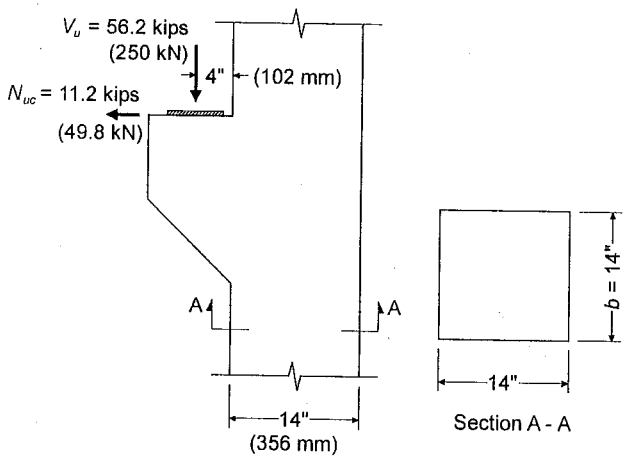

Fig. 3.1-1: Corbel geometry and loads

Material strengths:

$f_c' = 5$ ksi (34.5 MPa) (normal-weight concrete)

$f_y = 60$ ksi (414 MPa)

2 Design procedure

The entire structure under consideration is a D-Region because it has abrupt changes in geometry and is in the vicinity of concentrated forces. The structure will be designed using the strut-and-tie method according to ACI 318-02 Appendix A. The design is summarized as follows:

- Step 1: Determine the bearing plate dimensions.
- Step 2: Choose the corbel dimensions.
- Step 3: Establish the strut-and-tie model.
- Step 4: Determine the required truss forces.
- Step 5: Select the tie reinforcement.
- Step 6: Design the nodal zones and check the anchorages.
- Step 7: Check the struts.
- Step 8: Calculate the minimum reinforcement required for crack control.
- Step 9: Arrange the reinforcement.

3 Design calculations

3.1 Step 1: Determine the bearing plate dimensions

The nodal zone beneath the bearing plate is a compression-tension (CCT) node. The corresponding effective compressive strength is

$$f_{cu} = 0.85\beta_n f_c' = 0.85(0.80)(5000) = 3400 \text{ psi.} \quad \text{[ACI Sec. A.5.2 eq. (A-8)]}$$

Choose a 12 in. × 6 in. (305 mm × 152 mm) bearing plate. The bearing plate area is 12(6) = 72 in.^{2} (46452 mm.^{2}), and the bearing stress is 56.2(1000)/72 = 781 psi (5.38 MPa). Because this is less than the bearing stress limit, i.e., $\phi f_{cu} = 0.75(3400) = 2550$ psi (17.58 MPa), the bearing size is adequate.

3.2 Step 2: Choose the corbel dimensions

To be able to use ACI Appendix A, ACI Sec. 11.9.1 requires a span-to-depth ratio, *a/d*, of less than 2. Choose an overall corbel depth at column face of 18 in. (457 mm). In addition, ACI Sec. 11.9.2 requires that the depth at the outside of the bearing area is at least one-half of the depth at the column face. To satisfy this requirement, select a depth of 9 in. (229 mm) at the free end of the corbel. Fig. (3.1-2) summarizes the selected dimensions for the corbel.

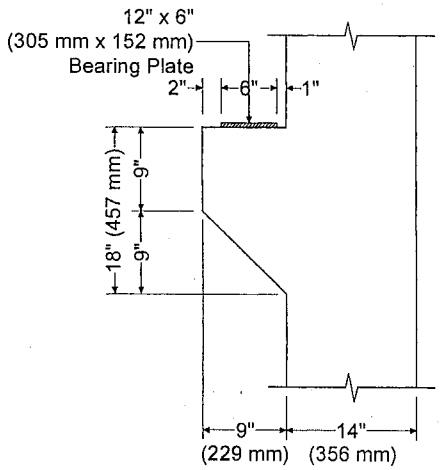

Fig. 3.1-2: Selected corbel dimensions

3.3 Step 3: Establish the strut-and-tie model

To consider load eccentricities and erection tolerances, the position of V_u is shifted 1 in. toward the outer edge of the corbel from center of bearing plate. Thus, the new position from the face of column is 1 + 6/2 + 1 = 5 in.

A simple strut-and-tie model is selected. The geometry is given in Fig. (3.1-3). The center of tie *CB* is assumed to be located 1.6 in. from the top of the corbel, considering one layer of steel bars and approximately 1 in. of concrete cover. Thus,

$$d = 18 - 1.6 = 16.4 \text{ in. (417 mm).} \qquad \text{[ACI Sec. 11.9.1]}$$

The horizontal tie *DA* is assumed to lie on the horizontal line passing through the sloping end of the corbel.

The position of strut *DD'* centerline is found by calculating the strut width w_s which can be obtained by taking moments about node *A* as follows:

$$56.2(0.32+5+12)+11.2(16.4)=F_{u,DD'}\left(12-\frac{w_s}{2}\right), \qquad (3.1\text{-}1)$$

where $F_{u,DD'} = \phi f_{cu} b w_s$ is the required compressive force in strut *DD'* and *b* is the out-of-plane dimension of the corbel. Like the node beneath the bearing plate (node *C*), node *D* is also a CCT node. Thus, its stress is limited to $\phi f_{cu} = 2550$ psi per ACI Sec. A.5.2, and $F_{u,DD'} = 2550(14)w_s/1000 = 35.7w_s$.

Substituting $F_{u,DD'}$ into eq. (3.1-1) and then solving it yield $F_{u,DD'}$ =111 kips (494 kN) and w_s=3.10 in. (79 mm).

This fixes the geometry of the truss.

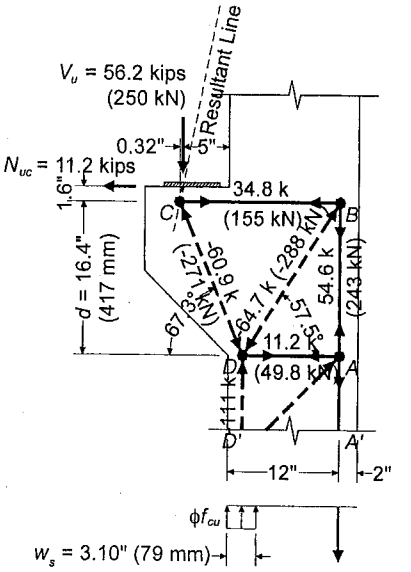

Fig. 3.1-3: Selected strut-and-tie model

3.4 Step 4: Determine the required truss forces

The required forces in all of the members of the truss are determined by statics and are shown in Table (3.1-1). A positive sign indicates that the member is tension. A negative sign indicates that the member is in compression.

Table 3.1-1: Truss forces

Member	*CD*	*CB*	*BD*	*BA*	*DA*	*DD'*
Force (kips)	-60.9 (-271 kN)	+34.8 (+155 kN)	-64.7 (-288 kN)	+54.6 (+243 kN)	+11.2 (+49.8 kN)	-111 (-494 kN)

3.5 Step 5: Select the tie reinforcement

The area of reinforcement required for tie *CB* is

$$\frac{F_{u,CB}}{\phi f_y} = \frac{34.8}{0.75(60)} = 0.77 \text{ in.}^2 \qquad \text{[ACI Secs. A.2.6 and A.4.1]}$$

The provided steel area must be at least

$$0.04\frac{f_c'}{f_y}bd = \frac{0.04(5)}{60}(14)(16.4) = 0.77 \text{ in.}^2 \qquad \text{[ACI Sec. 11.9.5]}$$

Choose 4 #4 (#13 mm) bars, $A_{st} = 4(0.20) = 0.80 \text{ in.}^2$ (516 mm^2).

As indicated in Table (3.1-1), tie *BA* has a larger tension than tie *CB*. However, this tie force should be resisted by column longitudinal reinforcement. Therefore, continue the 4 #4 bars down the column just to have a sufficient development length.

The area of reinforcement required for tie *DA* is

$$\frac{F_{u,DA}}{\phi f_y} = \frac{11.2}{0.75(60)} = 0.25 \text{ in.}^2 \qquad \text{[ACI Secs. A.2.6 and A.4.1]}$$

Choose 2 #3 (#10 mm) additional column ties at location *DA*, $A_{st} = 2(2)(0.11) = 0.44 \text{in.}^2$ (284 mm^2). These bars are spaced at 2 in. (51 mm) on center.

3.6 Step 6: Design the nodal zones and check the anchorages

The width w_s of nodal zone *D* was chosen in Sec. 3.3 to satisfy the stress limit on the nodal zone. Therefore, only nodal zone *C* is checked in this section.

To satisfy the stress limit of nodal zone *C*, the effective tie width, w_t must be at least equal to

$$\frac{F_{u,CB}}{\phi f_{cu} b} = \frac{34.8(1000)}{2550(14)} = 0.97 \text{ in. (25 mm).} \qquad \text{[ACI Secs. A.2.6 and A.5.1]}$$

This limit is easily satisfied because the available tie width is 2(1.6) = 3.2 in. (81 mm). See Fig. (3.1-4).

To anchor tie *CB*, weld the 4 #4 bars to a steel angle of 3½ in. × 3½ in. × ½ in. (89 mm × 89 mm × 13 mm). The details are shown in Fig. (3.1-5).

3.7 Step 7: Check the struts

Strut *CD* will be checked based on the sizes determined by nodal zones *C* and *D*. Other struts will be checked by computing the strut widths and checked whether they will fit within the space available.

The nominal strength of strut *CD* is limited to

$$F_{ns} = f_{cu} A_c, \qquad \text{[ACI Sec. A.3.1 eq. (A-2)]}$$

where

$$f_{cu} = 0.85\beta_s f_c' = 0.85(0.75)(5000) = 3188 \text{ psi} \qquad \text{[ACI Sec. A.3.2 eq. (A-3)]}$$

and A_c is the smaller area at the two ends of the strut. From Fig. (3.1-4), $A_c = 14(2.86) = 40.04 \text{in.}^2$. Thus, $F_{ns} = 3188(40.04)/1000 = 128$ kips. From Table 3.1-1, the factored load of strut *CD* is 60.9 kips (271 kN). Because this is less than the limit, i.e., $\phi F_{ns} = 0.75(128) = 96$ kips (427 kN), strut *CD* is adequate. Because β_s is assumed to be 0.75, minimum reinforcement will be provided; the calculations are presented in the next section.

The effective compressive strength of strut *BD* is also limited to $f_{cu} = 3188$ psi. Hence, the required width for strut *BD* is

$$\frac{F_{u,BD}}{\phi f_{cu} b} = \frac{64.7(1000)}{0.75(3188)(14)} = 1.93 \text{ in.} \qquad \text{[ACI Secs. A.2.6 and A.3.1]}$$

Choose 2 in. (51 mm) width for strut *BD*. The required width for strut *DD'* was determined in Sec. 3.2, i.e., 3.10 in. (79 mm).

As shown in Fig. (3.1-4), all the strut widths fit into the outline of the corbel region. Thus, this solution is accepted.

3.8 Step 8: Calculate the minimum reinforcement required for crack control

ACI Sec. 11.9.4 requires closed stirrups or ties parallel to the reinforcement required for tie *CB* to be uniformly distributed within 2/3 of the effective depth adjacent to tie *CB*, i.e., 2/3 (16.4) = 10.9 in. Use 10.5 in. The area of these ties must exceed

$$A_h = 0.5(A_{st} - A_n), \qquad \text{[ACI Sec. 11.9.4]}$$

where A_n is the area of reinforcement resisting the tensile force N_{uc} and $A_{st} \equiv A_s$ of ACI Sec. 11.9. Hence, the minimum area required is

$$A_h = 0.5(A_{st} - A_n)$$
$$= 0.5\left(A_{st} - \frac{N_{uc}}{\phi f_y}\right) = 0.5\left(0.80 - \frac{11.2}{0.85(60)}\right) = 0.29 \text{ in.}^2$$

Try 3 #3 closed stirrups, $A_v = 3(2)(0.11) = 0.66$ in.², with average spacing of 10.5/3 = 3.5 in.

Because β_s equal to 0.75 is used for the diagonal struts, minimum reinforcement provided must also satisfy

$$\sum \frac{A_{si}}{bs_i} \sin\gamma_i \geq 0.0030, \qquad \text{[ACI Sec. A.3.3.1 eq. (A-4)]}$$

where γ_i is the angle between the axis of minimum reinforcement and the axis of strut. According ACI Sec. A.3.3.2, γ_i has to be greater than 40° because only horizontal reinforcement is provided. Based on the provided reinforcement and the angle of strut *BD*, i.e., the smallest angle between strut and minimum reinforcement,

$$\sum \frac{A_{si}}{bs_i} \sin\gamma_i = \frac{2(0.11)}{14(3.5)} \sin 57.5° = 0.0038 > 0.003.$$

Because this amount of reinforcement satisfies both requirements, provide 3 #3 (#10 mm) closed stirrups at 3.5 in. (89 mm) spacing, distributed over a depth of 10.5 in. (267 mm) from tie *CB*.

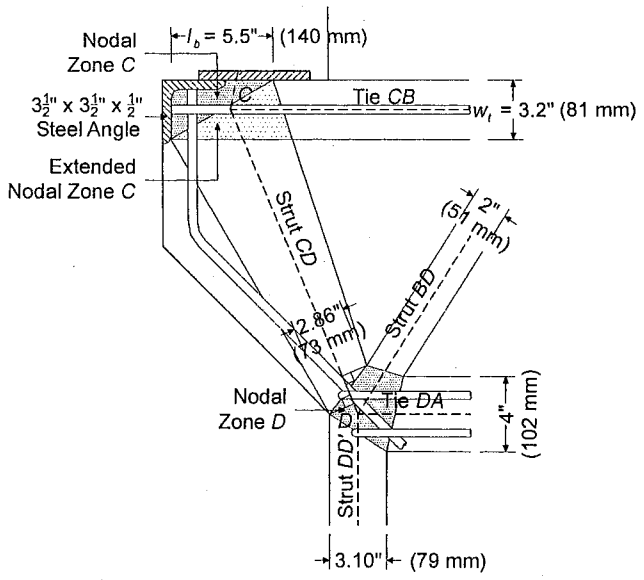

Fig. 3.1-4: Dimensions of strut-and-tie model components

3.9 Step 9: Arrange the reinforcement

The reinforcement details are shown in Fig. (3.1-5).

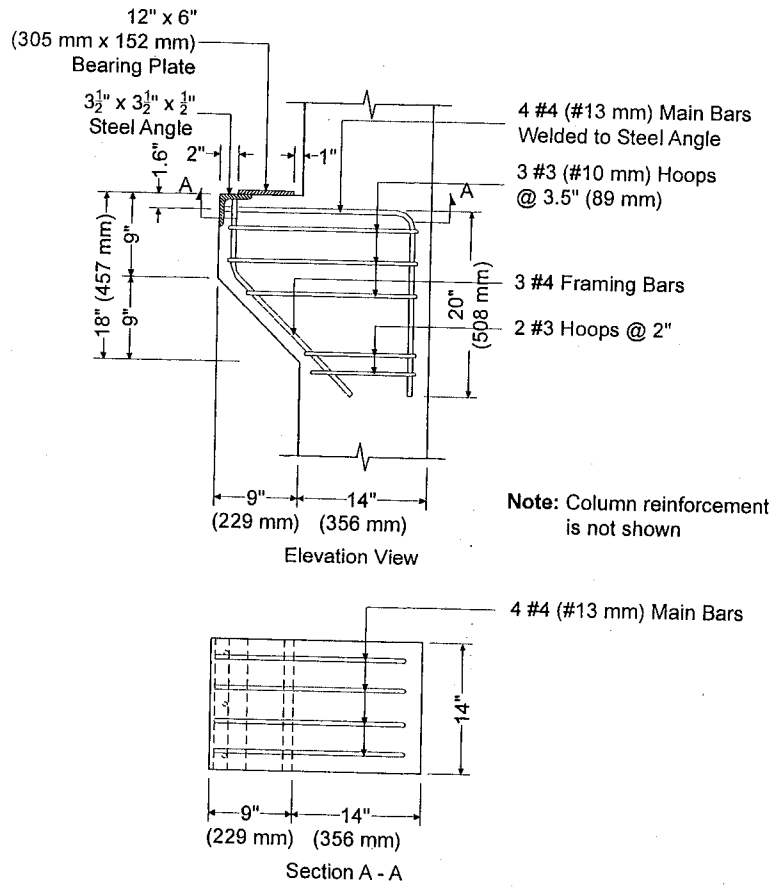

Fig. 3.1-5: Reinforcement details

4 Summary

The design of a single corbel has been presented. This design was completed using ACI 318-02 Appendix A "Strut-and-Tie Models" and the ACI 318-02 Sec. 11.9 "Special Provisions for Brackets and Corbels".

The main steps in this design involve defining the D-region and the boundary forces acting on the region, selecting a strut-and-tie model carrying the boundary forces in the D-region, solving for the member forces of the strut-and-tie model, providing reinforcement to serve as the steel ties, dimensioning the struts and nodes, and providing distributed reinforcement for crack control and ductility.

In this design, the entire corbel is the D-region, and a simple strut-and-tie model was employed.

The entire corbel is the D-region because there exist statical discontinuities, i.e., the concentrated forces, and geometrical discontinuities within one section flexural depth of the corbel on either side of the discontinuity. A simple strut-and-tie model was employed in the design. This strut-and-tie model resulted in the use of one layer of 4 #4 (#13 mm) bars for the main tie. Sufficient anchorage of this tie is required to ensure that it can carry the required force without having anchorage failure. This is achieved by welding all of the main bars to a structural steel angle.

References

ACI 318-02: *Building Code Requirements for Structural Concrete and Commentary*. ACI Committee 318, American Concrete Institute, Detroit, Michigan, 2002, 443 pp.

Example 3.2: Double corbel

Tjen N. Tjhin

Daniel A. Kuchma

Synopsis

A double corbel projecting from an interior column is designed using the strut-and-tie method according to ACI 318-02 Appendix A. The corbel transfers precast beam reaction forces, V_u of 61.8 kips (275 kN) acting at 6 in. (152 mm) from the face of the column at both ends. To account for beam creep and shrinkage deformations, a factored horizontal force, N_{uc} of 14.3 kips (63.6 kN) is assumed to develop at each side of the corbel top. The column is 14 in. (356 mm) square. The upper column carries a factored compressive axial load, P_u of 275 kips (1223 kN). The compressive strength of concrete, f'_c and yield strength of steel reinforcement, f_y are taken as 4 ksi (27.6 MPa) and 60 ksi (414 MPa), respectively. Normal-weight concrete is assumed.

The selected dimensions including the bearing plates are shown in Fig. (3.2-2). The shear span to depth ratio, *a/d*, is 0.38. A simple strut-and-tie model shown in Fig. (3.2-3) was used for the design. The provided main tie reinforcement is 7 #4 (#13 mm) bars. The anchorage of these bars is provided by welding each end of the bars to a structural steel angle of 4 in. × 4 in. × ½ in. (102 mm × 102 mm × 13 mm). The reinforcement details are shown in Fig. (3.2-5).

Tjen N. Tjhin is a doctoral candidate in the Department of Civil and Environmental Engineering at the University of Illinois at Urbana-Champaign. His research interests include nonlinear analysis and design of concrete structures.

Daniel (Dan) A. Kuchma is an Assistant Professor of Civil and Environmental Engineering at the University of Illinois at Urbana-Champaign. He is a member of ACI subcommittee 318E Shear and Torsion as well as joint ASCE/ACI Committee 445 Shear and Torsion and its subcommittee 445-A Strut and Tie.

1 Geometry and loads

The geometry and loads of the corbel to be designed are shown in Fig. (3.2-1).

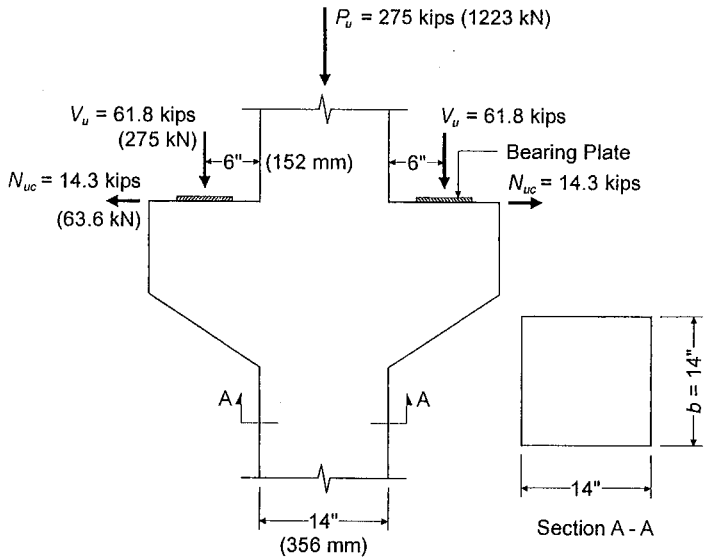

Fig. 3.2-1: Geometry and loads of the corbel

Material strengths:

$f_c^{'}$ = 4 ksi (27.6 MPa) (normal-weight concrete)

f_y = 60 ksi (414 MPa)

2 Design procedure

The entire corbel is a D-Region because it has abrupt changes in geometry and is in the vicinity of concentrated forces. The structure will be designed using the strut-and-tie method according to ACI 318-02 Appendix A. The step-by-step design procedure is as follows:

- Step 1: Determine the bearing plate dimensions
- Step 2: Choose the corbel dimensions.
- Step 3: Establish the strut-and-tie model.
- Step 4: Determine the required truss forces.
- Step 5: Select the tie reinforcement.
- Step 6: Design the nodal zones and check the anchorages.
- Step 7: Check the struts.
- Step 8: Calculate the minimum reinforcement required for crack control.
- Step 9: Arrange the reinforcement.

It is necessary only to consider a half portion of the corbel because the geometry and loading are symmetric about a vertical axis passing through the centroid of column. However, the entire corbel will be shown in almost all of the figures for better illustration.

3 Design calculations

3.1 Step 1: Determine the bearing plate dimensions

The nodal zone underneath the bearing plate is a compression-tension (CCT) node. The effective compressive strength of this node is limited to

$$f_{cu} = 0.85\beta_n f_c^{'} = 0.85(0.80)(4000) = 2720 \text{ psi.} \qquad \text{[ACI Sec. A.5.2 eq. (A-8)]}$$

Choose a 12 in. × 6 in. (305 mm × 152 mm) bearing plate. The bearing plate area is 12(6) = 72 in.^{2} (46452 mm.^{2}). The bearing stress is 61.8(1000)/72 = 858 psi (5.92 MPa). Because this is less than the bearing stress limit, i.e., $\phi f_{cu} = 0.75(2720) = 2040$ psi (14.07 MPa), the bearing size is adequate.

3.2 Step 2: Choose the corbel dimensions

To be able to use ACI Appendix A, ACI Sec. 11.9.1 requires a span-to-depth ratio, *a/d*, of less than 2. In addition, ACI Sec. 11.9.2. requires that the depth at the outside of the bearing area be at least 0.5*d*. Therefore, select a column face depth of 18 in. (457 mm) and select a depth of 10 in. (254 mm) at the free end of the corbel. The selected dimensions for the corbel are summarized in Fig. (3.2-2).

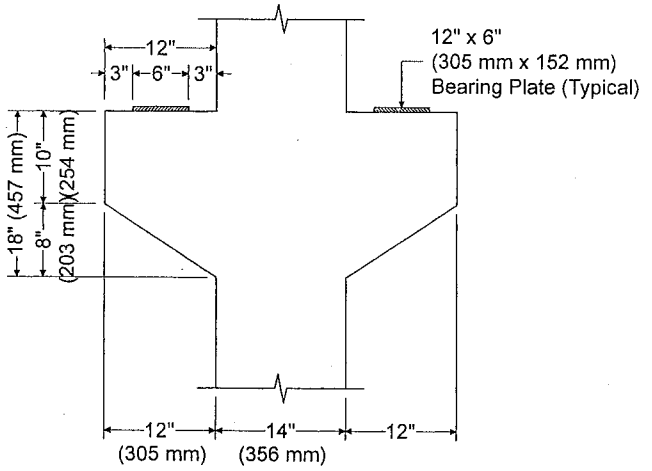

Fig. 3.2-2: Selected corbel dimensions

3.3 Step 3: Establish the strut-and-tie model

To allow for load eccentricities and erection tolerances, consider the reaction force, V_u to be placed 1 in. toward the edge of the corbel from center of bearing plate. Thus, the new position of V_u from the face of column is 3 + 6/2 + 1 = 7 in.

Fig. (3.2-3) shows the geometry of the assumed strut-and-tie model. The location of tie *AA'* is assumed to be 2 in. from the top of the corbel, considering two layers of steel bars and approximately 1 in. of concrete cover. Thus,

$$d = 18 - 2 = 16 \text{ in. (406 mm).} \qquad \text{[ACI Sec. 11.9.1]}$$

The horizontal strut *BB'* is assumed to lie on the horizontal line passing through the sloping end of the corbel.

As shown in Fig. (3.2-3), the column axial load, P_u is resolved into two even loads acting in line with strut *CB*. The location of strut *CB* centerline can be found by calculating its strut width, w_s This width can be obtained from

$$w_s = \frac{F_{u,CB}}{\phi f_{cu} b}, \qquad \text{[ACI Secs. A.3.1 and A.2.6] (3.2-1)}$$

where $F_{u,CB}$ is the required compressive force in strut *CB*, and b = 14 in. is the out-of-plane dimension of the corbel. The strut *CB* force is $F_{u,CB}$ = 275/2 + 61.8 = 199.3 kips. Because nodal zone *B* is an all-compression (CCC) node and strut *CB* is of prismatic type, the effective compressive strength, f_{cu}, is

$$f_{cu} = 0.85\beta_n f_c' = 0.85(1.0)(4000) = 3400 \text{ psi.} \qquad \text{[ACI Sec. A.3.2 eq. (A-3)]}$$

Substituting the above values into eq. (3.2-1) gives w_s = 5.58 in. (142 mm).

This fixes the geometry of the strut-and-tie model.

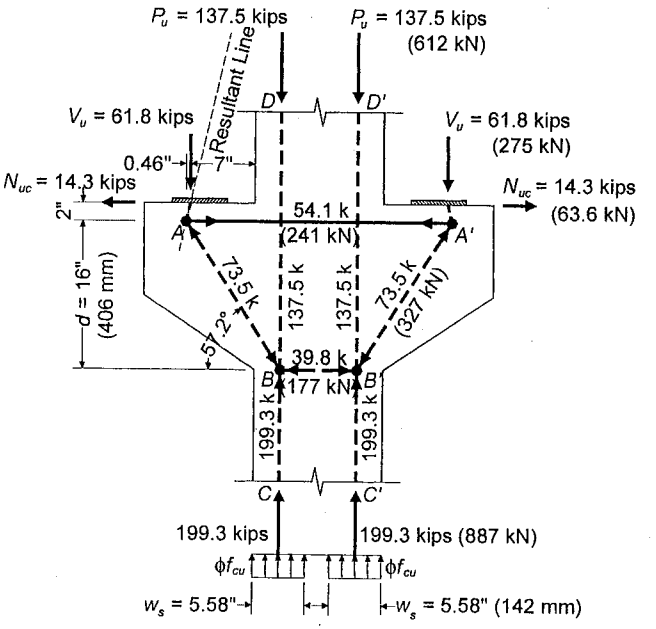

Fig. 3.2-3: Selected strut-and-tie model

3.4 Step 4: Determine the required truss forces

The required forces in all the members of the truss are determined by statics and are shown in Table (3.2-1). Note that positive sign indicates tension; negative sign indicates compression.

Table 3.2-1: Truss forces

Member	*AA'*	*AB= A'B'*	*BB'*	*CB = C'B'*	*BD = B'D'*
Force (kips)	+54.1 (+241 kN)	-73.5 (-327 kN)	-39.8 (-177 kN)	-199.3 (-887 kN)	-137.5 (-612 kN)

3.5 Step 5: Select the tie reinforcement

The required area of reinforcement for tie *AA'* is

$$\frac{F_{u,AA'}}{\phi f_y} = \frac{54.1}{0.75(60)} = 1.20 \text{ in.}^2 \qquad \text{[ACI Secs. A.2.6 and A.4.1]}$$

Further, the provided steel area must be at least

$$0.04\frac{f_c'}{f_y}bd = \frac{0.04(4)}{60}(14)(16) = 0.60 \text{ in.}^2 \qquad \text{[ACI Sec. 11.9.5]}$$

Choose 6 #4 (#13 mm) bars, $A_{st} = 6(0.20) = 1.20$ in.^{2} (774 mm^2). These bars are arranged in two layers as shown in Fig. (3.2-5).

3.6 Step 6: Design the nodal zones and check the anchorages

The width w_s of nodal zone *B* was determined in Sec. 3.3 to satisfy the stress limit on the nodal zone. Therefore, only nodal zone *A* is checked in this section.

To satisfy the stress limit of nodal zone *A*, the tie reinforcement must engage an effective depth of concrete, w_t at least equal to

$$\frac{F_{u,AA'}}{\phi f_{cu} b} = \frac{54.1(1000)}{2040(14)} = 1.89 \text{ in. (48 mm).} \qquad \text{[ACI Secs. A.2.6 and A.5.1]}$$

As shown in Fig. (3.2-4), this limit is easily satisfied because the nodal zone available is 2(2) = 4 in. (102 mm).

To anchor tie *AA'*, weld the 6 #4 bars to a steel angle of 4 in. × 4 in. × ½ in. (102 mm × 102 mm × 13 mm). The details are shown in Fig. (3.2-5).

3.7 Step 7: Check the struts

Strut *AB* will be checked based on the sizes determined by nodal zones *A* and *B*. Other struts will be checked by computing the strut widths and checked whether they will fit within the space available.

ACI defines the nominal strength of strut *AB* as

$$F_{ns} = f_{cu} A_c, \qquad \text{[ACI Sec. A.3.1 eq. (A-2)]}$$

where

$$f_{cu} = 0.85\beta_s f_c' = 0.85(0.75)(4000) = 2550 \text{ psi} \qquad \text{[ACI Sec. A.3.2 eq. (A-3)]}$$

and A_c is the smaller area at the two ends of the strut. From Fig. (3.2-4), $A_c = 14(4.88) = 68.32$ in.^{2} Thus, $F_{ns} = 2550(68.32)/1000 = 174$ kips. From Table 3.2-1, the factored load of strut *AB* is 73.5 kips (327 kN). Because this is less than the limit, i.e., $\phi F_{ns} = 0.75(174) = 131$ kips (583 kN), strut *AB* is adequate. Because β_s is assumed to be 0.75, minimum reinforcement has to be provided and is described in the next section.

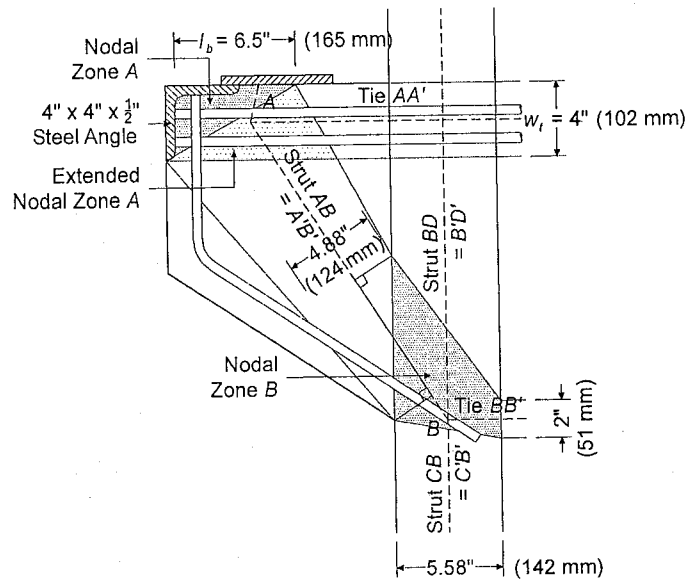

Fig. 3.2-4: Dimensions of strut-and-tie model components

The stress of the horizontal strut *BB'* is limited to

$$\phi f_{cu} = 0.75\left(0.85\beta_s f_c'\right) = 0.75[0.85(1.0)(4000)] = 2550 \text{ psi.} \quad \text{[ACI Secs. A.2.6 and A.3.2]}$$

Hence, the required width for strut *BB'* is

$$\frac{F_{u,BB'}}{\phi f_{cu} b} = \frac{39.8(1000)}{2550(14)} = 1.11 \text{ in.} \quad \text{[ACI Secs. A.2.6 and A.3.1]}$$

The stress of the vertical strut *BD* is limited to

$$\phi f_{cu} = 0.75\left(0.85\beta_s f_c'\right) = 0.75[0.85(0.6)(4000)] = 1800 \text{ psi.} \quad \text{[ACI Secs. A.2.6 and A.3.2]}$$

Hence, the required width for strut *BD* is

$$\frac{F_{u,BD}}{\phi f_{cu} b} = \frac{137.5(1000)}{1800(14)} = 5.46 \text{ in.} \quad \text{[ACI Secs. A.2.6 and A.3.1]}$$

Choose 2 in. (51 mm) width for strut *BB'*, and set the width of strut *BD* equals the width of strut *CB*. The required width for strut *CB* has been computed in Sec. 3.2, i.e., 5.58 in. (142 mm).

As shown in Fig. (3.2-4), all the strut widths fit into the outline of the corbel region. Thus, this solution is accepted.

3.8 Step 8: Calculate the minimum reinforcement required for crack control

ACI Sec. 11.9.4 requires closed stirrups or ties parallel to the reinforcement required for tie *AA'* to be uniformly distributed within 2/3 of the effective depth adjacent to tie *CB*, i.e., 2/3 (16) = 10.7 in. Use 10.5 in. In addition, the area of these ties must exceed

$$A_h = 0.5\left(A_{st} - A_n\right), \quad \text{[ACI Sec. 11.9.4]}$$

where A_n is the area of reinforcement resisting the tensile force N_{uc} and $A_{st} \equiv A_s$ of ACI Sec. 11.9. Hence, the minimum area required is

$$0.5\left(A_{st} - A_n\right) = 0.5\left(A_{st} - \frac{N_{uc}}{\phi f_y}\right) = 0.5\left(1.40 - \frac{14.3}{0.85(60)}\right) = 0.56 \text{ in.}^2$$

Try 3 #3 closed stirrups, $A_v = 3(2)(0.11) = 0.66 \text{ in.}^2$, with average spacing of 10.5/3 = 3.5 in.

Because $\beta_s$equal to 0.75 is used to calculate the strength of strut *AB*, minimum reinforcement provided must also satisfy

$$\sum \frac{A_{si}}{bs_i} \sin\gamma_i \geq 0.0030, \quad \text{[ACI Sec. A.3.3.1 eq. (A-4)]}$$

where γ_i is the angle between the axis of minimum reinforcement and the axis of strut. In this design, γ_i has to be greater than 40° per ACI Sec. A.3.3.2 because only horizontal reinforcement is provided. Based on the provided reinforcement,

$$\sum \frac{A_{si}}{bs_i} \sin\gamma_i = \frac{2(0.11)}{14(3.5)} \sin 57.2° = 0.0038 > 0.0030.$$

Because this amount of reinforcement satisfies both requirements, provide 3 #3 (#10 mm) closed stirrups at 3.5 in. (89 mm) spacing, distributed over a depth of 10.5 in. (267 mm) from tie *AA'*.

3.9 Step 9: Arrange the reinforcement

The reinforcement details are shown in Fig. (3.2-5).

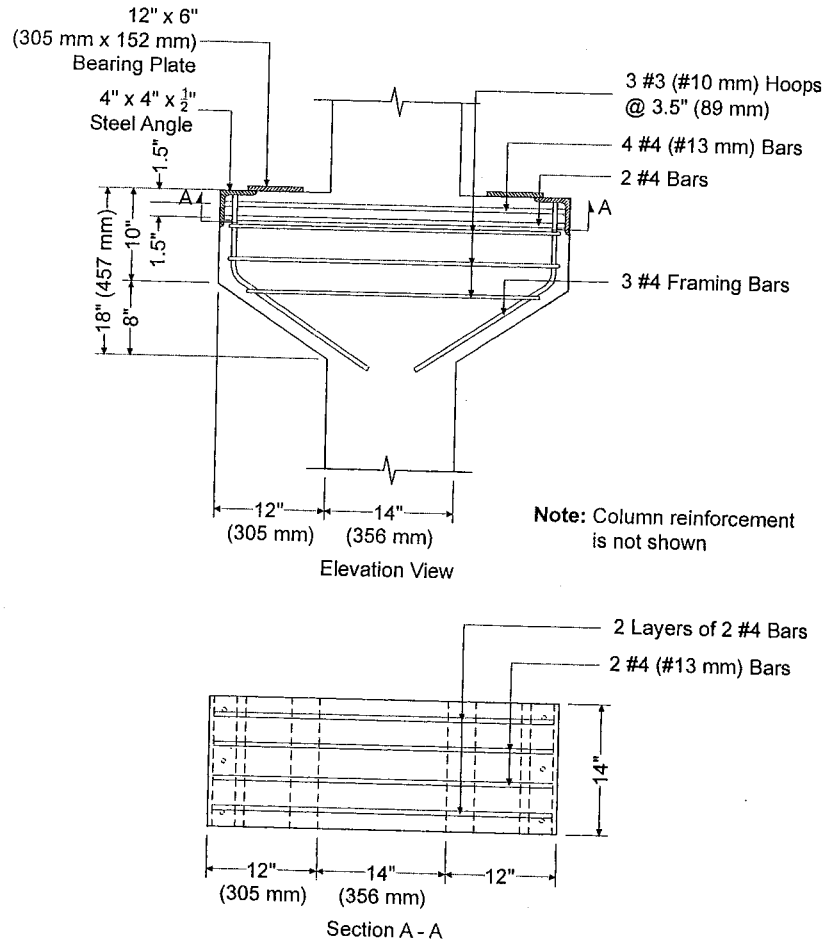

Fig. 3.2-5: Reinforcement details

4 Summary

The design of a double corbel has been presented. This design was completed using ACI 318-02 Appendix A "Strut-and-Tie Models" and the ACI 318-02 Sec. 11.9 "Special Provisions for Brackets and Corbels."

The main steps in this design involve defining the D-region and the boundary forces acting on the region, selecting a strut-and-tie model carrying the boundary forces in the D-region, solving for the member forces of the strut-and-tie model, providing reinforcement to serve as the steel ties, dimensioning the struts and nodes, and providing distributed reinforcement for crack control and ductility.

The entire corbel is the D-region because there exist statical discontinuities, i.e., the concentrated forces, and geometrical discontinuities within one section flexural depth of the corbel on either side of the discontinuity. A simple strut-and-tie model was employed in the design. This strut-and-tie model resulted in the use of 6 #4 (#13 mm) bars for the main tie. Particular attention was given to the anchorage of the main tie to ensure that it can carry the required force without having anchorage failure. To satisfy the anchorage requirements, all of the main bars are welded to a structural steel angle that is provided at each end.

References

ACI 318-02: *Building Code Requirements for Structural Concrete and Commentary*. ACI Committee 318, American Concrete Institute, Detroit, Michigan, 2002, 443 pp.

Example 4: Deep beam with opening

Lawrence C. Novak, SE

Heiko Sprenger

Synopsis:

The example problem of a deep beam with a rectangular opening represents a strong example of the application of Strut-and-Tie modeling of reinforced concrete structures. Since the entire beam constitutes a D-region, this example demonstrates the principles and methods that can be utilized to solve a wide range of problems. Example #4 has been fully evaluated per the requirements of Appendix A of ACI 318-02.

Lawrence C. Novak, SE is an Associate Partner with Skidmore, Owings & Merrill LLP, 224 South Michigan Ave., Chicago, IL 60604 (He is a member of ACI, SEAOI, ASCE and a voting member of ACI-209)

Heiko Sprenger recently graduated from University of Stuttgart and is an Intern Engineer with Skidmore, Owings & Merrill LLP, 224 South Michigan Ave., Chicago, IL 60604

1 System

The deep beam with an opening (Fig. 4.1) has been designed according to Appendix A of ACI 318-02 – Strut-and-Tie Models. The system as a whole is considered a D-Region because of force and geometric discontinuity.

For simplicity, the self-weight of the structure has been accounted for by an appropriate increase in the applied point load.

Materials:

Concrete – specified compression strength of concrete

$$f'_c = 4{,}500\,psi \qquad (31\frac{N}{mm^2})$$

Steel – specified yield strength of nonprestressed reinforcement

$$f_y = 60{,}000\,psi \qquad (414\frac{N}{mm^2})$$

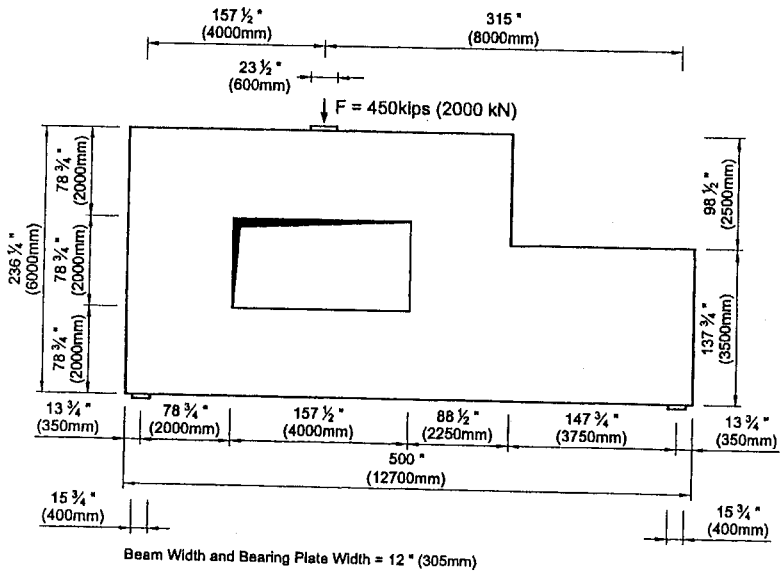

Fig. 4-1: Deep beam geometry

2 Strut-and-Tie Model

2.1 Finding the model

The structure behaves as an upper deep beam spanning to sloped columns supported on a lower deep beam. Based on that anticipated behavior, the internal strut-and-tie model (see Fig. 4-2) is developed. The strut-and-tie model can be based on either engineering judgement or a finite element analysis of the load flow. Usually the strut-and-tie model is selected such that the ties are located where the engineer anticipates the main reinforcement to be positioned for ease of constructability (in this case above and below the opening and at the bottom of the lower deep beam).

Note: According to ACI318-02, Section RA.1-Definitions – D-Region, the smallest angle permitted between a strut and a tie in a D-Region is 25 degrees. In this chosen model, the smallest angle is 34 degrees.

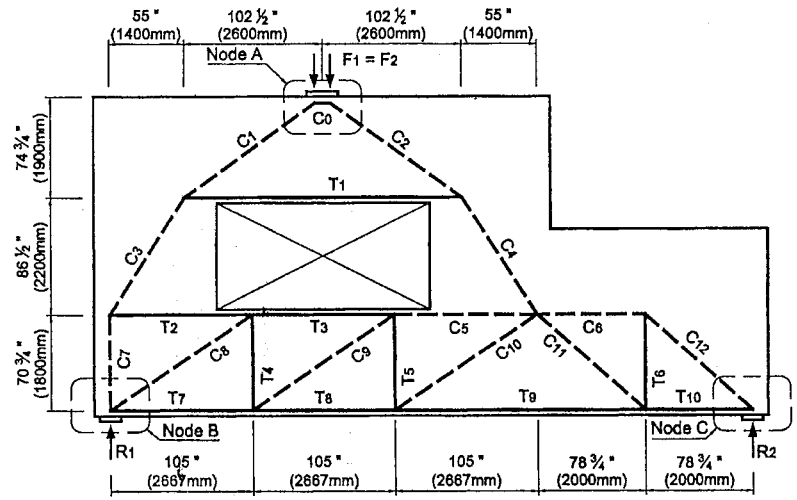

Fig. 4-2: The geometry of the chosen Strut-and-Tie Model

2.2 Forces

For the external forces determine reactions by summing moments about the lower left bearing (see Fig. 4-1).

$$M = 450kips \cdot 157.5" - R_2 \cdot 472.5"$$
$$\rightarrow R_2 = 150kips \quad (667kN)$$
$$\rightarrow R_1 = 300kips \quad (1{,}333kN)$$

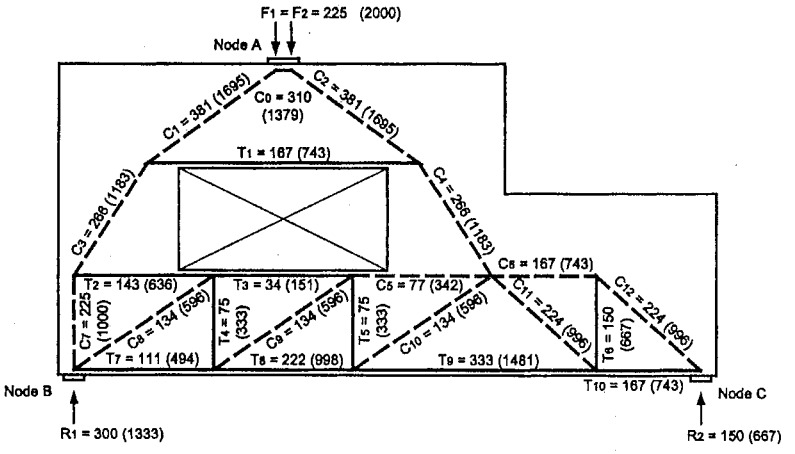

Fig. 4-3: Forces (C-Compression, T-Tension) of the Strut-and-Tie-Model (in *kips*, *kN* in parentheses) determined according to Method of Joints

3 Design calculations

Strength Reduction Factor according to ACI 318-02 Chapter 9.3.2.6

$$\phi = 0.75$$

3.1 Check bearing strength

Note: the width of the bearing plate matches the beam width.

ACI 318-02 Equation A-1

$$\phi \cdot F_n \geq F_u$$

and ACI 318-02 Equation 10.17.1

$$F_n = 0.85 \cdot f'_c \cdot A$$

with

$$f'_c = 4{,}500psi$$
$$\rightarrow F_n = 3{,}825psi \cdot A$$

Plate at node A

$$P = 450kips$$
$$A = 23\,1/2" \cdot 12" = 282in^2$$
$$\rightarrow 0.75 \cdot 3{,}825psi \cdot 282in^2 = 809kips \geq 450kips \quad (3{,}598kN \geq 2{,}000kN) \rightarrow \text{OK}$$

Plate at nodes B & C

$$R_1 = 300kips \geq 150kips = R_2$$
$$A = 15\,3/4" \cdot 12" = 189in^2$$
$$\rightarrow 0.75 \cdot 3{,}825kips \cdot 189in^2 = 542kips \geq 300kips \quad (2{,}410kN \geq 1{,}333kN) \rightarrow \text{OK}$$

Note: The node checks of Appendix A will typically govern over the bearing checks of ACI 318-02 Chapter 10

3.2 Ties

ACI 318-02 Equation A-1

$$\phi \cdot F_n \geq F_u \rightarrow F_n = \frac{F_u}{\phi}$$

with ACI 318-02 Equation A-6 – nominal strength of a tie

$$F_{nt} = A_{st} \cdot f_y + A_{ps} \cdot (f_{se} + \Delta f_p)$$

$$A_{ps} = 0 \text{ (no prestress)} \rightarrow F_{nt} = A_{st} \cdot f_y$$

and

$$f_y = 60{,}000 psi = 60 ksi$$

$$\rightarrow A_{st,req} = \frac{F_{nt}}{f_y} = \frac{F_u}{\phi \cdot f_y} = \frac{F_u}{0.75 \cdot 60 ksi} = \frac{F_u}{40 ksi} \qquad (\frac{F_u}{276 \frac{N}{mm^2}})$$

	F_u [kips]	F_u [kN]	$A_{st,req}$ [in²]	Bar size	A_{st}/bar [in²]	No. of Bars	$A_{st,prov}$ [in²]	Distribution
T_1 =	167	744	3.72	#10	1.27	4	5.08	4#10
T_2 =	143	636	3.18	#8	0.79	4	3.16	4#8
T_3 =	34	151	0.75	#8	0.79	4	3.16	4#8
T_4 =	75	333	1.66	#4	0.20	10	2.00	10#4@18in
T_5 =	75	333	1.66	#4	0.20	10	2.00	10#4@18in
T_6 =	150	667	3.33	#4	0.20	18	3.60	18#4@9in
T_7 =	111	493	2.46	#10	1.27	6	7.62	6#10
T_8 =	222	987	4.93	#10	1.27	6	7.62	6#10
T_9 =	333	1,480	7.40	#10	1.27	6	7.62	6#10
T_{10} =	167	741	3.70	#10	1.27	6	7.62	6#10

Tab. 4-1: Tie reinforcements

Table 4-1 shows the ties T_i with the forces (see Fig. 4-3), the required area of reinforcing steel, the bar size with the area of reinforcement for each bar, the number of bars, the provided area of reinforcement and the way the bars are distributed for each tie.

3.3 Struts

ACI 318-02 Equation A-1

$$\phi \cdot F_n \geq F_u$$

with ACI 318-02 Equation A-2 – nominal compressive strength of a strut without longitudinal reinforcement

$$F_{ns} = f_{cu} \cdot A_c$$

and ACI 318-02 Equation A-3 for the effective compressive strength of the concrete in a strut

$$f_{cu} = 0.85 \cdot \beta_s \cdot f'_c$$

with

$$f'_c = 4{,}500 psi$$

$\beta_s = 0.60 \cdot \lambda$ (without reinforcement satisfying ACI 318 - 02 Appendix A.3.3)

$\lambda = 1.0$ for normal weight concrete (ACI 318 - 02 Chapter 11.7.4.3)

$$A_{c,req} = w_{s,req} \cdot 12"$$

$$\rightarrow f_{cu} = 2{,}869 psi = 2.869 ksi$$

$$\rightarrow \phi \cdot F_n = 0.75 \cdot F_n = 0.75 \cdot 2.869 ksi \cdot A_c \geq F_u$$

$$\rightarrow A_{c,req} \geq \frac{F_u}{0.75 \cdot 2.869 ksi} = \frac{F_u}{2.152 ksi} \qquad (\frac{F_u}{14.85 \frac{kN}{mm^2}})$$

$$\rightarrow w_{s,req} = \frac{F_u}{2.152 ksi \cdot 12"} = \frac{F_u}{25.82 \frac{kips}{in}} \qquad (\frac{F_u}{4{,}525.9 \frac{kN}{mm}})$$

The factor $\beta_s = 0.60\ \lambda$ is taken conservatively, since bottle-shaped struts may develop. If the reinforcement satisfies ACI 318-02 Appendix A.3.3 (resistance against transverse tensile force in the strut), $\beta_s = 0.75$ could be used.

Table 4-2 shows the struts C_i with the forces (see Fig. 4-3) and the required and provided width of the strut with a 12" thickness. Where $w_{s,prov}$ is "ok", enough area is provided through the geometry of the model.

	F_u [kips]	F_u [kN]	$w_{s,req}$ [in]	$w_{s,prov}$ [in]
C_1 =	381	1,695	15	ok
C_2 =	381	1,695	15	ok
C_3 =	266	1,185	10	ok
C_4 =	266	1,185	10	ok
C_5 =	77	343	3	4", ok
C_6 =	167	741	6	ok
C_7 =	225	1,000	9	27½ ", ok
C_8 =	134	595	5	ok
C_9 =	134	595	5	ok
C_{10} =	134	595	5	ok
C_{11} =	224	997	9	ok
C_{12} =	224	997	9	ok

Tab. 4-2: Strut properties

3.4 Nodes

3.4.1 General

According to ACI 318-02 Chapter A-1, the node at point A is a C-C-C-Node consisting of three struts, therefore β_n = 1.0 (ACI 318-02 Section A.5.2.1), while the nodes at points B and C are C-C-T-Nodes, anchoring one tie each and therefore β_n = 0.8 for these nodes (ACI 318-02 Section A.5.2.2).

ACI 318-02 Equation A-7 – nominal compression strength of a nodal zone

$$F_{nn} = f_{cu} \cdot A_n$$

with ACI 318-02 Equation A-8 – the calculated effective stress on a face of a nodal zone

$$\phi \cdot f_{cu} = (0.75) \cdot 0.85 \cdot \beta_n \cdot f'_c$$

and ACI 318-02 Equation A-1

$$\phi \cdot F_n \geq F_u$$

3.4.2 Node A

$F_1 = 225 kips$

$C_0 = 310 kips$

$C_1 = 383 kips$

$\theta = \arctan\frac{69.8}{96.4} = 35.92°$

$\beta_n = 1.0$

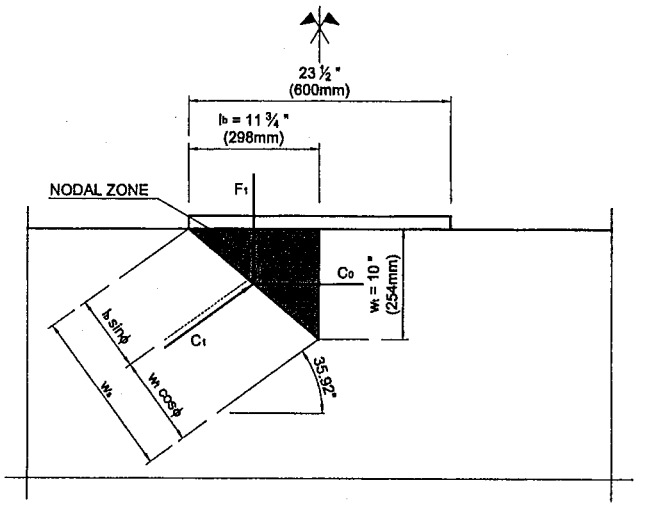

Fig. 4-4: Geometry of node A

$w_{F_1} = l_b = 11\frac{3}{4}"$

$w_{C_0} = 10"$ (approximate height of compression block C_0)

$w_{C_1} = w_s = l_b \sin\theta + w_t \cos\theta = 15"$

$A_{F_1} = 11\frac{3}{4}" \cdot 12" = 141 in^2$

$A_{C_0} = 10" \cdot 12" = 120 in^2$

$A_{C_1} = 15" \cdot 10" = 150 in^2$

$F_{nn,F_1} = 0.85 \cdot 1.0 \cdot 4{,}500 psi \cdot 141 in^2 = 539 kips$ (2,397kN)

$F_{nn,C_0} = 0.85 \cdot 1.0 \cdot 4{,}500 psi \cdot 120 in^2 = 459 kips$ (2,042kN)

$F_{nn,C_1} = 0.85 \cdot 1.0 \cdot 4{,}500 psi \cdot 150 in^2 = 574 kips$ (2,553kN)

$0.75 \cdot 539 kips = 404 kips \geq 225 kips = F_1$ ($1{,}797kN \geq 1{,}000kN = F_1$)

$0.75 \cdot 459 kips = 344 kips \geq 310 kips = C_0$ ($1{,}530kN \geq 1{,}379kN = C_0$)

$0.75 \cdot 574 kips = 431 kips \geq 383 kips = C_1$ ($1{,}917kN \geq 1{,}704kN = C_1$)

→ Node A is acceptable

3.4.3 Node B

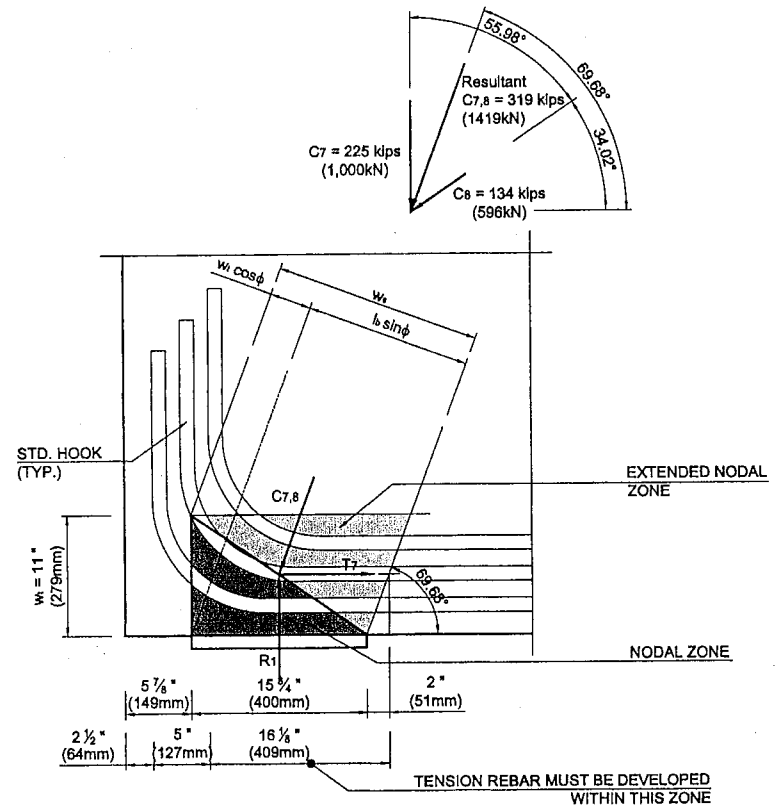

Fig. 4-5: Geometry of node B

$A_{C_{7,8}} = 18\frac{1}{2}" \cdot 12" = 222 in^2$

$F_{nn,R_1} = 0.85 \cdot 0.8 \cdot 4{,}500 psi \cdot 189 in^2 = 578 kips$ (2,571kN)

$F_{nn,T_7} = 0.85 \cdot 0.8 \cdot 4{,}500 psi \cdot 129 in^2 = 395 kips$ (1,757kN)

$F_{nn,C_{7,8}} = 0.85 \cdot 0.8 \cdot 4{,}500 psi \cdot 222 in^2 = 679 kips$ (3,020kN)

$0.75 \cdot 578 kips = 434 kips \geq 300 kips = R_1$ ($1{,}930kN \geq 1{,}333kN = R_1$)

$0.75 \cdot 395 kips = 296 kips \geq 111 kips = T_7$ ($1{,}317kN \geq 494kN = T_7$)

$0.75 \cdot 679 kips = 509 kips \geq 319 kips = C_{7,8}$ ($2{,}264kN \geq 1{,}418kN = C_{7,8}$)

$R_1 = 300kips$
$T_7 = 111kips$
$C_{7,8} = 319kips$
$\theta = 69.68°$
$\beta_n = 0.8$

$w_{R_1} = l_b = 15\,3/4"$
$w_{T_7} = w_t = 2 \cdot 2" + 3 \cdot 1\,1/4" + 2 \cdot 1\,1/2" = 10\,3/4"$
$w_{C_{7,8}} = w_s = l_b \sin\theta + w_t \cos\theta = 18\,1/2"$

$A_{R_1} = 15\,3/4" \cdot 12" = 189in^2$
$A_{T_7} = 10\,3/4" \cdot 12" = 129in^2$

3.4.4 Node C

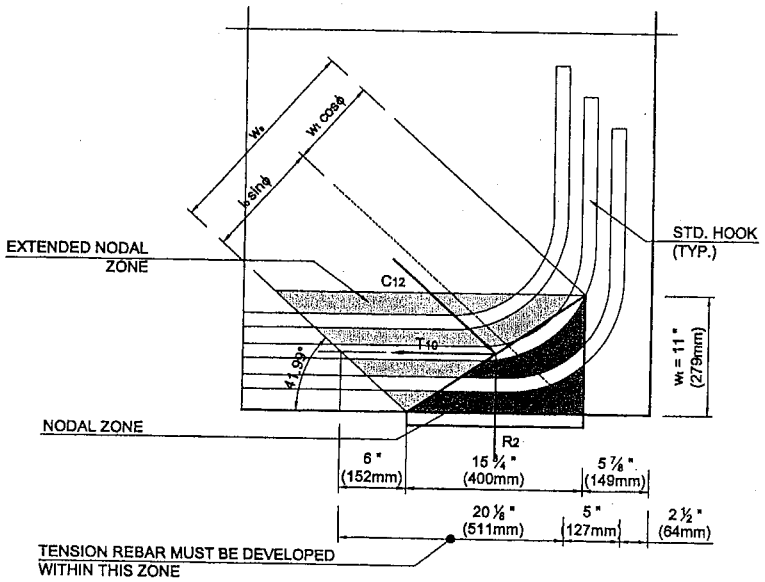

Fig. 4-6: Geometry of node C

$R_2 = 150kips$
$T_{10} = 167kips$
$C_{12} = 224kips$
$\theta = 41.99°$
$\beta_n = 0.8$

$w_{R_2} = l_b = 15\,3/4"$
$w_{T_{10}} = w_t = 2 \cdot 2" + 3 \cdot 1\,1/4" + 2 \cdot 1\,1/2" = 10\,3/4"$
$w_{C_{12}} = w_s = l_b \sin\theta + w_t \cos\theta = 18\,1/2"$

$A_{R_2} = 15\,3/4\,in \cdot 12in = 189in^2$
$A_{T_{10}} = 10\,3/4\,in \cdot 12in = 129in^2$
$A_{C_{12}} = 18\,1/2\,in \cdot 12in = 222in^2$

$F_{nn,R_2} = 0.85 \cdot 0.8 \cdot 4{,}500psi \cdot 189in^2 = 578kips \quad (2{,}571kN)$
$F_{nn,T_{10}} = 0.85 \cdot 0.8 \cdot 4{,}500psi \cdot 129in^2 = 395kips \quad (1{,}757kN)$
$F_{nn,C_{12}} = 0.85 \cdot 0.8 \cdot 4{,}500psi \cdot 222in^2 = 679kips \quad (3{,}020kN)$

$0.75 \cdot 578kips = 434kips \geq 150kips = R_2 \quad (1{,}930kN \geq 667kN = R_2)$
$0.75 \cdot 395kips = 296kips \geq 167kips = T_{10} \quad (1{,}317kN \geq 743kN = C_{10})$
$0.75 \cdot 679kips = 509kips \geq 224kips = C_{12} \quad (2{,}264kN \geq 997kN = C_{12})$

3.4.5 Development Length

Node B governs as the available hook anchorage length is less than the one at node C.

The development length l_{dh} in a standard hook according to ACI 318-02 Equation 12.5.2 is

$$l_{dh} = \frac{0.02 \cdot \beta \cdot \lambda \cdot f_y}{\sqrt{f_c'}} \cdot d_b$$

with

Following ACI 318-02 Chapter 12.5.4, which requires for a cover beyond the hook of less than 2.5" a spacing of stirrups not greater than $3d_b$ along l_{dh}, and the first stirrup being within $2d_b$ of the outside of the bent, l_{dh} may be multiplied by 0.7 according to ACI 318-02 Chapter 12.5.3(a) and therefore is reduced to

$$l_{dh} = 0.7 \cdot 22\,\tfrac{3}{4}" = 16" \quad (404mm)$$

The anchorage length is sufficient for both nodes with l_a being

$$l_{a,NodeB} = \frac{\frac{w_t}{2}}{\tan 69.68°} + 15\,\tfrac{3}{4}" + 5\,\tfrac{7}{8}" - 2\,\tfrac{1}{2}" - 5" = 16\,\tfrac{1}{8}" \quad (409mm)$$

$$l_{a,NodeC} = \frac{\frac{w_t}{2}}{\tan 41.99°} + 15\,\tfrac{3}{4}" + 5\,\tfrac{7}{8}" - 2\,\tfrac{1}{2}" - 5" = 20\,\tfrac{1}{8}" \quad (510mm)$$

$$l_{dh} = 16" \le 16\,\tfrac{1}{8}" \quad (404mm \le 409mm)$$

→ Node B and Node C are acceptable

l_{dh} could be further reduced by the ratio of $A_{s,req}$ to $A_{s,prov}$ (3.7/7.62 = 0.49) as per ACI 318-02 Chapter 12.5.3(d). This additional reduction in l_{dh} has not been taken as it will not change the results.

3.5 Minimum reinforcement for shrinkage and temperature

ACI 318-02 Equation 7.12.2.1(b) – the ratio between the area of reinforcement to gross concrete area is

$$\rho = \frac{A_S}{A_C} = 0.0018$$

Assume a reinforcement of #4 at 18", because following ACI 318-02 Chapter 7.12.2.2 the spacing shall not exceed 18", with $A_{st} = 0.20in^2$, therefore with the width of the wall being 12":

$$\rho = \frac{2 \cdot 0.20in^2}{18" \cdot 12"} = 0.0019 \ge 0.0018 \rightarrow \text{OK}$$

Conclusion: provide #4 at 18" minimum each way each face.

3.6 Minimum skin reinforcement

Checking the requirements in ACI 318-02 Chapter A.3.3, none other than the horizontal and vertical minimum reinforcement for shrinkage and temperature according to 3.2 will be provided. If the effective depth of a beam exceeds 36", skin reinforcement shall be distributed according to ACI 318-02 Chapter 10.6.7. The skin reinforcement is to be distributed for a distance of $d/2$ at a spacing not exceeding the least of $s_{sk} > d/6$, $s_{sk} > 12"$ and $s_{sk} > 1000A_b/(d - 30)$:

$$\frac{1000 \cdot 0.31in^2}{70\,\tfrac{1}{4}" - 30"} = 7\,\tfrac{1}{2}" \rightarrow s_{sk} \ge 7\,\tfrac{1}{2}" \quad (193mm)$$

Therefore the horizontal reinforcement of #4 at 18" shall be changed to #5 at 7½" for the bottom of the deep beam and above the opening in a depth of 37".

4 Rebar layout

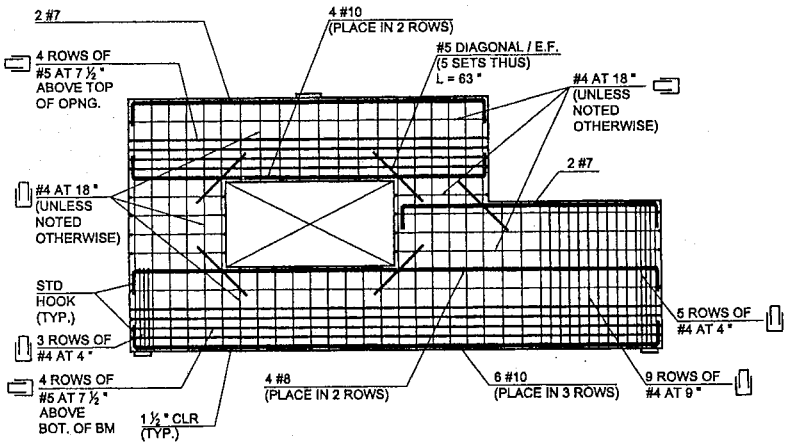

Fig. 4-7: Final rebar layout according to the strut-and-tie-model

Example 5 : Beam with indirect support and loading

Wiryanto Dewobroto

Karl-Heinz Reineck

Synopsis

Inadequate design of indirect supports resulted in a lot of structural damage and near failure of structural concrete beams. Most codes, including ACI 318, do not properly cover this case. However, strut-and-tie models almost automatically lead to correctly reinforcing these critical discontinuity regions. This example combines indirect supports as well as indirectly applied loads and demonstrates the application of strut-and-tie models following Appendix A of ACI 318-2002.

Wiryanto Dewobroto is a lecturer in civil engineering at the University of Pelita Harapan, Indonesia. He obtained BS in Civil Engineering from University of Gadjahmada in 1989. After that he worked in consulting engineer firm and has experience in design and supervision of many structures especially for high-rises, industrial buildings and bridges. In 1998 he obtained his MS in Structural Engineering from the University of Indonesia. From May to July 2002 he was a guest researcher at the University of Stuttgart, Germany.

Karl-Heinz Reineck received his Dipl.-Ing. and Dr.-Ing. degrees from the University of Stuttgart. He is involved in both research and teaching at the Institute for Lightweight Structures Conceptual and Structural Design, University of Stuttgart. His research covers design with strut-and-tie models, shear design and detailing of structural concrete. He is chairman of ASCE-ACI Committee 445-1 and member of the *fib* Task Group "Practical Design."

1 Geometry and loads

The T-beam shown in Fig. 5-1 is indirectly supported at support B by means of a transfer beam shown in section II-II. Likewise the loads are not directly applied to the web but are transferred by the beams shown in section I-I. The loads are symmetrically applied so that no torsion is induced.

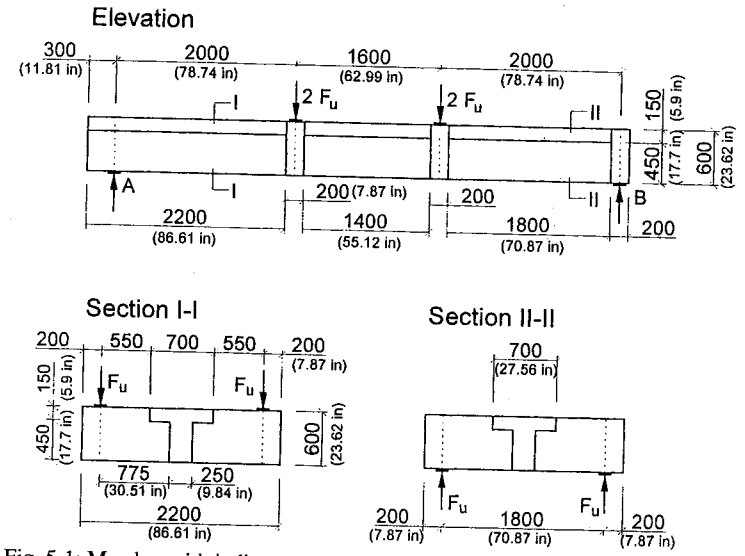

Fig. 5-1: Member with indirect support and factored loads (1 mm = 0.03937 in)

Design specification :

Factored load :	F_u =	160 kN	(36 kips)
Concrete :	f'_c =	31.6 MPa	(4,580 psi)
Reinforcement :	f_y =	500 MPa	(72,500 psi)

2 Design procedure

The design is based on Strut-and-Tie-Model according to Appendix A of the ACI 318-02 and is carried out in the following steps:

Step 1: Analysis
Step 2: Flexural design of main beam and calculation of internal lever arm
Step 3: Stirrup design for main beam and calculation of strut angle in web
Step 4: Check of anchorage length at node A and B
Step 5: Design of beam transferring the loads to the main beam
Step 6: Design of beam supporting the main beam
Step 7: Arrangement of reinforcement

Editorial note: The calculations are carried out in SI units; primary results are given in English units in brackets.

3 Design calculations

3.1 Step 1: Analysis

The shear force and moment diagram of the main beam are shown in Fig. 5-2.

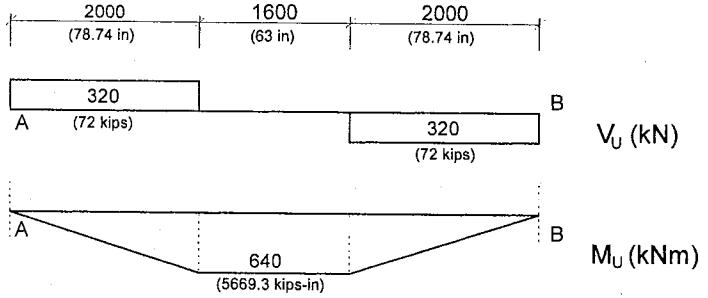

Fig. 5-2: Shear forces and flexural moment in the main beam
(1 kN = 0.2248 kips; 1 kN-m = 8.8496 kips-in)

Beams transferring the load to the main beam (Sec. I-I in Fig. 5-1):

M_u = 144 kN-m (1275 kips-in)
V_u = 160 kN (36 kips)

For the beam supporting the main beam at support B (Sec. II-II in Fig. 5-1) the same values apply.

3.2 Step 2: Flexural design of main beam

Use equivalent rectangular concrete stress distribution based on Sec.10.2.7:

$$f'_c = 31.6 \text{ MPa} \rightarrow \beta_1 = 0.85 - 0.005\,(31.6-27.6) / 6.89 = 0.82$$

$$\rho_{max} = 0.75\,\rho_b = \frac{0.638\,f'_c\,\beta_1}{f_y}\,\frac{600}{600+f_y} = 0.018$$

$$\omega_{max} = \frac{\rho_{max}\,f_y}{f'_c} = 0.285$$

$$M_n \geq \frac{M_u}{\phi} = \frac{640}{0.9} = 711.1\,\text{kN - m} \quad (6290\,\text{kips - in})$$

Make the assumptions that the compression zone is within the flange (Fig 5-3) and steel yields.

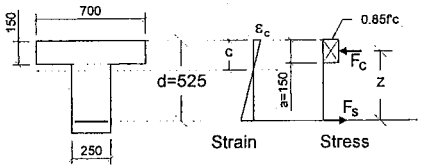

Fig. 5-3: Distribution of strains and stress at midspan of main beam (1 mm = 0.03937 in)

$$\frac{M_n}{bd^2f'_c} = \frac{711.1*10^6}{700*525^2*31.6} = 0.117 \rightarrow \omega = 0.126 < \omega_{max} = 0.285$$

$$A_s = \omega\frac{f'_c}{f_y}b\,d = 0.126*\frac{31.6}{500}*700*525 = 2926\,\text{mm}^2 \quad (4.54\,\text{in}^2)$$

use 6 ∅ 25 $A_s = 2945\ \text{mm}^2$ $(4.56\ \text{in}^2)$

Check the assumption:

$$a = \frac{A_s \cdot f_y}{0.85 \cdot f'_c \cdot b} = \frac{2926*500}{0.85*31.6*700} = 79\,\text{mm} < h_f = 150\,\text{mm} \quad \text{OK}$$

$$a = \frac{A_s \cdot f_y}{0.85 \cdot f'_c \cdot b} = 3.11\,\text{in} < h_f = 5.91\,\text{in}$$

The arrangement of the main bars is shown in Fig. 5-4. (1 mm = 0.03937 in)

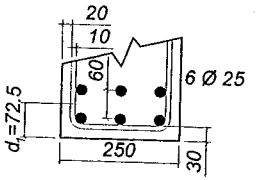

Fig. 5-4 : Proposed arrangement of bars for main beam (1 mm = 0.03937 in)

The updated values for the effective depth and the internal lever arm are as follows:

The updated lever arms are as follows:

$d = h - d_t = 600 - 72.5 = 527.5$ mm (20.78 in) > 525 mm (20.67 in)

$z = jd = d - 0.5a = 527.5 - (0.5 * 79) = 488$ mm (19.21 in)

$j = z / d = 0.925$

3.3 Step 4: Stirrup design for main beam

The dimensioning of the stirrups follows from chapter 11 of ACI 318. Subsequently the angle θ is derived for the inclined struts in the web so that the strut-and-tie model for the D-regions can be determined.

$$\phi V_n \geq V_u$$

$$V_n \geq \frac{V_u}{\phi} = \frac{320}{0.75} = 427\ \text{kN} \qquad (96\ \text{kips})$$

$$V_n = V_c + V_s$$

Eq. 11.3.1.1 for members subjected to shear and flexure only gives :

$$V_c = 0.17\sqrt{f'_c}\,b_w\,d$$

$$V_c = 0.17*\sqrt{31.6}*250*527.5 = 126024\ \text{N} = 126\ \text{kN} \quad (28.3\ \text{kips})$$

Alternative Eq. 11.3.2.1 gives :

$$V_c = \left(0.16\sqrt{f'_c} + 17\,\rho_w\frac{V_u\,d}{M_u}\right)b_w\,d \leq 0.29\sqrt{f'_c}\,b_w d$$

where

$$\frac{V_u\,d}{M_u} = \frac{320*0.5275}{640} = 0.2637 \leq 1.0$$

$$\rho_w = \frac{A_s}{b_w\,d} = \frac{2945}{250*527.5} = 0.0223$$

so that

$$V_c = \left(0.16\sqrt{31.6} + 17*0.0233*0.2637\right)250*527.5 \leq 0.29\sqrt{31.6}*250*527.5$$

$V_c = 132$ kN (29.67 kips) ≤ 215 kN (48.32 kips)

Use V_c from the alternative equation for designing the stirrups:

$V_s = V_n - V_c$

$V_s = 427 - 132 = 295$ kN (66.3 kips)

$< 0.68\sqrt{f_c'}\,b_w d = 504$ kN (113.3 kips)

$> 0.34\sqrt{f_c'}\,b_w d = 252$ kN (56.6 kips) → $s \le d/4 = 131$ mm (5.16 in)

$$\frac{A_v}{s} = \frac{V_s}{f_y \cdot d} = \frac{295{,}000}{500 * 527.5} = 1.12\ \frac{mm^2}{mm} = 1120\ \frac{mm^2}{m} \quad (0.0441\ \frac{in^2}{in})$$

use stirrups ∅ 10 at 125 mm spacing → $\left(\frac{A_v}{s}\right)_{prov} = 1250\ \frac{mm^2}{m}\ (0.0492\ \frac{in^2}{in})$

The angle θ of the inclined struts in the web of the truss model can be derived now because the amount of stirrups is known. The free-body diagram shown in Fig. 5-5 shows that the shear force in the B-region has to be taken by the stirrup forces over the length ($z \cot\theta$):

$$V_n = (A_v / s)\, f_y\, z \cot\theta$$

and from this the angle θ can be calculated as follows:

$$\cot\theta = \frac{s}{A_v} \cdot \frac{V_n}{f_y z} = \frac{1}{1.12} * \frac{427{,}000}{500 * 488} = 1.5625 \rightarrow \quad \theta = 32.6°$$

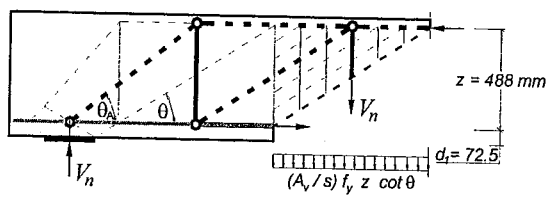

Fig. 5-5: Compression stress fields for the inclined struts (1 mm = 0.03937 in)

3.4 Step 4: Check the anchorage length at nodes A and B

3.4.1 Check the development length of longitudinal rebars

According to Sec. 12.11 ACI 318-02 the development of rebars should satisfy the following requirement (see also Fig. 5-6):

1. At least one-third the longitudinal reinforcement shall extend along the same face of member into the support at least 150 mm.
2. At simple supports the diameter of the reinforcement should be small enough so that computed development length l_d of the bar satisfies the following condition:

$$l_d \le \frac{M_n}{V_u} + l_a$$

where

M_n is nominal moment strength assuming all reinforcement at the section (at support) to be stressed to the specified yield strength f_y.

Therefore from Step. 2, it can be calculated as

$M_n = A_s f_y z$

$M_n = 2945 * 500 * 488 = 719.10^6$ N-mm = 719 kN-m.

V_u is factored shear force at the section (V_u = 320 kN).

l_a at the support shall be the embedment length beyond the center of the support.

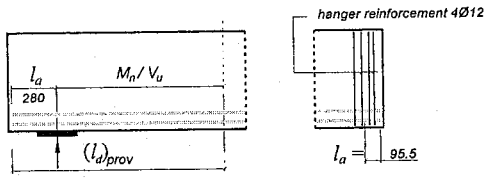

(a). Direct support (Node A) (b). Indirect support (Node B)

Fig. 5-6: Development length of the positive bar (1 mm = 0.03937 in)

Here for simplicity all bars are extended to the support.

The beam section at the support is similar to Fig. 5-4, the diameter of rebar is 25 mm, therefore according to Sec. 12.2.2 the development length can be calculated as follows:

$$l_d = \left(\frac{f_y \alpha \beta \lambda}{20\sqrt{f_c'}}\right) d_b \qquad \text{(in)}$$

This equation applies to normal weight concrete (λ=1.0), uncoated reinforcement (β=1.0) and bar diameters larger than bar No.7, or 22 mm (α = 1.0), for f_c' = 4,583 psi and f_y= 72,500 psi:

$$(l_d)_{req} = \left(\frac{72500*1.0*1.0*1.0}{20\sqrt{4583}}\right) d_b = 54 d_b = 1350 \text{ mm} \quad (53.15 \text{ in})$$

Check node A:

$$(l_d)_{prov} = 1.3 * M_n/V_u + l_a = 1.3 * 715{,}000/320 + 280 = 3{,}185 mm \quad (98.98 \text{ in})$$

$$(l_d)_{prov} = 3{,}185 mm \quad (98.98 in) > (l_d)_{req} \rightarrow \text{OK}$$

Check node B:

$$(l_d)_{prov} = M_n/V_u + l_a = 715{,}000/320 + 95 = 2{,}234 mm \quad (87.95 \text{ in}) > (l_d)_{req} \rightarrow \text{OK}$$

The requirements of Sec. 12.11 regarding the development of the longitudinal reinforcement have been satisfied, however this does not represent a check of the anchorage length directly at the support.

3.4.2 Check the anchorage length at direct support A

Use Standard hooks to terminate the rebars at the support. The check of the anchorage length at the direct support is carried out according to Sec. 12.5.2 for a standard hook according to A.4.3.2. According to ACI A.4.3.2 the development length starts at the point where the centroid of the reinforcement in the tie leaves the extended nodal zone. For simplicity here the inner face of the support is taken, and as shown in Fig. 5-7 the available development length (l_{dh}) computed in this way is 380 mm.

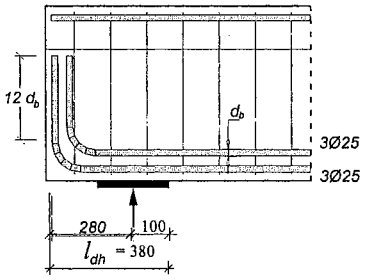

Fig. 5-7: Development length at direct support (Node A) (1 mm = 0.03937 in)

According to section 12.5.2 the development length is:

$$l_{dh} = (0.02\ \beta\ \lambda\ f_y / \sqrt{f_c'})\ d_b$$

where

β and λ are 1.0 for normal weight concrete and uncoated rebar

f_c' = 4,580 psi

f_y = 72,500 psi

therefore

$$l_{dh} = (0.02 * 1.0 * 1.0 * 72{,}500 / \sqrt{4{,}580})\ d_b = 21\ d_b$$

According to Sec.12.5.3 where anchorage or development for f_y is not specifically required, reinforcement in excess of that required by analysis can be multiplied by

$$l_{dh} = (A_{s,req} / A_{s,prov})\ 21\ d_b$$

In order to calculate $A_{s,req}$, the tension force (F_{sA}) shown in Fig. 5-8 is required. Based on the FIP Recommendations (1999), Sec.6.5.2.1, the angle θ_A for the resultant of the fan-shaped compression field follows the geometry of the fan (Fig. 5-8):

$$\cot\theta_A = [0.5a_1 / z + (d_1 / z + 0.5) \cot\theta\ ]$$

$$\cot\theta_A = [125 / 488 + (72.5 / 488 + 0.5)\ 1.5625\ ] = 1.2695 \rightarrow \theta_A = 38.2^\circ$$

$F_{sA} = V_n \cot\theta_A = 427 * 1.2695 = 542$ kN (122 kips)

$A_{s,req} = F_{sA} / f_y = 542{,}000 / 500 = 1084$ mm² (1.68 in²)

$A_{s,prov} = 6\ \varnothing\ 25$ (2945 mm²) (4.56 in²)

Therefore: $l_{dh,req} = (A_{s,req} / A_{s,prov})\ 21\ d_b$

$l_{dh,req} = (1084 / 2945)\ 21\ d_b = 7.73\ d_b = 193$ mm < $l_{dh,prov} = 280$ mm

$l_{dh,req} = 7.60$ in < $l_{dh,prov} = 11.02$ in

The anchorage length at direct support (Node A) is adequate.

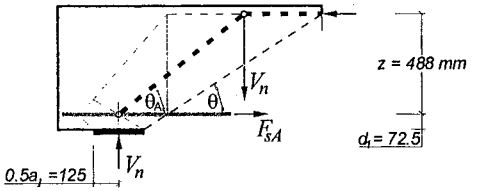

Fig. 5-8: Tension force (F_{sA}) to be anchored at the support (1 mm = 0,03937 in)

3.4.3 Hanger reinforcement at indirect support

At an indirect support the strut-and-tie model in the web is the same as that for direct supports [Reineck (1996)]. However, at node B the reaction of the main beam must be transferred to the supporting beam by hanger reinforcement (Fig. 5-9). The area of hanger reinforcement required can be calculated as follows:

$A_s = V_n / f_y = 427{,}000 / 500 = 854$ mm^2 (1.32 in^2)

Use 4 stirrups ∅ 12 $A_s = 905$ mm^2 (1.40 in²)

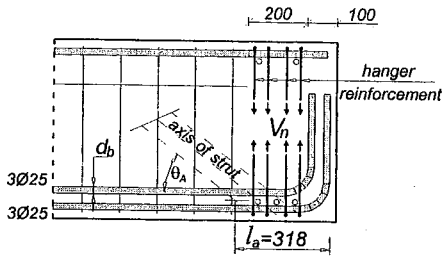

Fig. 5-9: Model and development length at the indirect support (Node B)
(1 mm = 0.03937 in)

3.4.4 Check the development length at indirect support B

In order to place the hanger reinforcement below the standard hooks at the indirect support, the main beam should be extended 100 mm beyond the edge of transfer beam (see Fig. 5-9). Otherwise the stirrup anchorage of the main reinforcement is not sufficient.

According to Sec. A.4.3.2 the development length can be calculated from the point where the centroid of the reinforcement in a tie leaves the extended nodal zone. As shown in Fig. 5-9 the development length (l_a) computed in this way is 318 mm, which is larger than use l_{dh} requirement from the previous calculation, therefore the development length at the indirect support is adequate.

Note: It is evident that in ACI 318 there is no difference between the requirements for the anchorage length for direct or indirect supports. However, the stress condition at an indirect support is clearly more unfavorable, because the transverse tensile stresses reduce the bond strength and thus the required anchorage length should be larger than for the case at a direct support.

3.5 Step 5 : Beam transferring the load to the main beam

3.5.1 Strut-and-tie model

The entire deep beam is a D-region. To satisfy equilibrium at point C in Fig. 5-10 for the tie forces in the upward direction, hanger reinforcement is required. These stirrups must be located within the intersection of the web of the main beam and the beam transferring the load.

The strut-and-tie model may be assumed as shown in Fig. 5-10:

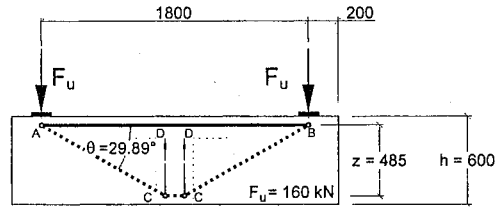

Fig. 5-10: Strut-and-tie configuration of beam transferring the load
(1 mm = 0.03937 in; kN = 0.2248 kips)

The angle of the strut is larger than 25°, therefore acceptable. However, a certain minimum amount of transverse reinforcement is required according to Appendix A.3.3 of ACI 318-2002 as calculated in the following. Because of that it may be stated that this model as such is not fully transparent (see also Schlaich et al (1987)), because it does not show the necessity to provide any transverse reinforcement. Therefore it may be considered to use the strut-and-tie model for point loads near a support used in the FIP Recommendations (1999) "Practical design of structural concrete", and this was also proposed by and MacGregor in part 2 of this Special Publication.

3.5.2 Design hanger reinforcement

The up-ward forces in C-D must be resisted by hanger reinforcement as calculated already in Section 3.4.3.

3.5.3 Design ties

Calculate the horizontal tie force (T_u) at node A through node B as follows

$T_u = F_u / \tan\theta = 160 / \tan 29.9° = 278.2$ kN (62.5 kips)

$T_n \geq T_u / \phi = 278.2 / 0.75 = 371$ kN (83.4 kips)

$A_s = T_n / f_y = 371{,}000 / 500 = 742$ mm^2 (1.15 in^2)

Use 3 ∅ 19, $A_s = 850$ mm^2 (1.31 in²)

3.5.4 Strength of nodal zone

The nominal compression strength of a nodal zone shall be

$$F_{nn} = f_{cu} A_n$$

where

$f_{cu} = 0.85 \beta_n f_c'$

$\beta_n = 0.8$

$f_{cu} = 0.85 * 0.8 * 31.6 = 21.5$ MPa (3.12 ksi)

A_n = area of the nodal zone taken perpendicular to the resultant force, mm²

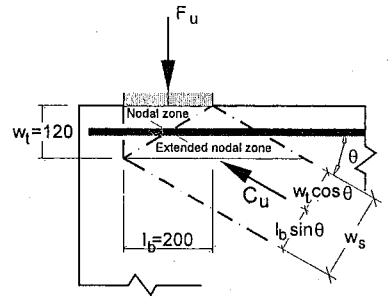

Fig. 5-11: Nodal zone at the load point (1 mm = 0.03937 in)

Check nodal zone under the bearing force (F_u) as shown in Fig 5-11:

$A_n = b l_b = 200 * 200 = 40{,}000$ mm² (62.0 in²)

so that

$F_{nn} = f_{cu} A_n = 21.5 * 40{,}000 = 860{,}000$ N = 860 kN (193 kips)

$\phi F_{nn} = 0.75 * 860$ kN = 645 kN (145 kips) > F_u = 160 kN → OK

Check nodal zone under the strut action (C_u)

$C_u = F_u / \sin\theta = 160 / \sin 29.9° = 321$ kN (72.2 kips)

$A_n = b w_s = b (w_t \cos\theta + l_b \sin\theta)$

$= 200 (120 \cos 29.9° + 200 \sin 29.9°) = 40{,}745$ mm² (63.15 in²)

so that

$F_{nn} = f_{cu} A_n = 21.5 * 40{,}745 = 876{,}000$ N = 876 kN (197 kips)

$\phi F_{nn} = 0.75 * 876 = 657$ kN (148 kips) > C_u = 321 kN → OK

For the anchorage of the reinforcement hooks are provided without further check.

3.5.5 Strength of inclined struts

The nominal compressive strength of a strut shall be taken as

$$F_{ns} = f_{cu} A_c$$

where

A_c = cross-sectional area at one end of the strut

$A_c = b w_s = b (w_t \cos\theta + l_b \sin\theta)$

$f_{cu} = 0.85 \beta_s f_c'$

$\beta_s = 0.75$ (bottle-shaped with reinforcing satisfying ACI 318-02 Sec. A.3.3)

therefore

$f_{cu} = 0.85 * 0.75 * 31.6 = 20.1$ MPa (2.92 ksi)

$A_c = 200 (120 \cos 29.9 + 200 \sin 29.9) = 40{,}700$ mm² (63.09 in²)

$F_{ns} = 20.1 * 40{,}700 = 819{,}000$ N = 819 kN (184 kips)

$\phi F_{ns} = 0.75 * 819 = 614$ kN (138 kips) > C_u → OK

Design the rebar crossing the diagonal strut to satisfy Appendix A.3.3 (Fig. 5-12):

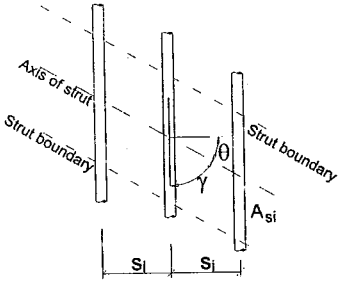

Fig. 5-12: Rebar crossing the diagonal strut

The reinforcement will be placed in one direction (vertical only) at an angle γ to the axis of diagonal strut so that γ shall not be less than 40°.

$\gamma = 90 - \theta = 90 - 29.9 = 60.1°$

For $f_c' \leq 41.4$ MPa (6000 psi) the amount of reinforcement is calculated as follows:

$$\left(\frac{A_{si}}{s_i}\right)_{prov} \geq 0.003\frac{b}{\sin\gamma}$$

so that

$$\left(\frac{A_{si}}{s_i}\right)_{min} = 0.003 * \frac{200}{\sin 60.1} = 0.692\,\frac{mm^2}{mm} = 692\,\frac{mm^2}{m} \quad (0.0272\,\frac{in^2}{in})$$

Try stirrup ∅ 10 at 200 mm (8 in) spacing $\left(\frac{A_{si}}{s_i}\right)_{prov} = 785\,\frac{mm^2}{m}$ $(0.031\,\frac{in^2}{in})$

3.6 Step 6: Beam supporting the main beam

The design is similar to that of the previous beam. Note that the model (Fig. 5-13) is inverted relative to the beam transferring the load.

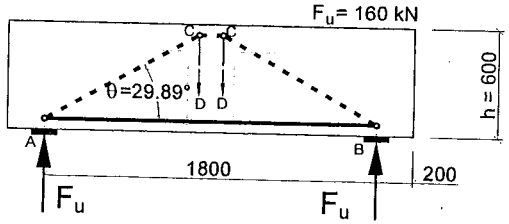

Fig. 5-13: Strut-and-tie model for the beam supporting the main beam
(1 mm = 0.03937 in; 1 kN = 0.2248 kips)

4 Reinforcement layout

The reinforcement layout is shown in Fig. 5-14 to Fig. 5-16

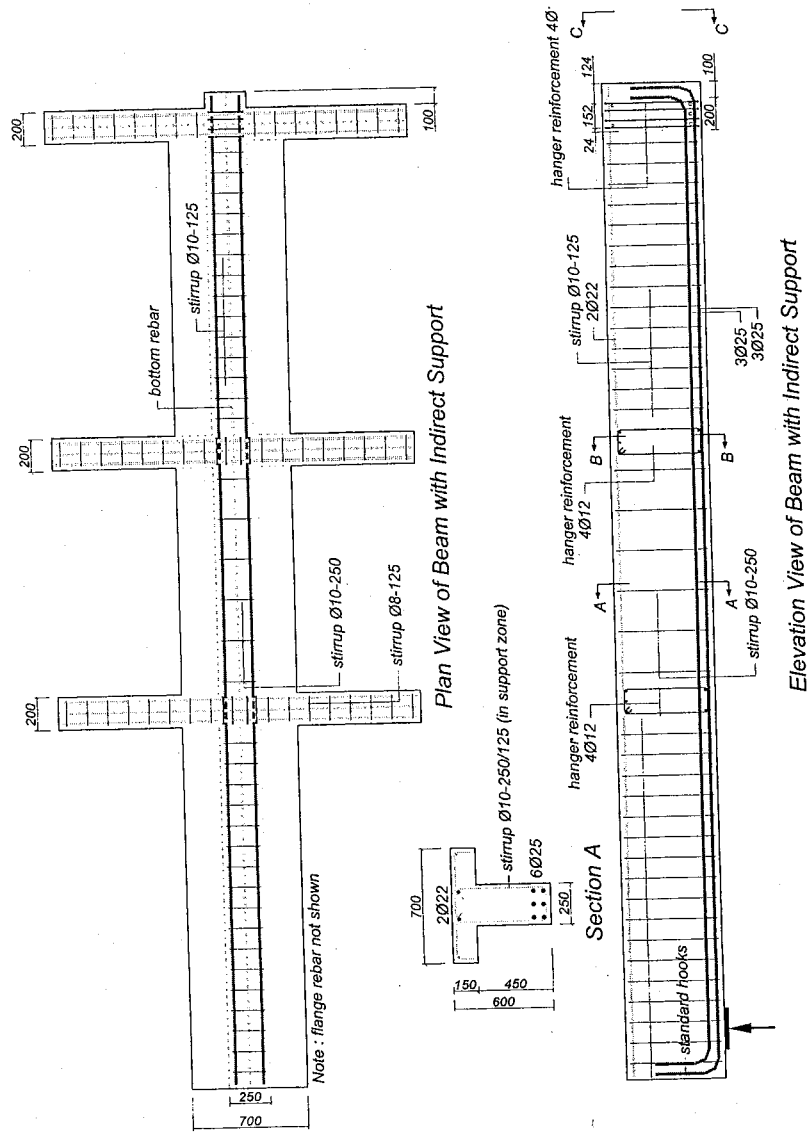

Fig. 5-14: Elevation and section of beam with indirect support
(1 mm = 0.03937 in)

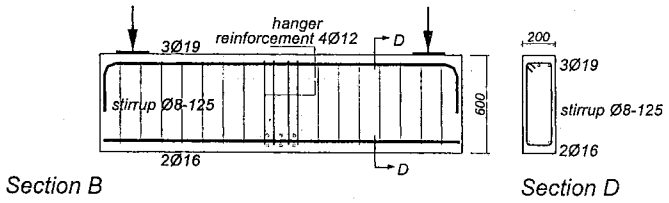

Fig. 5-15: Elevation and section of beam transferring load (Node A)
(1 mm = 0.03937 in)

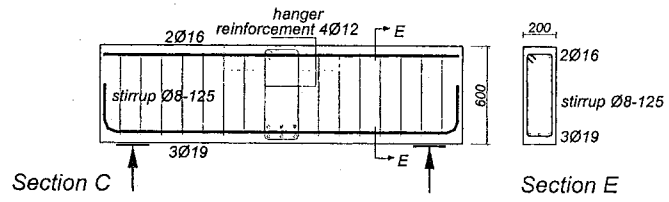

Fig. 5-16: Elevation and section of beam supporting the main beam (Node B)
(1 mm = 0.03937 in)

5 Summary

Indirect supports are presently dealt with by rules for the shear design although they represent a critical D-region. By using strut-and-tie models it becomes obvious that hanger stirrups have to be provided for the full support force. The shear design of the adjacent web is the same like for a direct support.

A critical issue is also the anchorage of the longitudinal reinforcement at an indirect support because at this TTC-node the transverse tensile stresses reduce the bond capacity. Therefore, longer anchorage lengths are required than at a direct support, a TCC-node, where transverse compression favorably influences the bond stresses and thus the required anchorage length.

Notation

f_c' = specified compressive strength of concrete
f_y = specified yield strength of nonprestressed reinforcement
d = distance from extreme compression fiber to centroid of tension rebar (effective depth)
d_b = nominal diameter of bar
F_u = factored force acting in a strut, tie, bearing area, or nodal zone in a strut-and-tie model kN
C_u = factored compression strut in a strut-and-tie model kN
T_u = factored tension tie in a strut-and-tie model kN
A_n = area of the face of the nodal zone that F_u acts on, taken perpendicular to the line of action of F_u, or the resultant force on the section, mm^2
A_c = effective cross-sectional area at one end of a strut in a strut-and-tie model, taken perpendicular to the axis of the strut, mm^2
s_i = spacing of reinforcement in the i^{th} layer adjacent to the surface of the member, mm
w_s = effective width of strut, mm
w_t = effective width of tie, mm
β_t = factor defined in Sec.10.2.7.3 of ACI 318-02
β_s = factor to account for the effect of cracking and confinement reinforcement on the effective compressive strength of a nodal zone
γ = angle between the axis of a strut and the bars crossing that strut
θ = angle between the axis of a strut or compressive field and the tension chord of the member
ϕ = strength reduction factor
l_b = width of bearing, mm
z = inner lever arm

References

American Concrete Institute (2002) : *Building Code Requirements for Structural Concrete* (ACI 318-02) and Commentary (ACI 318R-02) , Appendix A.

FIP Recommendations (1999): *Practical Design of Structural Concrete.* FIP-Commission 3 "*Practical Design*", Sept. 1996.
Publ.: SETO, London, Sept. 1999. (Distributed by: *fib*, Lausanne)

Reineck, K.-H. (1996): *Rational Models for Detailing and Design* , p. 101-134, in: Large Concrete Buildings: Rangan, B.V. and Warner, R. F. (Ed.)., Longman Group Ltd., Burnt Mill, Harlow, England, 1996

Schlaich, J.; Schäfer, K; Jennewein, M. (1987): *Toward a Consistent Design for Structural Concrete.* PCI-Journal Vol. 32 (1987), No.3, 75-150, 1987

Example 6: Prestressed beam

Adolfo Matamoros

Julio Ramirez

Synopsis

The design of the end region of a prestressed beam according to Appendix A of the 2002 ACI Building Code is presented. Two alternatives are considered, the first with straight strands and debonding toward the ends of the member in order to control stresses at transfer. The second case is with draped strands. Strut-and-tie models corresponding to each of the two alternatives are developed, analyzed, and the reinforcement is proportioned to resist the calculated internal forces. Anchorage length requirements were a critical factor in selecting the configuration of the truss models.

Adolfo Matamoros received his MS and Ph.D. degrees from the University of Illinois at Urbana Champaign. He is an Assistant Professor at the University of Kansas. His research covers shear design and detailing of structural concrete. He is Secretary of ACI Committee 408, Bond and Development of Reinforcement.

Julio Ramirez is a Professor of Structural Engineering at Purdue University. He is a Fellow of ACI and a recipient of the Delmar Bloem award. He is a member of the ACI Committees Technical Activities, Publications, 318, Structural Building Code, 408 Committee, Bond and Development of Reinforcement, Joint ACI-ASCE 445, Shear and Torsion, Joint ACI-ASCE 423, Prestressed Concrete.

1 Geometry and loads

The end region of a simply-supported prestressed beam subjected to a uniformly distributed load, w_u, is designed using Appendix A of the 318-02 Building Code (ACI, 2002). Beam dimensions are shown in Fig. 6-1. The distance between supports is 30 ft. (9144 mm) and the total length of the beam is 32 ft.–8 in. (9957 mm).

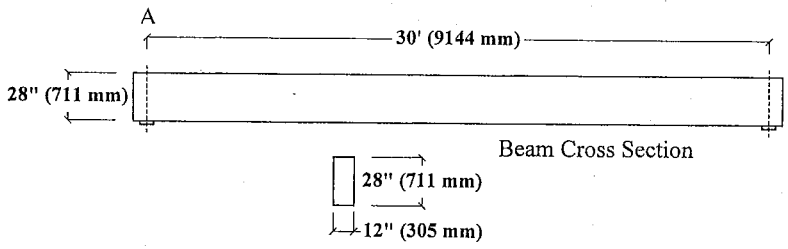

Fig.6-1: Member dimensions in mm.

The design loads and material properties for the beam are as follows:

$w_u = 0.30$ kip/in. (53 N/mm) $f_{se} = 150$ ksi (1034 MPa)

$f'_c = 7.5$ ksi (52 MPa) $f_y = 60$ ksi (414 MPa)

$b = 12$ in. (305 mm)

Two different alternatives are considered for the detailing of the end region. In the first case a straight strand profile, including the option of debonding some of the strands at sections located 15 in. (381 mm) and 45 in. (1143 mm) from the centerline of the supports (Fig 6-2), is considered. In the second alternative the end region is designed using a combination of straight strands and some strands draped at point D in Fig. 6-2, located 91 in. (2311 mm) from the end of the beam. The distance from the centerline of the support to the end of the beam is 16 in. (406 mm). The dimensions of the assumed bearing plate are 6 x 12 in. (152 x 305 mm):

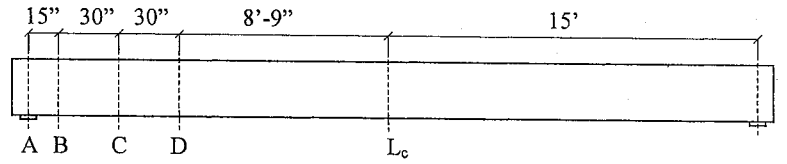

Fig.6-2: Beam dimensions and location of critical sections of strut-and-tie model.

2 Design procedure

The overall design of D- and B-regions of the member can be conducted using the Appendix A of the 318-02 Code (ACI, 2002). In practice, it is likely that the parts of the beam designated as B-regions will be designed using the procedures in the main body of the code. For the purpose of this paper, the member design is carried out using the requirements stated in Appendix A as well as other relevant sections from of the ACI 318-2002 Code. The steps are as follows:

- Step 1: Determine the boundaries between D- and B-regions of the beam and calculate moment and shear demands at these locations.
- Step 2: Establish an initial strut-and-tie model for the design region based on the dimensions of the horizontal strut and tie determined from flexure requirements. Check that the forces in the critical horizontal and inclined struts remain below the maximum effective strengths allowed by the ACI provisions. If the strength of the struts is adequate on the basis of the limits specified in Appendix A, proceed with the proportioning of the reinforcement. Otherwise choose the most feasible option between adjusting the height/width of the struts, the uniaxial compressive strength of the concrete, or the width of the beam.
- Step 3 : Determine the number of strands needed to satisfy the force demand on the main flexural tie. Check that the strands are properly anchored.
- Step 4 : Dimension mild reinforcement to satisfy force demands acting on the ties. In prestressed members, mild steel can be used to supplement the strength provided by the prestressing steel. This can be critical in regions near the ends of the beams where prestress transfer occurs by bond. Insure that minimum amount of reinforcement and the maximum spacing are in accordance with ACI 318-02 requirements.

3 Design calculations for end region with straight strands

The relevant portion of the beam for this design example is located between the edge of the beam and section D (in Fig. 6-2), which corresponds to the boundary between the D- and B-regions. The location of section D was selected to be at a distance approximately equal to the effective depth from the debonding section closest to the beam centerline. A strut-and-tie model capable of transferring forces between section D and the end of the beam is developed following the procedure outlined in Section 2.

Distance from support in. (mm)	$M_u \times 10^3$ kip in. (kN mm)	V_u kip (kN)
75 (1905)	3.21 (362)	31.5 (140)

Table 6-1: Calculated demands at boundary of design region

3.1 Determine moment and shear demands at boundary of the design region

The bending moment and shear force demand are determined at the boundary of the design region based on principles of equilibrium. The magnitude of the bending moment and shear force are summarized in Table 6-1.

3.2 Define strut and tie model

The configuration of the strut-and-tie model is defined based on the height of the horizontal strut and the height of the horizontal tie, as described in step 2 of the suggested procedure. The height of the main flexural tie is defined as twice the distance from the bottom of the beam to the centroid of the strands. Strands are distributed in two layers spaced at 2 in. (51 mm), as shown in Fig. 6-3.

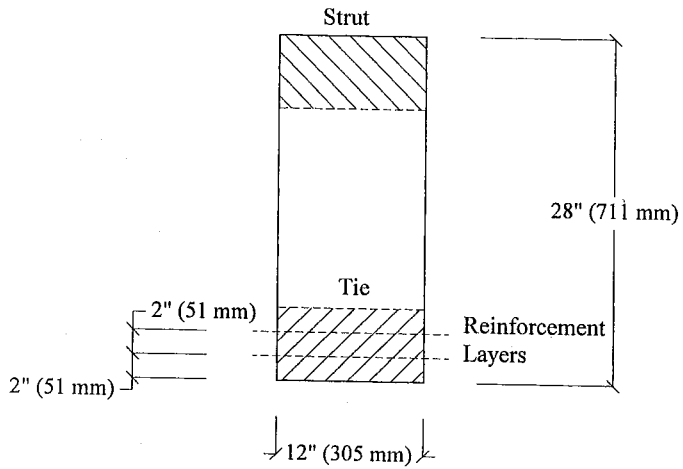

Fig.6-3: Location of strands for beam with horizontal pattern.

The idealized strut-and-tie model for the design region is shown in Fig. 6-4. Solid lines correspond to tension elements and the thicker broken lines represent struts. At section D, located 75 in. (1905 mm) from the support (Fig. 6-4), the total number of strands is assumed evenly distributed between the two layers (Fig. 6-3). Consequently, the height of the tie (N_6-N_4-N_2 in Fig. 6-4) is 6 in. (152 mm), and its centroid is located 3 in. (76 mm) from the bottom face of the beam. The height of the horizontal strut (N_5-N_3-N_1 in Fig. 6-4) is assumed to be 3 in. (76 mm), which corresponds approximately to the calculated width of the rectangular stress block at edge of the D-region (a = 2.5 in.). After internal forces are calculated, the possibility of debonding a portion of the total number of strands will be investigated, because it would be beneficial to achieve proper stress control at transfer and under service load levels.

The vertical loads applied at the nodes of the strut-and-tie model (Fig. 6-4) account for the effect of the distributed load acting on the beam. The configuration of the model was selected so that the angle of inclination for the first strut (element 9, Fig. 6-4) was steeper than the other two inclined struts, to provide a better representation of the compression fan that forms in the area surrounding the support. The angle of inclination of the second and third struts (designated α in Fig. 6-4) was calculated based on the dimensions of the horizontal tie, the horizontal strut, and the distance between vertical ties. For the strut-and-tie model shown (Fig. 6-4) $\alpha = 38.1°$, which is greater than the lower limit of 25° established by the ACI Code (2002).

3.3 Check overall height of model and determine internal forces in all struts and ties

The couple formed by forces C_c and T_s must be equal to the external moment acting at point D (Fig. 6-4). Therefore,

$$C_c = T_s = \frac{3.21 \times 10^3 \; kip\; in.}{23.5\; in.} = 136\; kip\; (607\; kN) \qquad (6\text{-}1)$$

Element forces are determined based on equilibrium for each of the 6 nodes shown in Fig. 6-4. Results are summarized in Table 6-2. A negative sign indicates compression.

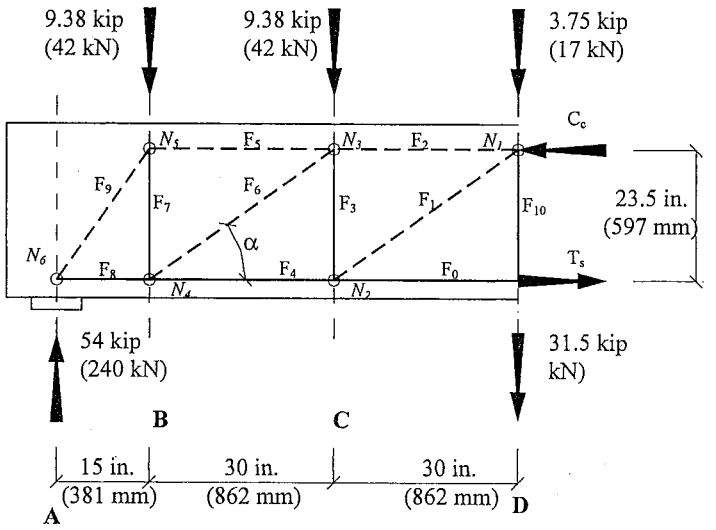

Fig.6-4: Strut-and-tie model for end region with horizontal strand pattern.

Element Type	Designation (Fig. 6-4)	Force kip (kN)
Horizontal Struts	F_2	-91 (-407)
	F_5	-34 (-153)
Inclined Struts	F_1	-57 (-254)
	F_6	-72 (-322)
	F_9	-64 (-285)
Horizontal Ties	F_0	136 (607)
	F_4	91 (407)
	F_8	34 (153)
Vertical Ties	F_3	35 (157)
	F_7	45 (199)
	F_{10}	32 (140)

Table 6-2: Element forces for strut-and-tie model in Fig. 6-4.

3.4 Verify capacity of horizontal and inclined struts

The nominal capacity of the struts is determined using the effective compressive strength given by Eq. A-3 of the ACI Building Code (2002):

$$f_{cu} = 0.85 \beta_s f_c' \qquad \text{[ACI Sec. A.3.2, Eq. (A-3)]}$$

According to Section A.3.2 of the ACI Code the effective strength should be the smaller of the strength of the concrete in the strut and the concrete in the nodal zone. The critical horizontal strut of the truss model shown in Fig. 6-4 is element 2, located near the boundary of the region being analyzed. Node 3, located at the left end of Strut 2, is classified as a C-C-T node because two struts and a tie converge in it. According to Appendix A of the ACI Code the strength factor for a strut located in the compression zone of a beam is $\beta_s = 1.0$, and the strength factor for a node with one tie is $\beta_n = 0.8$. Given the lower capacity of the concrete in the node, $\beta_n = 0.8$ controls the nominal capacity of the strut.

Therefore, the design strength of the horizontal strut is:

$$f_{cu} = 0.85 \times 0.8 \times 7.5\ ksi = 5.1\ ksi\ (35\ MPa) \quad (6\text{-}2)$$

$$\phi F_{ns} = 0.75 \times f_{cu} \times A_c \quad \text{[ACI Sec. A.3.1, Eq. (A-2)]}$$

$$\phi F_{ns} = 0.75 \times f_{cu} \times 12\ in. \times 3\ in. = 138\ kip\ (613\ kN) \quad (6\text{-}3)$$

where ϕ is the strength reduction factor, which according to Section 9.3.2.6 of the ACI Code, is 0.75 for struts, ties, nodal zones, and bearing areas of strut-and-tie models. Equation 6-3 shows that the capacity of the horizontal strut is greater than the demand on the strut of 91 kip (407 kN) (Table 6-2), therefore the strut has adequate strength.

Inclined Struts 6 and 9 were investigated to determine which of two had the largest demand. Because one tie is anchored in each of the two nodes 5 and 6, located at the ends of Strut 9 (F_9, Fig. 6-4), the strength reduction factor for the nodes is $\beta_n = 0.80$. Element 9 is considered a bottle-shaped strut because its width can spread between nodes. Consequently the strength factor for the strut according to Section A.3.2.2 of the ACI Code is $\beta_s = 0.6$, which is lower than the strength factor for the nodes. Although Section A.3.2.2 allows the use of a higher factor $\beta_s = 0.75$ if reinforcement is provided complying with Section A.3.3, in this case it was assumed that no such reinforcement was provided and the more conservative factor was used. Therefore, the nominal strength of the concrete in Strut 9 is:

$$f_{cu} = 0.85 \times 0.6 \times 7.5\ ksi = 3.83\ ksi\ (26 MPa) \quad (6\text{-}4)$$

The width of the strut must be calculated to determine its nominal capacity. Figure 6-5 shows Node 6, located at the support. The width at the bottom of Strut 9 is given by Eq. 6-5:

$$w_{st} = l_{bp} \sin\alpha + h_t \cos\alpha \quad (6\text{-}5)$$

where l_{bp} is the width of the support plate and h_t is the height of the horizontal tie. According to Eq. 6-5, the width of strut 9 at the bottom is:

$$w_{9b} = 6\ in. \sin 57.5° + 6\ in. \cos 57.5° = 8.3\ in.\ (210\ mm) \quad (6\text{-}6)$$

The width at the top of Strut 9 (w_{9t}), the bottom of Strut 6 (w_{6b}), and the top of Strut 6 (w_{6b}) (Fig. 6-4) are calculated also using Eq. 6-5. The geometric model of these nodes is similar to that shown in Fig. 6-5 except that the length l_{bp} is taken as half the width of the vertical tie converging into the node and h_t is taken as the height of the strut (3 in., 76 mm). Therefore, the width of Tie 7 must be calculated to obtain the width of Strut 9 at Node 5. Section RA.4.2 of the ACI Building Code Commentary (2002) suggests calculating a limit of the tie width based on the allowable bearing stress of the nodal region. Following this recommendation, the width of Tie 7 is obtained based on the allowable stress in Node 5:

$$w_{tie7} = \frac{F_7}{\phi\, 0.85 \beta_n f'_c b} = \frac{45\ kip}{0.75 \times 0.85 \times 0.80 \times 7.5 ksi \times 12\ in.} = 1\ in.\ (25\ mm) \quad (6\text{-}7)$$

The width of element 9 at the top of the strut is calculated based on the width of the tie and the width of the horizontal strut:

$$w_{9t} = {}^{w_{tie}}\!/_{2} \sin\alpha + h_t \cos\alpha = {}^{1\ in.}\!/_{2} \sin 57.5° + 3\ in. \cos 57.5° = 2in.\ (52\ mm) \quad (6\text{-}8)$$

Similarly, the width of Strut 6 at the top of the strut is calculated based on the height of the tie and the allowable stress in Node 3. The width of Tie 3 is:

$$w_{tie3} = \frac{F_3}{\phi\, 0.85 \beta_n f'_c b} = \frac{32\ kip}{0.75 \times 0.85 \times 0.80 \times 7.5\ ksi \times 12\ in.} = 0.7in.\ (18\ mm) \quad (6\text{-}9)$$

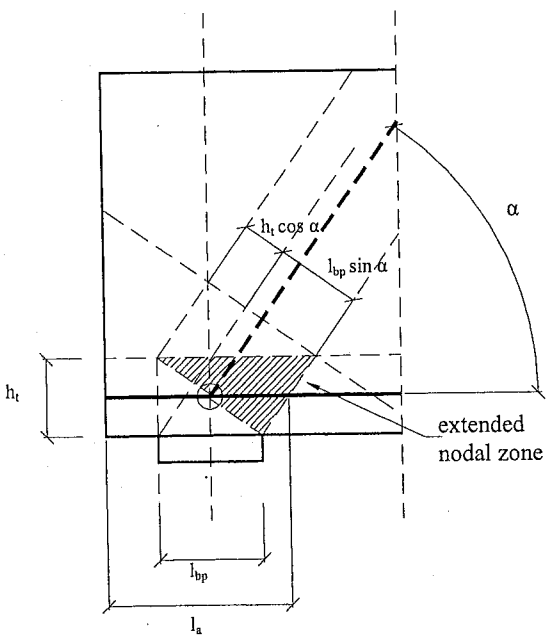

Fig.6-5: Width of strut in terms of nodal dimensions.

Therefore, the width of Strut 6 is given by:

$$w_{6t} = 0.35\ in. \sin 38.1° + 3\ in. \cos 38.1° = 2.6\ in.\ (65\ mm) \quad (6\text{-}10)$$

The capacity of Strut 9 is calculated at the section with the smallest width, which occurs at the top of the strut, and is given by:

$$\phi F_{ns} = 0.75 \times f_{cu} \times 12in. \times 2in. = 69\ kip\ (307\ kN) \quad (6\text{-}11)$$

Which is greater than the demand in strut (64 kip, 285 kN, Table 6-2). Similarly, the capacity of Strut 6 is given by:

$$\phi F_{ns} = 0.75 \times f_{cu} \times 12\,in. \times 2.6\,in. = 90\,kip\ (400\,kN) \qquad (6\text{-}12)$$

Which is also greater than the demand on the strut (72 kip, 322 kN). Having verified that the strength of the struts is adequate, the next step is to proceed with the proportioning of the reinforcement. In cases in which the struts fail to meet the minimum strength criteria, the depth of the struts, the compressive strength of the concrete, or the width of the beam must be adjusted in order to meet the Code requirements.

3.5 Calculate the reinforcement needed for horizontal ties

The force demand in each of the three horizontal ties is presented in Table 6-2. The number of strands required for each tie is determined using Eq. A-6 of the ACI Building Code, which defines the nominal strength of a tie as:

$$F_{nt} = A_{st} f_y + A_{ps}(f_{se} + \Delta f_p) \qquad \text{[ACI Sec. A.4.1, Eq. (A-6)]}$$

Strands with a nominal diameter of ½ in. (12.5 mm), which have a nominal area of 0.153 in^2 (99 mm^2) are used. Section A.4.1 of the ACI Code allows the designer to assume a value of Δf_p = 60 ksi (414 MPa). The total area of prestressing strands required is:

$$A_{ps} = \frac{T_{h\,tie}}{\phi\,(f_{se} + \Delta f_p)} \qquad (6\text{-}13)$$

The development length is critical for Ties 4 and 8. According to Section 12.9 of the ACI Code (2002), the development length of the strand is given by:

$$l_d = \left(\frac{f_{se}}{3}\right) d_b + (f_{ps} - f_{se})\, d_b \qquad \text{[ACI Sec. 12.9, Eq. (12-2)]}$$

Substituting the nominal diameter of the strand and the appropriate stress values into the previous equation, the anchorage length required to fully develop the stress in the strand is:

$$l_d = \left(\frac{150\,ksi}{3} + 60\,ksi\right) \times 0.5\,in. = 55\,in.\,(1397\,mm) \qquad (6\text{-}14)$$

For ties with anchorage length smaller than that required for Δf_p = 60 ksi (414 MPa), Section 12.9.1.1 allows the use of the smaller embedment provided the strand stress does not exceed values obtained with Eq. 12-2 of the Code. Accordingly, Eq. 12-2 can be rewritten to obtain the maximum stress that can be carried by the strand, in terms of the available anchorage length l_a:

$$f_{ps} = \frac{l_a}{d_b} + \frac{2\,f_{se}}{3} \qquad (6\text{-}15)$$

Equation 6-15 is meant to be applied only in cases where the anchorage length is between the transfer length (25 in., 635 mm for a ½ in. diameter strand) and the development length. A piecewise function approach as described in Section R12.9.1.1 of the ACI Building Code Commentary must be followed in other cases.

According to Section A.4.3.2 and A.4.3.3 of the ACI Building Code (2002), the force in the horizontal ties must be developed at the point where the centroid of the reinforcement leaves the extended nodal zone (Fig. 6-5). In the case of nodes 2, 4, and 6 the distance from the center of the node to the point where the centroid of the reinforcement leaves the extended nodal zone is given by:

$$l_{al} = \frac{w_{tie}}{2}\left[1 + \frac{\tan\alpha}{\tan(90-\alpha)}\right] \qquad (6\text{-}16)$$

where the angle α is the angle of inclination of the strut and w_{tie} is the width of the vertical tie converging in the node. The distance l_{al} is added to the distance between the center of the node and the edge of the beam to calculate the anchorage length available, which is shown in Table 6-3. For each tie, the maximum allowable stress is calculated using Eq. 6-15, and the amount of reinforcement required is calculated using Eq. 6-13 (Table 6-3).

Element Designation	$T_{h\,tie}$ kip (kN)	l_a in. (mm)	f_{ps} (6-15) ksi (MPa)	A_{ps} (6-13) in^2 (mm^2)	Number of Strands
F_0	136 (607)	61.6 (1564)	210 (1450)	0.86 (557)	6
F_4	91 (407)	31.8 (808)	164 (1128)	0.74 (477)	5
F_8	43 (153)	26.4 (671)	153 (1054)	0.37 (242)	3

Table 6-3: Proportioning of horizontal ties

Tests have shown that if an inclined crack (web shear) penetrates the transfer length at approximately $50d_b$, 25 in. (636 mm) in this case, the anchorage of the strand may be lost with catastrophic consequences (Peterman et. al, 2000). In this example, the configuration of the beam is such that the transfer length zone of the strands extends beyond the centerline of the support, where a shear crack is likely to occur. In order to address this problem, Tie 7 was designed for the full shear force so that it can effectively restrain the growth of the inclined crack. An alternative approach would be to calculate the strand stress afforded by the reduced anchorage length and provide mild reinforcement to carry the tension force in excess of the maximum stress that the strand can develop (Ramirez, 1994).

The results in Table 6-3 show that given the anchorage length requirements not much advantage can be taken of debonding in this case. One strand can be debonded at 6.6 in. (168 mm) from the edge. This is attributed in part to the proximity of the design region to the edge of the beam, which limits the available distance for proper anchorage of the strands. Another reason is the interaction between shear and tension in the horizontal reinforcement commonly observed in strut-and-tie models for slender beams. The horizontal component of the compression force in the inclined struts must be equilibrated by a force in the horizontal tie, which must be added to the force necessary to resist the demand for flexure.

3.5 Calculate reinforcement for vertical ties

Forces in the vertical ties are summarized in Table 6-2. The area of reinforcement is determined based on a yield stress of 414 MPa, as shown in Eq. 6-17:

$$A_{st} = \frac{F_{u\,tie}}{\phi f_y} \qquad (6\text{-}17)$$

Using U-stirrups made with No. 4 bars (9.5 mm diameter), the total area of vertical reinforcement for each tie is 0.4 in^2 (258 mm^2) stemming from two legs with 0.2 in^2 (129 mm^2) each. Section A.4.3.4 of the ACI Code stipulates that the stirrups must be anchored following standard practice, as specified in Section 12.13. The number of stirrups required for each vertical tie, which are placed near the center of the ties, is summarized in Table 6-4. In areas of the end region between vertical ties, the minimum amount of reinforcement required by the ACI Code is placed. According to Section 11.5.4 of the ACI Code (2002) the maximum spacing between stirrups for presstressed members is 0.75h, which is 21 in. (533 mm) for the beam being analyzed. A spacing of 15 in. (381 mm), corresponding to the distance between sections A and B (Fig. 6-4) is adopted. The minimum amount of web reinforcement is given by:

$$A_v = \frac{0.75\sqrt{f'_c}\, b_w\, s}{f_y} \geq \frac{50\, b_w\, s}{f_y} \qquad \text{[ACI Sec. 11.5.5.3, Eq. (11-13)]}$$

$$A_v = \frac{0.75\sqrt{7500}\,12\times 15}{60000} = 0.19\ in^2\ (126\ mm^2) \qquad (6\text{-}18)$$

To simplify the fabrication of the reinforcing cage, one No. 4 stirrup is placed between at the center point between sections B and C, and C and D (A_v = .4 in^2, 258 mm^2), in addition to the reinforcement required at the location of each vertical tie.

Element Designation	$F_{u\,tie}$ kip kN	A_{st} (6-17) in^2 (mm^2)	Number of stirrups, No. 4
F_3	35 (157)	0.78 (502)	2
F_7	45 (199)	1.00 (645)	3
F_{10}	32 (140)	0.71 (458)	2

Table 6-4: Proportioning of vertical ties

3.6 Verify bearing capacity

The bearing stresses in node N_6, located at the support of the beam (Fig. 6-4), must remain within the limit allowed by the Code. The bearing stress is calculated by dividing the reaction force by the area of the bearing plate:

$$f_b = \frac{54\ kip}{6\ in.\times 12\ in.} = 0.75\ ksi\ (5\ MPa) \qquad (6\text{-}19)$$

The support node N_6 is a C-C-T node given that one tie is anchored in it. The bearing strength is (β_n =0.8):

$$\phi f_{cu} = 0.75\times 0.85\times 0.8\times 7.5\ ksi = 3.83\ ksi\ (26\ MPa) \qquad (6\text{-}20)$$

Therefore the node has adequate bearing capacity.

3.7 Reinforcement layout for end region

The reinforcement layout of the end region with the horizontal strand profile is shown in Fig. 6-6.

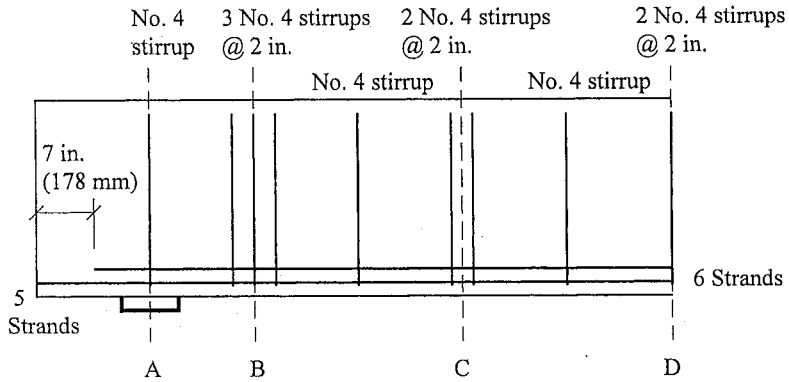

Fig.6-6: Reinforcement configuration for end region.

4 Design calculations for end region with draped strands

Given the differences in the location of the reinforcing strands within the design region, a different strut-and-tie model must be used between points A and D (Fig. 6-7).

4.1 Determine moment and shear demands for the beam

The bending moment and shear force demands at the edge of the end region are the same shown in Table 6-1.

4.2 Define truss configuration

The configuration of the truss is defined based on the height of the horizontal struts and the height of the horizontal ties. Similar to the horizontal strand alternative, the height of the horizontal ties was assumed to be 6 in. (152 mm) and the height of the horizontal struts 3 in. (76 mm). The inclination of the struts was similar to the case of the end region with the horizontal strands ($\alpha = 38.1°$). The model with draped strands (Fig. 6-7) has 9 additional truss elements and three additional nodes, which are necessary to model the stress gradient in the transfer length zone of the strands.

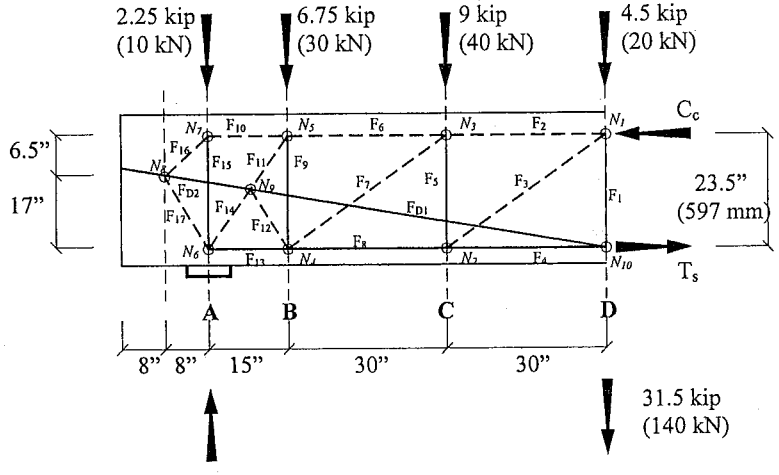

Fig.6-7: Strut-and-tie model for end region with draped strands.

Elements F_{D1} and F_{D2} represent the draped strands. The reason for using two separate elements and adding Node 9 (Fig. 6-7) is to model the effect of the transfer length on the stress in the draped strands. The truss shown in Fig. 6-7 is statically indeterminate. To facilitate the calculation of element forces in the truss, the forces in ties F_{D1} and F_{D2} are predetermined taking into consideration the development length of the strands. A total of two strands, corresponding to 33% of the total prestressing force, are draped at section D (Fig 6-7). As previously discussed Section A.4.3.2 of the ACI Building Code (2002) stipulates that the tie force must be developed at the point where the centroid of the reinforcement leaves the extended nodal zone. The dimensions of nodal zone 8 and the surrounding struts framing this nodal zone are analyzed to determine the anchorage length of the strand (Fig. 6-8).

The 6 in. dimension shown in Fig. 6-8 was selected to guarantee that struts 11 and 14 would have adequate capacity. The dimensions l_a and l_{ao} (Fig. 6-8) are determined using simple geometry:

$$l_{ao} = {}^{8\ in.}\!/_{\cos 11.58°} = 8.2\ in.\ (207\ mm) \tag{6-21}$$

The distance between the back of the node and the point where the tie leaves the extended nodal zone (Fig. 6-8) is calculated using the law of sines:

$$l_a - l_{ao} = 4.1\ in. \times \frac{\sin 53.2°}{\sin 36.8°} = 5.5\ in.\ (139\ mm) \tag{6-22}$$

Therefore the total anchorage length is:

$$l_a = 8.2\ in. + 5.5\ in. = 13.7\ in.\ (348\ mm) \tag{6-23}$$

In this case the anchorage length available is less than the transfer length. Therefore the minimum stress in the strand between Nodes 8 and 9 is given by:

$$f_{ps} = \frac{3\,l_a}{d_b} = \frac{3 \times 13.7}{0.5} = 82\ ksi\ (567\ MPa) \tag{6-24}$$

Because a total of two strands are draped, the force in Tie F_{D2} is given by

$$F_{D2} = 2\,A_{ps}\,f_{se} = 2 \times 0.153\ in^2 \times 82\ ksi = 25\ kip\ (111\ kN) \tag{6-25}$$

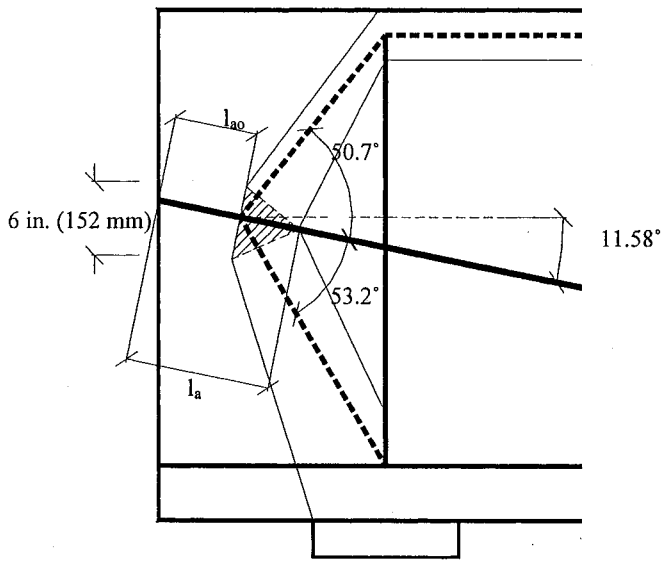

Fig.6-8: Development length of strands anchored in Node 8.

Similarly, the force in Tie F_{D1} is calculated based on the anchorage length at the point where the tie leaves the extended nodal zone of Node 9. The distance between nodes N8 and N9 can be calculated using the law of sines and is 17 in. (432 mm). The distance from the center of Node 9 to the point where the tie leaves the extended nodal zone is calculated based on the width of Strut 14 (8.3 in., 210 mm) as one half the width of the strut divided by the cosine of the angle between the normal to the strut and the axis of the tie (21°). The anchorage length is:

$$l_a = 8.2 + 17 + 4.4 = 29.6\ in.\ (752\ mm) \qquad (6\text{-}26)$$

Because the available anchorage length is greater than the transfer length, the minimum stress in the strand between Nodes 8 and 9 can be determined using Eq. 6-15:

$$f_{ps} = \frac{29.6}{0.5} + \frac{2\times150}{3} = 159\ ksi\ (1096\ MPa) \qquad (6\text{-}27)$$

The force in Tie F_{D1} is given by

$$F_{D1} = 2\ A_{ps}\ f_{se} = 2\times0.153\ in^2\times159\ ksi = 49\ kip\ (216\ kN) \qquad (6\text{-}28)$$

4.3 Calculate forces in truss elements

After the forces in Ties F_{D1} and F_{D2} are known, the internal forces in the truss can be calculated using principles of equilibrium. Results are summarized in Table 6-5.

Element Type	Designation (Fig. 6-7)	Force kip (kN)
Horizontal Struts	F_2	-103 (-458)
	F_6	-58 (-258)
	F_{10}	-16 (-71)
Inclined Struts	F_3	-42 (-187)
	F_7	-57 (-254)
	F_{11}	-78 (-347)
	F_{12}	-27 (-120)
	F_{14}	-55 (-245)
	F_{16}	-21 (-93)
	F_{17}	-20 (-89)
Horizontal Ties	F_4	88 (391)
	F_8	54 (240)
	F_{13}	21 (93)
Vertical Ties	F_1	22 (98)
	F_5	26 (116)
	F_9	59 (262)
	F_{15}	11 (49)

Table 6-5: Element forces

4.4 Verify capacity of horizontal and inclined struts

The critical horizontal strut of the truss model shown in Fig. 6-7 is element F_2. The capacity of this element was calculated in Section 3.4 (Eq. 6-3) to be 138 kip (613 kN), which is greater than the demand on element F_2.

The inclined strut with the largest demand is element F_{11}. In order to calculate the width of Strut 11 at Node 5, the width of Tie 9 must be calculated. The width of Tie 9 is calculated based on the allowable stress in Node 5:

$$w_{tie} = \frac{F_9}{\phi\ 0.85\beta_n\ f_{cu}\ b} = \frac{59\ kip}{0.75\times0.85\times0.80\times7.5\ ksi\times12\ in.} = 1.29\ in.\ (33\ mm) \qquad (6\text{-}29)$$

The width of element F_{11} at the top of the strut is calculated based on the width of the tie and the width of the horizontal strut framing the nodal zone. Using Eq. 6-6:

$$w_{11t} = \frac{1.29\ in.}{2}\sin 32.6° + 3\ in.\cos 32.6° = 2.9\ in.\ (73\ mm) \qquad (6\text{-}30)$$

The capacity of the strut is calculated using a factor $\beta_s = 0.6$ (for bottle-shaped struts and also because Node 9 is a C-T-T node):

$$\phi F_{ns} = 0.75 \times f_{cu} \times 12\ in. \times 2.9\ in. = 99\ kip\ (440\ kN) \qquad (6\text{-}31)$$

which is greater than the demand in the strut (78 kip, 347 kN).

4.5 Calculate the number of strands needed in horizontal ties

The force demand in each of the three horizontal ties is presented in Table 6-5. The procedure is similar to the calculations shown in Section 3.5 for the beam with the horizontal strand pattern. For each tie, the maximum allowable stress was calculated using Eq. 6-15, and the amount of reinforcement required was calculated using Eq. 6-13 (Table 6-6).

Table 6-6 shows that if 4 strands are maintained in the horizontal tie, the amount of reinforcement will be sufficient to sustain the calculated demand. The remarks made in Section 3.5 about the catastrophic consequences of a shear crack forming through the transfer length of a strand are applicable to this strut-and-tie model also.

Element Designation	$T_{h\ tie}$ kip (kN)	l_a in. (mm)	f_{ps} (6-15) ksi (MPa)	A_{ps} (6-13) in.^{2} (mm^2)	Number of Strands
F_4	88 (391)	61.6 (1564)	210 (1450)	0.56 (360)	4
F_8	54 (240)	31.8 (808)	164 (1128)	0.44 (283)	3
F_{13}	21 (93)	26.4 (671)	153 (1054)	0.18 (118)	2

Table 6-6: Proportioning of horizontal ties

4.6 Calculate reinforcement for vertical ties

The calculated forces in the vertical ties are shown in Tables 6-5 and 6-7. Similar to the case of the end region with horizontal strands, U-stirrups made with No. 4 bars (9.5 mm diameter) are used as vertical reinforcement (the total area of each tie is 0.4 in^2, 258 mm^2). The area of reinforcement required by each tie, determined with Eq. 6-17, and the corresponding number of stirrups are summarized in Table 6-7.

Element Designation	$F_{u\ tie}$ kip (kN)	A_{st} (6-17) in.^{2} (m^2)	Number of stirrups, No. 4
F_1	22 (98)	0.49 (315)	2
F_5	26 (116)	0.58 (373)	2
F_9	59 (262)	1.31 (846)	4
F_{15}	11 (49)	0.24 (158)	1

Table 6-7: Proportioning of Vertical Ties

As indicated in Table 6-7 the demand in element 9 is the highest and requires the use of 4 No. 4 stirrups. A significant part of the force carried by element 9 originates from the difference in the magnitude of forces F_{D1} and F_{D2}. This difference is caused by the approach followed to model the anchorage of the strands, which in effect lumps the force transferred between nodes 8 and 9 at Node 9 (Fig. 6-7). In reality the transfer of force occurs gradually throughout the length of the strand, and for this reason it is deemed more appropriate to distribute the reinforcement evenly between points A and B than to concentrate it at the location of Tie 9 (Fig. 6-9).

4.7 Reinforcement layout for end region

The reinforcement layout for the beam is shown in Fig. 6-9. Minimum transverse reinforcement is placed as indicated in Section 3.6.

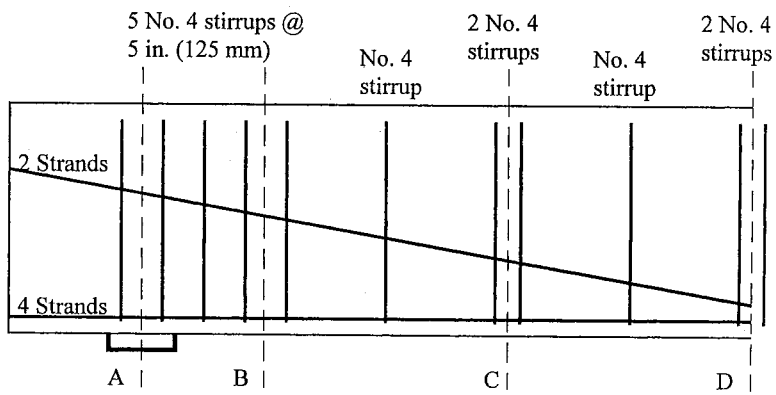

Fig.6-9: Reinforcement configuration for end region.

5 Summary

The design of the end region of a prestressed beam following Appendix A of the 2002 ACI Building Code for strut-and-tie models is presented. The configuration of the strut-and-tie models was selected to represent the effects of stress transfer in strands, the high shear stresses that take place near the support, and the effect of draping part of the strands.

The most critical factor for selecting the configuration of the strut-and-tie models was the development and anchorage length requirements for strands. The location of the nodes was chosen with the goal of developing models that could represent the increase in strand stress with anchorage length. After suitable models were selected, internal forces in truss elements were calculated, and their compliance with the strength requirements of the ACI Code (2002) was verified.

Among the main differences between the two models is the effect of the vertical component of the prestressing force in the beam with draped strands. Element 1 of the draped-strand model is subjected to a compression force equal to the vertical component of the force in the draped strands (Node 10, Fig. 6-7). Equilibrium of vertical forces at Node 1 (Fig. 6-7) dictates that the compression force in element 1 must be subtracted from the shear force of 31.5 kip (140 kN) applied at the node. As a result, the vertical ties and inclined struts in the model are designed for the shear force at section D reduced by the vertical component of the prestressing force in the draped strands.

Another significant difference between the two models is caused by the approach used to model the effect of bond stresses on the force in the ties. Conservatively, the force in the ties was assumed equal to the minimum that can be developed at the node closest to the edge of the beam. Following this approach resulted in a difference of 24 kip (107 kN) between forces F_{D1} and F_{D2} in Node 9 of the model with draped strands (Fig. 6-7). This 24-kip force, which is parallel to the orientation of the draped strands, is resisted by elements 11 and 12 of the model (Fig. 6-7). Because the compression force in both of these elements has a vertical component, it caused the tension force in Tie 9 (Fig. 6-7) to increase, resulting in a higher demand for vertical reinforcement. In the model with the horizontal strand pattern (Fig. 6-4) the effect of bond is not as significant given the interaction between the inclined struts and the horizontal ties. Although it seems that the additional stirrups imply a higher cost for the draped strand option, the strut-and-tie analysis only examines the ultimate condition. A final choice of reinforcement layout must be made taking into consideration stresses at the time of release and at service load levels.

Notation

A_{ps}	area of prestressed reinforcement
A_{st}	area of nonprestressed reinforcement
$A_{v,min}$	minimum area of shear reinforcement within a distance s
b	beam width
d_b	diameter of bar or strand
f_b	effective bearing strength of concrete
f_{cu}	effective compressive strength of concrete in a strut or nodal zone
f_{se}	effective stress in prestressed reinforcement
f_y	yield stress of reinforcement
f'_c	compressive strength of concrete
F_{ns}	nominal strength of strut
F_{nt}	nominal strength of tie
h_t	height of tie
l_{bp}	length of base plate
l_d	development length of bars
l_{dh}	development length of hook
M_u	factored bending moment at edge of D-region
V_u	factored shear force at edge of D-region
w_u	factored distributed load acting on beam
w_{st}	width of strut
α	angle of inclination of strut
β_s	factor to account for cracking and confining reinforcement on the effective compressive strength of concrete of a strut
β_n	factor to account for the effect of the anchorage of ties on the effective compressive strength of concrete of a nodal zone
Δf_p	increase in stress in prestressing tendons due to factored loads
ϕ	strength reduction factor

References

ACI 318-02: *Building Code Requirements for Reinforced Concrete and Commentary*. ACI Committee 318, American Concrete Institute, Farmington Hills, Michigan 2002.

Peterman, R., Ramirez, J., and Olek, J., "*Influence of flexure-shear cracking on strand development length in prestressed concrete members*," PCI Journal, v. 45, n. 5, Sep. 2000, pp. 76-94.

Ramirez, J., "*Strut-and-Tie Shear Design of Pretensioned Concrete*," ACI Structural Journal, v. 91, n. 5, Sep.-Oct. 1994, pp. 572-578.

Example 7: Strut-and-tie model cable stayed bridge pier table

Robert B. Anderson

Synopsis

Strut-and-tie models make the design of portions of complex structures transparent. This example, a pier table from a cable stayed bridge, is developed to show how strut-and-tie modeling can be used for an area that may be exposed to cyclic loading and how the results from alternate loads may be superimposed upon one another. The pier table transmits forces from the pylon, through an integral superstructure connection, to individual support legs. The pier table also creates an area for the transmission of superstructure forces. This example briefly describes the model development based upon the perceived flow of forces within the structure. The tie reinforcement is then detailed and the nodal zones checked.

Robert B. Anderson is a senior design engineer for URS Corporation, Tampa, Florida. He received his Master's degree in Engineering from the University of Texas at Austin and his Bachelor's degree in Civil Engineering from South Dakota State University. While attending the University of Texas, his research focused on the full scale testing of reinforced concrete models for strut-and-tie nodal regions. His design expertise includes both concrete and steel bridge types ranging from short-span grade separation structures to long span cable stayed structures.

1 Introduction and scope

This example is developed to show how strut-and-tie modeling can be used for an area that may be exposed to cyclic loading and how the results from alternate loadings may be superimposed upon one another. The example, shown in Figure 7-1, is a pier table from a cable stayed bridge. The pier table transmits forces from the pylon, through an integral superstructure connection, to individual support legs. The pier table also creates an area for the transmission of superstructure forces. The detailed isolated view also shown in Figure 7-1 shows how this region may be modeled with a plane frame or space frame analysis program and the free body forces that exist at the element connections. The framing of the structure transverse to the bridge axis is shown in Figure 7-2.

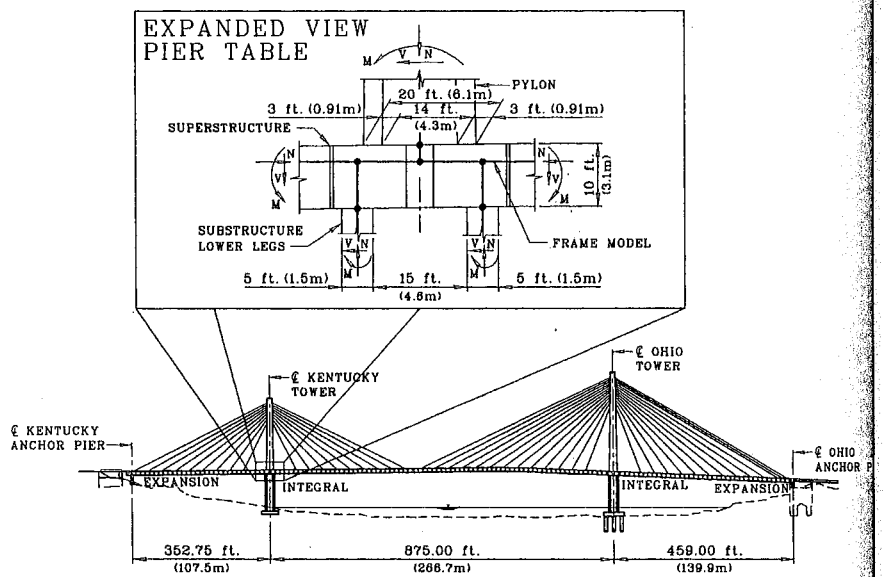

Figure 7-1: Bridge pier table layout

The scope of this example is limited to developing the strut-and-tie model for transmitting the pylon forces to the lower legs. The moments, shears, and axial loads developed at the top of the substructure lower legs, shown in Figure 7-1, will not be investigated. Fig. 7-3 shows a strut-and-tie model for examining forces from the superstructure elements.

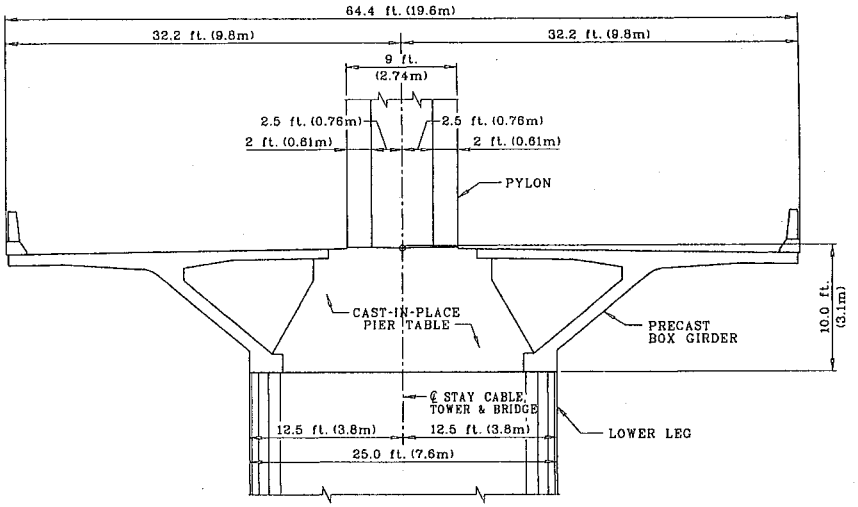

Fig. 7-2: Transverse section

Ties potentially exist in both the top and bottom of the girder because the integral connection sees both positive and negative moments during erection and its final load state. The strut-and-tie model shown in Fig.7-3 produces only one tie at either the top or bottom of the girder section which may be evaluated with a sectional approach (conventional flexural reinforcement design) versus the strut-and-tie model and also will not be studied as part of this example. Nevertheless, the tie reinforcing requirements from either of these omitted cases can be added to the tie requirement derived in the alternate strut-and-tie model developed in this example.

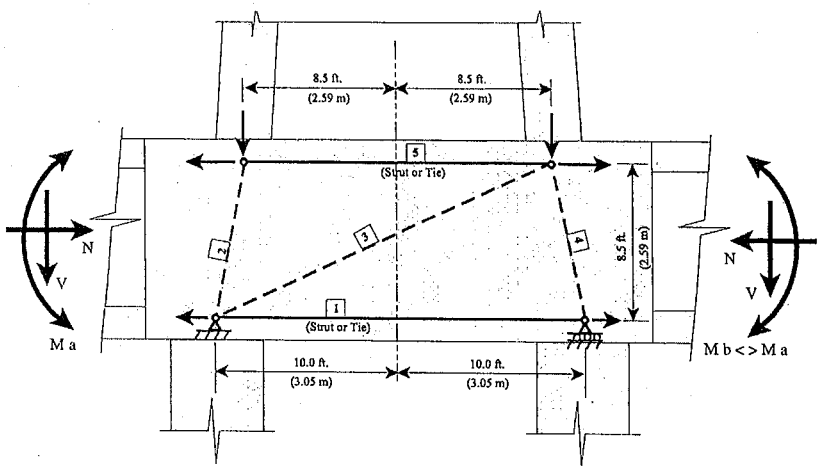

Fig. 7-3: Strut-and-tie model for superstructure moment transfer

2 Developing and analyzing the strut-and-tie model

Intuitively, the designer can visualize a force spreading from the pylon to the lower legs as shown in Fig. 7-4 due to the axial load N. The more difficult aspect is to derive the flow of forces for the moments and shears (M and V) also introduced at the base of the pylon. A first step is to divide the cross section of the pylon into four segments.

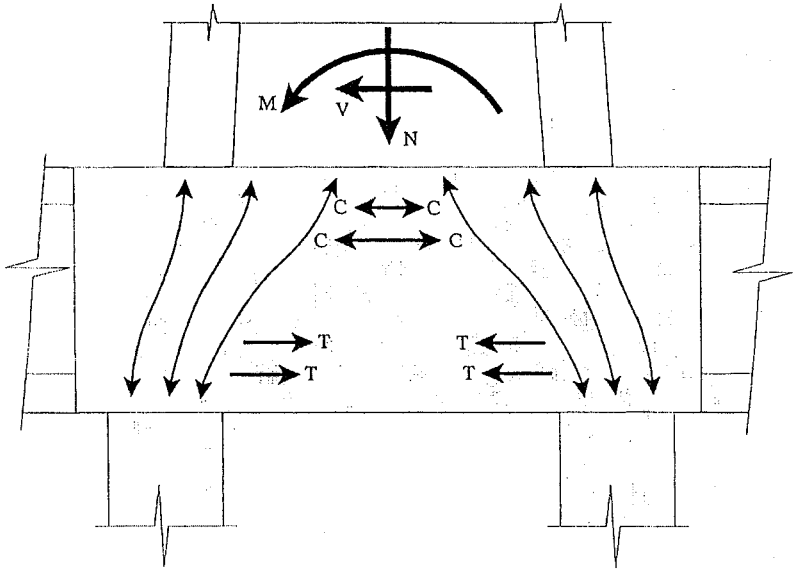

Fig. 7-4: Flow of pylon forces at pier table

Looking ahead, these segments will define discrete points (nodes) for the strut-and-tie model. In Fig.7-5, a unit downward force of 1,000 kips (4,448 kN) produces a uniform (P/A) pressure over the cross section and a set of discrete downward forces shown in Fig.7-5. Alternately, a unit moment of 1,000 kip-feet (1,356 kNm) produces flexural (Mc/I) stresses that are also represented discretely in Fig.7-5. Moment equilibrium is assured; however, the forces are dependent upon the selected location of the nodes. In Fig.7-6, the strut-and-tie model that accounts for spreading of forces from the pylon to the lower legs has been developed. The dimensions of the model with the node and member numbering, and unit load cases are shown in Fig.7-7. Nodes 5 through 7 at the top of the model correspond to the discrete points derived from the pylon's cross-sectional analysis. Load case 1 shows the loading for the unit downward force of 1,000 kips (4,448 kN) and Load case 2 shows the loading for a unit moment of 1,000 kip-feet (1,356 kNm).

Load case 3 is used for the transfer of shear forces for a unit shear force of 100 kips (445 kN) at the base of the pylon. Table 7-1 summarizes the forces developed in each of the strut-and-tie elements due to each of the unit loads.

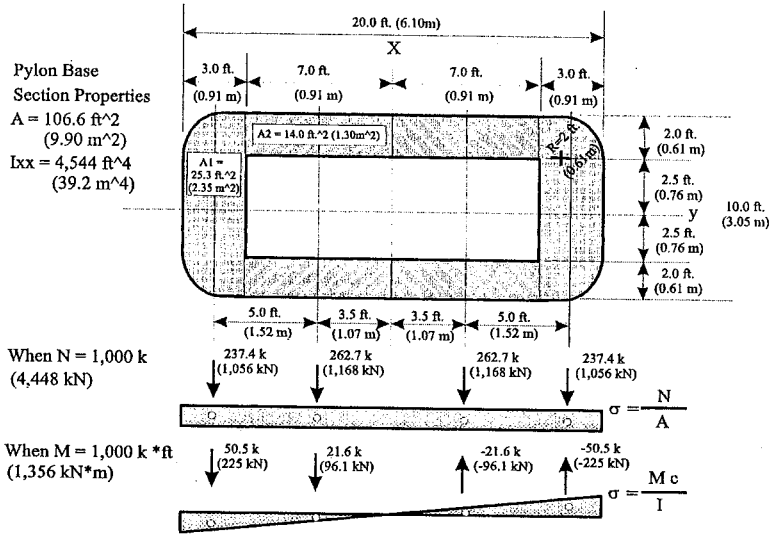

Fig. 7-5: Discrete force representation

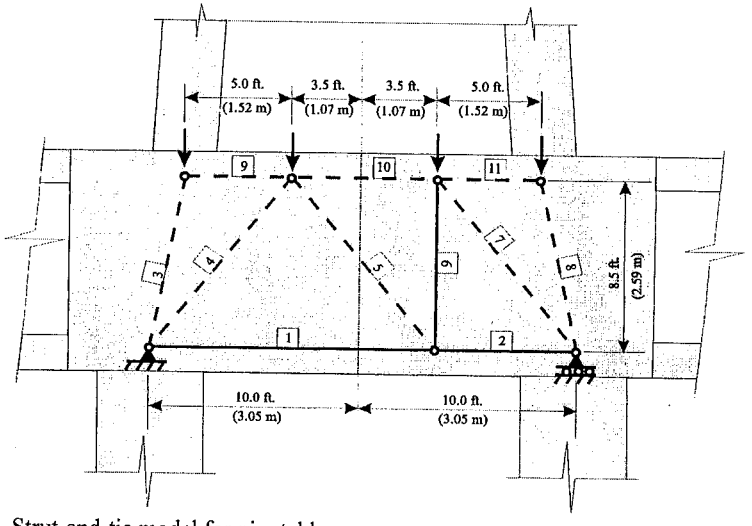

Fig. 7-6: Strut-and-tie model for pier table
(for transfer of pylon forces to substructure)

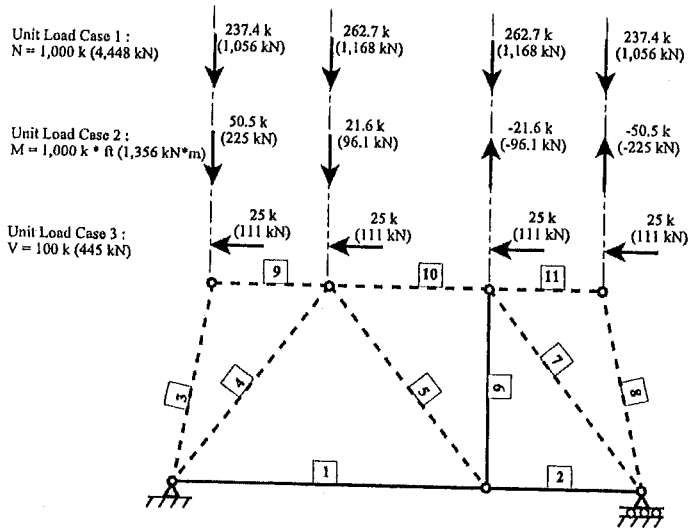

Fig.7-7: Application of unit loads

Member	Unit Loadings			Dead Loads			Live Loads			
	Unit Axial (N)	Unit Moment (M)	Unit Shear (V)	Dead Load Case 1 Time = Day 1	Dead Load Case 2 Time = Day oo	Maximum Dead Load (Most Tensile)	Live Load Case 1 Max Axial	Live Load Case 2 Max Moment	Live Load Case 3 Min Moment	Maximum Live Load (Most Tensile)
	1,000 k	1,000 k-ft	100 k	-21,401 k = N -17,793 k-ft = M 89 k = V	-21,072 k = N -19,450 k-ft = M 110 k = V		-1,984 k = N -22,570 k-ft = M 103 k = V	-474 k = N 17,905 k-ft = M -123 k = V	-1,525 k = N -37,856 k-ft = M 210 k = V	
1	242.8	8.9	-67.5	5,294.3	5,214.8	5,294.3	612.8	38.7	565.2	612.8
2	242.8	-8.9	-32.5	5,008.6	4,907.0	5,008.6	247.2	314.4	-35.1	314.4
3	-241.1	-51.3	0.0	-6,071.5	-6,077.2	-6,071.5	-1,635.7	803.9	-2,308.9	803.9
4	-330.7	0.0	-53.5	-7,124.6	-7,027.2	-7,027.2	-710.9	-91.3	-616.1	-91.3
5	0.0	-28.0	55.1	-449.4	-484.1	-449.4	-575.1	433.6	-944.2	433.6
6	0.0	21.6	-42.5	346.9	373.7	373.7	444.0	-334.7	728.9	728.9
7	-330.7	0.0	53.5	-7,030.4	-6,910.2	-6,910.2	-601.2	-222.2	-392.5	-222.2
8	-241.1	51.3	0.0	-4,246.7	-4,082.4	-4,082.4	679.2	-1,032.4	1,573.7	1,573.7
9	-41.9	-8.9	25.0	-1,033.0	-1,028.6	-1,028.6	-258.4	109.0	-348.7	109.0
10	-242.8	8.9	-17.5	-5,053.0	-4,962.0	-4,962.0	-298.9	-252.9	-70.1	-70.1
11	-41.9	8.9	-25.0	-760.2	-737.0	-737.0	92.2	-148.7	220.9	220.9

Table 7-1: Strut-and-tie forces for unit and applied loading

A cable stayed bridge must be analyzed for hundreds of load cases including: 1) permanent applied loading such as dead loads, post-tensioning loads, and forces due to creep and shrinkage effects, and 2) transient applied loads such as those from live load, wind, and temperature. Using a unit load approach offers an effective solution to develop group loading effects from the global analyses. The strut-and-tie model shown in Figures 7-5, 7-6 and 7-7 remains valid for all load cases as long as the struts remain struts (compression elements) and the ties remain ties (tension elements). It also gives the designer an appreciation for the forces developed at the pier table connection in terms of the applied forces. Table 7-2 shows an actual set of dead and live load forces and their factored sum based upon ACI load factors. It can be seen the downward pylon loads produced the majority of load in each of the strut-and-tie elements.

Member	Maximum Dead Load	Maximum Live Load	Group 1 (1.4DL + 1.7LL)
1	5,294.3	612.8	8,453.8
2	5,008.6	314.4	7,546.5
3	-6,071.5	803.9	-7,133.5
4	-7,027.2	-91.3	-9,993.1
5	-449.4	433.6	108.0 *
6	373.7	728.9	1,762.2
7	-6,910.2	-222.2	-10,052.0
8	-4,082.4	1,573.7	-3,040.1
9	-1,028.6	109.0	-1,254.8
10	-4,962.0	-70.1	-7,066.0
11	-737.0	220.9	-656.2

Tie Design Forces

* The tensile force for member 5 will be covered by orthogonal temperature and shrinkage reinforcement not explicitly designed in this example.

Table 10-2: Strut-and-tie forces for factored loadings

Of course, there maybe other situations where an overturning load, due to wind for example, would develop tensile forces in strut elements and alternate models would have to be developed.

3 Detailing the ties and nodes

This example has focused upon the development of a model for analyzing a complex structure with a single strut-and-tie model and unit load cases which are combined for group loading effects. Once the strut-and-tie forces are developed for each the loading combinations, the individual elements can be proportioned to resist these forces and detailed analyses of the nodal regions can commence. Different loading combinations may produce the worst condition for individual elements within the strut-and-tie model. The designer needs only to pick maximum tie forces developed by the various loading combinations. The calculation of reinforcing (mild steel and post-tensioning) requirements is undertaken as follows.

4 Calculations for the proportioning of ties and nodal zone check

Tie 1

Factored Design Force = F_{ut} = 1.4DL+1.7LL = 1.4 (5294.3 k)+1.7 (612.8 k)

= 8,453.8 k (37,600 kN)

ϕ = 0.75 Section 9.3.2.6

Select 60 – 1-1/4 " (32mm) Diameter Prestressing Rods

A_{ps} = 60 * 1.25 in.^{2} / rod = 75.0 in^2 (48,400 mm^2)

f_{py} = 150 ksi (1034 MPa)

f_{se} = 0.6 * 150 ksi = 90 ksi (621 MPa)

Δf_p = 60 ksi (414 MPa) (Bonded)

$\phi F_{nt} = \phi (A_{st} f_y + A_{ps} (f_{se} + \Delta f_p))$ Section A.4.1

= 0.75 (0 + (75.0 in.^{2} (90 ksi + 60 ksi))

= 8,437.5 k (0.2 % Overstress ~ OK)

Tie 6

Factored Design Force = F_{ut} = 1.4DL+1.7LL = 1.4 (373.7 k)+1.7 (728.9 k)

= 1,762.2 k (7,838 kN)

ϕ = 0.75 Section 9.3.2.6

Select 5 Layers at 1'-0" (305 mm) Spacing of 18 bars per layer of – #6 (19mm) Stirrups

16 Layers over 15'-0" (4.57m) are detailed in Figure 10-8

A_{ps} = 5 * 18 * 0.44 in.^{2} / bar = 39.6 in.^{2} (25,550mm^2)

f_y = 60 ksi (414 MPa)

$\phi F_{nt} = \phi (A_{st} f_y + A_{ps} (f_{se} + \Delta f_p))$ Section A.4.1

= 0.75 ((39.6 in.^{2}) 60 ksi + 0)

= 1,782.0 k > 1,762.2 k ~ OK

Space this reinforcing on each side of the tower centerline pylon to account for an alternate model (not shown in this example) which is mirrored from the one selected.

Nodal Zone at Intersection of Members 2, 7 and 8

$Fcu = 0.85\ \beta n\ f'c$ Section A.5.2

βn = 0.80

$f'c$ = 5.5 ksi (38 Mpa)

Fcu = 0.85 * 0.80 * 5.5 ksi = 3.74 ksi (25.8 Mpa)

Check Stress at Node:

Width of Cast-In-Place Portion of Pier Table

σ = 8,437.5 k / ((3 ft. * 12 in. / ft.) * (20 ft. * 12 in. / ft.)) = 0.98 ksi < 3.74 ksi ~ OK

The proportioning of this reinforcing is shown in Fig.7-8. Three layers of 1-1/4" (32 mm) diameter post-tensioning bars are utilized to provide the resisting element for the tie forces developed in Members 1 and 2 in the strut-and-tie model. For Member 6, 18 - #6 (19mm) stirrups are provided per 1''-0" (305 mm) space. These stirrups are provided at both sides of the centerline of the pylon to account for an alternate model which is mirrored from the one selected. The amount of stirrups provided is in excess of that required but assures shear ductility of the section for alternate load paths which may coexist with the model selected for this example.

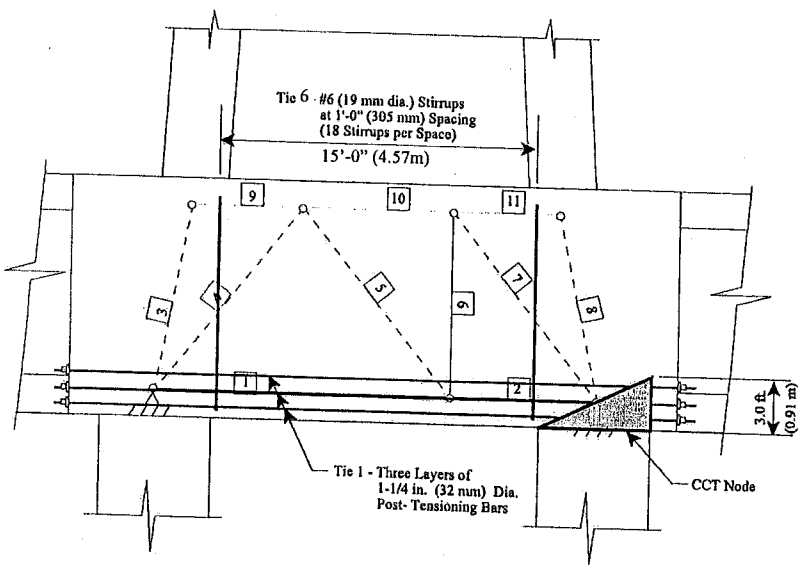

Fig. 7-8: Detailing of ties and CTT Node

5 Summary

Example 7 presents a strut-and-tie model for a situation that exists in a cable stayed bridge designed with a central pylon and dual legs for the substructure element. This example focuses on the load paths necessary to transfer the pylon loads to the lower legs and how to effectively and efficiently deal with multiple load cases that exist in complex structures.

Example 8: High wall with two openings

Robert W. Barnes

Synopsis

In this example, application of the new strut-and-tie modeling provisions of ACI 318-02 to the design of a wall with openings is summarized. Because the openings constitute a significant portion of the wall, earlier Code versions provide little relevant guidance for ensuring that the wall provides adequate resistance to the applied loads. Previous examples of the application of strut-and-tie models (STM's) to multiple load cases and/or lateral loads are rare. The wall in this example is designed to resist multiple combinations of both gravity and in-plane lateral loads.

Construction of the STM for each load combination is outlined. In addition, employment of statically indeterminate STM's to improve the efficiency and serviceability of the wall design is discussed. The example also covers selection and anchorage of tie reinforcement, as well as capacity checks for struts and nodal zones.

Robert W. Barnes received his M.S.E. and Ph.D. degrees from the University of Texas at Austin. He is an Assistant Professor in the Department of Civil Engineering at Auburn University; member of Joint ACI-ASCE Committee 423, Prestressed Concrete; and associate member of Joint ACI-ASCE Committee 445, Shear and Torsion.

1 Geometry, materials and loads

A 16-in. (405-mm) wall with a height of 640 in. (16.26 m) and a width of 320 in. (8.13 m) contains two 120-in. (3.05-m) square openings as shown in Fig. (8-1). The design concrete strength is 4000 psi (26 MPa), and the design yield strength of the steel reinforcement is 60,000 psi (410 MPa). Minimum cover is 2 in. (50 mm). The wall is to be designed for the following factored load cases:

- Load Case 1: two vertical loads of 450 kips (2.0 MN).
- Load Case 2: two lateral loads of 170 kips (0.76 MN) acting on right-hand side of wall.
- Load Case 3: combined loads from Load Cases 1 and 2.
- Load Case 4: two lateral loads of 170 kips (0.76 MN) acting on left-hand side of wall.
- Load Case 5: combined loads from Load Cases 3 and 4.

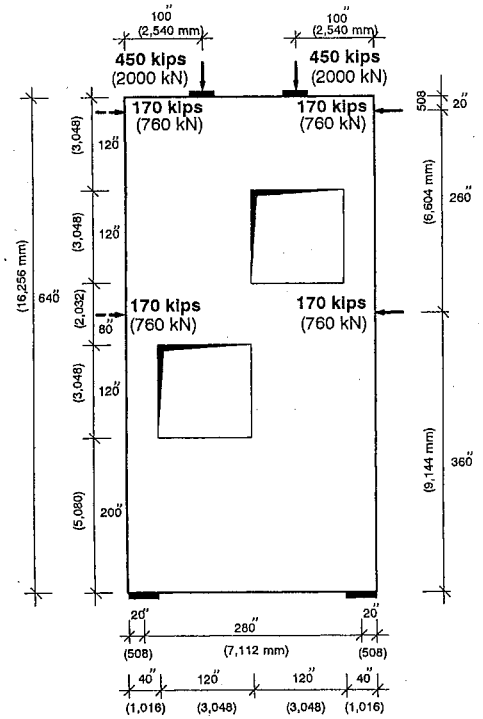

Fig.8-1: Wall geometry and loads

The wall rests on two footings. The available contact area at each support is 16 in. (406 mm) wide (the thickness of the wall) and 40 in. (1.02 m) long, so that the center of each support is located as shown in Fig. (8-1). The wall is modeled as simply supported. Under the influence of factored lateral loads, the concrete above the support in tension is expected to crack. The stiffness of this concrete with respect to lateral forces will be considerably less than that of the concrete above the compression support. Thus, the compression support is relied upon to transfer all the lateral forces to the foundation by shear-friction.

2 Design procedure

The whole wall is a D-region due to the openings and the concentrated loads and supports. ACI 318-99 gives little guidance for this type of structure. The design is based on the new *Appendix A—Strut-and-tie models* of ACI 318-02 as allowed by Section 11.10.1 of that document. Unless otherwise noted, all subsequent references in this example are to specific sections of ACI 318-02.

The first design step consists of conceiving a strut-and-tie model for each load case. Other steps include selecting tie reinforcement, checking capacity of nodal zones, and ensuring adequate anchorage of tie reinforcement at the nodes.

3 Modeling

The strut-and-tie models for the five load cases are shown in Fig. (8-2) through (8-6). Struts are indicated as dashed lines; solid lines represent ties. The struts and ties were positioned by considering 1) likely paths of the loads to the supports, and 2) orthogonal reinforcement patterns.

The model for Load Case 1 is not statically determinate. Thus, the forces in the struts and ties are not determined by equilibrium alone. For preliminary design, the model was developed by assuming approximately sixty percent of each vertical load traveled around the exterior of the opening beneath that load, while the remaining forty percent of both loads passed through the region between the two openings. The struts were then located to satisfy this assumption and equilibrium while exhibiting the clear flow of each force to the supports. The assumption was based on nothing more than engineering judgment about how the force paths might flow around the opening. As long as the resulting model satisfies equilibrium, and the stuts, ties, and nodal zones satisfy the provisions of Appendix A, the structure should develop the ultimate strength required.

Although not necessary for strength design, a linear elastic, plane-stress finite element analysis (FEA) was performed to refine the model for better performance under service conditions. Large disparities between the STM and the elastic stress distribution require will result in significant cracking as the structure deforms to redistibute the loads according to the reinforcement pattern. In addition, STM's that conform to the elastic stress distribution require less reinforcement than those that do not [Schlaich, Schäfer, and Jennewein (1987)]. Linear FEA was selected because it offers an adequate indication of the distribution of stresses under service loads. Nonlinear FEA might also be employed at the discretion of the designer.

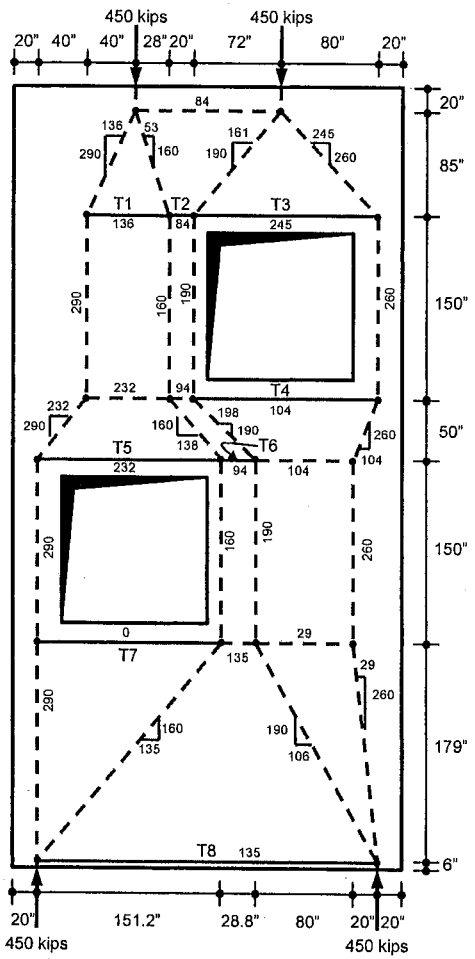

Fig.8-2: STM for Load Case 1

The use of the finite element analysis resulted in only a slight modification of model geometry and forces. For example, the FEA indicates that approximately 58 percent of the right-hand load travels around the outside of the top opening and 64 percent of the left-hand load travels around the outside of the bottom opening, rather than the sixty percent originally assumed for both locations. The final model is shown in Fig. (8-2).

In Fig. (8-2), the portion of the load that passes between the two openings in Load Case 1 is split into two distinct paths to clarify how each 450-kip (2.0-MN) load travels around each opening and proceeds to the foundation. This distinction is not necessary; the two paths could have been joined into a single load path in the central portion of the model. For simplicity, no attempt was made to separate the influence of the two vertical loads in the region between the openings for other load cases.

The necessary transformation of lateral loads into vertical reactions increases the difficulty of load-path visualization for Load Cases 2–5. The final strut-and-tie models chosen for these load cases are shown in Fig. (8-3) through (8-6). The desire for orthogonal reinforcement contributes to the relative complexity of the models for these cases. The requirement (A.2.4) that struts not cross or overlap prevents formation of the models for the combined load cases (3 and 5) by simply superimposing the models for more elementary cases (1, 2 and 4). The requirement (A.2.5) that struts and ties intersect at angles no smaller than 25 degrees also influenced the construction of portions of these models. Finally, an effort was made to obtain consistent tie locations among the five load cases. Although this may result in increased complexity when fine-tuning the individual STM's, it simplifies the reinforcement selection process (Section 3) and increases the efficiency of the final design.

As with Load Case 1, all of the models for the other load cases are statically indeterminate. Although it is possible to construct statically determinate models for these cases, this is not recommended for this structure because such models are differ markedly from the elastic flow of forces. Load Case 2 may be considered as an example. A statically determinate model for this case could have been constructed by omitting the tie (T1) on the right-hand side of the upper opening and adjusting the model geometry on the left-hand side of the opening. If such a model was employed, severe cracking could be expected in the region of the omitted tie, possibly under service conditions. In effect, the designer would be relying on the region to the left of the opening to resist the applied loads without any contribution from the region of the omitted tie. The statically determinate model would be less efficient; the *additional* reinforcement required to strengthen and extend T2 and T4 to the left of the opening would far outweigh the reinforcement saved by removing T1. Thus, while the use of an indeterminate model increases the complexity of the modeling procedure, it can improve efficiency and serviceability.

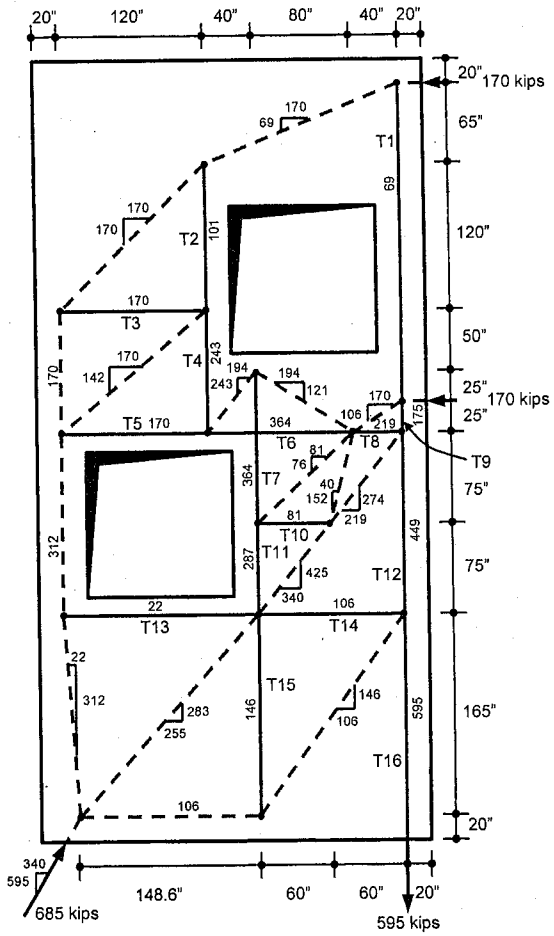

Fig.8-3: STM for Load Case 2

Analysis of statically indeterminate models requires the determination of enough redundant forces so that the remaining forces may be calculated using equilibrium considerations only. The general procedure used for Load Cases 2 though 5 included selecting the forces in the necessary redundants, and then determining the rest of the forces to satisfy equilibrium. Struts or ties located in the 40 in. (1.02 m) wide sections adjacent to the openings were chosen as redundants. As was done for Load Case 1, the magnitude of the force in each redundant strut or tie was estimated from a simple plane-stress finite element analysis of the structure.

Any rational estimate of the redundant force might have been used; only the efficiency and serviceability of the resulting design would have been affected by the accuracy of the estimate. Again, linear FEA was chosen to obtain an efficient and serviceable structure without undue effort.

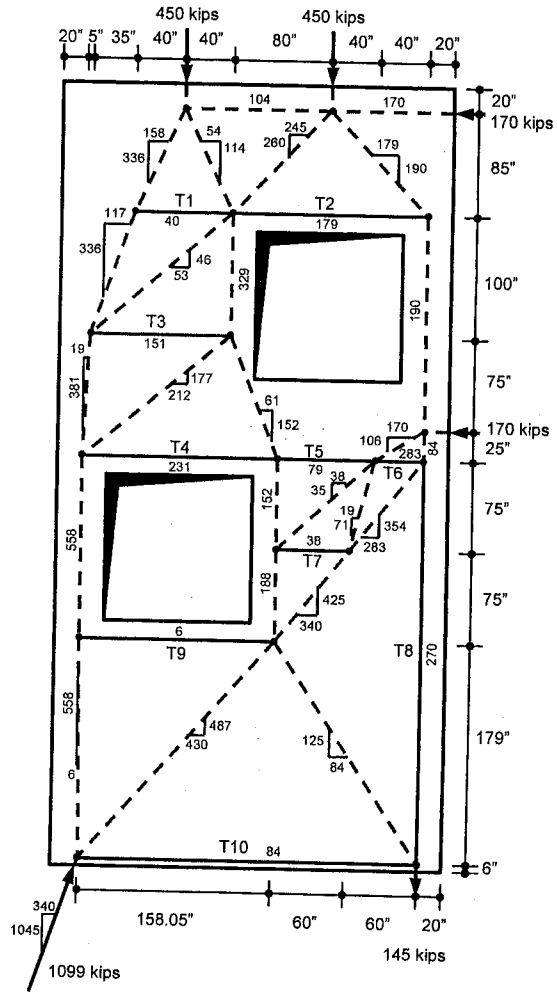

Fig.8-4: STM for Load Case 3

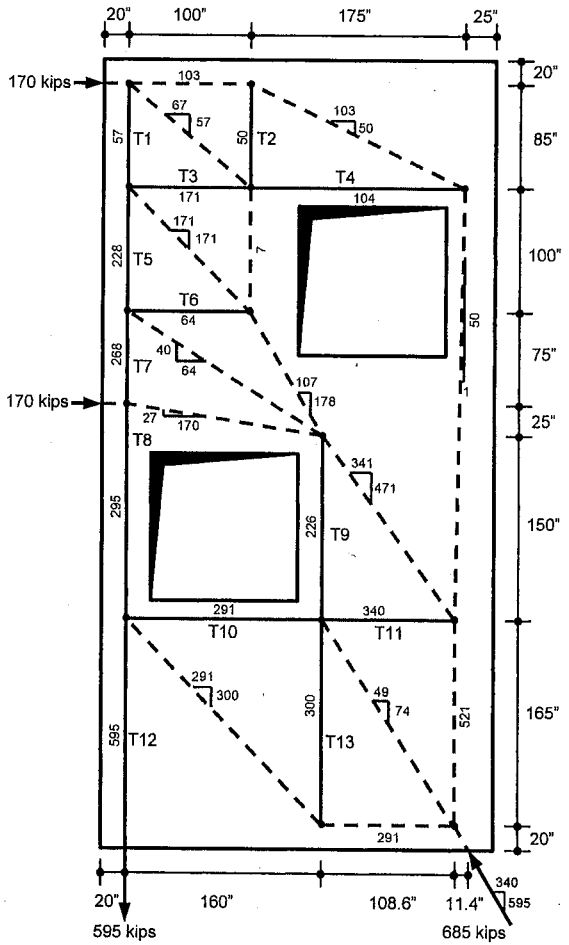

Fig.8-5: STM for Load Case 4

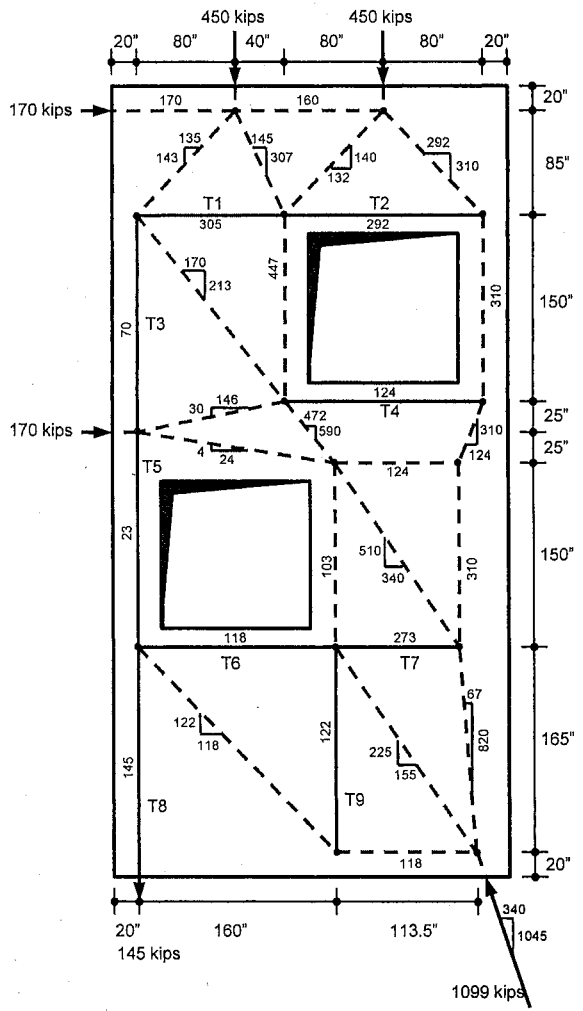

Fig.8-6: STM for Load Case 5

In order to control cracking and satisfy minimum reinforcement requirements, minimum orthogonal reinforcement should be included to satisfy Sections A.3.3.1 and A.3.3.2. Because a variety of strut orientations are present in the three models, the simplest means of satisfying Equation A-4 is by supplying a quantity of reinforcement that satisfies the expression

$$\frac{A_{si}}{bs} \geq 0.003$$

in each orthogonal direction. A mat of #5 bars spaced at 12 in. (300 mm) both ways in each face of the wall satisfies this expression. This pattern also satisfies the minimum reinforcement requirements of Sections 11.8, 11.10, and 14.3 of ACI 318-02. Once minimum reinforcement satisfying Section A.3.3 is provided, a value of 0.75 may be conservatively assumed for β_s (A.3.2) when calculating the effective compressive strength of concrete (f_{cu}) in each strut. An exception occurs at nodes anchoring more than one tie (CTT nodes). For the end of a strut that enters such a node, f_{cu} should be computed using a β_n value of 0.60 (A.3.1, A.5.2). The node located immediately above the right-hand support in Load Case 3 is an example of this node type.

3 Design of tie reinforcement

Since there is no prestressed reinforcement, the area of steel required for each tie is calculated from the expression

$$A_{st,req} = \frac{F_u}{\phi f_y}$$

where $\phi = 0.75$. For example, the strongest ties required are T16 from Load Case 2 and T12 from Load Case 4. The factored tension force in each of these ties is 595 kips (2.65 MN); therefore, 13.2 in^2 (8520 mm^2) of reinforcement is required. Placement of eleven #7 bars in each face of the wall provides a total tie reinforcement of 13.2 in^2. A bar spacing of 3.5 in. (89 mm) results in distribution of the tie force over at least 35 in. (890 mm). All of the tie regions are proportioned in a similar manner. Fig. (8-7) is a graphical summary of the tie requirements that result from considering all of the load cases. Each tie in this figure is labeled. The three numbers in each label represent the critical load case, the factored load (kips), and the area (in^2) of steel required for each tie, respectively. When establishing strut-and-tie models for multiple load cases, a concerted effort should be made to select consistent tie locations for the various cases. If so, tie reinforcement may often be efficiently utilized for more than one load case. Fig. (8-8) depicts one potential configuration of reinforcement that satisfies the tie requirements given in Fig. (8-7). The dashed lines represent minimum reinforcement that is not assigned to any particular tie.

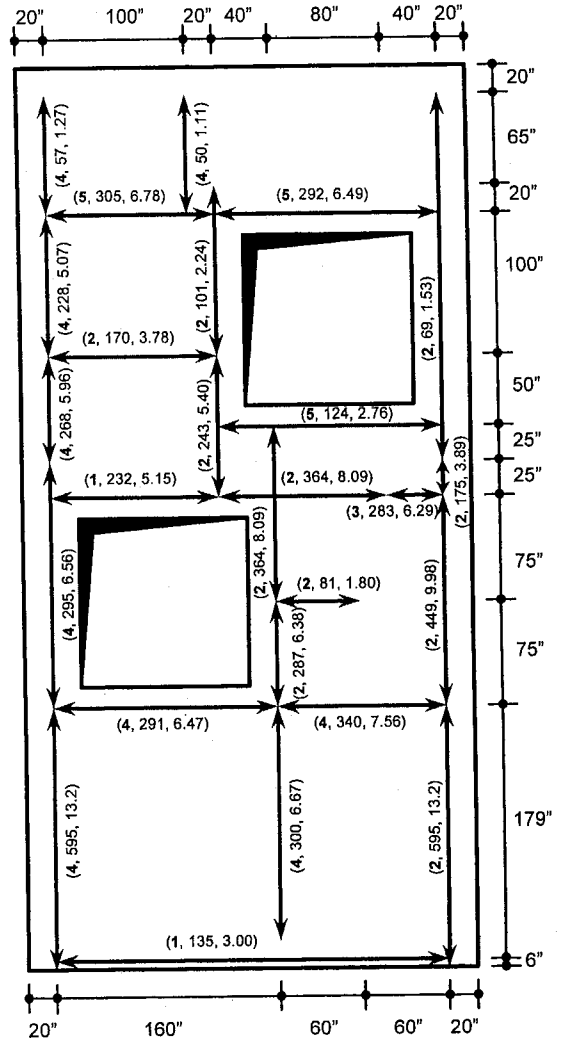

Fig.8-7: Critical tie requirements (load case, F_u, $A_{st,req}$)

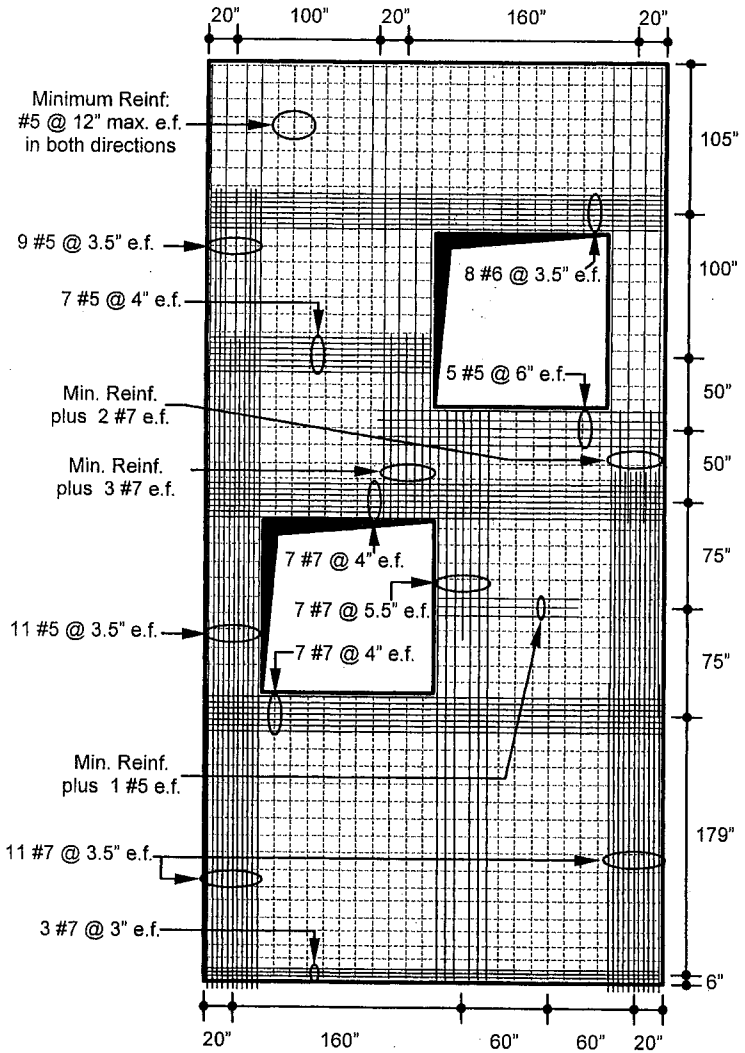

Fig.8-8: Wall reinforcement configuration (e.f. = each face of wall)

4 Nodal zones and bearing areas

Inspection of the strut-and-tie models for the five load cases reveals that the critical bearing location is at the compression support when the wall is subjected to Load Case 3 or 5. For Load Case 3, the compression support is the left-hand support. The corresponding nodal zone is shown in Fig. (8-9). Because the nodal zone represents the intersection of four forces, it is subdivided into two subnodes connected by a strut for easier visualization. Each subnode represents the intersection of three forces. In this manner, the geometry of the entire nodal zone can be constructed using the fundamental relationships for three-force nodes [Schlaich and Anagnostou (1990)]. The entire nodal zone consists of the two subnodes and the internal strut.

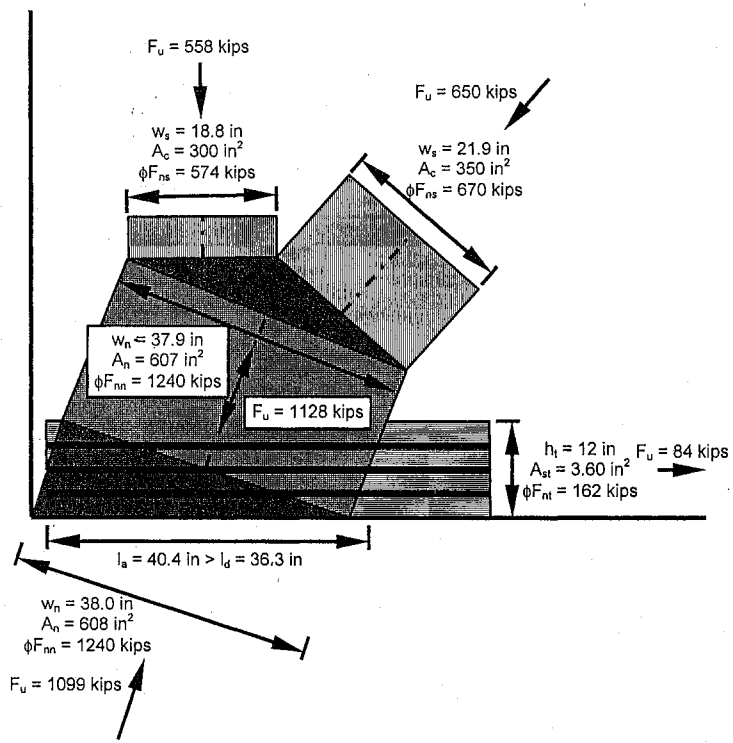

Fig.8-9: Nodal zone at compression support (Load Case 3)

The geometry of the lower subnode is defined by the available bearing width of 40 in. (1020 mm) and the assumed 12-in. (305-mm) thickness of the horizontal tie, which consists of three #7 bars in each face. The magnitude (1128 kips [5.02 MN]) and inclination angle (67.9° from horizontal) of the force in the internal strut are obtained from equilibrium. The available width of this internal strut (37.9 in. [963 mm]) can be obtained by considering the width of the other strut and tie as well as the angles between all three forces. Next, the upper subnode is constructed as a "hydrostatic" node with the stresses in the two exterior struts assumed equal to the stress in the internal strut. Thus, the lengths of each side of this subnode are proportional to the force carried by the corresponding strut. From equilibrium, lines of action of the tie and all struts coincide at the node point. The computed width, area, factored load, and factored strength of each strut and tie are shown in Fig. (8-9).

The lower subnode is of interest for checking the bearing capacity of the wall with respect to the support reaction. Due to the inclination of the reaction at the support, the available width of the nodal zone perpendicular to the reaction strut is given by:

$$w_n = 40\,\text{in}\left(\frac{1045}{1099}\right) = 38.0\,\text{in} \quad (966\,\text{mm})$$

The available area of the nodal zone with respect to the reaction is then:

$$A_n = (38.0\,\text{in})(16\,\text{in}) = 608\,\text{in}^2 \quad (0.393\,\text{m}^2)$$

The node anchors one tie (CCT node); therefore, a β_n value of 0.80 is selected. The effective compressive strength of the strut concrete is:

$$f_{cu} = 0.85\beta_n f'_c = 0.85(0.80)(4000\,\text{psi}) = 2.72\,\text{ksi} \quad (18.8\,\text{MPa})$$

The factored nominal strength of the nodal zone with respect to the reaction force is:

$$\phi F_{ns} = \phi f_{cu} A_c = (0.75)(2.72\,\text{ksi})(608\,\text{in}^2) = 1240\,\text{kips} \geq F_u = 1099\,\text{kips}$$

Thus, the bearing area appears large enough to provide adequate strength. However, the subnode faces bounded by the internal strut are subject to a larger force (1128 kips [5.02 MN]) than the bottom face of the nodal zone. As indicated in the figure, the capacity of these faces is also adequate.

The horizontal component of the reaction at this support is transferred to the footing by means of shear-friction. When designed according to the provisions of Section 11.7.4 of ACI 318-02, the required amount of shear-friction reinforcement is given by:

$$A_{vf,\text{req}} = \frac{V_u}{\phi f_y \mu} = \frac{340\,\text{kips}}{(0.75)(60\,\text{ksi})(0.6)} = 12.6\,\text{in}^2 \quad (8120\,\text{mm}^2)$$

A conservative value of 0.6 was assumed for μ. Thus, at least 12.6 in^2 (8120 mm^2) of reinforcement must cross the joint and be adequately developed in both the footing and the wall. This requirement will be satisfied by the 13.2 in^2 (8520 mm^2) of tension reinforcement provided as tie reinforcement for other load cases.

Sizing of the bearing plates (or bearing areas) for the applied loads is less complicated. Again, the full thickness (16 in.) of the wall is utilized. For each 450-kip load, a value of 1.0 may be selected for β_s and β_n, because the strut enters a compression-only node and is too short to spread significantly. The required bearing plate width for each of these loads is given by:

$$w \geq \frac{F_{us}}{\phi b f_{cu}} = \frac{450\,\text{kips}}{0.75(16\,\text{in})(3.4\,\text{ksi})} = 11.0\,\text{in} \quad (280\,\text{mm})$$

Therefore, 11 in. x 16 in. (280 mm x 406 mm) bearing plates are selected. A similar calculation can be performed for the 170-kip lateral loads. Each lateral load near the top of the wall immediately enters a node with one tie (CCT node) for one load case, so a β_n value of 0.80 should be selected for computing f_{cu}. This results in a required width of 5.21 in. (132 mm). However, for the lower 170-kip loads, a β_n value of 0.6 should be selected because each load enters a CTT node for one load case. A plate width of 6.94 in. (176 mm) is required. For simplicity, 7 in. x 16 in. (178 mm x 406 mm) bearing plates are selected for all the applied lateral loads.

The nodal zones and bearing areas described above are the most critical compression areas in the five strut-and-tie models. Despite the presence of the two openings, there is ample space to provide adequate widths for all the other struts and nodes in the models.

5 Anchorage of tie reinforcement

Fig. (8-10) illustrates the geometry of the nodal zone immediately above the left-hand support under the influence of Load Case 1. This load case produces the critical tension demand in the horizontal tie. Reinforcement was selected for this tie according to the procedure discussed above. Dimensioning of the nodal zone was performed as discussed in the previous section. Because of the small ratio of bar spacing to bar diameter, the reinforcement for this tie has the longest required straight bar development length of all the wall reinforcement, despite the fact that the horizontal reinforcement higher in the wall is subject to the reinforcement location factor (α) of 1.3 (Section 12.2.4). Neglecting any potential benefits of transverse reinforcement, the development length (l_d) for the #7 bars with a center-to-center spacing of 3 in. (76 mm) is

$$l_d = \frac{3}{40}\frac{f_y}{\sqrt{f'_c}}\frac{\alpha\beta\gamma\lambda}{\left(\frac{c+K_{tr}}{d_b}\right)}d_b = \frac{3}{40}\frac{60000}{\sqrt{4000}}\frac{1}{1.71}(0.875\,\text{in}) = 36.3\,\text{in} \quad (0.92\,\text{m})$$

As shown in Fig. (8-10), this is less than the available anchorage length (l_a) of 39.8 in. (1.01 m) (A.4.3(b)). Therefore, straight bar development is adequate for this tie.

In general, ensuring proper anchorage of the reinforcing steel is not difficult in this design. The bar sizes and spacings are such that the required straight bar development lengths are less than the available anchorage lengths. All the remaining nodes are located at least 15 in. away from wall surfaces, so there is adequate room for straight bar development of the #5, #6 and #7 bars within and behind the nodal zones (A.4.3), which typically extend 30–40 in. (0.76–1.02 m). If larger bars had been selected, hooks or mechanical anchorages may have been necessary.

When terminating reinforcement that is no longer required, such as the vertical #7 bars along the wall boundaries, care must be taken to extend these bars through the entire nodal zone at which they are no longer required. They must also extend at least one development length beyond the point at which they enter the extended nodal zone.

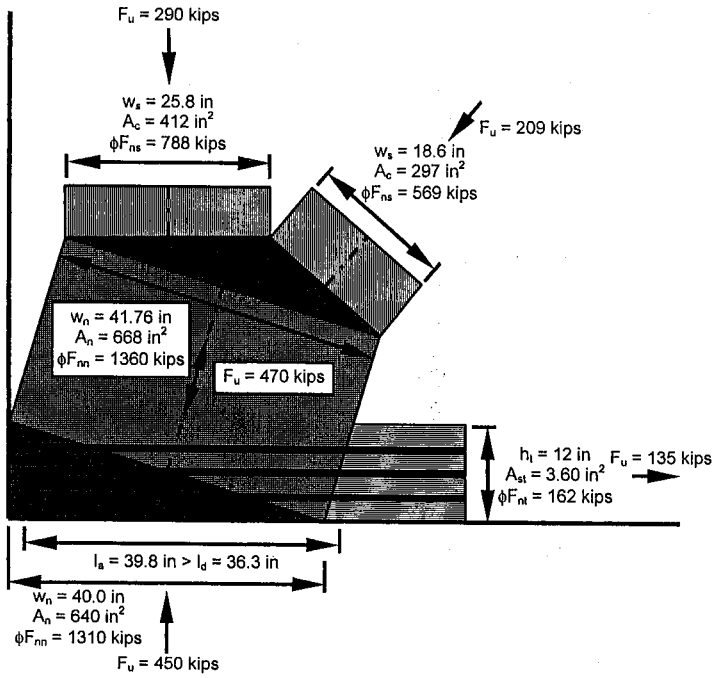

Fig.8-10: Nodal zone at support (Load Case 1)

Summary

Design of a reinforced concrete wall with two large openings is presented. The wall is designed according to the provisions of the new *Appendix A—Strut-and-tie models* of ACI 318-02. Issues related to the use of indeterminate models and the application of STM for multiple load cases are discussed. Tie reinforcement is selected after considering the STM's for all load cases. Capacity checks for typical struts and nodal zones are illustrated, and an example tie anchorage check is provided. Straight bar anchorage is adequate for all ties; no hooks or special anchorage devices are required.

Notation

Unless noted below, notation corresponds to that found in ACI 318-02.

$A_{st,req}$	required area of tie reinforcement
$A_{vf,req}$	required area of shear-friction reinforcement
l_a	tie anchorage length available in a nodal zone

References

ACI 318-99: *Building Code Requirements for Structural Concrete*. ACI Committee 318, American Concrete Institute, Farmington Hills, Michigan 1999

ACI 318-02: *Building Code Requirements for Structural Concrete*. ACI Committee 318, American Concrete Institute, Farmington Hills, Michigan 2002

Schlaich, J., Schäfer, K, and Jennewein, M. (1987): Toward a Consistent Design of Structural Concrete. *PCI Journal* Vol. 32 (1987), No. 3, p. 74-150

Schlaich, M., and Anagnostou, G. (1990): Stress Fields for Nodes of Strut-and-Tie Models. *Journal of Structural Engineering* Vol. 116 (1990), No. 1, p. 13-23

Example 9: Pile Cap

Gary J. Klein

Synopsis

The following example illustrates use of STM's for design of a pile cap. Two load cases are considered: 1) axial load only, and 2) axial load and overturning moment. The design is based on Appendix A of ACI 318-02 Results are compared to section design procedures per ACI 318-99. Compared to section design methods, STM design is more rational and leads to a more reliable structure. Because the reinforcing bars are located above the piles, overall footing depth is increased compared to traditional design in which the bars are placed between piles.

Gary J. Klein, FACI, is executive vice president of Wiss, Janny, Elstner Associates Inc., Northbrook, IL, where he has conducted structural investigations of buildings, Bridges, parking decks, and other structures. He is a member of ACI Committee 318, Structural Concrete Building Code; 342, Evaluation of Concrete Bridges and Bridge Elements; 345, Concrete Bridge Construction, Maintenance and Repair; 445, Shear and Torsion; and 546, Repair of Concrete.

1 Geometry and loads

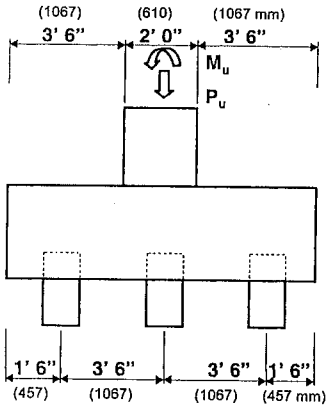

a)Elevation

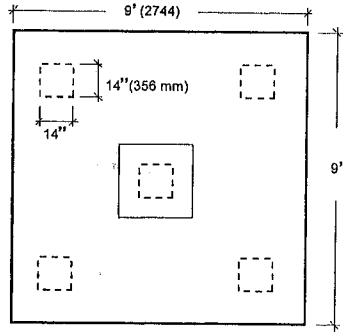

b)Plan

Fig. 9-1: Elevation and plan

General Data

Footing f'_c = 4000 psi

Column f'_c = 6000 psi

Reinf. f_y = 60,000 psi

Piles (14 in. sq.) Allow =70T (140^k)

Load Case 1:

P_D = 445^k M_D = 0

P_L = 222^k M_L = 0

P_u = $1.4P_D + 1.7P_L = 1000^k$

Load Case 2:

P_D = 445^k M_D = 0

P_L = 104^k M_L = 282 ft-k

P_u = 800^k M_u = 480 ft-k

Load and ϕ Factors:

- Per ACI 318-99, Chapter 9
- Per ACI 318-02, Appendix C

Pile Reactions

$$R=\frac{P}{N}+\frac{M}{SM}$$

$$SM_{piles}=\frac{\sum d^2}{d}=\frac{4x3^2}{3}=12$$

Row	Case	P/N	M/SM	Total	Factored
Left	1	133	0	133	200
	2	110	24	134	200
Center	1	133	0	133	200
	2	110	0	110	160
Right	1	133	0	133	200
	2	110	-24	86	120

Table 9-1: Pile reactions

2 Section design per ACI 318-99

Shear

Critical section at face of column: $V_u = 2x200^k = 400^k$

$V_u \le \phi V_c = \phi 2\sqrt{f'_c}\, bd = 0.85x2\sqrt{4000}\, x108d \ge 400{,}000^{\#}$

$\Rightarrow d \ge 34.4" \therefore use\ h = 39"; d = 39-3-1.5 = 34.5"$

Flexure

$M_u = 400^k\ x\,2ft = 800ft-k; Try 12\text{–}\#7, A_s = 7.2\ in^2$

$\rho = A_s / bd = 0.0019; \rho_{min} = 0.0018 \quad ok$

$\phi M_n = 0.9x7.2x60x34.5(1-.59x0.0019x60/4) = 13{,}200\ in-k = 1099\ ft-k \qquad ok$

Reinforcement Development

Straight #7 Bars: $\ell_d = \frac{60{,}000}{20\sqrt{4000}} x\,0.875 = 41.5"$

Hooked #7 Bars: $\ell_{db} = 1200db/\sqrt{4000} = 16.6"$

Although straight bars are fully developed at the face of the column, use hooked bars in accordance with common practice.

Cracking

Check service load flexural stress at column face SM = $9x3.25^2/6 = 15.8\ ft^4$

$M_s = 133^k\ x2x2' = 532ft-k \quad f_t = 532/15.8 = 33.7ksf = 233psi \approx 3.7\sqrt{f'_c}$

$\therefore$ Cracking is unlikely.

3 Strut-and-tie model per 318-02 Appendix A (Case 1)

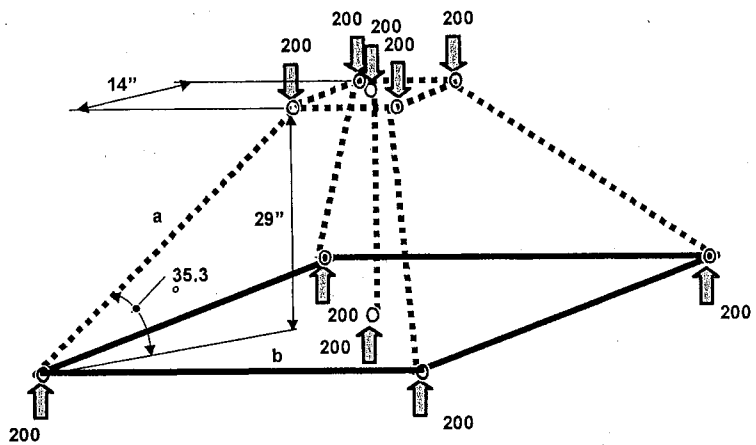

Strut a: 346k Compression

Tie b: 200k Tension

Fig. 9-2: Strut-and-tie model

Strut a = 200/sin 35.3 = 346^k Comp.

Tie b = 346 cos 35.3/$\sqrt{2}$ = 200^k Tens.

Strut c = 200^k Comp.

Tie Reinforcing

$\phi P_{nt} = \phi A_{st} f_y \geq P_u \Rightarrow 0.85 A_{st}\, 60 \geq 200 \Rightarrow A_{st} \geq 3.92 in^2$

Use 6–#8 ($A_{st} = 4.32 in^2$) *or* 9–#6 ($A_{st} = 3.96 in^2$)

Element	Type	β	$\phi\ 0.85\ \beta f_c'$ (ksi)
Struts	Comp. Zone	1.0	2.89
	Bottle	0.6	1.73
Nodes	CCC	1.0	2.89
	CCT	0.8	2.31
	CTT	0.6	1.73

Table 9-2: Elements

Strut:

$$A_{cs_{req'd}} = \frac{346}{1.73} = 200$$

$$A_{cs} = 14 h_2 = 14\left(14 \sin 35.3 + h_1 \cos 3.5\right)$$

$$\Rightarrow h_1 = 7.6", h_2 = 14.3"$$

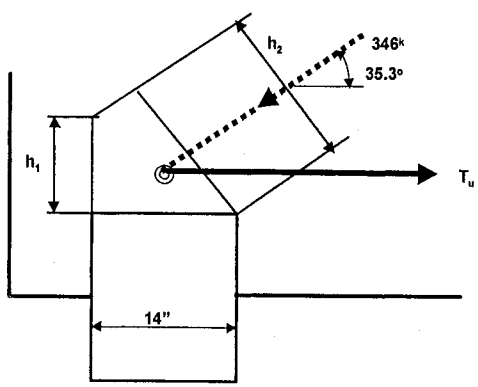

Fig. 9-3: Bottom node

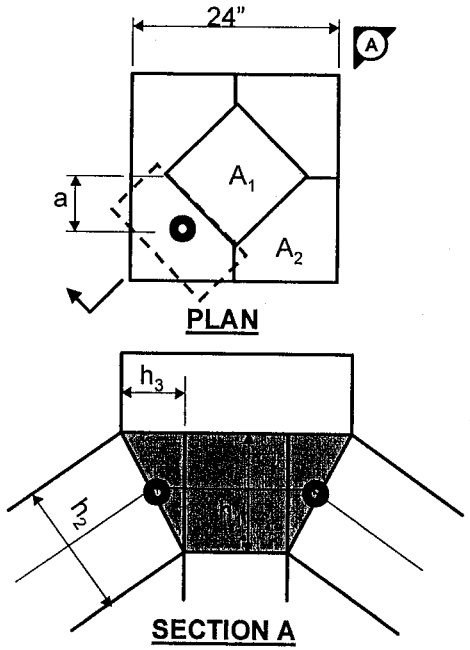

Fig. 9-4: Top node

Tension Tie

$T_u = 200^k$ $\quad H_{c_{req'd}} = \dfrac{200}{0.85\,x\,60} = 3.92\,in^2$

Use 6 - #8 bars in 2 layers at 2" & 6" above pile

Check development $\ell_{db} = 1200\ x1.0/\sqrt{4000} = 19.0"$ ok

Min. Reinf. $\rho_{min} = 0.0018$, Max spacing = 18"

Use #6 @ 6 between piles $\quad p = \dfrac{A_s}{bd} = \dfrac{0.44}{6\,x\,39} = 0.0019$

Top Node

$$A_1 = \frac{P_u}{\phi f_{cs}} = \frac{200}{1.73} = 116 in^2$$

$$A_2 = (24^2 - 116)/4 = 115 in^2$$

Assume diagonals are square:

$$h_2 = \sqrt{346/1.73} = 14.1"$$

$$h_3 = 115/14.1 = 8.2"$$

$$h_2 = h_3 \sin 35.3 + h_1 \cos 35.3$$

$$\Rightarrow h_1 = 11.5"$$

Check strut d

$$f_{cn} = \frac{346 \cos 35.3}{14.1 x 11.5}$$

$$= 1.74 \text{ ksi} < 2.89$$

$$a = (\sqrt{116}/2 + 8.2/2)/\sqrt{2}$$

$$= 6.70" \ (7" \textit{assumed})$$

Total Pile Cap Depth = 29" + pile embed. + $(h_1/2)_{bot}$ + $(h_1/2)_{top}$

= 29 + 9 + 7.6/2 + 11.5/2 = 47.5"

Use 4'0" + 48"

4 Strut-and-tie model per 318-02 Appendix A (Case 2)

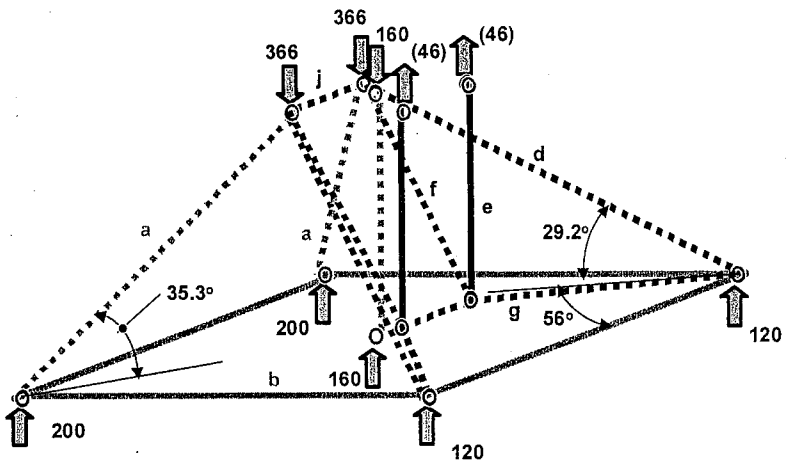

Strut d: 246^k Compression

Tie e: 46^k Tension

Strut f: 51^k Compression

Strut g: 31^k Compression

Tie h: 200^k Tension

Strut j: 320^k Compression

Fig. 9-5: Strut-and-tie model

Note: Truss members required to resolve eccentric load shown in black.

Bottom Node

Per Case 1

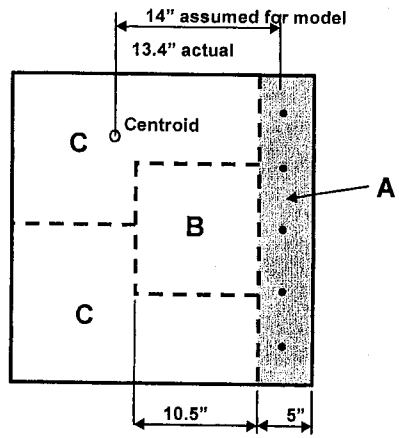

Fig. 9-6: Top node

Assuming square struts:

$h_2 = \sqrt{P_u / \phi f_{cs}}$

$\phi f_{cs} \, x \, h_2 \, x \, h_3 \geq P_u \sin\theta$

$\Rightarrow h_3 \geq P_u \sin\theta / (\phi f_{cs} h_2)$

$h_2 = h_3 \sin\theta + h_1 \cos\theta$

$\Rightarrow h_1 = (h_2 - h_3 \sin\theta) / \cos\theta$

Strut	Node	P_u	ϕf_{cs}	h_2	θ	ϕf_{cn}	h_3	h_1	$h_2 \times h_3$
Cent.	B	160	1.73	9.6	90	2.89	9.6	0.0	92
a	C	346	1.73	15.4	35.3	2.89	4.9	13.9	69
d	C	246	1.73	13.0	29.2	2.89	3.5	11.7	42
f	C	51	1.73	5.9	64.2	2.89	2.9	6.4	16
						Total = A + B + 2C = 120 + 92 + 2x127 =			466

Table 9-3: Node values

Total Column Area Available $= 24^2 = 576\ in^2 > 466\ in^2$

Total Pile Cap Depth $= 29" + \text{pile embed.} + (h_1/2)_{bot} + (h_1/2)_{top}$

$= 29 + 9 + 7.6/2 + 13.9/2 = 48.8"$

Use 4'0" = 48"

5 Summary

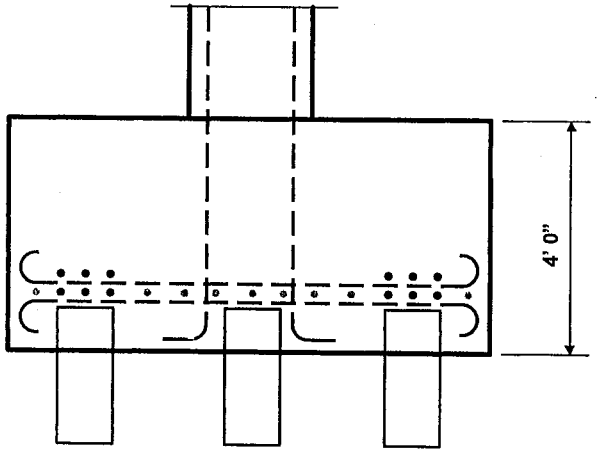

Fig. 9-7: STM Design per ACI 318-02:

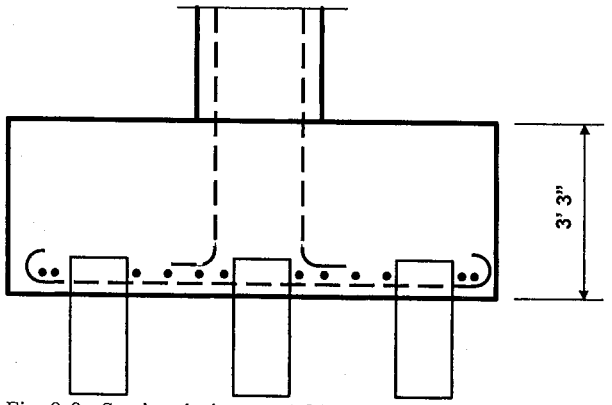

Fig. 9-8: Section design per ACI 318-99:

COMPARISON		
Method:	STM per 318-02	Section Design per 318-99
Footing Depth	4'-0"	3'-3"
Reinforcing	12 #8 concentrated over piles & 9 #6 (temperature) between piles, each way	12 #7 each way between piles

Table 9-4: Comparison

6 Conclusions

1 STM's are applicable to pile caps subjected to vertical load and overturning moment.

2 Design is dependent on judgment.

3 Detailed calculations at nodes are required to determine node height and thus the reinforcing details and overall footing depth; however, simplifying assumptions are needed:

- Assumption of square struts is needed to simplify complex geometry where struts intersect in three dimensions
- Geometric dissimilarities between struts and notes must be neglected (but checks should be made to assure the centoid is properly located and node area is sufficient)

4 Compared to traditional designs where reinforcing is located between piles, STM design results in greater footing depth and quantity of reinforcing.

5 STM design is more rational and leads to more reliable performance.

Part 5

Modeling structural concrete with strut-and-tie models - summarizing discussion of the examples as per Appendix A of ACI 318 - 2002

Karl - Heinz Reineck

Synopsis

After a brief summary of the contents of the SP and the examples, several general points are discussed which are based on observations made about the examples. The choice of a strut-and-tie model is a major issue and different engineers may propose various models for the same task. This leads to a discussion of the uniqueness of models and whether it is acceptable that different engineers may choose different models and thus different reinforcement arrangements and detailing for the same D-region. A further issue identified in some of the examples was the transition of a B-region to a D-region, and the procedure of modeling is shown. Finally the role and the importance of detailing is emphasized and some examples for this are given. Also some observations are made which led to recommendations for reconsidering some code provisions.

Karl-Heinz Reineck received his Dipl.-Ing. and Dr.-Ing. degrees from the University of Stuttgart. He is involved in both research and teaching at the Institute for Lightweight Structures Conceptual and Structural Design (ILEK), University of Stuttgart, and he is head of two research groups and managing director of the institute. His research covers the shear design of structural concrete, the design with strut-and-tie models and detailing of structural concrete and the design of high-performance concrete hot-water tanks. He is member of ASCE-ACI Committee 445 "Shear and Torsion" and chairs two subcommittees and also is a member of *fib* Task Group 1.1 "Practical Design".

1 Summary

The main objections of this Special Publication are to give background information on the use of strut-and-tie models (STM) following the new Appendix A of ACI 318-02 and to present design examples.

Part 2 describes the development of Appendix A and gives background information on the Commentary of ACI 318 itself. The strength values given in Appendix A are justified by comparison to other codes and with recommendations based on test results.

Part 3 presents important and well known test results which justify the use of strut-and-tie models for the design of structural concrete.

The examples presented in Part 4 may be classified in different groups:

- classical D-regions: Examples 1, 2, 3 and 6, which have already been designed using strut-and-tie models since long, and where test evidence is available, as described in Part 3.
- D-regions in beams: Example 5 with indirect supports, which so far have been addressed in some codes, often with an additional detailing rule to provide hanger reinforcement, which is not incorporated in ACI 318-02.
- D-regions in walls of buildings: Examples 4, 7 and 8.
- D-regions in 3D-structures: Examples 9 and 10.

In the following some general observations are made and some issues are discussed of general relevance for designing with strut-and-tie models.

2 Modeling and uniqueness of models

2.1 Finding a model

Finding a model for a given geometry and loading of a member or a D-region is the first and major task for the design engineer. The subsequent analysis of the forces and the check of the stresses then is relatively straight forward. The different modeling methods were presented by Schlaich, Schäfer and Jennewein (1987), and these are:

- using a standard example or adapting it to the given geometry or forces, as for the well known corbels or deep beams;
- using linear elastic stress distributions in decisive sections to determine the location of major struts or ties; and
- applying the load path method.

The first two methods are fairly obvious and have already been described by Schlaich et al. (1987). Therefore, in the following only the load path method is explained briefly with an example taken from the FIP Recommendations (1999).

The D-region shown in Fig. 1 with a point load applied in the direction of the member axis may occur at a beam end with a prestressing anchor or it may represent a column with an eccentric load. At the end of the D-region, the stress distribution is known and it is that of the B-region, and it can be calculated from well known formulae according to linear elastic theory, if the member is uncracked. So all the free-body diagrams shown in Fig. 1 are in equilibrium. The basic model in Fig. 1a demonstrates the overall equilibrium for a force applied at the end with a small eccentricity e. However, this model is not representative for the inner flow of forces within the D-region. The refined model in Fig. 1b is found by splitting the applied force F into two forces and correspondingly splitting the stress diagram at the right end into two parts with the strut forces C_1 and C_2 each equal to F/2 as resultants. The location of these two forces C_1 and C_2 is known and so only the location of node (N1) and the value for d_1 has to be assumed to finalize the strut-and-tie model and determine the tie force T_1 in Fig. 1b.

The load path method applied to a force with a large eccentricity leads to the strut-and-tie model shown in Fig. 1c. In this case, the load path for the force F only covers the lower part of the member and at the right end leaves a couple of equal forces in opposite direction in the upper part of the section. The magnitude and the location of these forces are also known so that the strut-and-tie model can fairly easily be completed.

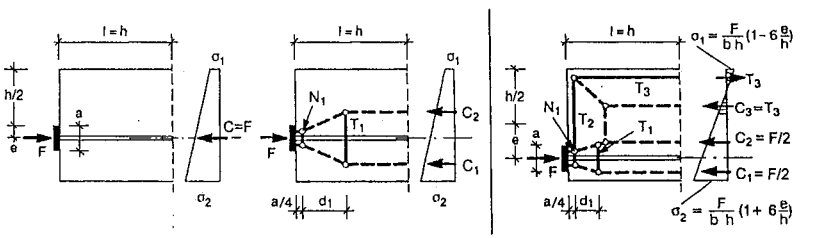

a) basic model b) refined model c) model for large eccentricities e

Fig. 1: Load path method applied to a D-region with a concentrated force in direction of the member axis with a small and with a large eccentricity

In a similar way the load path method can be applied to a beam end with a prestressing anchor as shown in Fig. 2, whereby at the border to the B-region in addition to the longitudinal stresses also shear stresses occur. Again the basic model (Fig. 2a) is not representative for the inner flow of forces. A refined model is required to find the transverse tie force T_1 (Fig. 2b). The further refined model in Fig. 2c is found by deviating the upper inclined strut C_1 slightly, and this exhibits the low tensile forces in the upper left corner.

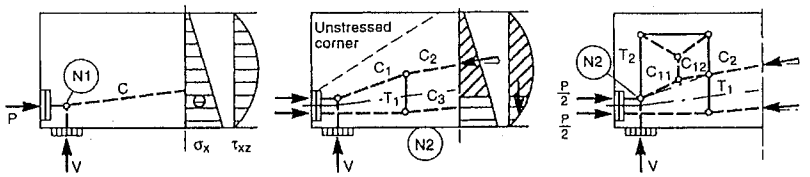

a) basic model b) refined model c) further refined model

Fig. 2: Load path method applied to the D-region at an end-support of a beam with a prestressing anchor

All of these tensile stresses or forces are traditionally covered in codes, as for example in the CEB-FIP MC 90, by rules for so-called "spalling stresses" or "bursting stresses". With the strut-and-tie models such artificial names are not required and all the tensile stresses and tensile forces clearly follow from applying the load path method.

Finally it should be pointed out that the load path method here did not require a Finite-Element analysis, because the required stresses at the border to the B-region could be found from basic mechanics. This orientation at the linear elastic stresses gave the major input for the choice of the model. Therefore, only few minor decisions had to be made for the locations of nodes and ties, like e.g. the location of node (N1) in Fig. 2a or the location of the tie T_1 in Fig. 2b.

2.2 Uniqueness of models

The above presented modeling techniques still imply that assumptions are made with respect to the location of nodes and struts or ties, so that several engineers may come to different solutions. In the above two cases, these differences are small and of minor importance because the linear elastic stress distributions gave the major input for the geometry of the model. In other design cases, the differences may be more significant and may lead to different forces of ties at possibly different locations and thus to different amounts of required reinforcement

All this poses the question regarding the uniqueness of strut-and-tie models for given loads and geometry of a D-region, which leads back to the basis for using strut-and-tie models (STM) in design. When applying STM, the following two conditions must be fulfilled: equilibrium and strength limits for the elements of strut-and-tie models. These two conditions comply with the static solution of the theory of plasticity, i.e. equilibrium and yield conditions are fulfilled, and this leads to a lower bound of the collapse load, as for example explained by Muttoni, Schwartz and Thürlimann (1996).

Thereby compatibility is not fulfilled, i.e. a mechanism is not necessarily found with a static solution. The different solutions lead to different ultimate loads, and only the maximum value of the collapse loads corresponds to a mechanism. The exact or right solution will comply with the lower bound of all the possible kinematic solutions.

The fact that different strut-and-tie models can be found is therefore an imminent condition of this design method based on the static solution of the theory of plasticity. A unique solution can only be expected if compatibility is fulfilled. Any consideration of compatibility requires the calculation of strains and deformations which requires assumptions for the constitutive laws for the elements of STM, and this leads to a non-linear analysis of the model. In order to avoid this complication, Schlaich et al. (1987) recommended to orientate the model in accordance with the stress fields of a linear elastic analysis. This firstly has the advantage that the changes in the flow of forces within the D-region are small from the elastic state of stresses to the cracked state of the member until the ultimate load is reached at the assumed model. Therefore, not much redistribution of the internal forces takes place which would require a large amount of ductility. Secondly, the model can also be used for checking the serviceability limit state, i.e. crack widths and deformations.

With respect to the ductility, which is assumed to be given in the theory of plasticity, and the check of the yield conditions, it should be noted that normally a design with strut-and-tie models leads to yielding of the reinforcements but not to failure of the struts. This is because the widths of the struts are often determined by given dimensions of loading plates or statical conditions or the widths of the struts are assumed so that the stress limits for struts are not attained. It is not advisable to always assume minimum values for the widths of struts so that stress limits are attained in all struts, because then the connected ties also are concentrated, leading to reinforcement congestion. Therefore, the practical conclusion for assuring a ductile behavior is to place reinforcement for all main tensile forces and to design such that struts and nodes do not govern the failure.

The fact that in design different strut-and-tie models can be found for a given problem and a single unique solution should not be expected has puzzled many engineers when STM was presented as a design tool. Perhaps the reason is that structural engineers are trained to find the only one exact analytical solution. This is true under given conditions and restrictions, e.g., when analyzing a structure for given geometry and loading according to linear elastic theory.

Contrary to analysis however, in design an engineer readily chooses a variety of solutions, and for the same task she/he has many options to satisfy the given conditions and the requirements for safety and economy and of quality. This is demonstrated by Fig. 3 showing the many different types of bridges which a designer may consider in the conceptual design or in the first design phases. The classification of structural systems for bridges in Fig. 3a by Schlaich and Bergermann (1992) discerns solutions where main structural parts are either in compression or in tension. Even after such basic decisions have been made and for example beams have been selected and only the material concrete is favored, there is still an enormous variety of systems as demonstrated in Fig. 3b. The range is from statically determinate or indeterminate parallel girders, to haunched beams without and with a hinge at midspan, to strutted beams shaped according to the moment diagram (like by Schlaich), to trussed bridges (like by Menn).

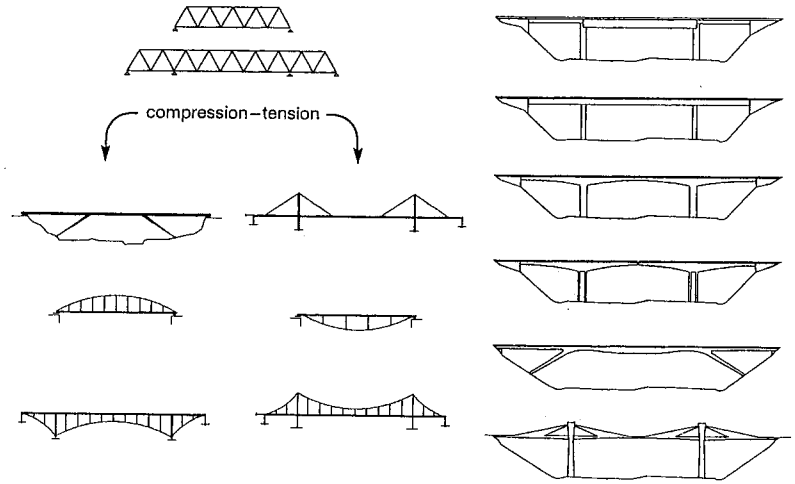

a) classification of structural systems for bridges acc. to Schlaich and Bergermann (1992)

b) variety of beams for concrete bridges

Fig. 3: Variety of statical systems for bridges

In view of this enormous variety in designing structures, it should be accepted that also in structural concrete design many solutions are possible, and thus different strut-and-tie models may be favored by different engineers leading to different reinforcement schemes. All the models will provide the required capacity of the member when tested, if the ductility is provided. The required ductility may be expected to be provided if the structural behavior near the ultimate load of the member or the D-region is governed by yielding of the steel and if the nodes and especially the anchorages are properly designed. Less ductility can be expected if struts and compressive stresses govern the design, which should not be the case in a well selected design.

A good example of different equally valid models is the dapped beam end, dealt with in Part 3 and in Example 2. Fig. 4 shows the models in question. The model in Fig. 4a requires a concentration of stirrups at the face of the beam end, whereas model in Fig. 4b leads to a second tie T_2 for anchoring the tie T_4 and thus promotes the distribution of the stirrups over some length. A third model (Fig. 4c) was proposed in the FIP Recommendations (1999), which was developed under the aspect of minimizing the corbel dimensions for the corbel.

Every model has both advantages and disadvantages as identified by different researchers. The model in Fig. 4a may lead to short lengths for the horizontal tie (force 281), but the inclined strut from node D to the node B (force 195) seems not to comply with the observed failure mechanism, because it crosses the inclined crack starting from the inner corner (see Fig. 9b of Part 3).

This is avoided by the model in Fig. 4b, but this model like that in Fig. 4a is based on orthogonal reinforcement, which is not favorable for limiting the width of the inclined crack starting from the inner corner. The inclined reinforcement for tie T_5 in Fig. 4c more efficiently controls the width of the inclined crack which opens widely at failure, but this model is not capable of dealing with horizontal forces at the support, which may unintentionally occur due to friction at the support. Therefore, the FIP Recommendations (1999) recommend a combination of the latter two models.

Finally it should be pointed out that all three models may exhibit the full desired capacity if properly designed and detailed as demonstrated in Part 3 for the model in Fig. 4a.

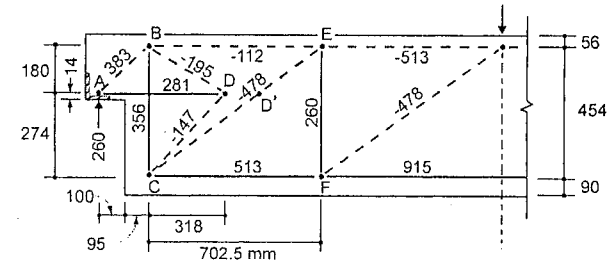

a) model for the test by Cook and Mitchell (1988), see Fig. 9c in Part 3

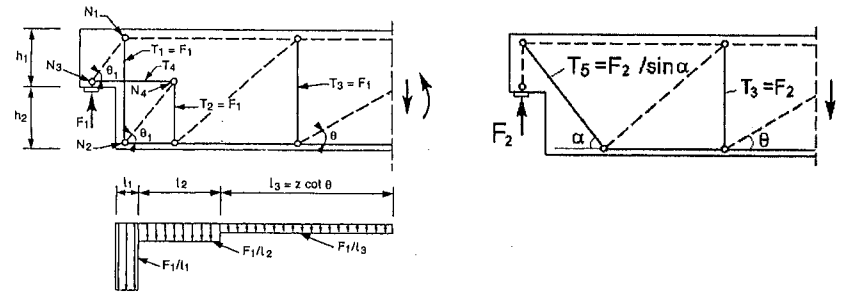

b) model 1 proposed by the FIP Recommendations (1999)

c) model 2 proposed by the FIP Recommendations (1999)

Fig. 4: Different models for dapped beam ends

A similar discussion was carried out for the proper design model for corbels, and this is demonstrated in Fig. 5 for a corbel loaded at the bottom. The first model in Fig. 5a follows the practical request to use only orthogonal reinforcement, whereas the model in Fig. 5b shows an inclined tie that directly follows the trajectories according to linear elastic theory. Such an inclined reinforcement is more efficient and this is visualized by the shorter length of the ties in this model.

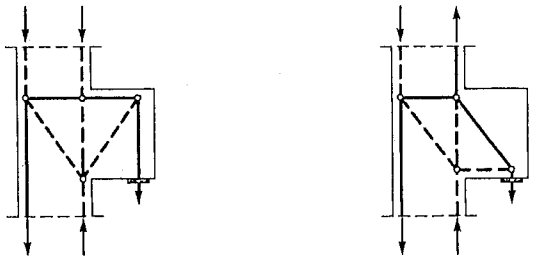

a) model for orthogonal reinforcement b) model for inclined reinforcement

Fig. 5: Strut-and-tie models for corbels loaded at the bottom [Schlaich and Schäfer (2001)]

However, such a discussion on the flow of forces is not sufficient for deciding on the better model. Such a decision requires the detailing of the nodes and anchorages, which may govern the whole design of the D-region.

2.3 Discussion on the uniqueness of models for different examples

2.3.1 Example 1

Example 1 is a basic example of deep beams for which the design principles and different design models can be studied and discussed well, as was done in Example 1a. Additionally, in section 3.6 of part 3 an extensive report is given on a test of this deep beam which gave insight into the structural behavior and validity of the models shown in Fig. 6.

The three models shown in Fig. 6 differ in the amount of required transverse reinforcement and subsequently in the distribution of the tie force in the bottom chord. The first model in Fig. 6a was selected for the design of Example 1a, and is surely on the safe side for the design of the transverse reinforcement, because the force of the vertical tie is equal to the applied load. The force in the bottom chord is staggered and the anchorage at the support has to be designed for a far smaller force (i.e. 50%) than that at midspan.

The model in Fig. 6b appears to be a simpler model. It does not exhibit a vertical tie and the force in the bottom tie is constant from support to support. As a consequence the anchorage at the support has to be designed for 100% of the force at midspan. The fact that there is no vertical tie in the model does not mean that no stirrups are required, but these stirrups would be added following the rules for minimum reinforcement, as shown in section 3.6 of Example 1b.

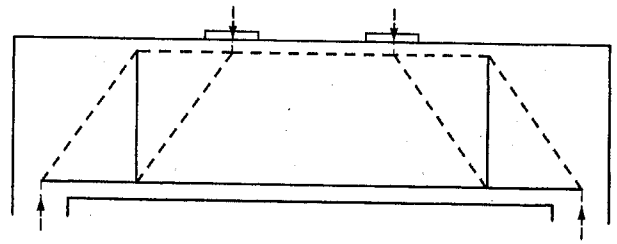

a) model assumed for Example 1a

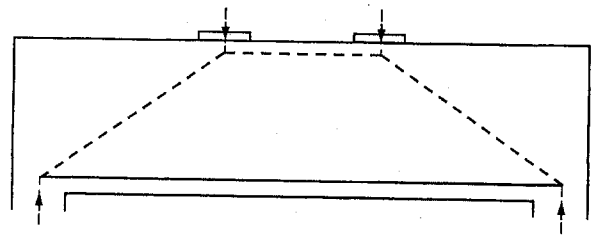

b) model assumed for Example 1b

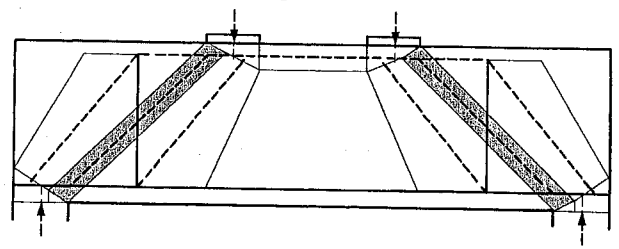

c) model according to the FIP Recommendations (1999)

Fig 6: Different models for Example 1

The third model in Fig. 6c lies between the previous two models and is internally statically indeterminate. An empirically derived rule is given in the FIP Recommendations (1999) to determine which part of the applied load should be assigned to the vertical tie; this depends on the distance of the load from the support axis. This provides a consistent transition for the design of a deep beam with loads near the support to a slender beam, where the total applied load has to be transferred by means of a truss with no direct load transfer to the support by an inclined strut.

The lack of an explicit transverse tie fact in the model in Fig. 6b may appear critical, since it requests the designer to remember to specify minimum required reinforcement. On the other hand it may be argued, that by placing a minimum transverse reinforcement it will carry some load, so that in fact the model of Fig. 6c is effective. The difference is only that the capacity of the transverse tie representing the minimum reinforcement is always the same and does not depend on the distance of the load from the support axis.

In concluding this discussion, the model of Fig. 6c appears to be a proper and practical solution, which demonstrates the necessity for an increasing amount of transverse reinforcement with increasing a in the range between $a = 0.5\ z$ and $a = 2\ z$ (a = distance of load from support axis; z = inner lever arm). Therefore, in section 8.3 of Part 2 MacGregor (2002) proposes that a similar provision should be considered by ACI Subcommittee 318 E as a possible addition to Appendix A.

2.3.2 Example 4

Example 4 presents a new and unknown problem for which no solutions are available in textbooks and no tests have been carried out. It is therefore not surprising that completely different models were proposed by several engineers to which this example was given, some of which are shown in Fig. 7.

The model selected in Example 2 (Fig. 4-3) is shown in Fig. 7 a1, and it may be described as a "beam on beam" solution, which means that the upper part is regarded as a statically determinate member supported on inclined supports. Because the support reactions of this member are equal, i.e. half of the load is carried in each inclined strut, the lower beam has to transfer a part of the load below the opening to the left support so that the overall equilibrium is fulfilled, which resulted in a support reaction at the left support higher than half the applied load (see section 2.2 in Example 4). The upper part is regarded as a deep beam and the model selected is the same as for Example 1b shown in Fig. 6b.

The model in Fig. 7 a2 is a variant of this first model where the right inclined strut is split into a vertical and an inclined strut. The vertical strut carrying the part of the load to be transferred to the left support is nearer to this support than in the previous model. The model for the upper deep beam is that of Fig. 6c.

The models in Fig. 7b are based on the assumption that the vertical short members besides the opening provide a flexural stiffness that may be assessed by a frame analysis. The upper part of the model in Fig. 7 b1 then reflects a deep beam clamped at both sides with a tension chord over the opening. Contrary to that, the model of Fig. 7 b2 may be described as two corbels branching out from the vertical members besides the opening up to the load point and picking up there half of the load each. The corbels are just touching each other under the load but are not connected there, so that tension only occurs in the top chord and no reinforcement is required in the bottom chord directly over the opening.

For all models addressed so far, the upper beam was symmetrically supported, but this assumption is abandoned for the model presented in Fig. 7c. The load is split into two portions equal to the support reactions and consequently no load is transferred by the beam under the opening. Therefore, no transverse reinforcement must be provided in the lower beam. The left upper part over the opening dominantly exhibits a corbel-like action, whereas the right part is a simple beam like the model shown in Fig. 7 a1.

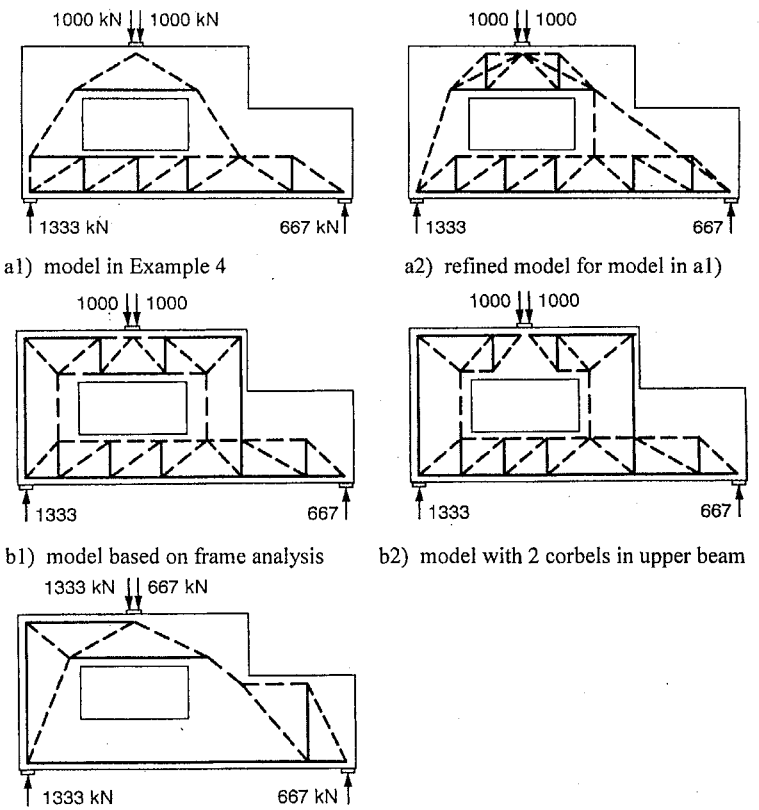

a1) model in Example 4

a2) refined model for model in a1)

b1) model based on frame analysis

b2) model with 2 corbels in upper beam

c) load path model with no load transfer in lower beam

Fig. 7: Different possible models for Example 4

In view of the remarkable differences between all these models the designer may seek some direction in choosing among the possible models. This is provided by a linear-elastic analysis of the wall. However, even without such an analysis, sound engineering judgement will provide a critical perspective:

- the models in Fig. 7b are less likely than those in Fig. 7a because they are less stiff, which is visualized by the longer ties required.
- the model in Fig. 7 b2 is obviously violating compatibility at the midspan of the upper beam over the opening, because there is no connection at all.
- in the model in Fig. 7c the lower beam only acts as a tension member, but with the tension at the bottom; this is not compatible with the flexural stiffness of this member.

Therefore, a combination of the models in Fig. 7 a2 and Fig. 7 b1 may be a sensible solution with some preference for the first model so that it carries more than the second. However, other options are possible.

3 Transition between D- and B-regions of beams

The transition between D- and B-regions of beams has already been addressed when explaining the load path method in Figs. 1 and 2. It is clear that a consistent transition has to be modeled and that is guaranteed by applying the stress distribution of the B-region at the border section of the D-region. In Figs. 1 and 2 these stresses were calculated from a linear-elastic analysis, but likewise the stresses from a cracked section design may be applied, like a flexural design for the moment and axial compressive force in case of Fig. 1c if the stresses would show that the section was cracked.

In case of shear forces acting at the border section like in Fig. 2, the model for a cracked section in the B-region is the well-known truss model as shown in Fig. 8 for a beam with a cantilever [Reineck (1996)].

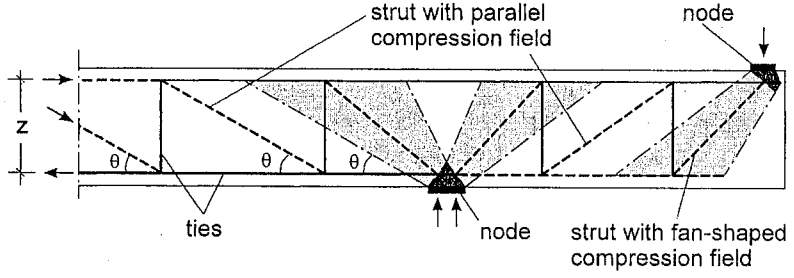

Fig. 8: Truss model and stress fields for a beam with a cantilever

In the D-regions the load is transferred by fan-shaped stress fields, and in the B-regions the truss model is characterized by a parallel stress field inclined at an angle θ to the x-axis. A section in the B-region of the beam contains the forces of the truss as shown on the left end of the beam in Fig. 8, and likewise these forces must be applied at the border of a D-region if the member is cracked.

Therefore, in order to have a consistent transition between B- and D-regions in concrete structures, like in beams, the inner lever arm z and the angle θ must be known. This poses the problem to derive the angle θ for the inclined struts in the web from the shear design carried out according to chapter 11 of ACI 318. As shown in Example 5, the angle θ of the inclined struts in the web of the truss model can be derived because the amount of stirrups is known. The model in Fig. 8 (see also Fig. 5-5 of Example 5) shows that the shear force in the B-region has to be taken by the stirrup forces over the length (z cotθ):

$$V_n = (A_v / s_v)\, f_y\, z \cot\theta$$

and from this expression the angle θ can be calculated as follows:

$$\cot\theta = \frac{V_n}{f_y\, z} \cdot \frac{s_v}{A_v}$$

In this way the shear design of ACI 318 using a V_s- and a V_c-term is interpreted by a truss model, in order to model the transition of a B-region to a D-region.

4 Detailing

Finally the important topic of detailing has to be addressed, as pointed out ever so often by Leonhardt (1965, 1973) and Leonhardt and Mönnig (1977). With strut-and-tie models (STM) this emphasis has continued, because the nodes are defined as an element to be checked. The STM method automatically forces engineers to look at nodes and anchorages. Thus many problems may be detected in early design stages so that the necessary changes can be made to avoid damage through better detailing. In addition to presenting the design concept of STM Schlaich and Schäfer (2001) give many examples for detailing in the continuation of the article by Leonhardt (1973) in the Beton Kalender.

Based on the experience with the examples presented in this report some detailing issues are addressed in this section. They show that detailing again means dimensioning and modeling of the stress fields, only on a smaller scale; the overall equilibrium of struts and ties at a node must be refined and consequently followed up to the stress fields.

The first issue is the use of standard hooks in several of the examples. The hook shortens the required anchorage length in comparison to a straight bar but not to an overwhelming extent, and in European codes the benefit is only 30%. In addition, a hook is critical in case of a support directly at a beam end as in Example 1, because there is the danger that the unreinforced corner below the bend may spall off as shown in Fig. 9. This is especially true for bars with large diameters which are customary in American practice.

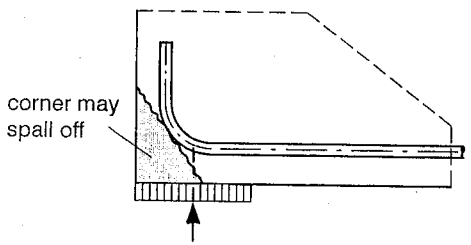

Fig 9: A standard hook at an end support directly at the beam end

In such cases it is necessary to provide some length behind the support as shown in Fig. 10. In principle such details have to be looked at 3-dimensionally (see Figs. 10b and 10c) in order to secure good anchorage as well as not to congest the detail with too much reinforcement so that the concrete cannot be cast properly.

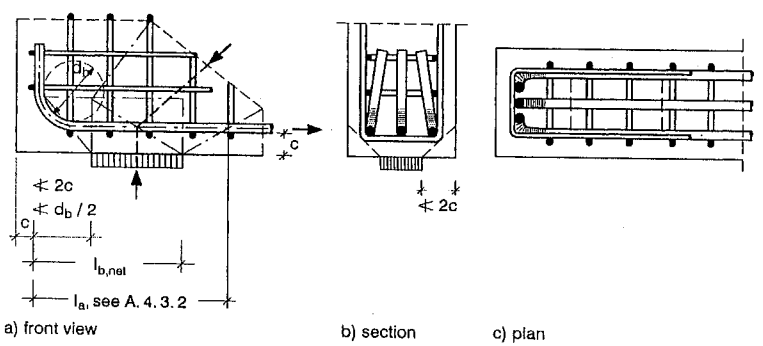

Fig. 10: Detailing at an end support with a standard hook

A more generally experience gained from the examples is, that the provisions for the development length in ACI 318 should be discussed further. The rules in Appendix A do not comply with the rules in the main body of the code, and there are many discrepancies between ACI and European codes.

For example, the influence of transverse pressure or tensile stresses on the anchorage length is not clearly addressed in ACI 318 nor in Appendix A of ACI 318. As the Example 5 showed, there is no difference between a TCC-node, like a direct end support, and a TTC-node, like an indirect end-support. Tests have showed that the anchorage at indirect supports is a critical issue [Leonhardt, Koch and Rostasy (1971); Leonhardt, Walther and Dilger (1968); Baumann and Rüsch (1970)].

Further, the definition of the anchorage length of Appendix A as shown in Fig. 10a should be reviewed, because in European codes the anchorage length starts from the inner face of the support.

The relation between standard hooks and 180°-hooks should also be reconsidered. In all codes there is no difference with respect to shortening the anchorage length as compared to a straight bar; e.g. in European codes there is the same benefit of 30% for both anchorage elements. However, any180°-hook confining the concrete within its bend is a better anchorage at the ultimate limit state (ULS) as compared with a hook. The reason for this discrepancy is that presently the rules for the development of anchorage lengths are based on serviceability considerations, that for e.g. only a slip of 0.10 mm should occur. If the conditions at ULS would be considered, then the anchorage values would show a clear benefit for using 180°-hooks.

The use of 180°-hooks certainly means that possibly smaller bar diameters are selected in order to account for the diameter of bend. However, there is a clear advantage if short anchorages occur as in the case of the corbel shown in Fig. 11. Here Schlaich and Schäfer (2001) showed that thorough considerations are required to design and detail such a critical detail.

Generally, it is indispensable to define realistic values for bond strength and realistic factors for the different anchorage elements when determining the development length at the ULS. Only then the designer can consider the different conditions for TCC- or TTC-nodes where reinforcing bars are anchored. There should be more investigations on the dimensioning of the nodes and development of reinforcement like that carried out by Bergmeister, Breen and Jirsa (1991).

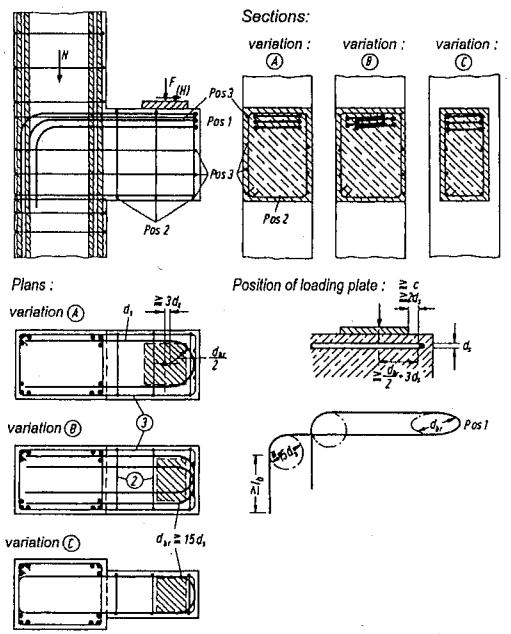

Fig. 11: Detailing of a corbel at a column with a short anchorage length according to Schlaich and Schäfer (2001)

5 Closure

The Appendix A of ACI 318 is a major step forward towards a consistent design of structural concrete. It should enable improved design and detailing of D-regions of concrete structures. This report gives the background for this important achievement and should encourage designer to use strut-and-tie models. The nine examples presented in this Special Publication of ACI should help practicing engineers to apply Appendix A in their daily work.

6 References

ACI 318 (1999): Building Code Requirements for Structural Concrete (ACI 318-02) and Commentary (ACI 318R-02). Reported by ACI Committee 318. American Concrete Institute, Farmington Hills, MI. 445 pp

Baumann, Th.; Rüsch, H. (1970): Schubversuche mit indirekter Krafteinleitung (Shear test with indirect load application). Deutscher Ausschuss für Stahlbeton, Report 210, 1-42, W. Ernst u. Sohn, Berlin, 1970

Bergmeister, K.; Breen, J. E.; Jirsa, J. O. (1991): Dimensioning of the nodes and development of reinforcement. p. 551 - 556 in: IABSE Rep. V.62 (1991)

FIP Recommendations (1999): "Practical Design of Structural Concrete". FIP-Commission 3 "Practical Design", Sept. 1996. Publ.: SETO, London, Sept. 1999. (distributed by: *fib*, Lausanne)

Leonhardt, F. (1965): Über die Kunst des Bewehrens von Stahlbetontragwerken (On the art of reinforcing concrete structures). Beton- und Stahlbetonbau 60 (1965), H.8, pp.181; H.9, pp. 212

Leonhardt, F.; Walther, R.; Dilger, W. (1968): Schubversuche an indirekt gelagerten, einfeldrigen und durchlaufenden Stahlbetonbalken (shear tests at indirectly supported single-span and continuous reinforced concrete beams). Deutscher Ausschuss für Stahlbeton Report 201. 1968

Leonhardt, F.; Koch, R.; Rostásy, F.S. (1971): Aufhängebewehrung bei indirekter Lasteintragung von Spannbetonträgern, Versuchsbericht und Empfehlungen (Hanger reinforcement at indirect load transfer in prestressed concrete beams, test report and recommendations). Beton- und Stahlbetonbau 66 (1971), H.10, 233-241. Discussion by: Baumann, Th.. Beton- und Stahlbetonbau 67 (1972), H.10, 238-239

Leonhardt, F. (1973): Das Bewehren von Stahlbetontragwerken. Beton Kalender 1973, W. Ernst & Sohn, Berlin. (The reinforcing of concrete structures. Reprint translated by B. Maisel, C&Ca, London)

Leonhardt, F.; Mönnig, E. (1977): Vorlesungen über Massivbau - Teil 3: Grundlagen zum Bewehren im Stahlbetonbau. Springer Verlag, Berlin, 1977

MacGregor, J. G. (2002): Derivation of strut-and-tie models for the 2002 ACI Code. p. 7 - 40 in: Examples for the design of structural concrete with strut-and-tie models, Special Publication of ACI. American Concrete Institute, Farmington Hills, 2002

Muttoni, A.; Schwartz, J.; Thürlimann, B. (1996): Design of concrete structures with stress fields. Birkhäuser, Basel, 1996

Reineck, K.-H. (1996): Rational Models for Detailing and Design. p. 101-134 in: Large Concrete Buildings. Rangan, B.V.; Warner, R.F. (Ed.). Large Concrete Buildings. Longman Group Ltd., Burnt Mill, Harlow, England, 1996

Schlaich, J.; Bergermann, R. (1992): Fußgängerbrücken. Katalog zur Ausstellung an der ETH Zürich, 1992 (Pedestrian bridges. Catalogue of an exhibition)

Schlaich, J.; Schäfer, K; Jennewein, M. (1987): Toward a consistent design for structural concrete. PCI-Journ. V.32 (1987), No.3, 75-150

Schlaich, J.; Schäfer, K. (2001): Konstruieren im Stahlbetonbau (Detailing of reinforced concrete). Betonkalender 90 (2001), Teil II, 311 - 492. Ernst & Sohn Verlag, Berlin 2001

Acknowledgements

The authors wishes to acknowledge the contribution by Arndt Goldack and Uwe Burckhardt from the University of Stuttgart as well as by Robert Zechmann from the University of Kansas who proposed and investigated some of the models for the Example 4 presented in Fig. 7.

The authors acknowledge the editing of the drawings by Elfriede Schnee and Ali Daghighi. The authors also gratefully appreciate the thorough work by Angela Siller for editing the final version considering the comments by reviewers.

CONVERSION FACTORS—INCH-POUND TO SI (METRIC)*

To convert from	to	multiply by
	Length	
inch	millimeter (mm)	25.4E†
foot	meter (m)	0.3048E
yard	meter (m)	0.9144E
mile (statute)	kilometer (km)	1.609
	Area	
square inch	square centimeter (cm^2)	6.451
square foot	square meter (m^2)	0.0929
square yard	square meter (m^2)	0.8361
	Volume (capacity)	
ounce	cubic centimeter (cm^3)	29.57
gallon	cubic meter (m^3)‡	0.003785
cubic inch	cubic centimeter (cm^3)	16.4
cubic foot	cubic meter (m^3)	0.02832
cubic yard	cubic meter (m^3)‡	0.7646
	Force	
kilogram-force	newton (N)	9.807
kip-force	newton (N)	4448
pound-force	newton (N)	4.448
	Pressure or stress (force per area)	
kilogram-force/square meter	pascal (Pa)	9.807
kip-force/square inch (ksi)	megapascal (MPa)	6.895
newton/square meter (N/m^2)	pascal (Pa)	1.000E
pound-force/square foot	pascal (Pa)	47.88
pound-force/square inch (psi)	kilopascal (kPa)	6.895
	Bending moment or torque	
inch-pound-force	newton-meter (Nm)	0.1130
foot-pound-force	newton-meter (Nm)	1.356
meter-kilogram-force	newton-meter (Nm)	9.807

To convert from	to	multiply by
	Mass	
ounce-mass (avoirdupois)	gram (g)	28.34
pound-mass (avoirdupois)	kilogram (kg)	0.4536
ton (metric)	megagram (Mg)	1.000E
ton (short, 2000 lbm)	megagram (Mg)	0.9072
	Mass per volume	
pound-mass/cubic foot	kilogram/cubic meter (kg/m^3)	16.02
pound-mass/cubic yard	kilogram/cubic meter (kg/m^3)	0.5933
pound-mass/gallon	kilogram/cubic meter (kg/m^3)	119.8
	Temperature§	
deg Fahrenheit (F)	deg Celsius (C)	$t_C = (t_F - 32)/1.8$
deg Celsius (C)	deg Fahrenheit (F)	$t_F = 1.8t_C + 32$

* This selected list gives practical conversion factors of units found in concrete technology. The reference source for information on SI units and more exact conversion factors is "Standard for Metric Practice" ASTM E 380. Symbols of metric units are given in parentheses.

† E indicates that the factor given is exact.

‡ One liter (cubic decimeter) equals 0.001 m^3 or 1000 cm^3.

§ These equations convert one temperature reading to another and include the necessary scale corrections. To convert a difference in temperature from Fahrenheit to Celsius degrees, divide by 1.8 only, i.e., a change from 70 to 88 F represents a change of 18 F or 18/1.8 = 10 C.